Photoredox-Catalyzed Direct Allylic C−H Functionalization of Enol Silyl Ethers

NAKASHIMA Tsubasa

Department of Molecular & Macromolecular Chemistry
Graduate School of Engineering
Nagoya University

**Contents**

Chapter 1. Introduction and General Summary

1.1 General transformations of C(sp^3)−H bonds

C(sp^3)−H bond is one of the most fundamental covalent bonds to constitute organic molecules. The selective transformations of C(sp^3)−H bonds into C−C or C−X (carbon−heteroatom) bonds can streamline the molecular synthesis. Therefore, the development of new reactions and new catalysts for this type of transformations is a subject of central importance in synthetic chemistry. While a great number of C(sp^3)−H functionalizations based on the heterolytic cleavage in acid-base equilibrium have been reported, this type of methodologies often encounters any limitation due to the pK_a values of C−H bonds. Since the deprotonation of C−H bonds in non-activated hydrocarbons is far difficult, the transformations of C(sp^3)−H bonds usually rely on the activating functional groups, such as carbonyl group, which allow for the decrease of the pK_a of neighboring methyl, methylene, or methine C−H bonds, leading to the facile generation of carbanion intermediates and the subsequent bond-forming events (Figure 1).
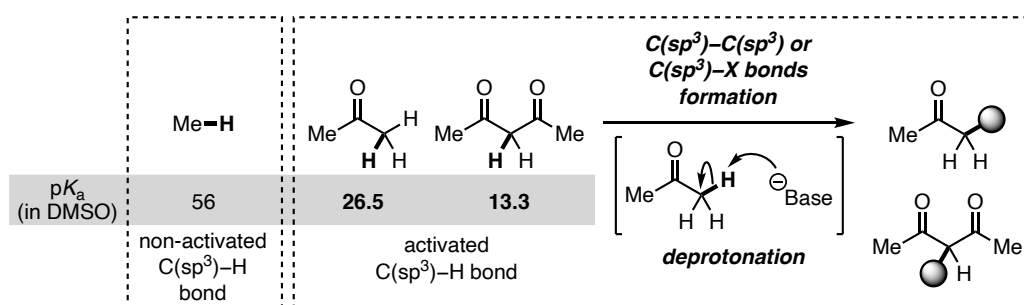
Figure 1. Functionalization of C(sp^3)−H bonds based on heterolytic cleavage.

Radical reaction through the homolytic cleavage of C(sp^3)−H bonds is a complementary strategy with polar reaction based on heterolytic cleavage. For instance, hydrogen atom transfer (HAT) of organic molecules with radical species leads to the generation of sp^3-hybridized carbon-centered radicals through the cleavage of a range of weakly acidic or non-acidic C(sp^3)−H bonds. While HAT process is largely affected by the bond dissociation enthalpy (BDE), reactive radical species, such as halogen radicals, enables the cleavage of not only the relatively active, benzylic or allylic C−H bonds having low BDE (about 90 kcal/mol) but also the strong C−H bonds in aliphatic hydrocarbons (Figure 2).
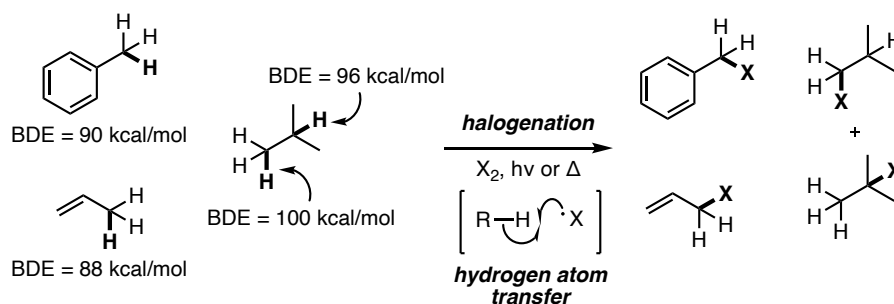
Figure 2. Homolytic cleavage of C(sp^3)−H bonds.

## 1.2 Catalytic functionalization of non-acidic C(sp^3)−H bonds

In past few decades, the development of novel catalytic methods for the functionalization of simple alkyl framework possessing non-acidic C(sp^3)−H bonds have been widely investigated. Especially, the methodologies using transition metal catalysis have made a great stride within this issue, where a wide variety of activation modes and structurally diverse catalysts and ligands have been demonstrated.

1.2.1 Transition metal carbene- and nitrene complexes

Catalytic transformations mediated by transition metal carbenes and nitrenes is one of the most straightforward methods for the conversion of C−H bonds to C−C and C−N bonds.[1] The preeminent reactivity of these complexes allows direct functionalization of non-acidic C(sp^3)−H bonds including simple hydrocarbons. For examples, dirhodium(II)-carbenes formed from dinuclear rhodium complexes and diazoesters have been utilized as the most versatile reactive intermediates for C−H bond insertion reactions to form new C(sp^3)−C(sp^3) bonds. Davies *et al.* have developed bridged rhodium catalyst with chiral carboxylate ligand and applied it to stereoselective insertion of chiral rhodium carbene species into C−H bonds of cycloalkanes (Scheme 1).[2] Further investigations into the modification of the electronical property of ligands have affected the selectivity in C−H bond activation to achieve the synthesis of complex natural products and bioactive molecules. Metal nitrenes also show similar reactivity as metal carbene species and have successfully utilized in the intra- or intermolecular amination of non-acidic C−H bonds with amides and hypervalent iodines (Scheme 2).[3]
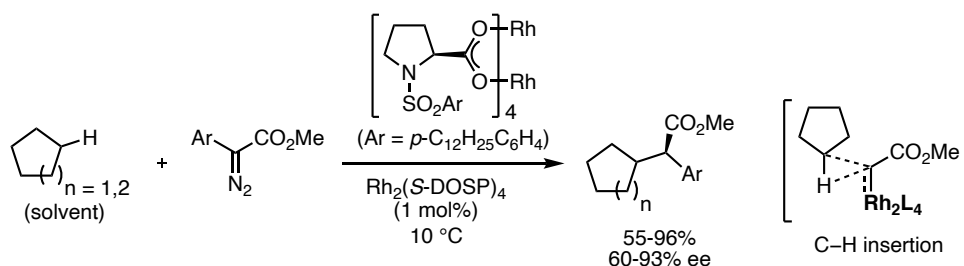

Scheme 1. Insertion of metal carbenes into C(sp^3)−H bonds.
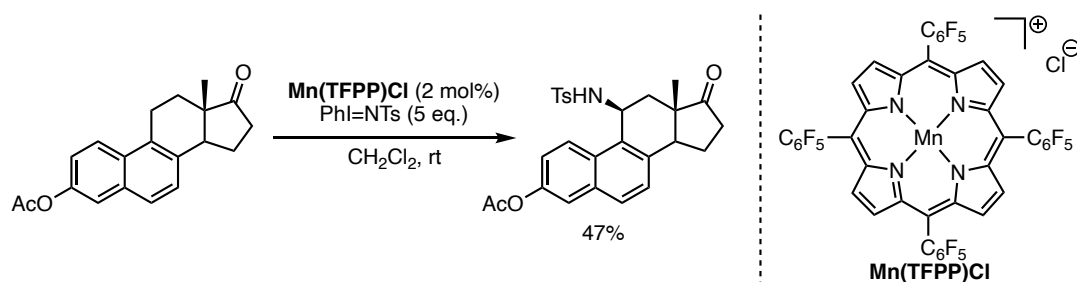
Scheme 2. Metal nitrenes catalysis for C(sp^3)−H amination.

1.2.2 Transition metal oxo complexes

The oxidation of C(sp^3)−H bonds is one of the most fundamental transformations in organic synthesis, in which transition metal oxo complexes have been known to show high reactivity.[4] Transition metal oxo complexes attached with a wide variety of ligands undergo oxygen atom transfer to substrates through concerted insertion into C−H bonds or C−H abstraction followed by radical rebound mechanism. Earth abundant transition metals, such as iron and manganese, are superior in terms of sustainability as well as excellent catalytic performance for the control of stereo-, regio-, and chemoselectivity. For example, White *et al.* have developed Fe- or Mn-based catalysts toward the selective C−H oxidation. By tuning the subtle electronic and steric properties of catalysts depending on substrates, they succeeded in the efficient synthesize of complex molecules (Scheme 3).[5]
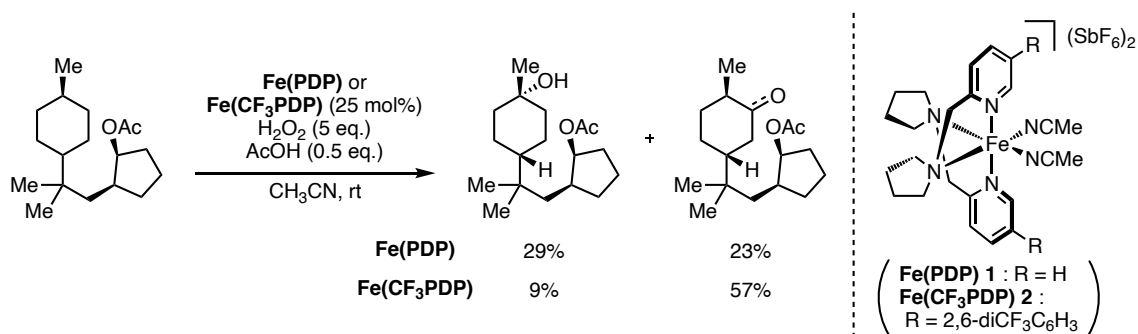
Scheme 3 Catalyst-controlled C−H oxidation.

1.2.3 Transition metal-catalyzed directed C(sp^3)−H functionalization

Recently, methods for the direct oxidative addition into inert C(sp^3)−H bonds with transition metal complexes have attracted a great deal of attention as it would offer a novel strategy in C−H functionalization chemistry. In 2004, a pioneering study on transition metal-catalyzed direct oxidation of non-activated primary C(sp^3)−H bonds was reported by Sanford group (Scheme 4).[6] They successfully achieved palladium-catalyzed, nitrogen-directed intramolecular C(sp^2)−H acetoxylation of aliphatic oximes and alkylated pyridines.

MeO—N ... (Scheme 4 structures)
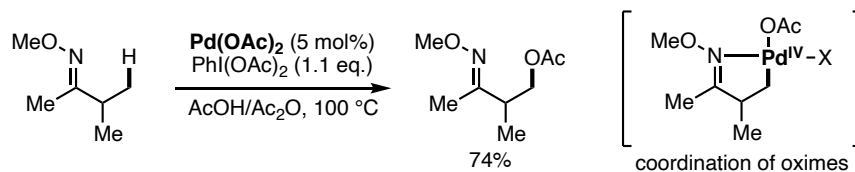
Scheme 4. Palladium-catalyzed acetoxylation of unactivated C(sp^3)−H bonds.

The Yu[7] and Daugulis[8] groups have also made the leading contributions for the establishment of concept and methodology for the directing groups-assisted transformation of C(sp^3)−H bonds. In addition to palladium catalysis, other noble transition metals (iridium and ruthenium, etc.) and earth-abundant metals (nickel, iron and cobalt, etc.) have been also applied to this chemistry and a lot of efforts on the improvement of the applicability have been conducted in last few decades.[9]

1.2.4 Hydrogen atom transfer (HAT)

Radicals are highly reactive intermediates and exhibit unique reactivities which are not found in ionic reactions or transition metal catalysis. As mentioned above, halogen radicals can promote the hydrogen abstraction reaction with a range of C(sp^3)−H bonds in hydrocarbons due to their high BDE of X−H bonds (X = halogens, BDE (H−Cl) = 102 kcal mol^{-1}).[10] The nitrogen-centered radicals also have high BDE, as aminium radical cations generated by photolysis or thermolysis of *N*-halogenated ammonium ions undergo intramolecular 1,5-HAT to generate carbon radicals, known for Hoffmann-Loffler-Freytag reaction (Scheme 5).[11]
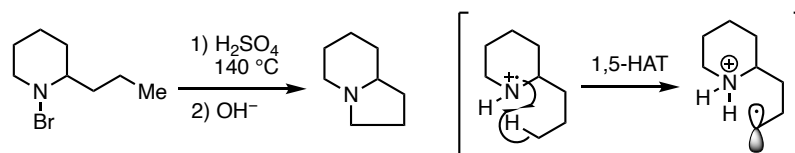
Scheme 5. Hoffmann-Loffler-Freytag reaction.

The recent advances in photoredox catalysis and photochemical reactions have enabled the facile generation of *N*-centered radicals or oxy radicals and following intramolecular HAT for the remote C(sp^3)−H activation under mild conditions (Scheme 6).[12] While these strategies are advantageous for regioselective activation of non-activated C(sp^3)−H bonds, the pre-installation of functional groups, such as amides or alcohols, is required.
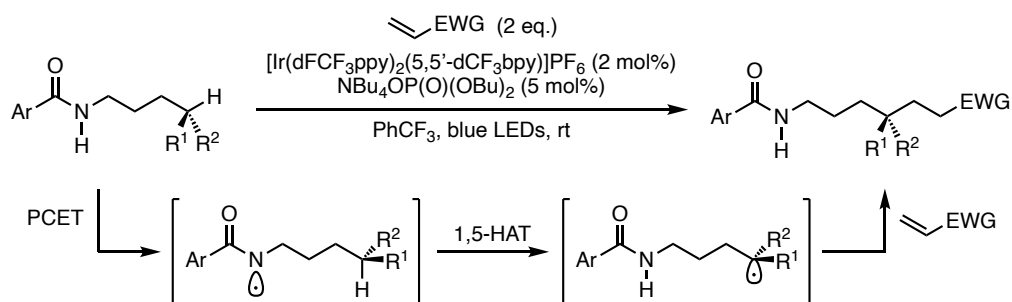
Scheme 6. Catalytic remote C(sp^3)−H activation.

On the other hand, the functionalization of non-acidic C(sp^3)−H bonds through catalytic intermolecular HAT process is one of the most attractive yet highly challenging transformations in organic synthesis, since it might enable the C−H bond cleavage without the aid of directing groups or intramolecular HAT process. With the spread of light-induced photoredox catalysis, a large number of researches for the development of novel HAT catalysts have been reported to enable the direct functionalization of C(sp^3)−H bonds (Figure 3).[13] The advantages of catalytic intermolecular HAT strategy have been seen in site-specific functionalization of organic molecules having multiple C(sp^3)−H bonds. For instance, MacMillan group reported catalytic alkylation of α-C−H bonds of alcohols with quinuclidine HAT catalyst and phosphates for C−H bond weakening catalyst.[13c] They demonstrated high applicability of their HAT system in selective functionalization of complex molecules (Scheme 7). Furthermore, the combination with transition-metal catalysis has broaden the utilities of these selective C−H activation modes.[14]
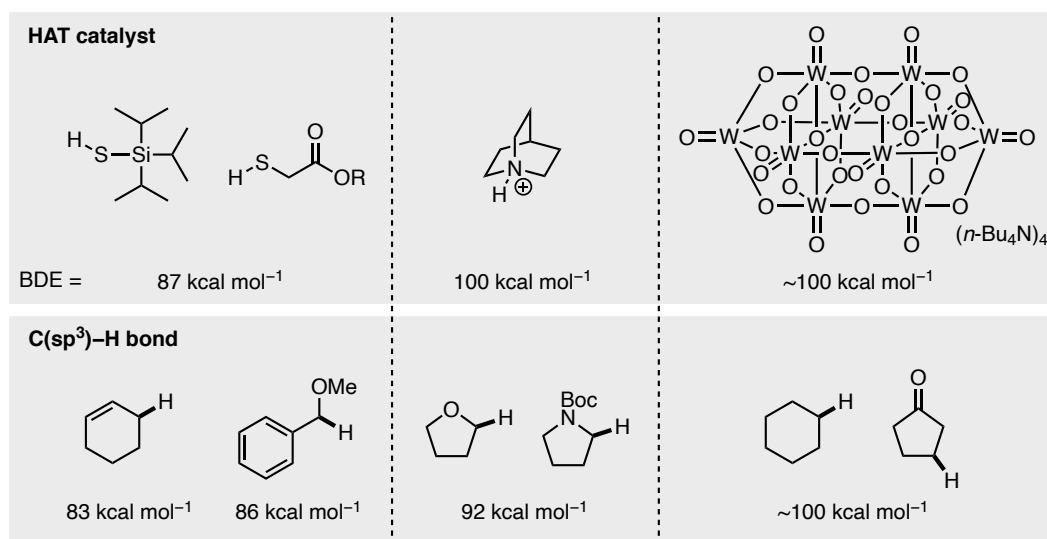

Figure 3. Representative HAT catalysts and BDE of C(sp^3)−H bonds.
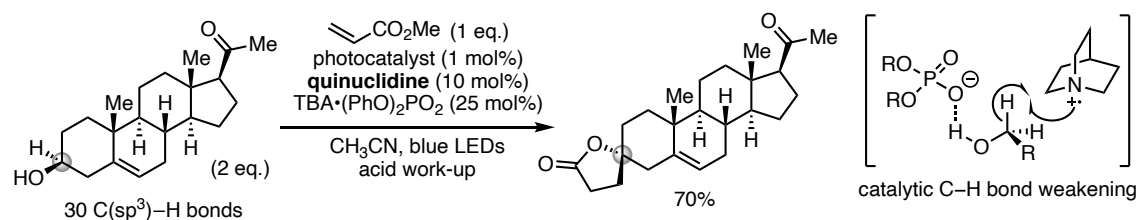
**Scheme 7.** Selective alkylation of complex alcohol C−H bonds via intermolecular HAT.

1.2.5 Single electron transfer (SET)

The single electron transfer (SET) is well known chemical reactions to afford radical ion intermediates and has been employed in organic synthesis, as seen in Birch reduction, Ullmann reaction, to name a few. The recent advances in photoredox catalysis, sometimes combined with organic molecular catalysis or transition metal catalysis, have enabled challenging bond forming reactions through the catalytic generation of radical ion species via SET under mild conditions.[15] In terms of activation of inert C−H bonds, radical cation intermediates generated by single-electron oxidation of organic molecules increase the acidity of neighboring C−H bonds[16] to promote the deprotonation and formation of carbon radical intermediates. With these properties, Nishibayashi *et al.* disclosed the generation of α-aminoalkyl radicals through the single-electron oxidation of tertiary amines and subsequent deprotonation. Based on this method, α-C−H alkylation of amines with electro-deficient olefins under the visible-light-mediated photoredox catalysis was achieved (Scheme 8).[17]
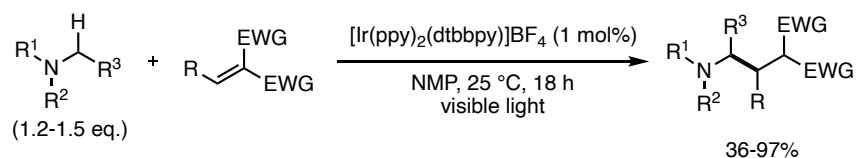
Scheme 8. Photoredox-catalyzed utilization of α-aminoalkyl radicals.

According to the related literatures, the pK_a value of a radical cation derived from triethylamine is presumed to be ca. 14.7 in acetonitrile whereas that of α-C−H bond of triethylamine is over 40 (Scheme 9).[18] This observation could be explained by considering the interaction of molecular orbitals between singly occupied sp^3 orbital on nitrogen atom and neighboring C−H σ-bond, leading the drastic weakening of neighboring C−H bond. An electron from C−H bond is transferred to nitrogen of radical cation in the elementary reaction of C−H bond cleavage to form the corresponding alkyl radicals (Figure 4). In addition to α-C−H functionalization of amines[19], the activation of allylic, benzylic[20] and imidoyl[21] C−H bonds have been achieved via single-electron oxidation-deprotonation sequence. These methodologies are much important to enable the selective cleavage of C(sp^3)−H bonds which are adjacent to electron-rich functionalities.
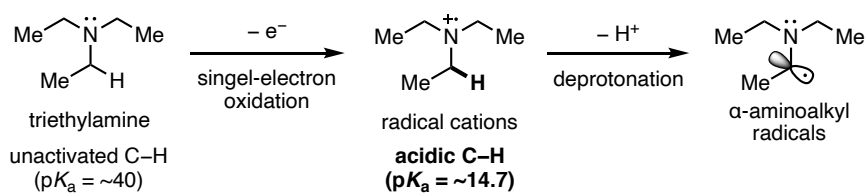
Scheme 9. Dramatically increased acidity of α-C−H bonds in radical cations.
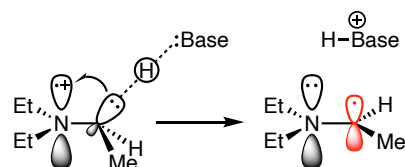
**Figure 4.** Model of deprotonation from radical cations.

1.3 Selective C(sp^3)−H functionalization

As described above, the development of direct functionalization of C(sp^3)−H bonds has enabled straightforward access to functionalized molecules without need for pre-installation of activating groups. For instance, the direct transformation of C−H bonds would dramatically decrease the number of process in the synthesis of natural products, and chemoselective late-stage functionalization of complex molecules can improve the efficiency of the drug discovery (Figure 5a,b).[22] On the other hand, the selective C−H functionalization of organic molecules which have multiple functional groups affords the powerful method for the synthesis of more complex molecules. Transformation of C(sp^3)−H bonds with preservation of reactive sites generates another synthetic intermediates and further reaction of potent reactive sites enables the rapid construction of highly functionalized molecules. (Figure 5c).
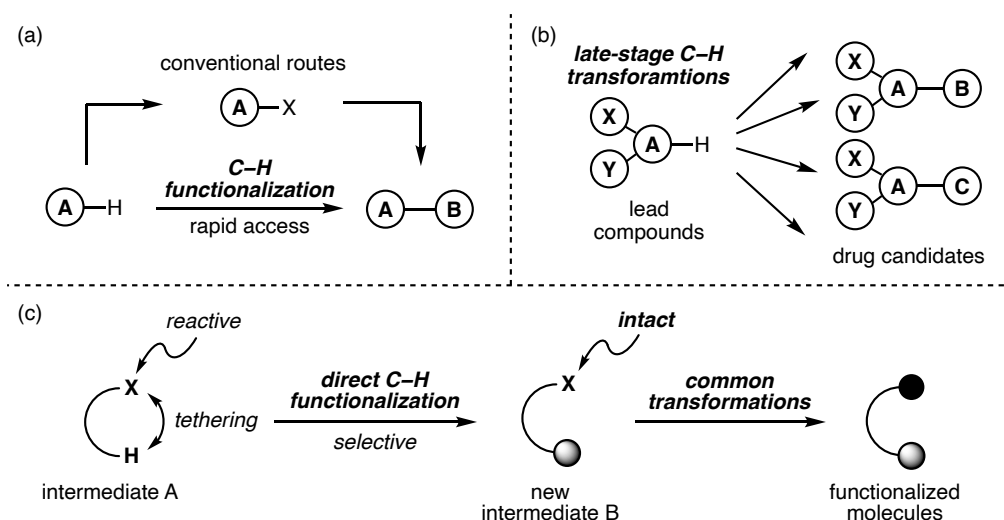
Figure 5. Direct C(sp^3)−H functionalization. (a) Efficient access to targeting molecules. (b) Diversification of drug compounds. (c) Transformations of C(sp^3)−H bonds with reactive functional groups.

1.3.1 Catalytic allylic C(sp^3)−H functionalization

Alkenes are widely available and versatile building blocks for the synthesis of not only small molecules but also natural products, and selective functionalization of C=C bonds have been well developed. In addition to the reactivity of olefins, allylic C(sp^3)−H bonds have been also recognized as potential reactive sites due to its low BDE and a large number of catalytic methods for direct allylic C−H functionalization have been reported using transition metal catalysts and organocatalysts.[23] Thus, the consecutive allylic functionalization and common transformation of olefins allow the efficient organic synthesis (Scheme 10).
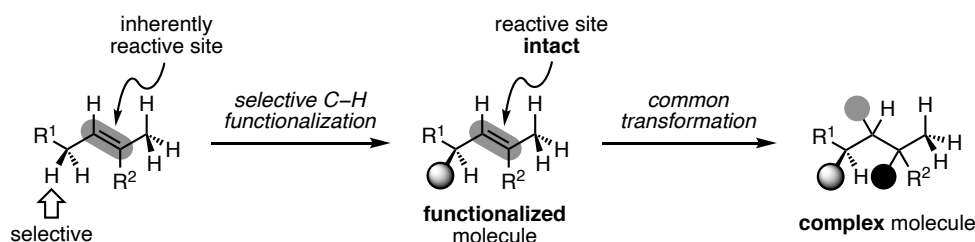
Scheme 10. Allylic C(sp^3)−H functionalization and transformation of olefins.

1.4 Enol silyl ethers

Enol silyl ethers and their analogues have long been utilized as enolate equivalents and are one of the most versatile reagents in organic synthesis. These reagents are applicable to various transformations, such as C−C, C−N, C−O, C−X (X = halogens) bond forming reactions, to afford α-functionalized carbonyl compounds.[24] In addition to their synthetic utilities, these analogues can be prepared not only from ketones but also from aldehydes, esters and amides, thus providing the attractive platform for the construction of diverse molecular architectures (Figure 6).
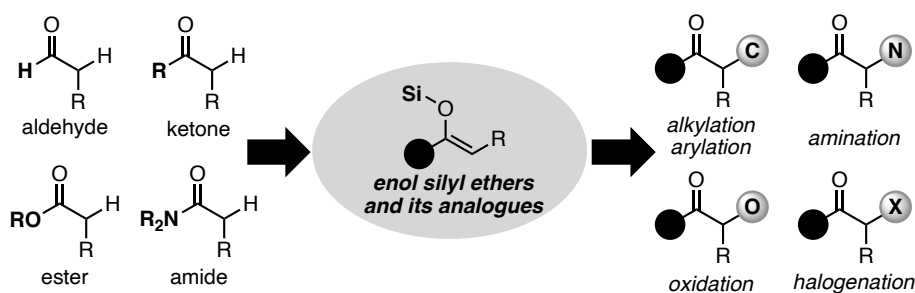
Figure 6. Enol silyl ethers in organic synthesis.

On the other hand, the preparation of enol silyl ethers and their derivatives typically requires strong bases, such as lithium amides, or strong silyl Lewis acids, such as silyl triflates. These conditions sometimes suffer from the use of functional groups which are prone to react under basic or acidic

conditions (Scheme 11). The structure of carbonyl compounds having more than one active methyl, methylene, or methine group is inappropriate for the preparation of enol silyl ethers because these carbonyls are often afford the mixture of structural isomer. In other words, the synthesis of complex enol silyl ethers has remained difficult.
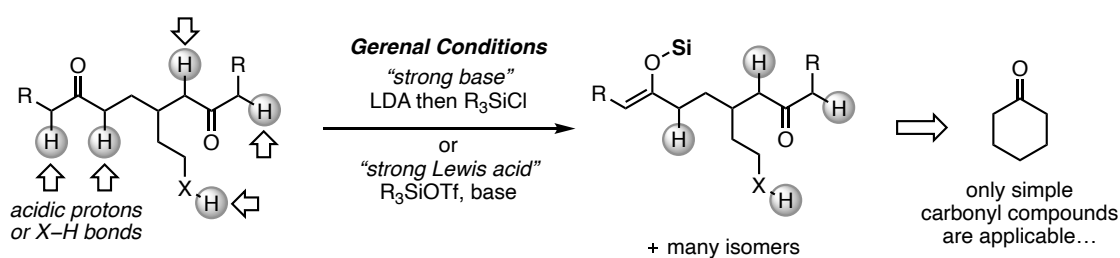
Scheme 11. Synthetic problems in preparation of enol silyl ethers.

In this context, the author has paid attention to enol silyl ethers for their synthetic utilities in organic synthesis and the potential reactivity of their allylic C(sp^3)−H bonds contributed by electron-rich enol moiety. If the allylic C−H functionalization of enol silyl ethers could be achieved with reactive enol moiety intact, the following common polar reactions of resulting enol silyl ethers can afford α,β-difunctionalized, complex carbonyl compounds (Scheme 12). The development of new methodologies to enable the selective "complexation" of the structure of commonly utilized reactive reagents should have large impact on the efficient organic synthesis.
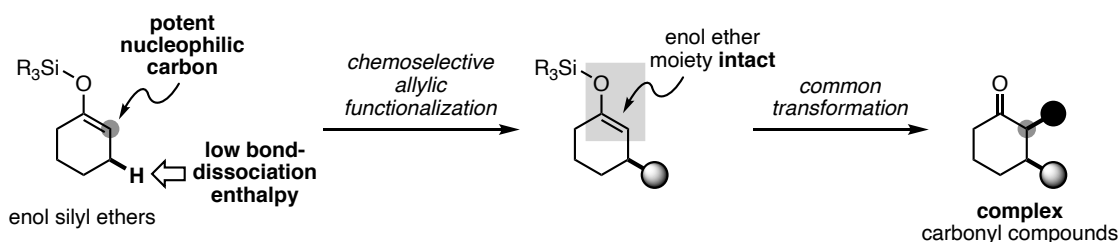
Scheme 12. The outline of this thesis.

1.4.1 Allylic C(sp^3)−H functionalization of enol silyl ethers through hydrogen atom transfer

Despite the high demands and utilities in organic synthesis, only a few catalytic methods for the functionalization of allylic C−H bonds of enol silyl ethers have been reported. Transition metal catalyzed chemo- and stereoselective C−H insertion of enol silyl ethers was reported by Davies group to afford alkylated products at the allylic position with preservation of enol ether moiety (Scheme 13).[25] While this system provided enantio-enriched enol silyl ethers, the regio-, chemo- and

stereoselectivity heavily relied on the structure of both enol silyl ethers and diazoesters and further synthetic application was not conducted.
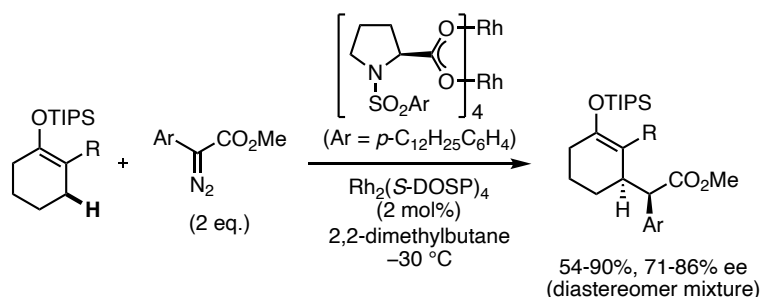
Scheme 13. Catalytic C−H insertion of metal carbenes.

In 2015, MacMillan group disclosed the direct arylation of allylic C(sp^3)−H bonds with combined organic and photoredox dual catalysis (Figure 7).[26] The electron deficient cyano-substituted (hetero)arenes were reduced by the photoexcited state of iridium^{III} complex to afford the long-lived radical anion and transiently generated Ir^{IV} would oxidize thiol catalyst through the proton-coupled electron transfer. Then, thiyl radical acted as HAT catalyst to form allylic radical intermediate from enol silyl ether which underwent radical-radical coupling with radical anion. This reaction is highly
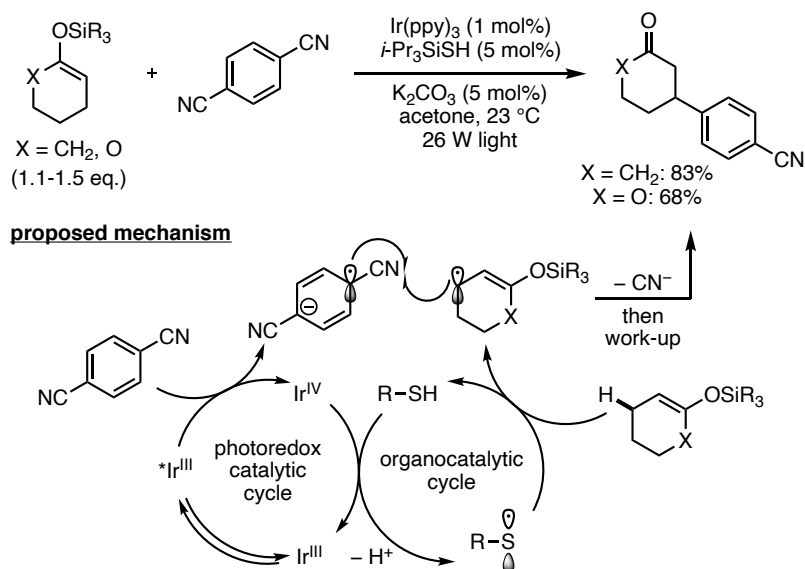
Figure 7. Organo- and photoredox-catalyzed allylic C−H arylation.

practical and straightforward methods to construct valuable compounds from simple olefin substrates. While enol silyl ethers and ketene silyl acetals were also applicable for the formation of β-arylated

carbonyl compounds, only a few examples were shown and enol ether moiety was not preserved through the reaction.

More recently, Chang *et al.* reported copper-catalyzed direct allylic C−H perfluoroarylation of enol silyl ethers through the hydrogen atom abstraction of allylic C−H bonds via copper catalyst to form allylic radicals (Scheme 14).[27] The radical intermediates would be captured by perfluoroarene-bounded copper catalyst and following bond formation afforded β-arylated ketones, esters and aldehydes.
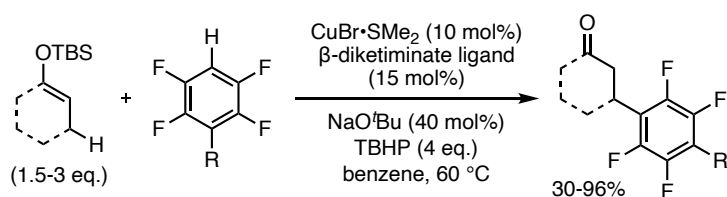
Scheme 14. Copper-catalyzed allylic C−H perfluoroarylation.

In this way, the nature of weak allylic C−H bonds in enol silyl ethers has been recognized and applied to several transformations to catalytically construct new carbon-carbon bonds, however, such a methodology with preservation of enol ether moiety and further synthetic applications has been elusive in spite of their high potential utilities.

1.4.2 Single electron oxidation of enol silyl ethers

It has also been known that enol silyl ethers are amenable to single-electron oxidations and generate corresponding radical cations. In 1988, Gassman and Bottorff reported that cyclohexanone-derived trimethylsilyl enol ether could undergo photoinduced single-electron transfer with 1-cyanonaphthalene as a strong oxidant under the irradiation of 300 nm UV lamp to generate a corresponding radical cation intermediate and resulted in the formation of unfunctionalized ketone (Scheme 15).[28] This transformation would proceed with the loss of trimethylsilyl cation from radical cation intermediate to give α-carbonyl radicals followed by hydrogen atom abstraction from methanol to afford the corresponding ketone.
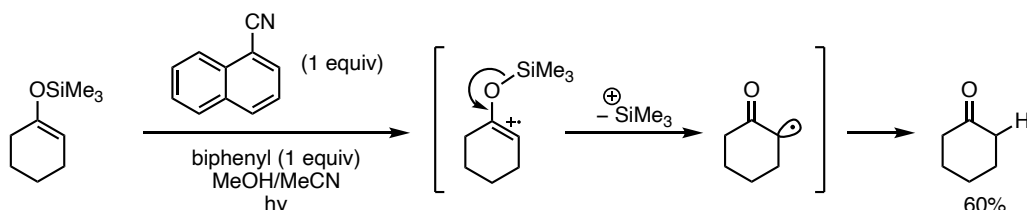
Scheme 15. Electron transfer-induced desilylation.

The reaction of trimethylsilyl enol ethers with 2,3-dichloro-5,6-dicyano-1,4-benzoquinone (DDQ) was investigated by Bhattacharya and co-workers (Scheme 16).[29] In that report, they revealed that enol silyl ethers smoothly reacted with DDQ through the formation of charge transfer complexes to generate radical ion pairs. Subsequent radical coupling to afford a mixture of C−O coupled adduct and C−C quinone adduct followed by the formation of 2-cyclohexan-1-one. The similar study with chloranil as an electron acceptor under the UV light irradiation also showed the same affection as C−O adduct and enone formation.[30] The identification of intermediate upon the photo-oxidation was conducted by time-resolved spectroscopy and radical cations derived from enol silyl ethers were exactly observed with the decay of excited state of chloranil.
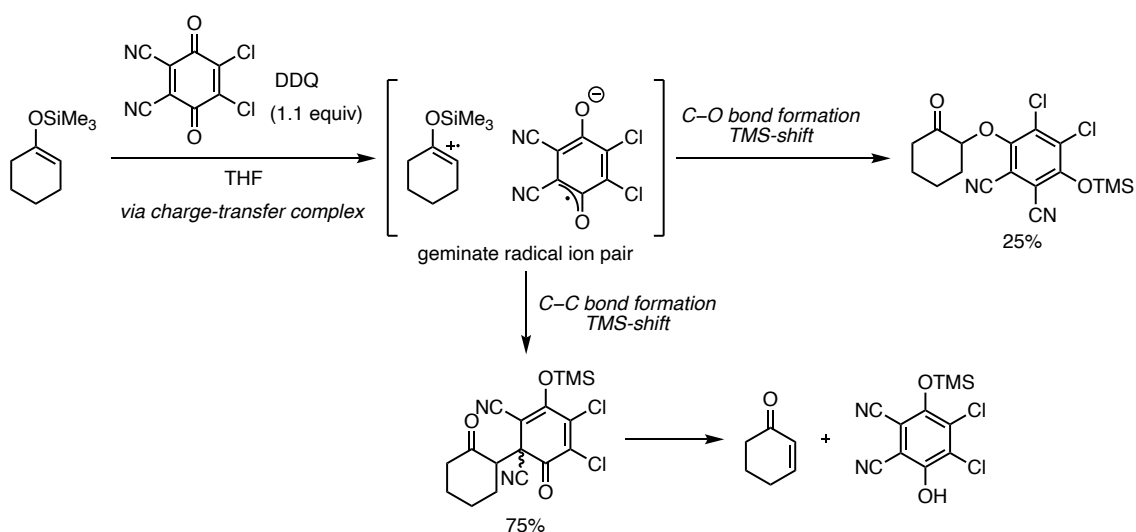
Scheme 16. Radical coupling reaction with DDQ.

Kochi and Rathore reported α-nitration of enol silyl ethers with tetranitromethane (TNM) (Scheme 17).[31] Spectral investigation revealed that the red colored solution of reactants stemmed from the 1:1 complexation of enol silyl ethers and TNM, which caused thermal decomposition to afford α-nitro ketone and trimethylsilyl trinitromethane via radical cation intermediates at ambient temperature. While the formation of α-nitro ketone was suppressed at −40 °C, the irradiation of visible light facilitated the product formation through the excitation of the EDA complex and generation of radical cations derived from enol silyl ethers.
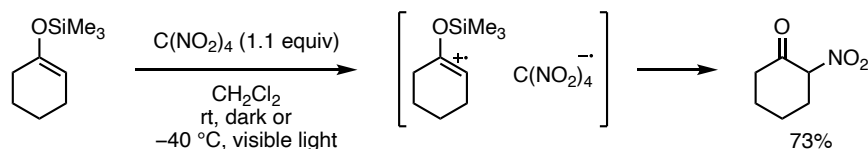
Scheme 17. α-Nitration of enol silyl ethers.

Enol silyl ethers which have δ,ε- or ε,ζ-unsaturated moieties could be oxidized by excess amount of copper (II) triflate ($Cu(OTf)_2$) or ceric ammonium nitrate ($Ce(NH_4)_2(NO_3)_6$, CAN) to form radical cation intermediates followed by cascade desilylative intramolecular cyclization, second cyclization, terminal oxidation, and deprotonation to provide the tricyclic ketones (Scheme 18).[32] This method showed high efficiency to construct the fused polycyclic ketones from readily prepared enol silyl ethers in a single manipulation.
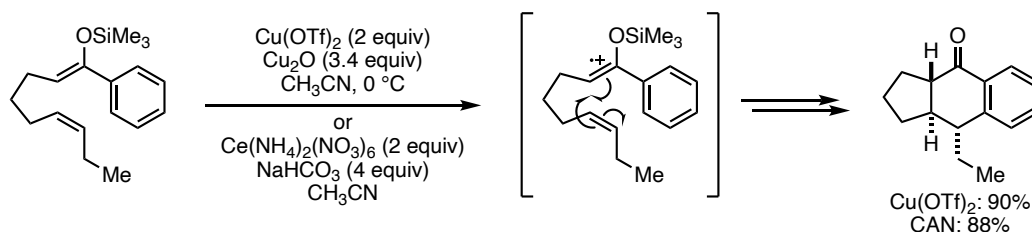
Scheme 18. Oxidative cyclization of unsaturated enol silyl ethers.

In addition to these reactions, several transformations regarding single-electron oxidation of enol silyl ethers have been reported,[33-39] however, in terms of the reactivity of radical cations derived from enol silyl ethers, desilylation reaction or bond-formation at α-position to carbonyl groups have only been achieved.

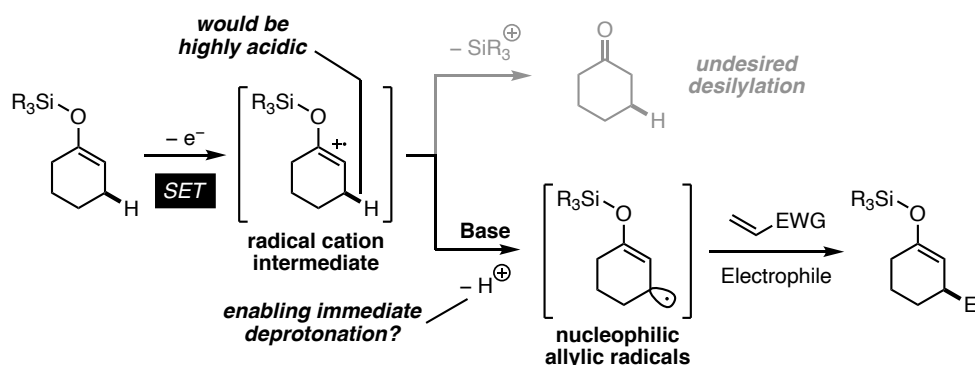## 1.4.3 Direct allylic C−H alkylation of enol silyl ethers enabled by photoredox-Brønsted base hybrid catalysis: Chapter 2

As described in section **1.2.5**, considering the properties of radical cations, the acidity of neighboring C−H bonds was dramatically increased. With this information and properties of enol silyl ethers in SET conditions mentioned in section **1.4.2**, the allylic C−H bond in radical cations generated via single-electron oxidation of enol silyl ethers should be highly acidic (Figure 8). The author envisioned that rapid deprotonation from radical cations over desilylation would produce nucleophilic allylic radicals to enable the bond-forming reaction with electrophiles at allylic position. To deeply understand the property of radical cations and the elemental step for the generation of allylic radical, several computational- and photochemical experiments were conducted, and it was revealed that pK_a value of radical cations generated from cyclohexanone-derived enol silyl ethers in acetonitrile was similar to that of p-TsOH. As a result of rational optimization of reaction conditions, allylic C−H alkylation with electron-deficient olefins was achieved by the use of appropriate Brønsted base under a photoredox condition. In addition to the discovery of the new transformations, derivatizations of alkylated enol silyl ethers demonstrated the high availability to access to an array of complex carbonyl compounds.

Figure 8. The reaction design of allylic C−H alkylation of enol silyl ethers.

1.5.1 Brønsted acid catalysts in photoredox catalysis

Recent development of photoredox catalysis has supplied chemists methodologies which enabled new manner of bond-forming reactions and the combination with Brønsted acid catalysts often decreases the activation energies to accelerated the radical reaction.[40] The one role of Brønsted acid is electrophilic activation of electrophiles via protonation or hydrogen bonding to enhance the reactivity toward nucleophilic radical species (Figure 9a).[41] The other one is lowering the reduction potentials of substrates to proceed SET for the generation of radical intermediates (Figure 9b).[42]
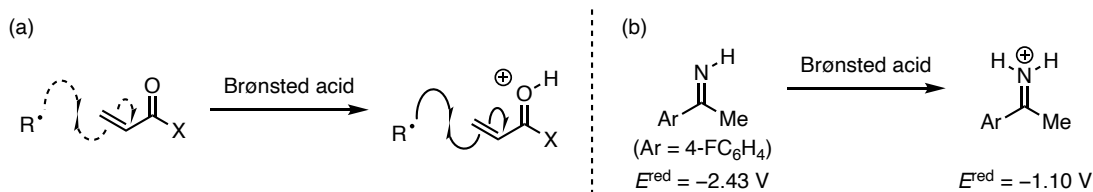
Figure 9. (a) Radical addition with olefins accelerated by Brønsted acid. (b) Reduction potential highly decreased by protonation.

1.5.2 Photoinduced allylic heteroarylation of enol silyl Ethers: Chapter 3

In section **1.4.3** and chapter **2**, the high acidity of radical cations derived from enol silyl ethers which was close to that of sulfonic acids was disclosed. Then, the author wondered if radical cation intermediates could be utilized as Brønsted acid catalyst to activate Brønsted basic substrates. Enormous trials of substrates revealed that cyanopyridine derivatives undergo coupling reaction with allylic radicals from enol silyl ethers promoted by the high acidity of radical cations (Figure 10).
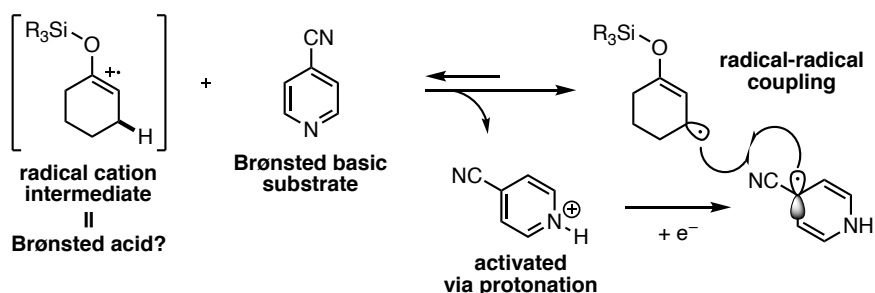
Figure 10. The reaction design of radical cations-initiated coupling reaction.

1.6.1 Mannich-type allylic C−H functionalization of enol silyl ethers under photoredox-thiol hybrid catalysis: Chapter 4

Having established reaction system of allylic functionalization of enol silyl ethers via single-electron oxidation-deprotonation sequence, the author next tried to extend it to aminoalkylation reaction with imines as radical acceptors.[43] However, the product inhibition of aniline derivatives generated after the coupling reactions seemed to be problematic under the use of highly oxidizing photoredox catalysis. As a solution of this problem, considering the lower BDE of allylic C−H bonds in enol silyl ethers (~80 kcal mol^{-1}), HAT catalysis with thiol[44] was selected to avoid the oxidation of products by using mildly oxidizing photoredox catalyst (Figure 11).
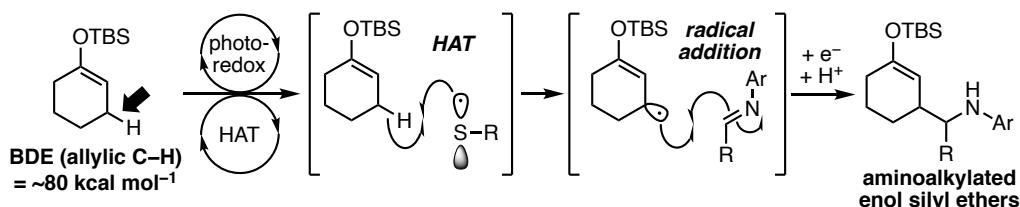
Figure 11. Allylic aminoalkylation under photoredox-thiol catalysis.

1.7 Conclusion

In this thesis, the direct allylic C−H functionalization of enol ethers with the preservation of enol ether moiety was achieved by the use of photoredox catalysis. The consideration of the property of radical cations and the appropriate selection of Brønsted base directed by the computational estimation of pK_a of radical cations generated from enol silyl ethers enabled efficient deprotonation to form nucleophilic allylic radicals and bond formation with electron-deficient olefins. The use of high acidity of radical cations derived from enol silyl ethers was utilized for the activation of Brønsted basic substrates such as cyanopyridines to give allylic heteroarylated products. In addition to single-electron oxidation-deprotonation process, HAT catalyst combined with mildly oxidizing Ir-complex could also generate allylic radicals enabling the reaction with imines to avoid product inhibitions by highly

oxidizing photocatalyst. In the whole reaction developed in this thesis, allylic-functionalized enol silyl ethers could be transformed to highly functionalized carbonyl compounds to demonstrate the availability of these transformations.

References

(1) (a) Taber, D. F.; Ruckle Jr., R. E. *J. Am. Chem. Soc.* **1986**, *108*, 7686. (b) Doyle, M. P.; Westrum, L. J.; Wolthuis, W. N. E.; See, M. M.; Boone, W. P.; Bagheri, V.; Pearson, M. M. *J. Am. Chem. Soc.* **1993**, *115*, 958. (c) Taber, D. F.; You, K. K.; Rheingold, A. L. *J. Am. Chem. Soc.* **1996**, *118*, 547.

(2) (a) Davies, H. M. L.; Hansen, T. *J. Am. Chem. Soc.* **1997**, *119*, 9075. (b) Davies, H. M. L.; Beckwith, R. E. J. *Chem. Rev.* **2003**, *103*, 2861. (c) Davies, H. M. L.; Manning, J. R. *Nature* **2008**, *451*, 417.

(3) (a) Dauban, P.; Dodd, R. *Synlett* **2003**, 1571. (b) Park, Y.; Kim, Y.; Chang, S. *Chem. Rev.* **2017**, *117*, 9247. (c) Hazelard, D.; Nocquet, P.-A.; Compain, P. *Org. Chem. Front.* **2017**, *4*, 2500.

(4) (a) Gunay, A.; Theopold, K. H. *Chem. Rev.* **2010,** *110,* 1060. (b) Chen, Z.; Yin, G. *Chem. Soc. Rev.* **2015**, *44*, 1083. (c) Nesterov, D. S.; Nesterova, O. V.; Pombeiro, A. J. L. *Coor. Chem. Rev.* **2018**, *355*, 199. (d) Larson, V. A.; Battistella, B.; Ray, K.; Lehnert, N.; Nam, W. *Nat. Rev. Chem.* **2020**, *4*, 404.

(5) (a) Chen, M. S.; White, M. C. *Science* **2007**, *318*, 783. (b) Gormisky, P. E.; White, M. C. *J. Am. Chem. Soc.* **2013**, *135*, 14052. (c) Howell, J. M.; Feng, K.; Clark, J. R.; Trzepkowski, L. J.; White, M. C. *J. Am. Chem. Soc.* **2015**, *137*, 14590.

(6) Desai, L. V.; Hull, K. L.; Sanford, M. S. *J. Am. Chem. Soc.* **2004**, *126*, 9542.

(7) Giri, R.; Chen, X.; Yu, J.-Q. *Angew. Chem. Int. Ed.* **2005**, *44*, 2112.

(8) Zaitsev, V. G.; Shabashov, D.; Daugulis, O. *J. Am. Chem. Soc.* **2005**, *127*, 13154.

(9) (a) Jazzar, R.; Hitce, J.; Renaudat, A.; Sofack-Kreutzer, J.; Baudoin, O. *Chem. Eur. J.* **2010**, *16*, 2654. (b) Baudoin, O. *Chem. Soc. Rev.* **2011**, *40*, 4902. (c) Saint-Denis, T. G.; Zhu, R.-Y.; Chen, G.; Wu, Q.-F.; Yu, J.-Q. *Science* **2018**, *359*, 759.

(10) Luo, Y.-R. *Handbook of Bond Dissociation Energies in Organic Compounds* CRC Press, Boca Raton, FL, **2003**.

(11) (a) Hoffmann, A. W. *Ber.* **1883**, *16*, 558. (b) Loffler, K.; Freytag, C. *Ber.* **1909**, *42*, 3427. (c) Wolff, M. E. *Chem. Rev.* **1963**, *63*, 55.

(12) (a) Martínez, C.; Muñiz, K. *Angew. Chem. Int. Ed.* **2015**, *54*, 8287. (b) Choi, G. J.; Zhu, Q.; Miller, D. C.; Knowles, R. R. *Nature* **2016**, *539*, 268. (c) Chu, J. C.; Rovis, T. *Nature* **2016**, *539*, 272. (d) Zhang, J.; Li, Y.; Zhang, F.; Hu, C.; Chen. Y. *Angew. Chem. Int. Ed.* **2016**, *55*, 1872.

(13) (a) Tzirakis, M. D.; Lykakis, I. N.; Orfanopoulos, M. *Chem. Soc. Rev.* **2009**, *38*, 2609. (b) Qvortrup, K.; Rankic, D. A.; MacMillan, D. W. C. *J. Am. Chem. Soc.* **2014**, *136*, 626. (c) Jeffrey, J. L.; Tarrett, J. A.; MacMillan, D. W. C. *Science* **2015**, *349*, 1532. (d) Mukherjee, S.; Maji, B.; Tlahuext-Aca, A.; Glorius, F. *J. Am. Chem. Soc.* **2016**, *138*, 16200.

(14) (a) Shaw, M. H.; Shurtleff, V. W.; Terrett, J. A.; Cuthbertson, J. D.; MacMillan, D. W. C. *Science* **2016**, *352*, 1304. (b) Le, C.; Liang, Y.; Evans, R. W.; Li, X.; MacMillan, D. W. C. *Nature* **2017**,

547, 79. (c) Kato, S.; Saga, Y.; Kojima, M.; Fuse, H.; Matsunaga, S.; Fukatsu, A.; Kondo, M.; Masaoka, S.; Kanai, M. *J. Am. Chem. Soc.* **2017**, *139*, 2204.

(15)(a) Shaw, M. H.; Twilton, J.; MacMillan, D. W. C. *J. Org. Chem.* **2016**, *81*, 6898. (b) Romero, N. A.; Nicewicz, D. A. *Chem. Rev.* **2016**, *116*, 10075. (c) McAtee, R. C.; McClain, E. J.; Stephenson, C. R. J. *Trends in Chemistry* **2019**, *1*, 111.

(16)Schmittel, M.; Burghart, A. *Angew. Chem. Int. Ed. Engl.* **1997**, *36*, 2550.

(17)Miyake, Y.; Nakajima, K.; Nishibayashi, Y. *J. Am. Chem. Soc.* **2012**, *134*, 3338.

(18)Beatty, J. W.; Stephenson, C. R. J. *Acc. Chem. Res.* **2015**, *48*, 1474.

(19)McManus, J. B.; Onuska, N. P. R.; Nicewicz, D. A. *J. Am. Chem. Soc.* **2018**, *140*, 9056.

(20)Zhou, R.; Liu, H.; Tao, H.; Yu, X.; Wu, J. *Chem. Sci.* **2017**, *8*, 4654.

(21)Ashley, M. A.; Rovis, T. *J. Am. Chem. Soc.* **2020**, *142*, 18310.

(22)(a) Gutekunst, W. R.; Baran, P. S. *Chem Soc. Rev.* **2011**, *40*, 1976. (b) Qiu, Y.; Gao, S. *Nat. Prod. Rep.* **2016**, *33*, 562. (c) Kawamata, T.; Nagatomo, M.; Inoue, M. *J. Am. Chem. Soc.* **2017**, *139*, 1814. (d) White, M. C.; Zhao, J. *J. Am. Chem. Soc.* **2018**, *140*, 13988. (e) Abrams, D. J.; Provencher, P. A.; Sorensen, E. J. *Chem. Soc. Rev.* **2018**, *47*, 8925. (f) Zhao, J.; Nanjo, T.; de Lucca Jr., E. C.; White, M. C. *Nat. Chem.* **2019**, *11*, 213. (g) Shang, M.; Feu, K. S.; Vantourout, J. C.; Barton, L. M.; Osswald, H. L.; Kato, N.; Gagaring, K.; McNamara, C. W.; Chen, G.; Hu, L.; Ni, S.; Fernández-Canelas, P.; Chen, M.; Merchantm R. R.; Qin, T.; Schreiber, S.; Melillo, B.; Yu, J.-Q.; Baran, P. S. *PNAS* **2019**, *116*, 8721. (h) Feng, K.; Quevedo, R. E.; Kohrt, J. T.; Oderinde, M. S.; Reilly, U.; White, M. C. *Nature* **2020**, *580*, 621.

(23)(a) Johannsen, M.; Jørgensen, K. A. *Chem. Rev.* **1998**, *98* 1689. (b) Howell, J. M.; Liu, W.; Young, A. J.; White, M. C. *J. Am. Chem. Soc.* **2014**, *136*, 5750. (c) Liu, W.; Ali, S.; Ammann, S.; White, M. C. *J. Am. Chem. Soc.* **2018**, *140*, 10658. (d) Liron, F.; Oble, J.; Lorion M. M.; Poli, G. *Eur. J. Org. Chem.* **2014**, *5863*. (e) Bayeh, L.; Le, P. Q.; Tambar, U. K. *Nature* **2017**, *546*, 196. (f) Fernandes, R. A.; Nallasivam, J. L. *Org. Biomol. Chem.* **2019**, *17*, 8647. (g) Huang, H.-M.; Bellotti, P.; Glorius, F. *Chem. Soc. Rev.* **2020**, *49*, 6186. (h) Tanabe, S.; Mitsunuma, H.; Kanai, M. *J. Am. Chem. Soc.* **2020**, *142*, 12374. (i) Kazarouni, A. M.; McKoy, Q. A.; Blakey, S. B. *Chem. Commun.* **2020**, *56*, 13287.

(24)(a) Stork, G.; Hudrlik, P. F. *J. Am. Chem. Soc.* **1968**, *90*, 4462. (b) Kan, S. B. J.; Ng, K. K. H.; Paterson, I. *Angew. Chem. Int. Ed.* **2013**, *52*, 9097. (c) Matsuo, J.; Murakami, M. *Angew. Chem. Int. Ed.* **2013**, *52*, 9109.

(25)Davies, H. M. L.; Ren, P. *J. Am. Chem. Soc.* **2001**, *123*, 2070.

(26)Cuthbertson, J. D.; MacMillan, D. W. C. *Nature* **2015**, *519*, 74.

(27)Xie, W.; Kim, D.; Chang, S. *J. Am. Chem. Soc.* **2020**, *142*, 20588.

(28)Gassman, P. G.; Bottorff, K. J. *J. Org. Chem.* **1988**, *53*, 1097.

(29) Bhattacharya, A.; DiMichele, L. M.; Dolling, U.-H.; Grabowski, E. J. J.; Grenda, V. J. *J. Org. Chem.* **1989**, *54*, 6118.

(30) Bockman, T. M.; Shukla, D.; Kochi, J. K. *J. Chern. Soc. Perkin Trans.* **1996**, *2*, 1623.

(31) Rathore, R.; Kochi, J. K. *J. Org. Chem.* **1996**, *61*, 627.

(32) Snider, B. B.; Kwon, T. *J. Org. Chem.* **1992**, *57*, 2399.

(33) Ramsden, C. A.; Smith, R. G. *Org. Lett.* **1999**, *1*, 1591.

(34) Hudson, C. M.; Marzabadi, M. R.; Moeller, K. D. *J. Am. Chem. Soc.* **1991**, *113*, 7372.

(35) Heidbreder, A.; Mattay, J. *Tetrahedron Lett.* **1992**, *33*, 1973.

(36) Hintz, S.; Mattay, J.; van Eldik, R.; Fu, W.-F. *Eur. J. Org. Chem.* **1998**, *1998*, 1583.

(37) Wright, D. L.; Whitehead, C. R.; Sessions, E. H.; Ghiviriga, I.; Frey, D. A. *Org. Lett.* **1999**, *1*, 1535.

(38) Ackermann, L.; Heidbreder, A.; Wurche, F.; Klärner, F.-G.; Matty, J. *J. Chern. Soc. Perkin Trans.* **1999**, *2*, 863.

(39) Bunte, J. O.; Rinne, S.; Schäfer, C.; Neumann, B.; Stammler, H.-G.; Matty, J. *Tetrahedron Lett.* **2003**, *44*, 45.

(40) (a) Proctor, R. S.; Colgan, A. C.; Phipps, R. J. *Nat. Chem.* **2020**, *12*, 990. (b) Yin, Y.; Zhao, X.; Qiao, B.; Jiang, Z. *Org. Biomol. Chem.* **2020**, *7*, 1283.

(41) (a) Espelt, L. R.; Wiensch, E. M.; Yoon, T. P. *J. Org. Chem.* **2013**, *78*, 4107. (b) Uraguchi, D.; Kinoshita, N.; Kizu, T.; Ooi, T. *J. Am. Chem. Soc.* **2015**, *137*, 13768. (c) Hepburn, H. B.; Melchiorre, P. *Chem. Sci.* **2016**, *52*, 3520. (d) Pitzer, L.; Sandfort, F.; Strieth-Kalthoff, F.; Glorius, F. *J. Am. Chem. Soc.* **2017**, *139*, 13652.

(42) (a) Nakajima, M.; Fava, E.; Loescher, S.; Jiang, Z.; Rueping, M. *Angew. Chem. Int. Ed.* **2015**, *54*, 8828. (b) Miller, D. C.; Tarantino, K. T.; Knowles, R. R. *Top. Curr. Chem.* **2016**, *374*, 30. (c) Leitch, J. A.; Rossolini, T.; Rogova, T.; Maitland, J. A. P.; Dixon, D. J. *ACS Catal.* **2020**, *10*, 2009.

(43) (a) Jeffrey, J.; Petronijević, E. R.; MacMillan, D. W. C. *J. Am. Chem. Soc.* **2015**, *137*, 8404. (b) Lee, K. N.; Ngai, M.-Y. *Chem. Commun.* **2017**, *53*, 13093. (c) Pantaine, L. R. E.; Milligan, J. A.; Matsui, J. K.; Kelly, C. B.; Molander, G. A. *Org. Lett.* **2019**, *21*, 2317. (d) Garrido-Castro, A. F.; Maestro, M. C.; Alemán, J. *Catalysts* **2020**, *10*, 562.

(44) (a) Hager, D.; MacMillan, D. W. C. *J. Am. Chem. Soc.* **2014**, *136*, 16986. (b) Jia, J.; Kancherla, R.; Rueping, M.; Huang, L. *Chem. Sci.* **2020**, *11*, 4954.

Chapter 2

Direct Allylic C−H Alkylation of Enol Silyl Ethers Enabled by Photoredox-Brønsted Base Hybrid Catalysis
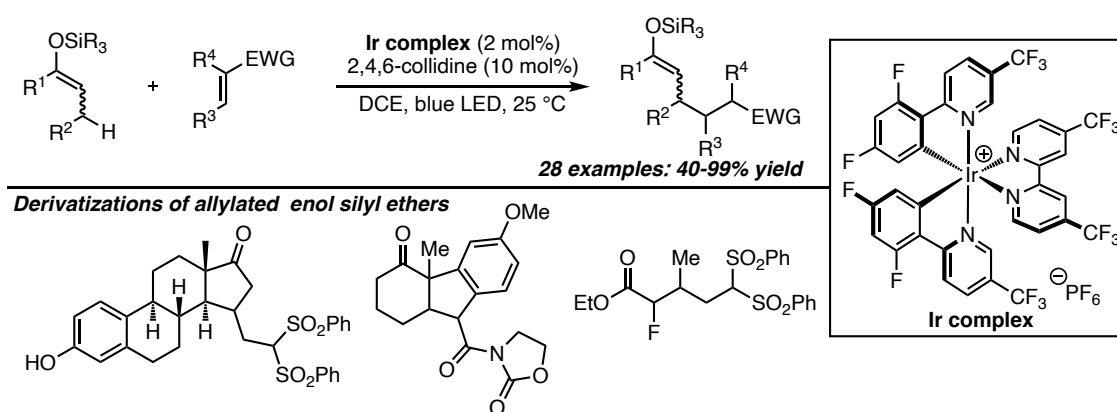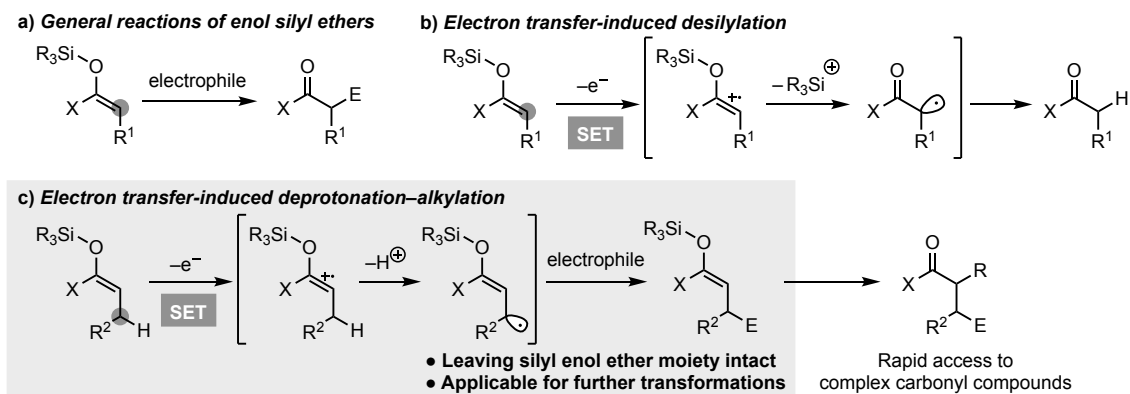

Abstract:

Strategies for altering the reaction pathway of reactive intermediates are of significant importance in diversifying organic synthesis. Enol silyl ethers, versatile enolate equivalents, are known to undergo one-electron oxidation to generate the radical cations that spontaneously form electrophilic α-carbonyl radicals via elimination of the silyl group. Here, the author demonstrate that close scrutiny of the property of the radical cations as strong C−H acids enables the identification of a catalyst system consisting of an iridium-based photosensitizer and 2,4,6-collidine for the generation of nucleophilic allylic radicals from enol silyl ethers through one-electron oxidation-deprotonation sequence under light irradiation without the desilylation of the radical cation intermediates. The resultant allylic radicals engage in the addition to electron-deficient olefins, establishing the selective allylic C−H alkylation of enol silyl ethers. The strategy is broadly applicable, and the alkylated enol silyl ethers can be transformed into highly functionalized carbonyl compound by exploiting their common polar reactivity.

1. Introduction

Enol silyl ethers and their analogs are one of the most versatile substrate classes and enjoy widespread applications in organic synthesis (Fig. 1a).[1-3] They can be prepared from carbonyl compounds of all oxidation states, such as aldehydes, ketones, esters and amide, by reliable protocols and exhibit preeminent reactivity as enolate anion equivalents amenable to various catalysis manifolds. These distinct features render enol silyl ethers attractive yet powerful handles for selective α-functionalization of a wide array of carbonyl entities.

On the other hand, the allylic sp^3-hybridized carbons of the enol silyl ethers are potential reaction sites as the electron-rich enol moiety contributes to decreasing bond-dissociation enthalpy of the allylic C−H bonds. In particular, selective bond formation at the allylic carbons[4] with preservation of the enol silyl ether component offers an opportunity to harness the reactivity of the resulting functionalized enol silyl ethers for the conventional polar reactions, enabling access to α,β-difunctionalized carbonyl compounds.[5-7] However, despite their potential synthetic utility, only a few catalytic systems are available for direct allylic C−H functionalization of enol silyl ethers or their analogs, which rely on transition metal catalysis and synergistic photoredox-thiol catalysis.[8,9]

In addition to the common polar reactivity useful for a diverse set of transformations, it has long been recognized that enol silyl ethers undergo single-electron oxidation to generate the corresponding radical cations.[10] Yet, previous efforts for exploiting this radical reactivity in reaction development have been restricted to coupling with concomitantly generated heteroatom radicals[11-15] or tethered olefins at the α-carbon of the carbonyl group; this is largely due to the strong property of the radical cation to undergo elimination of a silyl cation to produce parent carbonyls (Fig. 1b).[10.16-22] Under these circumstanced, the author considered the intrinsic properties of this class of radical cations, specially the presumed high acidity of allylic protons.[23-27] For instance, MacMillan[28-31] reported that radical cations generated from aldehyde- or cyclic ketone-derived enamines underwent deprotonation to form allylic radicals that were susceptible to radical addition reactions for β-functionalizations of the parent carbonyls. With this profile in mind, the author envisioned that the allylic proton of the radical cation derived from an enol silyl ether could be readily deprotonated to generate an allylic radical nucleophilic enough to be captured by an external electrophile (Fig. 1c). If the employment of an appropriate Brønsted base allows this proton abstraction event to occur predominantly over the desilylation, the single-electron oxidation-deprotonation sequence would provide a broadly applicable platform to execute bond construction exclusively at the allylic carbon, leaving the enol silyl ether component intact for further synthetic manipulations. Here, the author disclose the successful implementation of this strategy through the development of a direct allylic C−H functionalization of a variety of enol silyl ethers with electron-deficient olefins under hybrid catalysis of an iridum-based photosensitizer and pyridine derivative with the irradiation of visible light. The utility of this unique C−H alkylation protocol is also demonstrated.

21

a) *General reactions of enol silyl ethers*

b) *Electron transfer-induced desilylation*

c) *Electron transfer-induced deprotonation–alkylation*

- Leaving silyl enol ether moiety intact
- Applicable for further transformations

Rapid access to complex carbonyl compounds

Fig. 1 Transformations of enol silyl ethers. **A** General reaction pathway. **B** Known desilylation reaction initiated by single-electron oxidation. **C** The reaction design of allylic C−H alkylation

2. Results

2.1 Analysis of the Property of Enol Silyl Ether and Its Radical Cation.

The author selected the cyclohexanone-derived enol silyl ether **1a** as a model substrate and investigated the physical properties requisite to establish a catalytic system for effecting the target allylic functionalization. First, the oxidation potential (E_{ox}) of **1a** was determined to be 1.52 V vs. saturated calomel electrode (SCE) by square wave voltammetry measurement in MeCN, which led us to use a Ir^{III} photocatalyst bearing ligands suitable for imparting sufficient single-electron oxidation ability to the visible light-excited $*Ir^{III}$ to generate a radical cation from **1a**. Second, the pK_a value of the resulting radical cation $[1a]^{\bullet+}$ in MeCN was estimated from the calculated reaction free energy (ΔG) of deprotonation process. Since the direct determination of pK_a from the calculated free energy is liable to give deviated value, the author conducted statistical manipulation using experimentally available values. Specifically, the pK_a of $[1a]^{\bullet+}$ was obtained by considering acid-base equilibria with a series of substituted anilines (Fig. 2), whose pK_a values were experimentally determined (5-12 in MeCN).[32] As shown in Fig. 2, the values for the reaction free energy calculated at the SMD(MeCN)-(U)CAM-B3LYP/6-311+G(d, p) level and the experimental pK_a values of anilines showed excellent linear correlation. The intercept of this plot corresponded to the pK_a of $[1a]^{\bullet+}$ and was determined to be 8.4, which is close to that of TsOH [pK_a(MeCN) = 8.6],[33] meaning that $[1a]^{\bullet+}$ can be readily deprotonated by an appropriate Brønsted base. In view of structural tunability, the author sought to employ an organic base with recognition that essential requirements for ensuring the function of the base are not only the pK_a value but also the redox potential not to be involved in the single-electron redox processes operated by the photocatalyst.
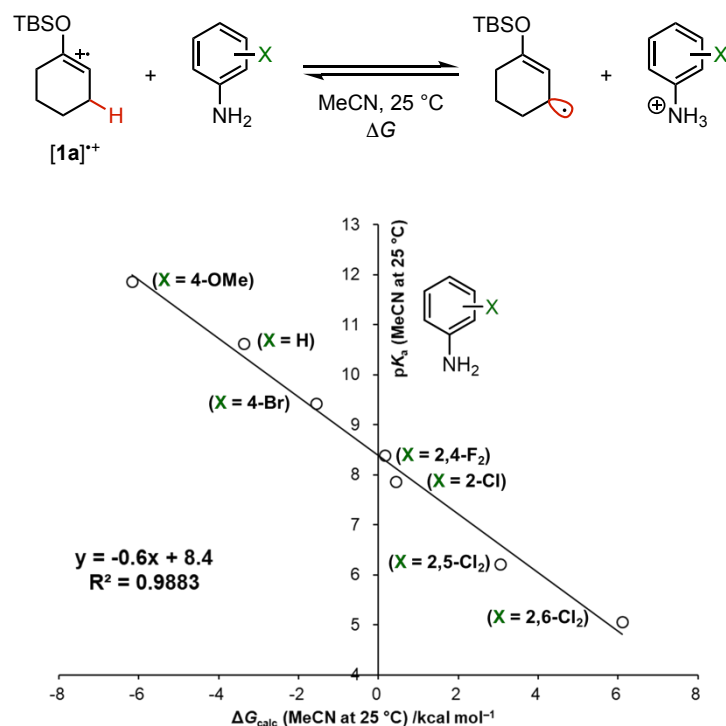
Fig. 2 Estimation of pK_a of radical cation [**1a**]$^{•+}$. **a** Acid-base equilibria between [**1a**]$^{•+}$ and substituted anilines. **b** Linear free energy plot for the acid-base equilibria

2.2 Design of Catalysis and Optimization of Reaction Conditions.

Based on these initial results and considerations, the author began to evaluate the viability of his strategy in the reaction of **1a** with banzalmalononitrile (**2a**) as an acceptor in the presence of [Ir(dF(CF$_3$)ppy)$_2$(4,4'-dCF$_3$bpy)]PF$_6$ (**4a**, 2 mol%) (*$E_{1/2}^{red}$ = 1.65 V vs. SCE)[34] and 2,4,6-collidine (1 equiv) (pK_a = 14.98 in MeCN, $E_{1/2}^{ox}$ = ≥2.0 V vs. SCE)[32] in MeCN at ambient temperature. Under the irradiation of a blue ligh-emitting diode (LED), bond formation occurred at the allylic carbon (β-position to the latent carbonyl) to give the alkylated enol silyl ether **3a** in 78% nuclear magnetic resonance (NMR) yield (Table 1, entry 1). The nature of the Brønsted base was of critical importance as the use of the sterically demanding 2,6-di-tert-butyl-4-methylpyridine (DTBMP) substantially decreased the yield of **3a** and inorganic bases, such as potassium phosphate, were totally ineffective (entries 2 and 3). Furthermore, attempted alkylations with Ir^{III} complexes **4b** or **4c**, having different bipyridine ligand, resulted in low conversion or no reaction, respectively, indicating that the reduction potential of the Ir^{III} complex in the excited state as well as the oxidation potential of the transient Ir^{II} complex have a significant impact on reaction efficiency (enries 4 and 5). Interestingly, solvent screening revealed that 1,2-dichloroethane (DCE) was optimal, allowing the reaction to proceed with higher efficiency under the influence of **4a** and 2,4,6-collidine to afford **3a** in 89% yield (entry 6). Although the catalytic use of the Brønsted base (10 mol%) appeared feasible, slight decrease in the

Table 1. Optimization of conditions for reaction of enol silyl ether **1a** with banzalmalononitrile (**2a**)

TBSO
+ NC CN / Ph →
4 (2 mol%), base, MeCN, blue LED, 25 °C →
TBSO ... CN CN Ph

1a   **2a**   **3a**

4a (R^1 = H, R^2 = CF_3)
$E_{1/2}^{*III/II}$ = 1.65 V; $E_{1/2}^{III/II}$ = -0.79 V

4b (R^1 = F, R^2 = H)
$E_{1/2}^{*III/II}$ = 1.61 V; $E_{1/2}^{III/II}$ = -1.16 V

4c (R^1 = H, R^2 = t-Bu)
$E_{1/2}^{*III/II}$ = 1.21 V; $E_{1/2}^{III/II}$ = -1.37 V

Entry	4	Base (mol%)	d.r.[a]	Yield (%)[b]
1	4a	2,4,6-collidine (100)	1.7:1	78
2	4a	DTBMP (100)	1.7:1	27
3	4a	K_3PO_4 (100)	-	0
4	4b	2,4,6-collidine (100)	1.7:1	14
5	4c	2,4,6-collidine (100)	-	0
6[c]	4a	2,4,6-collidine (100)	2.0:1	89
7[c]	4a	2,4,6-collidine (10)	1.9:1	78
8[d]	4a	2,4,6-collidine (10)	2.0:1	95 (98)
9[e]	4a	2,4,6-collidine (10)	1.8:1	(96)

Unless otherwise noted, the reactions were performed with **1a** (0.1 mmol), **2a** (1.2 equiv), base and **4** (2 mol%) in MeCN (1.0 mL) at 25 °C for 12 h under argon atmosphere with light irradiation (blue LED, 750 W m⁻²). *¹H NMR* proton nuclear magnetic resonance, *d.r.* diastereomeric ratios, *LED* light-emitting diode, *DTBMP* 2,6-di-*tert*-butyl-4-methylpyridine, *TBS* t-butyldimethylsilyl, *DCE* 1,2-dichloroethane. [a]Determined by ¹H NMR from crude reaction mixture. [b]NMR yield with mesitylene as an internal standard. The value within parentheses id an isolated yield. [c]The reaction was conducted in DCE (1.0 mL). [d]In DCE (0.5 mL). [e]Carried out with **1a** (2.0 mmol, 0.42 g), **2a** (1.1 equiv), 2,4,6-collidine (10 mol%) and **4a** (0.5 mol%) in DCE (10 mL) at 25 °C for 18 h under argon atmosphere with light irradiation (blue LEDs, total 5000 W m⁻²).

product yield was inevitable because of undesired desilylated ketone formation (entry 7). This problem was overcome by performing the reaction at higher substrate and catalyst concentration; desilylation was completely suppressed and **3a** was isolated almost quantitatively (entry 8). The direct allylic C−H alkylation protocol thus developed was scalable as demonstrated by the reaction of 0.42 g of **1a** with

2a, which proceeded smoothly with a reduced amount of **4a** (0.5 mol%) but with increased light intensity under otherwise identical conditions to yield 0.71 g of **3a** (96%) (entry 9).

To gain an insight into the reaction mechanism, especially the pathway for the generation of the reactive intermediate, Steern-Volmer luminescence quenching experiments were performed. Banzalmalononitrile (**2a**) and 2,4,6-collidine did not quench the excited state of photocatalyst **4a** (Supplementary Fig. 3). In contrast, increasing the concentration of enol silyl ether **1a** caused a significant decrease in emission intensity. These observations confirmed that the allylic C−H alkylation was initiated by the single-electron oxidation of **1a**.

2.3 Investigation of Substrate Scope.

Having established the optimized reaction conditions, the author explored the scope of this alkylation under photoredox-Brønsted case hybrid catalysis (Fig. 3). As demonstrated in the reactions of **1a**, a range of arylidene malononitriles were employable as electrophilic acceptors and the corresponding alkylated enol silyl ethers **3b-3e** were obtained in uniformly good yield. Alkylidene malononitrile could also be coupled with **1a** to form **3f** with moderate efficiency. Furthermore, α,β-unsaturated ketones and sulfones proved viable acceptors to furnish **3g-3j** in moderate to good yield. With respect to enol silyl ether nucleophiles, it is important to note that trimethylsilyl and triethylsilyl derivatives underwent deprotonation-allylic alkylation to afford **3k** and **3l** in high yield, clearly indicating that the selectivity of deprotonation over desilylation does not rely on the steric demand of the silyl groups. In addition to the cyclohexanone derivatives, seven- and eight-membered cyclic enol silyl ethers smoothly reacted with 1,1-bis(phenylsulfonyl)ethylene to give good yields of **3m** and **3n**. The acyclic enol silyl ethers were also found to be suitable substrates; *primary*-alkyl ketone- and mesityl ketone-derived enol silyl ethers gave rise to the desired products **3o-3r** in excellent yield, whereas the phenyl ketone-derived substrate provided **3s** in lower yield (see below for theoretical investigations and associated discussion). Relatively low reactivity was also observed in the reaction of the α-tetralone derivative, resulting in the formation of **3t** in 57% yield. Notably, butyryl pyrazole-derived ketene silyl hemiaminal was amenable to alkylation and afforded **3u** in high yield. Enol silyl ethers with additional common functional groups, such as chlorine, ether, ester, imide and nitrile, were compatible with this protocol and could be converted into the corresponding alkylated enol silyl ethers **3v-3z** with equally high efficiency. When the ethyl *t*-butyl ketone-derived enol silyl ether was subjected to the optimized conditions, the C−C bond formation occurred at the terminal, *primary* allylic carbon to yield **3Aa**. On the other hand, 2-methylcyclohexanone-derived enol silyl ether was alkylated predominantly on the *secondary* allylic carbon to give **3Ab**. An additional noteworthy aspect of this hybrid catalytic system was that it accommodated complex substrate setting; the allylic alkylation of the estrone derivative featuring a fused polycyclic framework delivered the enol silyl ether **3Ac** in excellent yield.
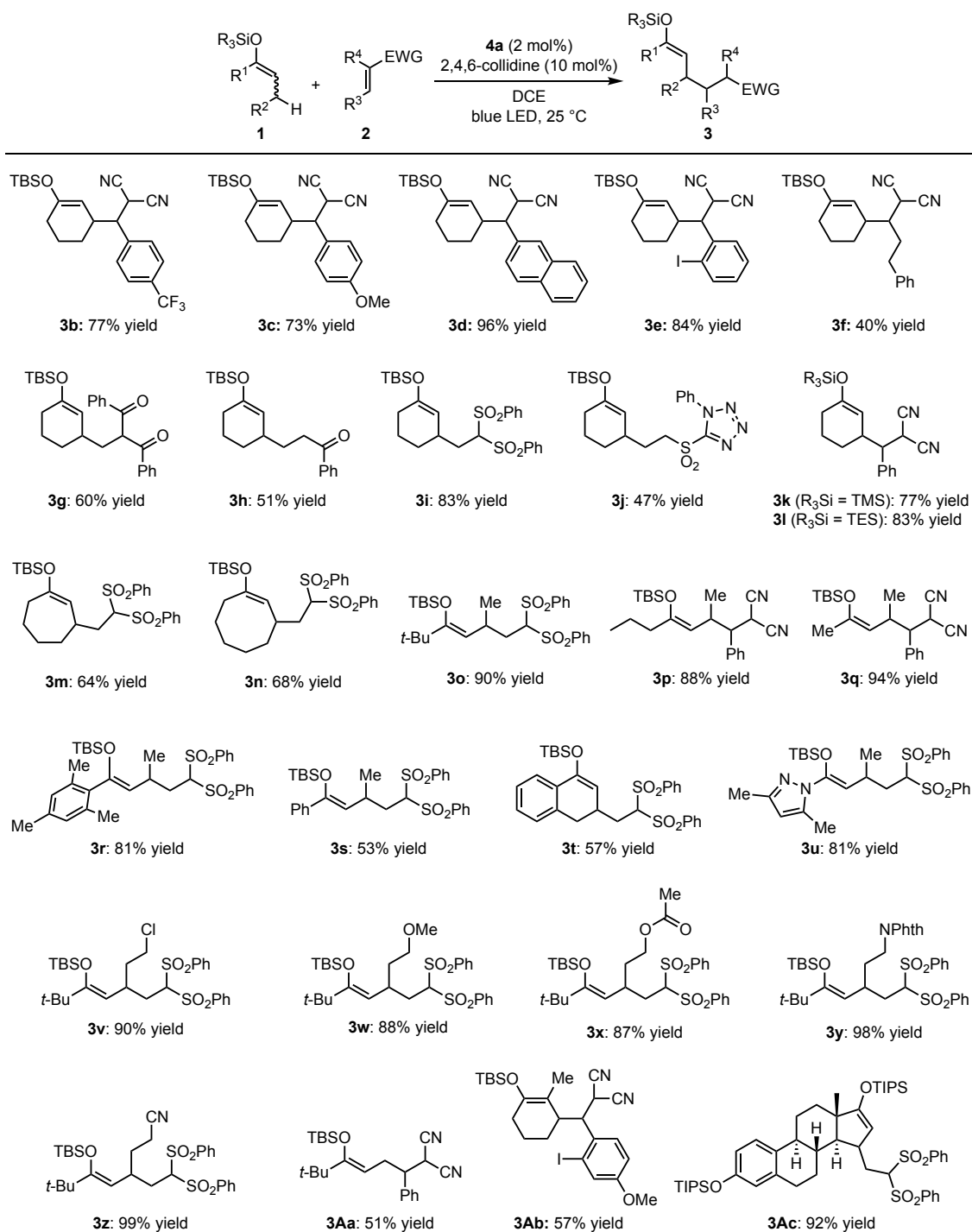
Fig. 3 Substrate scope. Isolated yields are shown. Diastereomeric ratios (d.r.) of the products with consecutive two stereocenters were 1.5:1-2.0:1. See the Supplementary Information for details.

26

3. Analysis to rationalize the reactivity difference.

The reactivity profile of the enol silyl ethers, particularly that observed with **1o** (R^1 = *t*-Bu), **1r** (R^1 = 2,4,6-Me$_3$C$_6$H$_2$) and **1s** (R^1 = Ph), prompted him to conduct density functional theory calculations at the CAM-B3LYP/6-311+G(d, p) level for these substrates in order to rationalize the differences in reactivity (Table 2). The pK_a values of the corresponding radical cations in MeCN were calculated to

Table 2. Summary of spin density and SOMO level of the radical **[1]**˙ and activation barrier of their addition to 1,1-bis(phenylsulfonyl)ethylene

[1o]˙ (R^1 = *t*-Bu)
[1r]˙ (R^1 = 2,4,6-Me$_3$C$_6$H$_2$)
[1s]˙ (R^1 = Ph)
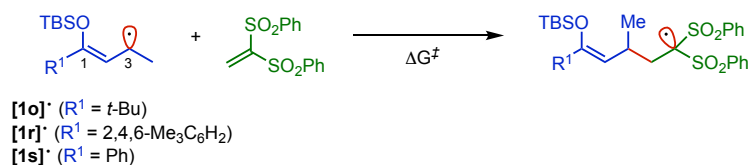
| **[1]**˙	**Spin density**		**SOMO**[a] (eV)	**ΔG**$^{\neq}$[b] (kcal mol^{-1})	**Yield (%) of the reaction**
	C1	**C3**			
[1o]˙	0.75	0.70	−5.77	21.2	90
[1r]˙	0.62	0.64	−5.77	21.6	81
[1s]˙	0.58	0.51	−5.77	23.3	53

SOMO singly occupied molecular orbital [a] Calculated at (U)CAM-B3LYP/6-311 + G(d, p) [b] Values for Gibbs free energy (298.15 K and 1 atm) were calculated at SMD(DCE)-(U)CAM-B3LYP/6-311 + G(d, p).

be 8.4 (**1o**), 6.5 (**1r**) and 4.8 (**1s**), respectively (Supplementary Figs. 6-11). These values suggested that the deprotonation process to generate an allylic radical would be much easier for the **1s**-derived radical cation ([**1s**]˙$^+$) than for the others, albeit the reaction of **1s** provided the lowest yield (**3s**, 53%), indicating that acidity of the radical cation was not the sole factor governing the present radical addition reaction. The author then calculated the singly occupied molecular orbital (SOMO) levels and spin density of **1o**-, **1r**- and **1s**-derived allylic radicals as well as the activation barrier of their additions to 1,1-bis(phenylsulfonyl)ethylene ($\Delta G^{\neq}$), respectively, and the results are summarized in Table 2. According to the frontier orbital theory, the reactivity of a radical generally depends on both the SOMO level and spin density at the reactive site. Considering almost the same SOMO level (=−5.77 eV), the reactivity difference between the three allylic radicals, [**1o**]˙, [**1r**]˙ and [**1s**]˙, would stem from differences on the spin density at the allylic C3 position. For [**1o**]˙, from which the reaction proceeded with the lowest $\Delta G^{\neq}$ of 21.2 kcal mol^{-1} to afford high yield of the product **3o** (90%), a relatively large spin density (=0.70) was located at the allylic position. Although the large spin density was estimated to be at the C1 position (=0.75), alkylation at this carbon would be highly unfavorable due to steric congestion, and in fact, the corresponding product was not detected experimentally. In

27

contrast, the electron in the radical [**1s**]$^{\cdot}$ can be delocalized over the phenyl group, decreasing the spin density at the C3 position (=0.51) compared to that of [**1o**]$^{\cdot}$. The difference in spin density was clearly reflected in the larger activation barrier ($\Delta G^{\neq} = 23.3$ kcal mol^{-1}) and lower experimental yield of the product **3s** (53%). The importance of spin localization for ensuring productive bond formation was also corroborated by the similar analysis of with **1r** in comparison to the outcome with **1s**. Radical conjugation with the mesityl group is partially inhibited in [**1r**]$^{\cdot}$ because of the torsional relationship between the allyl and mesityl moieties (Supplementary Fig. 12); this leads to a higher spin density (=0.64) at the C3 position and lower activation barrier ($\Delta G^{\neq} = 21.6$ kcal mol^{-1}), thereby accounting for the experimentally observed higher efficiency in the formation of the product **3r** (81% yield).

4. Transformation of Alkylated Enol Silyl Ethers.

The alkylation products have two different reactive sites, the enol silyl ether and active methane or methylene. This salient structural feature enables diverse transformations to access a variety of complex carbonyl compounds, providing a powerful demonstration of the utility of this method (Fig. 4). For instance, treatment of the alkylated enol silyl ether **3i** with Selectfluor facilitated smooth
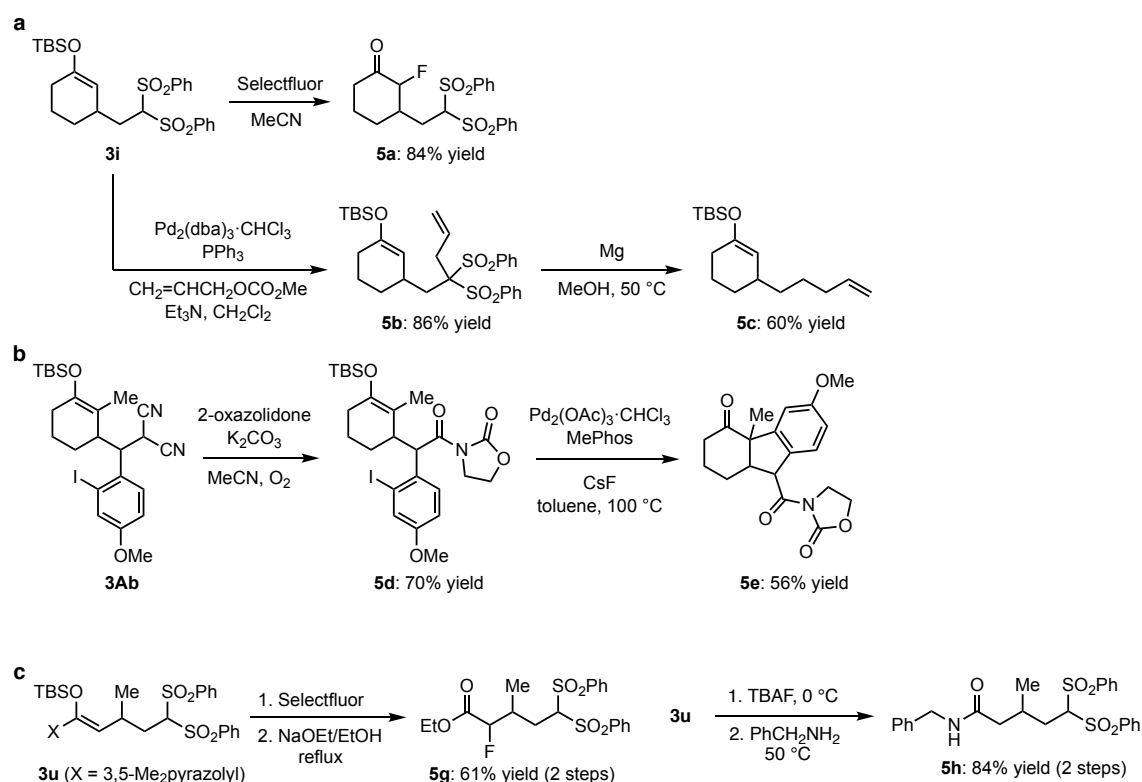
Fig. 4 Diverse transformations of alkylated products. **a** Derivatizations of alkylated enol silyl ether **3i**. **b** Synthesis of complex fused tricyclic ketone **5e** from alkylated enol silyl ether **3Ab**. **c** Derivatizations of alkylated ketene silyl hemiaminal **3u**

fluorination of the enol silyl ether component to produce the α-fluoro-β-alkylated ketone **5a**. On the other hand, selective functionalization of the bis(sulfonyl)methyl moiety of **3i** was feasible by the palladium-catalyzed allylation with allyl carbonate, affording **5b** in high yield. Subsequent exposure of **5b** to magnesium metal in MeOH effected desulfonylation to give **5c**. The malononitrile subunit of the enol silyl ether **3Ab** could be selectively converted into imide by reaction with 2-oxazolidoneunder oxygen atmosphere.[35] The resulting **5d** underwent intramolecular arylation under palladium catalysis to furnish the fused tricyclic ketone **5e**, of which structure is often found in diterpenoids, such as taiwaniaquinol A.[36] Moreover, functionalized esters and amides, such as **5f** and **5g**, were accessible through the common derivatizations of pyrazole-substituted ketene silyl hemiaminal **3u**; the reaction with Selectfluor followed by solvolysis in ethanol gave rise to α-fluoro-β-alkylated ester **5f**, while desilyltion and subsequent condensation with benzylamine proceeded with high efficiency to yield **5g**.

5. Conclusions

The author has developed a strategy for the allylic C–H alkylation of enol silyl ethers and their derivatives, which relies heavily on the combined use of appropriate photoredox and Brønsted base catalysts for the generation of requisite allylic radicals while suppressing undesired desilylation process. Under the hybrid catalysis, a series of enol silyl ethers smoothly react with electron-deficient olefins to give the corresponding functionalized enol silyl ethers. This operationally simple protocol, in concert with the ready availability of enol silyl ethers and their conventional polar reactivity, provides rapid and reliable access to an array of complex carbonyl compounds and will find widespread use among practitioners of organic synthesis.

6. Experimental Section

General Information: ^{1}H NMR spectra were recorded on a JEOL JNM-ECS400 (400 MHz) and JEOL JNM-ECA600II (600 MHz) spectrometer. Chemical shifts are reported in ppm from the tetramethylsilane (0.0 ppm) resonance as the internal standard (CDCl$_3$). Data are reported as follows: chemical shift, integration, multiplicity (s = singlet, d = doublet, t = triplet, q = quartet, quin = quintet, sext = sextet, sept = septet, m = multiplet, and br = broad) and coupling constants (Hz). ^{13}C NMR spectra were recorded on a JEOL JNM-ECA600II (151 MHz) spectrometer with complete proton decoupling. Chemical Shifts are reported in ppm from the solvent resonance as the internal standard (CDCl$_3$; 77.16 ppm). The high-resolution mass spectra were conducted on Thermo Fisher Scientific Exactive Plus (ESI). Analytical thin layer chromatography (TLC) was performed on Merck precoated TCL plates (silica gel 60 GF254, 0.25 mm). Flash column chromatography was performed on Silica gel 60 N (spherical, neutral, 40~50 μm; Kanto Chemical Co., Inc.).

All air- and moisture-sensitive reactions were performed under an atmosphere of argon (Ar) in dried glassware. Dichloromethane (CH$_2$Cl$_2$), 1,2-dichloroethane (DCE), diethyl ether (Et$_2$O), and tetrahydrofurane (THF) were supplied from Kanto Chemical Co., Inc. as "Dehydrated" and further purified by both A2 alumina and Q5 reactant using a GlassContour solvent dispensing system. The photocatalysts (**4a-4c**) and enol silyl ethers were synthesized according to the previously reported procedures.[34,37-39] Other simple chemicals were purchased and used as such.

Synthesis of Ketones
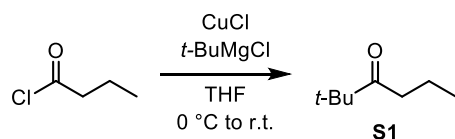
To a solution of butyryl chloride (3.1 mL, 30 mmol) and CuCl (0.15 g, 1.5 mmol) in THF (60 mL, 0.5 M), a 1 M THF solution of *t*-BuMgCl (31 mL, 31 mmol) was added dropwise via syringe under Ar atmosphere. The resulting mixture was allowed to warm to room temperature and stirred overnight. The reaction was then quenched by the addition of water at 0 °C and the aqueous phase was extracted with Et$_2$O twice. The combined organic phases were washed with 1 N aqueous solution of HCl three times, dried over Na$_2$SO$_4$, filtered, and concentrated. The residue was purified by distillation to afford **S1** in 57% yield (2.2 g, 17 mmol). ^{1}H NMR (400 MHz, CDCl$_3$) δ 2.46 (2H, t, J = 6.8 Hz), 1.63-1.54 (2H, m), 1.13 (9H, s), 0.90 (3H, t, J = 7.2 Hz).
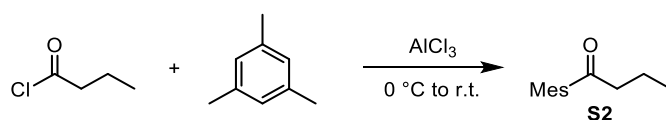
To a round-bottom flask was charged with mesitylene (8.4 mL, 60 mmol) and the reaction flask was cooled to 0 °C. Anhydrous AlCl$_3$ (0.67 g, 5 mmol) was added one-portion and the mixture was stirred at the same temperature for several minutes. To this mixture was added butyryl chloride (2.1 mL, 20 mmol) dropwise over 1 h at 0 °C. The whole reaction mixture was then allowed to warm to room temperature and stirred for 6 h. The reaction was quenched by the addition of water and the extractive work-up was conducted with Et$_2$O. The combined organic layers were washed with saturated aqueous solution of NaHCO$_3$, dried over Na$_2$SO$_4$, filtered, and concentrated. The resulting crude material was purified by column chromatography on silica gel (hexane 100% to hexane/EtOAc = 5:1 as eluent) to afford **S2** in 99% yield (3.7 g, 19.4 mmol). ^{1}H NMR (400 MHz, CDCl$_3$) δ 6.83 (2H, s), 2.67 (2H, t, J = 7.6 Hz), 2.27 (3H, s), 2.19 (6H, s), 1.73 (2H, sext, J = 7.6 Hz), 1.00 (3H, t, J = 7.6 Hz).
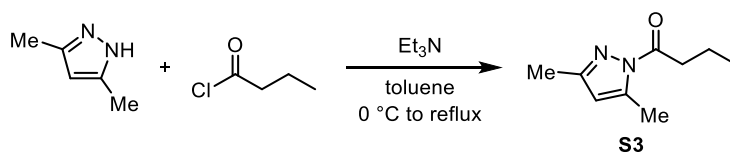

To a two-necked round-bottom flask was added 3,5-dimethylpyrazole (0.96 g, 10 mmol), butyryl chloride (1.2 mL, 11 mmol), toluene (50 mL, 0.2 M) and the flask was degassed by alternating vacuum evacuation/Ar backfill. The mixture was cooled to 0 °C, and Et$_3$N (2.8 mL, 20 mmol) was added. The whole mixture was then heated to reflux. After stirring for 1 h, the reaction mixture was cooled to room temperature and filtered through a pad of Celite with the aid of EtOAc. The filtrates were

evaporated under reduced pressure and the crude product was purified by column chromatography on silica gel (hexane/EtOAc = 10:1 as eluent) to afford **S3** quantitatively (1.7 g, 10 mmol). ^{1}H NMR (400 MHz, CDCl$_3$) δ 5.95 (1H, s), 3.08 (2H, t, J = 7.6 Hz), 2.54 (3H, s), 2.24 (3H, s), 1.77 (2H, sext, J = 7.6 Hz), 1.02 (3H, t, J = 7.6 Hz).
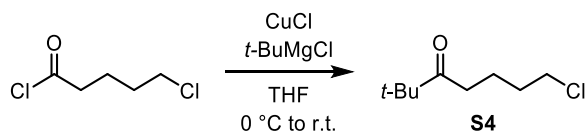
To a solution of 5-chlorovaleryl chloride (7.7 mL, 60 mmol) and CuCl (5.9 g, 60 mmol) in THF (60 mL, 1 M), a 1 M THF solution of t-BuMgCl (63 mL, 63 mmol) was added dropwise via syringe under Ar atmosphere at 0 °C. The reaction mixture was then allowed to warm to room temperature and stirred overnight. The reaction was quenched with ice water and filtered through a pad of Celite. The organic layer of resulting filtrates was washed with 1 N HCl aq. three times, dried, and concentrated. The crude product was purified by silica gel column chromatography (hexane/EtOAc = 15:1 as eluent) to give **S4** in 92% yield (9.75 g, 55.2 mmol). ^{1}H NMR (400 MHz, CDCl$_3$) δ 3.53 (2H, t, J = 6.4 Hz), 2.52 (2H, t, J = 6.8 Hz), 1.85-1.65 (4H, m), 1.14 (9H, s).
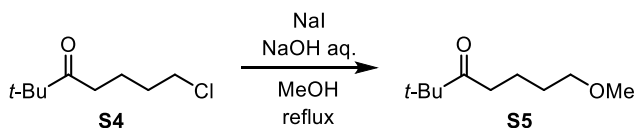
The mixture of **S4** (0.53 g, 3 mmol) and NaI (0.90 g, 6 mmol) in 1 N NaOH aq. (20 mL) and MeOH (100 mL) was refluxed with stirring for 12 h. The reaction mixture was then cooled to room temperature and evaporated to remove MeOH. The resulting mixture was extracted with EtOAc twice, and the combined organic layers were washed with brine, dried over Na$_2$SO$_4$, filtered, and concentrated. The residue was purified by column chromatography on silica gel (hexane/EtOAc = 15:1) to afford **S5** in 54% yield (0.28 g, 1.63 mmol). ^{1}H NMR (400 MHz, CDCl$_3$) δ 3.37 (2H, t, J = 6.4 Hz), 3.32 (3H, s), 2.51 (2H, t, J = 7.0 Hz), 1.66-1.50 (4H, m), 1.13 (9H, s).
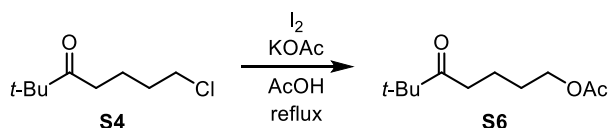

The solution of **S4** (2.6 g, 15 mmol), KOAc (2.9 g, 30 mmol), and I$_2$ (31 mg, 0.12 mmol) in AcOH (150 mL, 0.1 M) was refluxed with stirring overnight. The reaction mixture was allowed to cool to room temperature and acetic acid was removed by rotary evaporator. The residue was diluted with water and extracted with EtOAc. The combined organic layers were washed with brine, dried over Na$_2$SO$_4$, filtered, and concentrated. The crude material was purified by column chromatography on

silica gel (hexane/EtOAc = 10:1) to afford **S6** in 60% yield (1.8 g, 9.0 mmol). ^{1}H NMR (400 MHz, CDCl₃) δ 4.06 (2H, t, *J* = 6.2 Hz), 2.52 (2H, t, *J* = 7.0 Hz), 2.05 (3H, s), 1.62 (4H, m), 1.14 (9H, s).
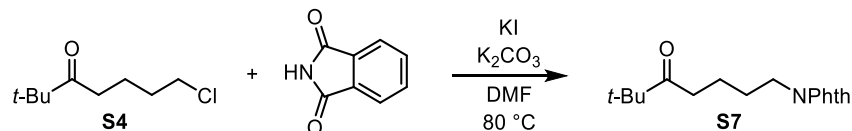
The suspension of **S4** (0.88 g, 5 mmol), phthalimide (0.88 g, 6 mmol), K₂CO₃ (1.38 g, 10 mmol), and KI (0.33 g, 2 mmol) in DMF (20 mL) was stirred at 80 °C overnight. After cooling to room temperature, the reaction mixture was diluted with water and the extractive work-up was performed with EtOAc. The combined organic layers were washed with water three times, dried over Na₂SO₄, and concentrated. The resulting crude residue was purified by column chromatography on silica gel (hexane/EtOAc = 3:1) to afford **S7** in 90% yield (1.3 g, 4.5 mmol). ^{1}H NMR (400 MHz, CDCl₃) δ 7.87-7,81 (2H, m), 7.74-7.68 (2H, m), 3.69 (2H, t, *J* = 7.2 Hz), 2.54 (2H, t, *J* = 7.2 Hz), 1.74-1.55 (4H, m), 1.13 (9H, s).
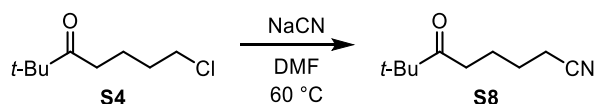
The mixture of **S4** (0.49 g, 2.8 mmol) and NaCN (0.41 g, 8.3 mmol) in DMF (3 mL) was vigorously stirred at 60 °C for 10 h. After cooling to room temperature, the reaction mixture was diluted with water and the extractive work-up was conducted with EtOAc. The combined organic layers were washed with water three times, dried over Na₂SO₄, filtered, and concentrated. The crude material was purified by column chromatography on silica gel (hexane/EtOAc = 10:1 to 4:1) to furnish **S8** quantitatively (0.47 g, 2.8 mmol). ^{1}H NMR (400 MHz, CDCl₃) δ 2.54 (2H, t, *J* = 6.8 Hz), 2.35 (2H, t, *J* = 7.2 Hz), 1.79-1.59 (4H, m), 1.14 (9H, s).

Characterization of Enol Silyl Ethers
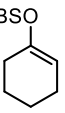
TBSO
^{1}H NMR (400 MHz, CDCl₃) δ 4.89-4.84 (1H, brm), 2.03-1.96 (4H, m), 1.69-1.61 (2H, m), 1.53-1.47 (2H, m), 0.91 (9H, s), 0.12 (6H, s); ^{13}C NMR (151 MHz, CDCl₃) δ 150.6, 104.5, 30.0, 25.9, 24.0, 23.3, 22.5, 18.2, –4.2.
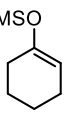
TMSO
^{1}H NMR (400 MHz, CDCl₃) δ 4.88-4.85 (1H, m), 2.03-1.96 (4H, m), 1.68-1.62 (2H, m), 1.53-1.48 (2H, m), 0.18 (9H, s); ^{13}C NMR (151 MHz, CDCl₃) δ 150.4, 104.4, 30.0, 24.0, 23.3, 22.5, 0.5.

TESO
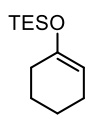
^{1}H NMR (400 MHz, CDCl$_3$) δ 4.89-4.83 (1H, m), 2.04-1.96 (4H, m), 1.68-1.60 (2H, m), 1.54-1.46 (2H, m), 0.97 (9H, t, J = 8.0 Hz), 0.64 (6H, q, J = 8.0 Hz); ^{13}C NMR (151 MHz, CDCl$_3$) δ 150.6, 104.1, 30.0, 24.0, 23.4, 22.5, 6.9, 5.2.

TBSO
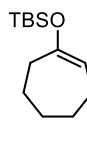
^{1}H NMR (400 MHz, CDCl$_3$) δ 5.01 (1H, t, J = 6.4 Hz), 2.26-2.19 (2H, brm), 1.98 (2H, dd, J = 11.6, 6.4 Hz), 1.71-1.63 (2H, m), 1.61-1.48 (4H, m), 0.91 (9H, s), 0.11 (6H, s); ^{13}C NMR (151 MHz, CDCl$_3$) δ 156.3, 108.7, 35.7, 31.6, 27.9, 25.9, 25.5, 25.4, 18.1, –4.3.

TBSO
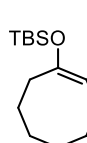
^{1}H NMR (400 MHz, CDCl$_3$) δ 4.74-4.66 (1H, m), 2.20-2.14 (2H, brm), 2.04-1.96 (2H, br), 1.61-1.45 (8H, brm), 0.91 (9H, s), 0.14 (6H, s); ^{13}C NMR (151 MHz, CDCl$_3$) δ 153.4, 105.0, 31.1(9), 31.1(5), 27.9, 26.5(2), 26.5(0), 25.9, 25.7, 18.2, –4.2.

TBSO
t-Bu
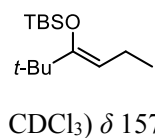
^{1}H NMR (400 MHz, CDCl$_3$) δ 4.44 (1H, t, J = 7.2 Hz), 1.99 (2H, quin, J = 7.2 Hz), 1.06 (9H, s), 0.98 (9H, s), 0.93 (3H, t, J = 7.2 Hz), 0.17 (6H, s); ^{13}C NMR (151 MHz, CDCl$_3$) δ 157.3, 105.5, 29.1, 26.7, 25.9, 19.5, 19.4, 14.9, –2.9.

TBSO
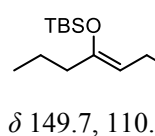
^{1}H NMR (400 MHz, CDCl$_3$) δ 4.40 (1H, t, J = 7.4 Hz), 2.06-1.90 (4H, m), 1.52-1.46 (2H, m), 0.95 (9H, s), 0.93-0.88 (6H, m), 0.12 (6H, s); ^{13}C NMR (151 MHz, CDCl$_3$) δ 149.7, 110.0, 38.8, 26.0, 20.5, 18.7, 18.4, 14.7, 13.8, –3.9.

TBSO
Me
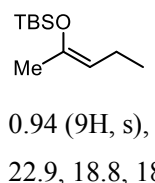
This compound was synthesized by the literature method.[3]
^{1}H NMR (400 MHz, CDCl$_3$) δ 4.93 (1H, t, J = 7.2 Hz), 1.97-2.04 (2H, m), 1.76 (3H, s), 0.94 (9H, s), 0.91 (3H, t, J = 7.8 Hz), 0.13 (6H, s); ^{13}C NMR (151 MHz, CDCl$_3$) δ 146.2, 110.7, 25.9, 22.9, 18.8, 18.4, 14.6, –3.8.

TBSO
Mes
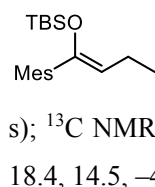
^{1}H NMR (400 MHz, CDCl$_3$) δ 6.81 (2H, s), 4.52 (1H, t, J = 7.2 Hz), 2.28 (6H, s), 2.25 (3H, s), 2.21 (2H, quin, J = 7.2 Hz), 1.01 (3H, t, J = 7.2 Hz), 0.91 (9H, s), –0.21 (6H, s); ^{13}C NMR (151 MHz, CDCl$_3$) δ 145.8, 136.9, 136.5, 136.4, 128.2, 115.0, 25.8, 21.2, 20.4, 18.8, 18.4, 14.5, –4.4.

TBSO
Ph
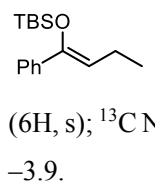
^{1}H NMR (400 MHz, CDCl$_3$) δ 7.43 (2H, d, J = 6.8 Hz), 7.31-7.25 (3H, m), 5.09 (1H, t, J = 7.6 Hz), 2.22 (2H, quin, J = 7.6 Hz), 1.03 (3H, t, J = 7.6 Hz), 0.98 (9H, s), –0.05 (6H, s); ^{13}C NMR (151 MHz, CDCl$_3$) δ 148.9, 140.0, 128.0, 127.4, 126.0, 114.0, 26.0, 19.6, 18.5, 14.4, –3.9.
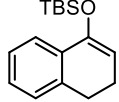
¹H NMR (400 MHz, CDCl₃) δ 7.46 (1H, d, J = 7.2 Hz), 7.22-7.08 (3H, m), 5.17 (1H, t, J = 4.6 Hz), 2.76 (2H, t, J = 8.0 Hz), 2.35-2.27 (2H, m), 1.01 (9H, s), 0.20 (6H, s); ¹³C NMR (151 MHz, CDCl₃) δ 148.4, 137.3, 133.8, 127.4, 127.1, 126.3, 122.0, 105.1, 28.4, 26.1, 22.4, 18.5, –2.8.
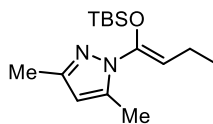
¹H NMR (400 MHz, CDCl₃) δ 5.79 (1H, s), 4.76 (1H, t, J = 7.6 Hz), 2.23 (3H, s), 2.21 (3H, s), 2.18 (2H, quin, J = 7.6 Hz), 1.03 (3H, t, J = 7.6 Hz), 0.92 (9H, s), –0.08 (6H, s); ¹³C NMR (151 MHz, CDCl₃) 148.1, 141.3, 139.8, 109.3, 105.7, 25.7, 18.9, 18.2, 14.1, 13.6, 11.6, –5.2.
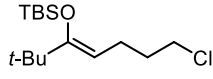
¹H NMR (400 MHz, CDCl₃) δ 4.43 (1H, t, J = 7.2 Hz), 3.53 (2H, t, J = 7.2 Hz), 2.13 (2H, q, J = 7.2 Hz), 1.79 (2H, quin, J = 7.2 Hz), 1.06 (9H, s), 0.98 (9H, s), 0.18 (6H, s); ¹³C NMR (151 MHz, CDCl₃) δ 159.1, 101.7, 45.0, 36.7, 33.3, 29.1, 26.7, 23.8, 19.4, –2.7.
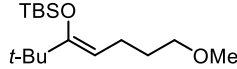
¹H NMR (400 MHz, CDCl₃) δ 4.45 (1H, t, J = 7.0 Hz), 3.36 (2H, t, J = 7.0 Hz), 3.32 (3H, s), 2.03 (2H, q, J = 7.0 Hz), 1.59 (2H, quin, J = 7.0 Hz), 1.05 (9H, s), 0.98 (9H, s), 0.17 (6H, s); ¹³C NMR (151 MHz, CDCl₃) δ 158.3, 102.9, 72.7, 66.0, 58.7, 30.3, 29.1, 26.7, 22.7, 19.4, –2.8.
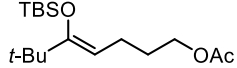
¹H NMR (400 MHz, CDCl₃) δ 4.44 (1H, t, J = 7.0 Hz), 4.06 (2H, t, J = 6.6 Hz), 2.07 (2H, q, J = 7.0 Hz), 2.04 (3H, s), 1.70-1.60 (2H, m), 1.05 (9H, s), 0.98 (9H, s), 0.18 (6H, s); ¹³C NMR (151 MHz, CDCl₃) δ 171.4, 158.7, 102.3, 64.5, 36.7, 29.3, 29.0, 26.7, 22.8, 21.2, 19.4, –2.8.
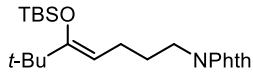
¹H NMR (400 MHz, CDCl₃) δ 7.86-7.80 (2H, m), 7.73-7.67 (2H, m), 4.47 (1H, brt, J = 6.6 Hz), 3.69 (2H, t, J = 7.6 Hz), 2.04 (2H, q, J = 7.6 Hz), 1.71 (2H, quin, J = 7.6 Hz), 1.04 (9H, s), 0.94 (9H, s), 0.15 (6H, s); ¹³C NMR (151 MHz, CDCl₃) δ 168.5, 158.7, 134.0, 132.4, 123.3, 102.2, 37.9, 36.7, 29.2, 29.0, 26.6, 23.7, 19.3, –2.8.
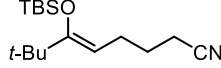
¹H NMR (400 MHz, CDCl₃) δ 4.41 (1H, t, J = 7.2 Hz), 2.32 (2H, t, J = 7.2 Hz), 2.13 (2H, q, J = 7.2 Hz), 1.69 (1H, quin, J = 7.2 Hz), 1.06 (9H, s), 0.98 (9H, s), 0.18 (6H, s); ¹³C NMR (151 MHz, CDCl₃) δ 159.9, 120.0, 101.0, 36.8, 29.0, 26.6, 26.1, 25.2, 19.3, 16.7, –2.7.
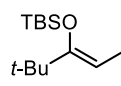
TBSO / t-Bu structure — ¹H NMR (400 MHz, CDCl₃) δ 4.57 (1H, q, *J* = 7.2 Hz), 1.53 (3H, d, *J* = 7.2 Hz), 1.06 (9H, s), 0.99 (9H, s), 0.18 (6H, s); ¹³C NMR (151 MHz, CDCl₃) δ 159.1, 97.0, 31.7, 29.0, 26.7, 25.9, 12.0, –2.7.
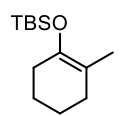
TBSO methylcyclohexene structure — ¹H NMR (600 MHz, CDCl₃) δ 2.04-1.99 (2H, m), 1.97-1.92 (2H, m), 1.67-1.61 (2H, m), 1.57 (3H, s), 1.56-1.51 (2H, m), 0.95 (9H, s), 0.11 (6H, s); ¹³C NMR (151 MHz, CDCl₃) δ 143.1, 111.7, 30.5(4), 30.4(5), 26.3, 24.0, 23.2, 18.3, 16.6, –3.7.
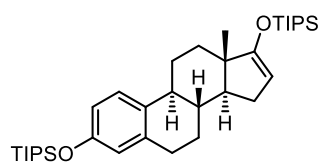
OTIPS steroid structure — ¹H NMR (400 MHz, CDCl₃) δ 7.08 (1H, d, *J* = 8.4 Hz), 6.64 (1H, d, *J* = 8.4 Hz), 6.59 (1H, s), 4.42 (1H, s), 2.90-2.74 (2H, m), 2.34-2.18 (2H, m), 2.21-2.03 (1H, m), 1.94-1.78 (3H, m), 1.64-1.31 (5H, m), 1.31-1.14 (6H, m), 1.10 (36H, br), 0.90 (3H, s); ¹³C NMR (151 MHz, CDCl₃) δ 165.4, 153.8, 138.0, 133.4, 125.8, 119.9, 116.9, 97.4, 54.3, 45.3, 44.8, 37.3, 33.8, 29.7, 28.3, 27.3, 26.4, 18.2(3), 18.1(6), 15.7, 12.9, 12.7.

General Experimental Procedure for Allylic Alkylation of Enol Silyl Ethers

To a flame-dried test tube were added electron-deficient olefin (0.12 mmol, 1.2 equiv), [Ir(dFCF₃ppy)₂(4,4′-dCF₃bpy)]PF₆ (2.29 mg, 0.002 mmol, 2 mol%) and DCE (0.5 mL, 0.2 M). The reaction tube was sealed with a rubber septum and then evacuated in *vacuo* and backfilled with Ar five times. Enol silyl ether (0.1 mmol, 1 equiv) and 2,4,6-collidine (1.3 μL, 0.01 mmol, 10 mol%) were successively introduced. The whole reaction mixture was stirred at 25 °C under the irradiation of blue LED (448 nm, 750 W/m²) with a fan to keep the temperature. After 12 h, the reaction mixture was evaporated. Purification of the resulting crude residue by column chromatography on silica gel (hexane 100% to hexane/EtOAc = 5:1) afforded the corresponding alkylated enol silyl ether.

Proposed Catalytic Cycle of Allylic C–H Alkylation

While it is difficult to precisely establish the entire reaction mechanism, particularly the closing step of the catalytic cycle, we illustrate the plausible mechanism of the present allylic alkylation of enol silyl ethers in Fig. S1. The light-excited Ir^III complex would engage in the oxidation of enol silyl ether to generate radical cation intermediate **A** and the reduced Ir^II complex. This oxidation process would then be relayed to the deprotonation of the radical cation by 2,4,6-collidine to furnish nucleophilic allylic radical **B**. The subsequent radical addition to electron-deficient olefin could form a new carbon–carbon bond with the generation of electrophilic radical **C**. The single-electron reduction of **C** by Ir^II

complex would give the carbanion intermediate **D**, which could be protonated by collidinium salt to afford the alkylated product and return both catalyst species back to the initial forms.
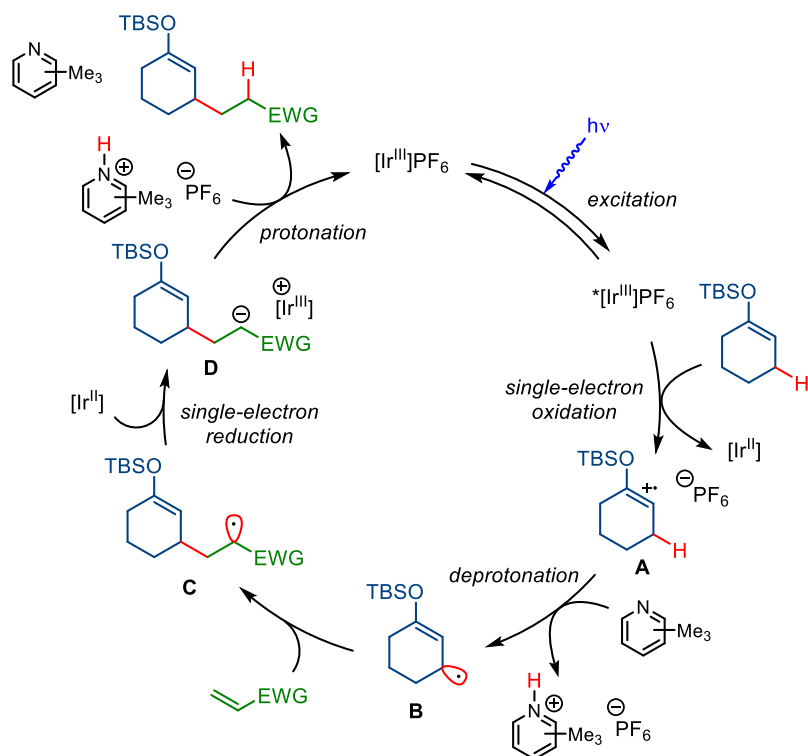
Fig. S1. Proposed catalytic cycle

Characterization of alkylated enol silyl ethers

3a: ^{1}H NMR (600 MHz, CDCl$_3$) (for major diastereomer) δ 7.45-7.32 (5H, m), 4.35 (1H, br), 4.16 (1H, d, J = 4.8 Hz), 2.99 (1H, dd, J = 10.2, 4.8 Hz), 2.91-2.85 (1H, m), 2.02-1.94 (3H, m), 1.88-1.82 (1H, m), 1.70-1.61 (1H, m), 1.28-1.22 (1H, m), 0.82 (9H, s), –0.06 (3H, s), –0.07 (3H, s), (for minor diastereomer) δ 7.45-7.32 (5H, m), 4.94 (1H, d, J = 4.2 Hz), 4.24 (1H, d, J = 4.8 Hz), 3.00-2.94 (1H, m), 2.91-2.85 (1H, m), 2.05-2.01 (2H, m), 1.71-1.61 (1H, m), 1.61-1.55 (1H, m), 1.49-1.42 (1H, m), 1.22-1.17 (1H, m), 0.94 (9H, s), 0.17 (6H, s); ^{13}C NMR (151 MHz, CDCl$_3$) (for major diastereomer) δ 153.4, 136.6, 129.3, 128.7, 112.1, 111.9, 103.8, 52.1, 37.1, 29.6, 27.7, 27.6, 21.6, 18.1, –4.3, –4.5, (for minor diastereomer) δ 155.3, 136.7, 129.0, 128.4, 112.4, 112.0, 103.0, 52.0, 36.1, 30.0, 27.9, 25.8, 19.6, 18.2, –4.0, –4.2; HRMS (ESI) Calcd for C$_{22}$H$_{29}$ON$_2$Si$^-$ ([M−H]$^-$) 365.2044. Found 365.2052.
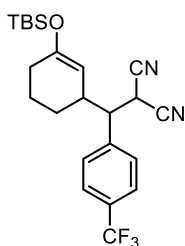
3b (dr = 1.8:1): ^{1}H NMR (600 MHz, CDCl$_3$) (for major diastereomer) δ 7.69 (2H, d, J = 8.4 Hz), 7.49 (2H, d, J = 8.4 Hz), 4.27 (1H, br), 4.18 (1H, d, J = 3.6 Hz), 3.02-2.95 (2H, m), 2.02-1.94 (3H, m), 1.89-1.82 (1H, m), 1.72-1.63 (1H, m), 1.29-1.21 (1H, m), 0.82 (9H, s), −0.07 (6H, s), (for minor diastereomer) δ 7.69 (2H, d, J = 7.5 Hz), 7.51 (2H, d, J = 7.5 Hz), 4.92 (1H, d, J = 4.2 Hz), 4.27 (1H, d, J = 4.8 Hz), 3.06 (1H, dd, J = 10.5, 4.8 Hz), 2.93-2.86 (1H, m), 2.04 (2H, t, J = 6.0 Hz), 1.70-1.56 (2H, m), 1.51-1.42 (1H, m), 1.18-1.12 (1H, m), 0.94 (9H, s), 0.17 (6H, s); ^{13}C NMR (151 MHz, CDCl$_3$) (for major diastereomer) δ 154.0, 140.5, 131.4 (q, $J_{C\text{-}F}$ = 32.8 Hz), 129.3, 126.3 (q, $J_{C\text{-}F}$ = 4.4 Hz), 123.9 (q, $J_{C\text{-}F}$ = 273.0 Hz), 111.7, 111.4, 103.1, 51.8, 37.0, 29.5, 27.5, 27.2, 25.7, 21.5, 18.1, −4.3, −4.5, (for minor diastereomer) δ 155.8, 140.6, 131.3 (q, $J_{C\text{-}F}$ = 33.2 Hz), 128.9, 126.3, 123.9 (q, $J_{C\text{-}F}$ = 272.0 Hz), 112.0, 111.5, 102.3, 51.7, 36.0, 29.9, 25.7, 25.5, 19.4, 18.2, −4.0, −4.2; HRMS (ESI) Calcd for C$_{23}$H$_{28}$ON$_2$F$_3$Si$^-$ ([M−H]$^-$) 433.1918. Found 433.1917.
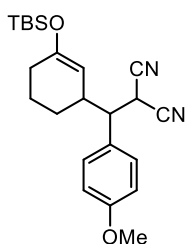
**3c** (dr = 1.9:1): The reaction of **1a** (0.1 mmol) with electron-deficient olefin (0.2 mmol, 2 equiv) was carried out for 24 h.
^{1}H NMR (600 MHz, CDCl$_3$) (for major diastereomer) δ 7.26 (2H, d, J = 9.0 Hz), 6.93 (2H, d, J = 9.0 Hz), 4.39 (1H, brs), 4.12 (1H, d, J = 4.8 Hz), 3.83 (3H, s), 2.96-2.89 (1H, m), 2.84 (1H, dd, J = 10.2, 4.8 Hz), 2.04-1.91 (3H, m), 1.88-1.81 (1H, m), 1.70-1.61 (1H, m), 1.27-1.18 (1H, m), 0.83 (9H, s), −0.04 (6H, s), (for minor diastereomer) δ 7.28 (2H, d, J = 7.8 Hz), 6.93 (2H, d, J = 7.8 Hz), 4.91 (1H, d, J = 4.2 Hz), 4.21 (1H, d, J = 4.8 Hz), 3.82 (3H, s), 2.94 (1H, dd, J = 10.8, 4.8 Hz), 2.86-2.80 (1H, m), 2.02 (2H, t, J = 6.3 Hz), 1.68-1.55 (2H, m), 1.48-1.42 (1H, m), 1.24-1.18 (1H, m), 0.94 (9H, s), 0.16 (6H, s); ^{13}C NMR (151 MHz, CDCl$_3$) (for major diastereomer) δ 160.0, 153.3, 129.8, 128.5, 114.6, 112.3, 111.9, 104.0, 55.5, 51.5, 37.1, 29.6, 27.8(3), 27.7(6), 25.8, 21.7, 18.2, −4.3, −4.5, (for minor diastereomer) δ 160.0, 155.2, 129.5, 128.6, 114.7, 112.6, 112.0, 103.1, 55.4, 51.4, 36.2, 30.0, 28.1, 25.8, 25.5, 19.5, 18.2, −4.0, −4.2; HRMS (ESI) Calcd for C$_{23}$H$_{32}$O$_2$N$_2$NaSi$^+$ ([M+Na]$^+$) 419.2125. Found 419.2139.
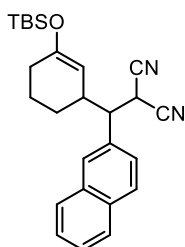
3d (dr = 1.8:1): ^{1}H NMR (600 MHz, CDCl$_3$) (for major diastereomer) δ 7.90 (1H, d, J = 8.4 Hz), 7.88-7.82 (2H, m), 7.80 (1H, s), 7.52 (1H, d, J = 7.2 Hz), 7.52 (1H, t, J = 5.4 Hz), 7.46 (1H, d, J = 7.8 Hz), 4.41 (1H, brs), 4.23 (1H, brd), 3.13-3.06 (2H, m), 2.05-1.95 (3H, m), 1.90-1.83 (1H, m), 1.74-1.65 (1H, m), 1.34-1.24 (1H, m), 0.79 (9H, s), −0.10 (3H, s), −0.11 (3H, s), (for minor diastereomer) δ 7.90 (1H, d, J = 8.4 Hz), 7.88-7.84 (2H, m), 7.82 (1H, s), 7.55-7.51 (2H, m), 7.49 (1H, d, J = 9.0 Hz), 5.00 (1H, d, J = 4.2 Hz), 4.32 (1H, d, J = 4.8 Hz), 3.17 (1H, dd, J = 10.2, 4.8 Hz), 3.04-2.98 (1H, m), 2.04 (2H, t, J = 6.3 Hz), 1.72-1.64 (1H, m), 1.63-1.56 (1H, m), 1.50-1.44 (1H, m), 1.27-1.19 (1H, m), 0.95 (9H, s), 0.18 (6H, s); ^{13}C NMR (151 MHz, CDCl$_3$) (for major isomer) δ 153.5, 134.0,

133.4(9), 133.4(5), 129.2, 128.4, 128.2, 127.9, 126.8, 126.7, 125.6, 112.1, 112.0, 103.9, 52.2, 37.3, 29.6, 27.8, 27.6, 25.7, 21.6, 18.1, −4.3, −4.5, (for minor diastereomer) δ 155.4, 134.1, 133.5(4), 133.4(6), 129.3, 128.3, 128.2, 127.9, 126.8, 126.7, 125.3, 112.4, 112.0, 103.0, 52.2, 36.2, 30.0, 27.9, 25.8, 25.7, 19.6, 18.2, −4.0, −4.2; HRMS (ESI) Calcd for $C_{26}H_{31}ON_2Si^-$ ([M−H]⁻) 415.2200. Found 415.2210.
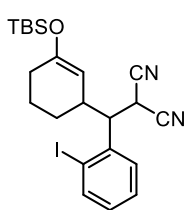
3e (dr = 1.6:1): ¹H NMR (400 MHz, CDCl₃) (for major diastereomer) δ 7.97-7.93 (1H, m), 7.49 (1H, d, J = 2.1 Hz), 7.46-7.42 (1H, m), 7.07 (1H, t, J = 2.0 Hz), 4.26 (1H, brs), 4.05 (1H, d, J = 1.2 Hz), 3.64 (1H, dd, J = 2.6, 1.2 Hz), 3.02-2.97 (1H, m), 2.09-1.96 (3H, m), 1.94-1.88 (1H, m), 1.72-1.60 (1H, m), 1.42-1.35 (1H, m), 0.83 (9H, m), −0.01 (3H, s), −0.05 (3H, s), (for minor diasteromer) δ 7.97-7.93 (1H, m), 7.54 (1H, d, J = 2.0 Hz), 7.46-7.42 (1H, m), 7.07 (1H, t, J = 1.9 Hz), 4.98 (1H, d, J = 1.2 Hz), 4.18 (1H, d, J = 1.4 Hz), 3.74 (1H, dd, J = 2.6, 1.3 Hz), 2.90-2.84 (1H, m), 2.09-1.96 (2H, m), 1.88-1.79 (1H, m), 1.72-1.60 (1H, m), 1.45-1.40 (1H, m), 1.21-1.15 (1H, m), 0.95 (9H, s), 0.19 (3H, s), 0.18 (3H, s); ¹³C NMR (151 MHz, CDCl₃) (for major diastereomer) δ 171.5, 152.2, 141.1, 139.5, 129.7, 129.0, 104.4, 103.0, 67.0, 56.1, 47.0, 43.0, 39.9, 29.9, 25.8, 21.4, 18.1, −4.1(8), −4.2(3), (for minor diastereomer) δ 171.5, 152.6, 141.6, 139.7, 129.6, 129.1, 107.4, 102.3, 67.0, 56.0, 47.1, 42.9, 40.7, 30.2, 28.1, 21.8, 18.2, −4.0, −4.1; HRMS (ESI) Calcd for $C_{22}H_{29}ON_2INaSi^+$ ([M+Na]⁺) 515.0986. Found 515.0983.
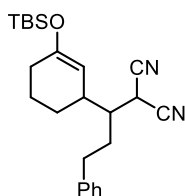
3f (dr = 1.6:1): ¹H NMR (400 MHz, CDCl₃) (for major diastereomer) δ 7.35-7.30 (2H, m), 7.26-7.20 (3H, m), 4.62 (1H, brs), 3.89 (1H, d, J = 2.4 Hz), 2.88-2.68 (2H, m), 2.68-2.60 (1H, m), 2.14-1.68 (5H, m), 1.64-1.49 (2H, m), 1.33-1.18 (2H, m), 0.92 (9H, s), 0.15 (6H, s), (for minor diastereomer) δ 7.35-7.28 (2H, m), 7.26-7.20 (3H, m), 4.62 (1H, brs), 3.79 (1H, d, J = 4.4 Hz), 2.88-2.68 (2H, m), 2.68-2.60 (1H, m), 2.14-1.68 (7H, m), 1.64-1.49 (2H, m), 0.92 (9H, s), 0.15 (6H, s); ¹³C NMR (151 MHz, CDCl₃) (for major diastereomer) δ 155.1, 140.5, 128.9, 128.4, 126.6, 113.5, 112.6, 104.6, 45.2, 37.9, 33.7, 31.5, 30.0, 25.8, 25.2, 24.2, 22.2, 18.2, −4.1(1), −4.1(4), (for minor diastereomer) δ 154.5, 140.4, 128.9, 128.4, 126.7, 113.2, 112.4, 103.9, 44.1, 37.8, 33.9, 31.2, 29.9, 25.8, 25.1, 24.7, 21.7, 18.1, −4.1; HRMS (ESI) Calcd for $C_{24}H_{34}ON_2NaSi^+$ ([M+Na]⁺) 417.2333. Found 417.2346.
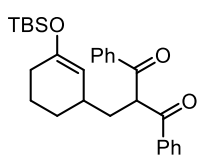
3g: ¹H NMR (600 MHz, CDCl₃) δ 7.97 (4H, d, J = 7.2 Hz), 7.56 (2H, t, J = 7.2 Hz), 7.48-7.43 (4H, m), 5.34 (1H, t, J = 6.6 Hz), 4.83 (1H, brs), 2.31 (1H, brs), 2.17-2.06 (2H, m), 2.04-1.92 (2H, m), 1.80-1.72 (2H, m), 1.58-1.49 (1H, m), 1.22-1.17 (1H, m), 0.91 (9H, s), 0.12 (6H, s); ¹³C NMR (600 MHz, CDCl₃) δ 196.1,

196.0, 152.0, 136.2(2), 136.1(7), 133.6, 129.0, 128.8, 128.7, 108.0, 55.0, 36.3, 33.5, 30.1, 29.0, 25.8, 21.5, 18.2, –4.2, –4.3; HRMS (ESI) Calcd for $C_{28}H_{36}O_3NaSi^+$ ([M+Na]$^+$) 471.2326. Found 471.2324.
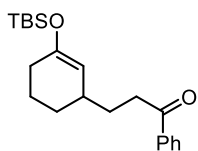
3h: The reaction was conducted with vinyl phenyl ketone (0.3 mmol, 3 equiv). ^{1}H NMR (600 MHz, CDCl$_3$) δ 7.96 (2H, d, J = 7.8 Hz), 7.56 (1H, t, J = 7.8 Hz), 7.46 (2H, t, J = 7.8 Hz), 4.82 (1H, brs), 2.99 (1H, t, J = 7.8 Hz), 2.28-2.22 (1H, m), 2.06-1.94 (2H, m), 1.82-1.67 (4H, m), 1.61-1.52 (1H, m), 1.20-1.13 (1H, m), 0.92 (9H, s), 0.13 (6H, s); ^{13}C NMR (151 MHz, CDCl$_3$) δ 200.8, 151.5, 137.2, 133.1, 128.7, 128.2, 108.8, 36.2, 34.5, 31.4, 30.1, 28.8, 25.9, 21.8, 18.2, –4.1, –4.3; HRMS (ESI) Calcd for $C_{21}H_{32}O_2NaSi^+$ ([M+Na]$^+$) 367.2064. Found 367.2063.
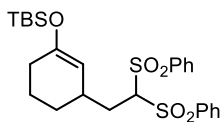
3i: ^{1}H NMR (600 MHz, CDCl$_3$) δ 7.97 (2H, d, J = 8.4 Hz), 7.95 (2H, d, J = 8.4 Hz), 7.72-7.70 (2H, m), 7.61-7.57 (4H, m), 4.64 (1H, brd), 4.46 (1H, t, J = 5.4 Hz), 2.46 (1H, br), 2.12-2.02 (2H, m), 1.96-1.91 (2H, m), 1.66-1.58 (2H, m), 1.52-1.46 (1H, m), 1.06-0.99 (1H, m), 0.91 (9H, s), 0.11 (6H, s); ^{13}C NMR (151 MHz, CDCl$_3$) δ 152.6, 138.1, 137.9, 134.7, 129.9, 129.8, 129.3, 106.6, 81.9, 32.8, 32.2, 29.9, 27.6, 25.8, 20.7, 18.2, –4.2; HRMS (ESI) Calcd for $C_{26}H_{36}O_5NaS_2Si^+$ ([M+Na]$^+$) 543.1666. Found 543.1667.

3j: The reaction was performed for 24 h. ^{1}H NMR (600 MHz, CDCl$_3$) δ 7.70 (2H, d, J = 7.8 Hz), 7.65-7.58 (3H, m), 4.72 (1H, brs), 3.80-3.69 (2H, m), 2.42-2.36 (1H, m), 2.09-1.86 (4H, m), 1.82-1.72 (2H, m), 1.63-1.56 (1H, m), 1.22-1.14 (1H, m), 0.92 (9H, s), 0.14 (6H, s); ^{13}C NMR (151 MHz, CDCl$_3$) δ 153.6, 152.9, 133.2, 131.6, 129.9, 125.2, 106.6, 54.2, 33.7, 29.9, 28.5, 28.1, 25.8, 21.5, 18.2, –4.1(6), –4.2(3); HRMS (ESI) Calcd for $C_{21}H_{32}O_3N_4NaSSi^+$ ([M+Na]$^+$) 471.1857. Found 471.1855.
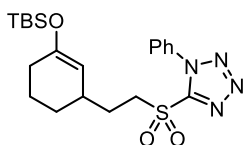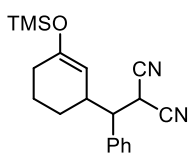
3k (dr = 2.0:1): ^{1}H NMR (600 MHz, CDCl$_3$) (for major diastereomer) δ 7.43-7.33 (5H, m), 4.36 (1H, brs), 4.15 (1H, d, J = 4.8 Hz), 3.01-2.95 (1H, m), 2.91-2.87 (1H, m), 2.02 (1H, t, J = 6.3 Hz), 2.01-1.94 (2H, m), 1.88-1.82 (1H, m), 1.71-1.62 (1H, m), 1.29-1.23 (1H, m), 0.02 (9H, s), (for minor diastereomer) δ 7.43-7.33 (5H, m), 4.95 (1H, d, J = 4.2 Hz), 4.24 (1H, d, J = 4.8 Hz), 3.01-2.95 (1H, m), 2.91-2.87 (1H, m), 2.01-1.94 (2H, m), 1.71-1.62 (1H, m), 1.62-1.56 (1H, m), 1.49-1.43 (1H, m), 1.22-1.17 (1H, m), 0.22 (9H, s); ^{13}C NMR (151 MHz, CDCl$_3$) (for major diastereomer) δ 153.2, 136.6, 129.3, 128.7, 112.1, 111.9, 103.9, 52.1, 37.1, 29.6, 27.6(4), 27.5(5), 21.6, 0.3, (for minor diastereomer) δ 155.0, 136.7, 129.0, 128.4, 112.4, 111.9, 103.1, 52.0, 36.1, 30.0, 27.8, 25.5, 19.6, 0.6; HRMS (ESI) Calcd for $C_{19}H_{23}ON_2Si^-$ ([M−H]$^-$) 323.1574. Found 323.1580.
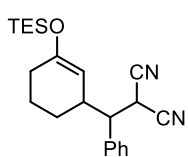
3l (dr = 2.0:1): ^{1}H NMR (600 MHz, CDCl$_3$) (for major diastereomer) δ 7.43-7.33 (5H, m), 4.34 (1H, brs), 4.15 (1H, d, J = 5.4 Hz), 3.01-2.95 (1H, m), 2.91-2.85 (1H, m), 2.05 (1H, t, J = 6.3 Hz), 2.02-1.95 (2H, m), 1.89-1.83 (1H, m), 1.71-1.63 (1H, m), 1.29-1.22 (1H, m), 0.83 (9H, t, J = 7.8 Hz), 0.47 (6H, q, J = 7.8 Hz), (for minor diastereomer) δ 7.43-7.33 (5H, m), 4.94 (1H, d, J = 4.2 Hz), 4.23 (1H, d, J = 4.8 Hz), 3.01-2.95 (1H, m), 2.91-2.85 (1H, m), 2.02-1.95 (2H, m), 1.71-1.63 (1H, m), 1.63-1.56 (1H, m), 1.49-1.43 (1H, m), 1.22-1.17 (1H, m), 1.00 (9H, t, J = 8.0 Hz), 0.69 (6H, q, J = 8.0 Hz): ^{13}C NMR (151 MHz, CDCl$_3$) (for major diastereomer) δ 153.3, 136.6, 129.3, 128.7, 112.1, 111.8, 103.4, 52.1, 37.1, 29.5, 27.7, 27.6, 21.6, 6.7, 5.0, (for minor diastereomer) δ 155.3, 136.7, 129.0, 128.4, 112.4, 111.9, 102.6, 52.0, 36.1, 29.9, 27.8, 25.5, 19.6, 6.9, 5.3; HRMS (ESI) Calcd for C$_{22}$H$_{29}$ON$_2$Si$^-$ ([M−H]$^-$) 365.2044. Found 365.2048.
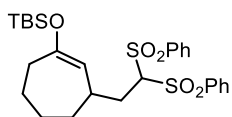
3m: ^{1}H NMR (600 MHz, CDCl$_3$) δ 7.96 (2H, d, J = 8.4 Hz), 7.93 (2H, d, J = 7.8 Hz), 7.72-7.68 (2H, m), 7.58 (4H, t, J = 7.8 Hz), 4.61 (1H, d, J = 4.2 Hz), 4.43 (1H, d, J = 5.4 Hz), 2.28-2.16 (3H, m), 2.09-2.03 (1H, m), 2.00 (1H, dd, J =15.9, 7.5 Hz), 1.84-1.77 (1H, m), 1.61-1.52 (1H, m), 1.52-1.46 (1H, m), 1.45-1.34 (1H, m), 1.28-1.21 (1H, m), 0.92 (9H, s), 0.12 (6H, s); ^{13}C NMR (151 MHz, CDCl$_3$) δ 157.7, 138.4, 137.9, 134.7(1), 134.6(7), 129.9, 129.6, 129.3, 129.2, 109.8, 82.0, 35.3, 34.7, 33.8, 32.2. 29.7, 25.9, 24.8, 18.2, −4.2, −4.3; HRMS (ESI) Calcd for C$_{27}$H$_{38}$O$_5$NaS$_2$Si$^+$ ([M+Na]$^+$) 557.1822. Found 557.1823.
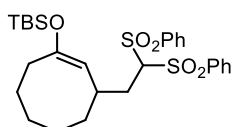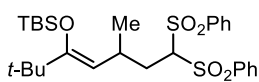
3n: ^{1}H NMR (600 MHz, CDCl$_3$) δ 7.96 (2H, d, J = 7.8 Hz), 7.91 (2H, d, J = 7.8 Hz), 7.70 (1H, t, J = 7.8 Hz), 7.69 (1H, t, J = 7.8 Hz), 7.58 (2H, t, J = 7.8 Hz), 7.57 (2H, t, J = 7.8 Hz), 4.55 (1H, dd, J = 8.7, 1.5 Hz), 4.13 (1H, d, J = 9.0 Hz), 2.42-2.34 (1H, m), 2.22-2.14 (2H, m), 2.06 (1H, ddd, J = 15.0, 8.7, 3.9 Hz), 1.87 (1H, dt, J = 13.8, 3.9 Hz), 1.72-1.59 (2H, m), 1.52-1.38 (4H, m), 1.24-1.10 (2H, m), 0.93 (9H, s), 0.17 (3H, s), 0.15 (3H, s); ^{13}C NMR (151 MHz, CDCl$_3$) δ 156.3, 138.5, 138.2, 134.6, 129.9, 129.6, 129.3, 129.2, 105.7, 82.3, 38.1, 35.3, 32.8, 32.0, 28.5, 27.0, 26.0, 25.8, 18.2, −4.0, −4.4; HRMS (ESI) Calcd for C$_{28}$H$_{40}$O$_5$NaS$_2$Si$^+$ ([M+Na]$^+$) 571.1979. Found 571.1976.

3o (Z/E = >20:1): ^{1}H NMR (600 MHz, CDCl$_3$) δ 7.87(9) (2H, d, J = 7.8 Hz), 7.87(6) (2H, d, J = 8.4 Hz), 7.64 (1H, t, J = 7.8 Hz), 7.61 (1H, t, J = 8.4 Hz), 7.50 (2H, t, J = 8.4 Hz), 7.48 (2H, t, J = 7.8 Hz), 4.59 (1H, d, J = 8.4 Hz), 4.22 (1H, d, J = 10.8 Hz), 3.23-3.14 (1H, m), 2.26 (1H, ddd, J = 15.0, 9.0, 4.2 Hz), 1.94-1.87 (1H, m), 1.06 (9H, s), 1.04 (9H, s), 0.33 (3H, s), 0.17 (3H, s); ^{13}C NMR (151 MHz, CDCl$_3$) δ 161.1, 139.6, 137.3, 134.5, 134.0, 130.3, 129.1, 129.0, 108.3, 81.6, 37.1, 33.0, 29.1, 26.9, 21.9, 19.5, −1.8, −4.1; HRMS (ESI) Calcd for C$_{28}$H$_{42}$O$_5$NaS$_2$Si$^+$ ([M+Na]$^+$) 573.2135. Found 573.2155.
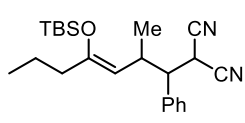
3p (dr = 1.6:1): ^{1}H NMR (600 MHz, CDCl$_3$) (for major isomer) δ 7.45-7.38 (5H, m), 4.37 (1H, d, J = 10.2 Hz), 4.34 (1H, d, J = 4.2 Hz), 2.99-2.91 (1H, m), 2.78 (1H, dd, J = 10.2, 4.2 Hz), 2.27 (1H, dt, J = 13.8, 8.4 Hz), 2.20 (1H, dt, J = 13.8, 7.2 Hz), 1.61-1.54 (2H, m), 0.97 (3H, t, J = 6.6 Hz), 0.95 (9H, s), 0.86 (3H, d, J = 6.6 Hz), 0.19 (3H, s), 0.17 (3H, s), (for minor isomer) δ 7.44-7.33 (5H, m), 4.30 (1H, d, J = 4.2 Hz), 4.27 (1H, d, J = 9.6 Hz), 3.33-3.25 (1H, m), 2.78 (1H, dd, J = 11.1, 4.2 Hz), 2.11 (1H, ddd, J = 15.0, 9.0, 5.7 Hz), 2.04 (1H, ddd, J = 15.0, 9.0, 6.8 Hz), 1.63-1.48 (2H, m), 1.01 (9H, s), 0.96 (3H, t, J = 7.2 Hz), 0.81 (3H, d, J = 6.8 Hz), 0.21 (6H, s); ^{13}C NMR (151 MHz, CDCl$_3$) (for major isomer) δ 155.7, 135.8, 129.3, 129.1, 128.8, 112.7, 112.1, 109.5, 53.6, 34.7, 34.1, 28.8, 25.8, 20.8, 20.5, 18.3, 14.0, –3.8, –4.4, (for minor isomer) δ 154.6, 136.1, 129.2, 128.9, 113.2, 112.0, 109.7, 53.7, 38.7, 32.2, 28.5, 26.0, 20.6, 19.5, 18.5, 13.9, –3.5, –3.6; HRMS (ESI) Calcd for C$_{23}$H$_{34}$ON$_2$NaSi$^+$ ([M+Na]$^+$) 405.2333. Found 405.2348.
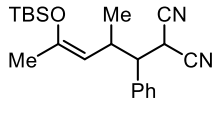
3q (dr = 1.5:1): ^{1}H NMR (400 MHz, CDCl$_3$) (for major diastereomer) δ 7.45-7.33 (5H, m), 4.32 (1H, d, J = 4.0 Hz), 4.24 (1H, d, J = 9.6 Hz), 3.34-3.22 (1H, m), 2.79 (1H, dd, J = 11.4, 4.0 Hz), 1.88 (3H, s), 1.01 (9H, s), 0.81 (3H, d, J = 7.2 Hz), 0.22 (6H, s), (for minor diastereomer) δ 7.40-7.31 (3H, m), 7.20-7.14 (2H, m), 4.14 (1H, d, J = 9.2 Hz), 4.00 (1H, d, J = 10.0 Hz), 3.39-3.29 (1H, m), 3.19 (1H, dd, J = 9.2, 5.6 Hz), 1.77 (3H, s), 0.98 (9H, s), 0.98 (3H, d, J = 7.2 Hz), 0.20 (3H, s), 0.18 (3H, s); ^{13}C NMR (151 MHz, CDCl$_3$) (for major diastereomer) δ 150.8, 136.2, 129.2, 128.9, 113.2, 112.1, 110.3, 53.6, 32.4, 28.6, 25.9, 23.1, 19.4, 18.5, –3.4, –3.5, (for minor diastereomer) δ 149.8, 135.2, 129.0, 128.6, 113.3, 112.5, 107.6, 52.8, 32.0, 27.3, 26.0, 23.1, 19.9, 18.5, –3.2, –3.6; HRMS (ESI) Calcd for C$_{21}$H$_{30}$ON$_2$NaSi$^+$ ([M+Na]$^+$) 377.2020. Found 377.2021.
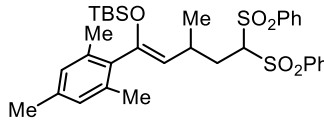
3r (*Z/E* = 5:1): ^{1}H NMR (600 MHz, CDCl$_3$) (for *Z* isomer) δ 8.04 (2H, d, J = 7.8 Hz), 7.78 (2H, d, J = 7.8 Hz), 7.70 (1H, t, J = 7.8 Hz), 7.57 (2H, t, J = 7.8 Hz), 7.49 (1H, t, J = 7.8 Hz), 7.30 (2H, t, J = 7.8 Hz), 6.82 (2H, s), 4.57 (1H, dd, J = 7.5, 2.1 Hz), 3.64 (1H, d, J = 9.6 Hz), 3.36-3.28 (1H, m), 2.34-2.28 (1H, m), 2.29 (3H, s), 2.24 (3H, s), 2.20 (3H, s), 1.94-1.88 (1H, m), 1.08 (3H, d, J = 6.6 Hz), 0.95 (9H, s), –0.13 (3H, s), –0.25 (3H, s): ^{13}C NMR (151 MHz, CDCl$_3$) (for *Z* isomer) δ 149.2, 139.2, 137.4(2), 137.4(0), 136.1, 135.7, 135.6, 134.4, 134.3, 129.8, 129.6, 129.0(2), 128.9(8), 128.5, 128.4, 115.7, 82.0, 32.5, 29.6, 25.8, 21.2, 21.0, 20.5, 18.4, –4.3; HRMS (ESI) Calcd for C$_{33}$H$_{44}$O$_5$NaS$_2$Si$^+$ ([M+Na]$^+$) 635.2292. Found 635.2305.
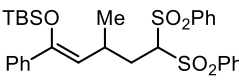
3s (*Z/E* = 6.7:1): ^{1}H NMR (600 MHz, CDCl$_3$) (for *Z* isomer) δ 8.12 (2H, d, *J* = 7.2 Hz), 7.71 (1H, d, *J* = 7.2 Hz), 7.60 (2H, t, *J* = 7.2 Hz), 7.57 (2H, d, *J* = 8.4 Hz), 7.40-7.26 (5H, m), 7.34 (1H, t, *J* = 7.2 Hz), 7.05 (2H, dd, *J* = 8.4, 7.2 Hz), 4.50 (1H, d, *J* = 8.4 Hz), 3.92 (1H, d, *J* = 10.2 Hz), 3.32-3.24 (1H, m), 2.46-2.42 (1H, m), 1.81-1.75 (1H, m), 1.06 (3H, d, *J* = 6.6 Hz), 0.98 (9H, s), 0.06 (3H, s), –0.11 (3H, s): ^{13}C NMR (151 MHz, CDCl$_3$) (for *Z* isomer) δ 152.1, 139.7, 139.6, 137.5, 134.5, 134.2, 129.8, 129.3, 129.1, 129.0, 128.3, 126.5, 114.7, 81.3, 33.0, 30.5, 26.1, 21.4, 18.6, –3.7, –3.9; HRMS (ESI) Calcd for C$_{30}$H$_{38}$O$_5$NaS$_2$Si$^+$ ([M+Na]$^+$) 593.1822. Found 593.1819.
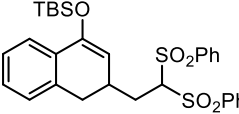
3t: ^{1}H NMR (600 MHz, CDCl$_3$) δ 7.92 (2H, d, *J* = 8.4 Hz), 7.80 (2H, d, *J* = 8.4 Hz), 7.69 (1H, t, *J* = 7.2 Hz), 7.64 (1H, t, *J* = 7.2 Hz), 7.55 (2H, dd, *J* = 8.4, 7.2 Hz), 7.48 (2H, dd, *J* = 8.4, 7.2 Hz), 7.33 (1H, d, *J* = 7.2 Hz), 7.17 (1H, t, *J* = 7.2 Hz), 7.14 (1H, t, *J* = 7.2 Hz), 7.00 (1H, d, *J* = 7.2 Hz), 4.97 (1H, d, *J* = 5.4 Hz), 4.40 (1H, t, *J* = 5.4 Hz), 2.92 (1H, dd, *J* = 15.0, 6.2 Hz), 2.90-2.83 (1H, m), 2.50 (1H, dd, 15.0, 5.4 Hz), 2.14-2.04 (2H, m), 1.00 (9H, s), 0.19 (3H, s), 0.16 (3H, s); ^{13}C NMR (151 MHz, CDCl$_3$) δ 149.5, 137.9, 137.8, 134.8, 134.6, 132.6, 129.8, 129.5, 129.3, 128.1, 126.6, 122.4, 105.6, 81.7, 33.6, 31.1, 29.7, 26.0, 18.4, –4.2, –4.4; HRMS (ESI) Calcd for C$_{30}$H$_{36}$O$_5$NaS$_2$Si$^+$ ([M+Na]$^+$) 591.1666. Found 591.1664.
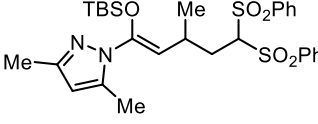
3u (*Z/E* = 1.7:1): ^{1}H NMR (600 MHz, CDCl$_3$) (for *Z* isomer) δ 8.03 (2H, d, *J* = 7.8 Hz), 7.83 (2H, d, *J* = 7.8 Hz), 7.69 (1H, t, *J* = 7.8 Hz), 7.56 (2H, t, *J* = 7.8 Hz), 7.53 (1H, t, *J* = 7.8 Hz), 7.36 (2H, t, *J* = 7.8 Hz), 5.83 (1H, s), 4.54 (1H, dd, *J* = 7.5, 2.4 Hz), 3.83 (1H, d, *J* = 11.0 Hz), 3.21-3.12 (1H, m), 2.35 (1H, ddd, *J* = 11.0, 7.5, 4.2 Hz), 2.24 (3H, s), 2.17 (3H, s), 1.93 (1H, ddd, *J* = 15.3, 11.0, 2.4 Hz), 1.09 (3H, d, *J* = 7.5 Hz), 0.94 (9H, s), –0.06 (6H, s), (for *E* isomer) δ 8.04 (2H, d, *J* = 7.8 Hz), 7.93 (2H, d, *J* = 7.8 Hz), 7.65 (1H, t, *J* = 7.8 Hz), 7.61 (1H, t, *J* = 7.8 Hz), 7.54 (2H, t, *J* = 7.8 Hz), 7.46 (2H, t, *J* = 7.8 Hz), 5.86 (1H, s), 5.58 (1H, dd, *J* = 6.6, 1.8 Hz), 4.61 (1H, d, *J* = 10.8 Hz), 2.21-2.16 (1H, m), 2.19 (3H, s), 2.18 (3H, s), 2.10-2.01 (2H, m), 0.95 (3H, d, *J* = 6.6 Hz), 0.89 (9H, s), 0.17 (3H, s), 0.00(4) (3H, s); ^{13}C NMR (151 MHz, CDCl$_3$) (for *Z* isomer) δ 148.4, 143.4, 139.4, 138.9, 137.4, 134.5, 134.3, 129.7(4), 129.6(5), 129.1(0), 129.0(8), 109.0, 106.3, 81.5, 32.4, 30.2, 25.7, 21.2, 18.3, 13.6, 11.9, –5.0, –5.3, (for *E* isomer) δ 148.9, 143.2, 140.0, 138.5, 137.9, 134.2(0), 134.1(8), 129.9, 129.7, 128.8(9), 128.8(6), 111.0, 106.0, 80.0, 31.7, 31.6, 25.6, 22.4, 18.1, 13.7, 11.1, –5.0, –5.1; HRMS (ESI): Calcd for C$_{29}$H$_{40}$O$_5$N$_2$NaS$_2$Si$^+$ ([M+Na]$^+$) 611.2040. Found 611.2035.
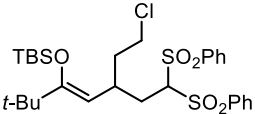
3v (*Z/E* = >20:1): ^{1}H NMR (600 MHz, CDCl$_3$) δ 7.89 (2H, d, *J* = 7.8 Hz), 7.87 (2H, d, *J* = 7.8 Hz), 7.66 (1H, t, *J* = 7.8 Hz), 7.64 (1H, t, *J* = 7.8 Hz), 7.52 (2H, t, *J* = 7.8 Hz), 7.50 (2H, t, *J* = 7.8 Hz), 4.57 (1H, d, *J* = 8.4 Hz), 4.21 (1H, d, *J* = 10.2 Hz), 3.60-3.49 (2H, m), 3.26-3.17 (1H, m), 2.36-2.30 (1H, m), 1.99-1.93 (1H, m), 1.93-1.82 (2H, m), 1.08 (9H, s), 1.04 (9H, s), 0.34 (3H, s), 0.22 (3H, s); ^{13}C NMR (151 MHz, CDCl$_3$) δ 162.4, 138.8, 137.3, 134.7, 134.3, 130.1, 129.3, 129.2, 129.1, 105.6, 81.1, 41.9, 39.5, 37.3, 33.0, 30.4, 29.1, 26.9, 19.6, −1.8, −3.5; HRMS (ESI) Calcd for C$_{29}$H$_{43}$O$_5$ClNaS$_2$Si$^+$ ([M+Na]$^+$) 621.1902. Found 621.1909.
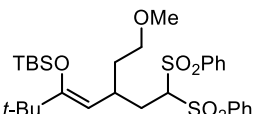
3w (*Z/E* = >20:1): ^{1}H NMR (600 MHz, CDCl$_3$) δ 7.90 (2H, d, *J* = 8.4 Hz), 7.87 (2H, d, *J* = 7.8 Hz), 7.65 (1H, t, *J* = 7.2 Hz), 7.62 (1H, t, *J* = 7.2 Hz), 7.51 (2H, dd, *J* = 7.8, 7.2 Hz), 7.49 (2H, dd, *J* = 8.4, 7.2 Hz), 4.61 (1H, d, *J* = 6.6 Hz), 4.24 (1H, d, *J* = 11.4 Hz), 3.49-3.40 (2H, m), 3.32 (3H, s), 3.22-3.15 (1H, m), 2.36 (1H, ddd, *J* = 15.9, 8.7, 4.2 Hz), 1.97 (1H, dd, *J* = 13.8, 11.4 Hz), 1.71-1.61 (2H, m), 1.07 (9H, s), 1.04 (9H, s), 0.35 (3H, s), 0.20 (3H, s); ^{13}C NMR (151 MHz, CDCl$_3$) δ 161.4, 139.2, 137.4, 134.5, 134.1, 130.2, 129.3, 129.1, 129.0, 106.6, 81.3, 70.5, 58.8, 37.3, 35.9, 32.1, 30.7, 29.2, 26.9, 19.6, −1.9, −3.8; HRMS (ESI) Calcd for C$_{30}$H$_{46}$O$_6$NaS$_2$Si$^+$ ([M+Na]$^+$) 617.2397. Found 617.2408.
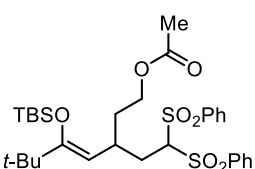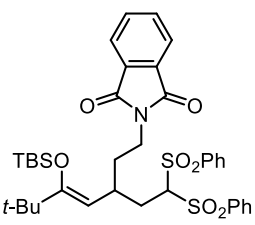
3x (*Z/E* = >20:1): ^{1}H NMR (600 MHz, CDCl$_3$) δ 7.89 (2H, d, *J* = 8.4 Hz), 7.87 (2H, d, *J* = 8.4 Hz), 7.65 (1H, t, *J* = 7.8 Hz), 7.63 (1H, t, *J* = 7.8 Hz), 7.50 (2H, dd, *J* = 8.4, 7.8 Hz), 7.49 (2H, dd, *J* = 8.4, 7.8 Hz), 4.61 (1H, d, *J* = 8.4 Hz), 4.24 (1H, d, *J* = 10.2 Hz), 4.18-4.08 (2H, m), 3.30-3.21 (1H, m), 2.40-2.33 (1H, m), 2.04 (3H, s), 1.92 (1H, t, *J* = 13.2 Hz), 1.81-1.66 (2H, m), 1.08 (9H, s), 1.04 (9H, s), 0.37 (3H, s), 0.21 (3H, s); ^{13}C NMR (151 MHz, CDCl$_3$) δ 171.2, 162.0, 139.1, 137.3, 134.6, 134.2, 130.2, 129.2, 129.1, 129.0, 106.2, 81.1, 62.1, 37.3, 34.8, 31.8, 30.4, 29.1, 26.9, 21.2, 19.6, −1.8, −3.8; HRMS (ESI) Calcd for C$_{31}$H$_{46}$O$_7$NaS$_2$Si$^+$ ([M+Na$^+$]) 645.2346. Found 645.2352.

3y (*Z/E* = >20:1): ^{1}H NMR (600 MHz, CDCl$_3$) δ 7.94 (2H, d, *J* = 7.8 Hz), 7.91 (2H, d, *J* = 7.8 Hz), 7.87-7.82 (2H, m), 7.74-7.69 (2H, m), 7.67 (1H, t, *J* = 7.8 Hz), 7.64 (1H, t, *J* = 7.8 Hz), 7.54 (2H, t, *J* = 7.8 Hz), 7.51 (2H, t, *J* = 7.8 Hz), 4.62 (1H, d, *J* = 8.4 Hz), 4.24 (1H, d, *J* = 10.8 Hz), 3.80-3.67 (2H, m), 3.30-3.22 (1H, m), 2.42 (1H, ddd, *J* = 14.7, 8.4, 3.6 Hz), 2.06-1.98 (1H, m), 1.82-1.78 (1H, m), 1.77-1.69 (1H, m), 1.06 (9H, s), 1.05 (9H, s), 0.41 (3H, s), 0.25 (3H, s); ^{13}C NMR (151 MHz, CDCl$_3$) δ 168.2, 162.2, 139.0, 137.3, 134.6, 134.2, 134.1,

132.4, 130.2, 129.4, 129.2, 129.1, 123.3, 105.7, 81.2, 37.3, 35.6, 34.6, 32.5, 30.4, 29.1, 26.9, 19.6, –1.8, –3.6; HRMS (ESI) Calcd for $C_{37}H_{47}O_7NNaS_2Si^+$ ([M+Na]$^+$) 732.2455. Found 732.2424.
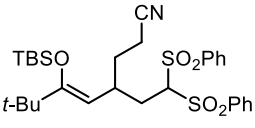
3z (Z/E = >20:1): ^{1}H NMR (600 MHz, CDCl$_3$) δ 7.88 (2H, d, J = 8.4 Hz), 7.85 (2H, d, J = 7.8 Hz), 7.67 (1H, t, J = 8.4 Hz), 7.65 (1H, t, J = 7.8 Hz), 7.55-7.48 (4H, m), 4.51 (1H, d, J = 8.4 Hz), 4.18 (1H, d, J = 10.2 Hz), 3.21-3.12 (1H, m), 2.41-2.31 (2H, m), 2.30-2.24 (1H, m), 1.96 (1H, t, J = 12.6 Hz), 1.88-1.80 (1H, m), 1.74-1.65 (1H, m), 1.08 (9H, s), 1.03 (9H, s), 0.31 (3H, s), 0.24 (3H, s); ^{13}C NMR (151 MHz, CDCl$_3$) δ 163.3, 138.6, 137.2, 134.8, 134.4, 130.0, 129.3, 129.2, 129.1, 119.9, 104.6, 81.0, 37.4, 33.8, 31.9, 30.3, 29.1, 26.8, 19.5, 14.4, –1.8, –3.3; HRMS (ESI) Calcd for $C_{30}H_{43}O_5NNaS_2Si^+$ ([M+Na]$^+$) 612.2244. Found 612.2258.
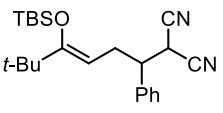
3Aa (Z/E = >20:1): ^{1}H NMR (600 MHz, CDCl$_3$) δ 7.42-7.34 (3H, m), 7.33-7.30 (2H, m), 4.33 (1H, t, J = 6.6 Hz), 3.98 (1H, d, J = 5.4 Hz), 3.21 (1H, td, J = 7.8, 5.4 Hz), 2.78 (1H, ddd, J = 14.8, 7.8, 6.6 Hz), 2.60 (1H, ddd, J = 14.8, 7.8, 6.6 Hz), 1.01 (9H, s), 1.00 (9H, s), 0.24 (3H, s), 0.21 (3H, s); ^{13}C NMR (151 MHz, CDCl$_3$) δ 162.0, 137.1, 129.2, 128.9, 128.1, 112.3, 111.9, 98.5, 47.2, 37.0, 29.2, 29.0, 28.9, 26.6, 19.3, –2.3, –2.6; HRMS (ESI): Calcd for $C_{23}H_{33}ON_2Si^-$ ([M−H]$^-$) 381.2357. Found 381. 2356.
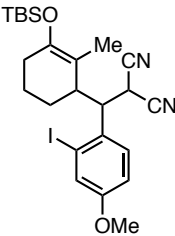
3Ab (dr = 2.0:1): ^{1}H NMR (600 MHz, CDCl$_3$) (for major diastereomer) δ 7.49 (1H, d, J = 8.4 Hz), 7.44 (1H, d, J = 3.0 Hz), 6.97 (1H, dd, J = 8.4, 3.0 Hz), 4.03 (1H, d, J = 6.0 Hz), 3.98 (1H, dd, J = 8.1, 6.0 Hz), 3.81 (3H, s), 2.78-2.72 (1H, m), 2.18-2.04 (2H, m), 1.79-1.64 (4H, m), 1.31 (3H, s), 0.92 (9H, s), 0.13 (3H, s), 0.11 (3H, s); ^{13}C NMR (151 MHz, CDCl$_3$) (for major diastereomer) δ 159.7, 147.9, 132.0, 128.2, 125.6, 114.9, 112.6, 111.9, 111.1, 103.3, 55.7, 50.5, 42.6, 30.0, 26.2, 25.9, 25.4, 19.9, 18.3, 16.6, –3.2, –3.3; HRMS (ESI) Calcd for $C_{24}H_{33}O_2N_2INaSi^+$ ([M+Na]$^+$) 559.1248. Found 559.1255.
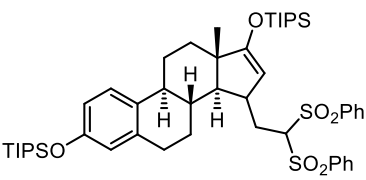
3Ac (dr = 9.2:1): ^{1}H NMR (600 MHz, CDCl$_3$) (for major isomer) δ 8.06 (2H, d, J = 7.8 Hz), 7.88 (2H, d, J = 7.8 Hz), 7.73 (1H, t, J = 7.8 Hz), 7.66 (1H, t, J = 7.2 Hz), 7.61 (2H, t, J = 7.8 Hz), 7.54 (2H, t, J = 7.8 Hz), 7.05 (1H, d, J = 9.0 Hz), 6.65 (1H, dd, J = 8.1, 2.4 Hz), 6.61 (1H, s), 4.50 (1H, d, J = 3.0 Hz), 4.47 (1H, dd, J = 10.2, 2.4 Hz), 3.00-2.94 (1H, m), 2.80-2.78 (2H, m), 2.32-2.21 (3H, m), 2.15 (1H, ddd, J = 14.7, 10.2, 4.8 Hz), 1.85 (1H, dd, J = 11.7, 7.2 Hz), 1.82-1.74 (2H, m), 1.60-1.37 (4H, m), 1.30-1.18 (6H, m), 1.12 (18H, br), 1.10 (18H, br), 0.91 (3H, s); ^{13}C NMR (151 MHz, CDCl$_3$) (for major isomer) δ 167.7,

45

154.0, 138.2, 138.1, 137.8, 134.7, 134.6, 133.2, 129.9, 129.7, 129.2(2), 129.1(8), 125.4, 119.8, 116.9, 98.6, 83.5, 55.1, 45.4, 45.3, 38.6, 35.9, 35.1, 29.2, 27.5, 26.2, 25.6, 21.5, 18.1, 12.9, 12.7; HRMS (ESI) Calcd for $C_{50}H_{73}O_6S_2Si_2^-$ ([M−H]$^-$) 889.4382. Found 889.4387.

Derivatization of Alkylated Enol Silyl Ethers

TBSO ... SO$_2$Ph / SO$_2$Ph **3i** → Selectfluor, MeCN, 0 °C to r.t. → O ... F, SO$_2$Ph / SO$_2$Ph **5a**
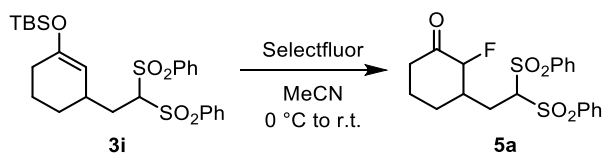
To a solution of **3i** (30.7 mg, 0.059 mmol) in MeCN (0.6 mL, 0.1 M) was added Selectfluor (23.0 mg, 0.065 mmol) at 0 °C, and the resulting reaction mixture was allowed to warm to room temperature. After stirring for 3 h, the solvent was removed under reduced pressure. The crude residue was purified by column chromatography on silica gel (hexane/EtOAc = 1:1 as eluent) to afford **5a** in 84% yield (21.1 mg, 0.050 mmol, dr = 1.4:1). ^{1}H NMR (400 MHz, CDCl$_3$) (for major diastereomer) δ 7.93 (2H, dd, J = 8.4, 1.2 Hz), 7.89 (2H, dd, J = 8.8, 1.2 Hz), 7.70 (1H, t, J = 7.6 Hz), 7.68 (1H, t, J = 8.0 Hz), 7.62-7.52 (4H, m), 4.82-4.77 (1H, m), 4.57 (1H, dd, J_{H-F} = 49.8 Hz, J_{H-H} = 11.0 Hz), 2.57-2.48 (2H, m), 2.46-2.24 (3H, m), 2.10-1.98 (2H, m), 1.69-1.44 (2H, m), (for minor diastereomer) δ 7.97 (2H, dd, J = 8.4, 1.0 Hz), 7.92 (2H, dd, J = 8.8, 1.6 Hz), 7.76-7.70 (2H, m), 7.64-7.57 (4H, m), 4.70 (1H, dd, J_{H-F} = 50.6 Hz, J_{H-H} = 3.8 Hz), 4.45 (1H, t, J = 5.8 Hz), 2.76-2.63 (1H, m), 2,63-2,53 (1H, m), 2.36-2.16 (3H, m), 1.94-1.68 (4H, m); ^{13}C NMR (151 MHz, CDCl$_3$) (for major diastereomer) δ 203.2 (d, J_{C-F} = 14.3 Hz), 138.1, 137.1, 134.9, 134.8, 129.8, 129.6, 129.4, 129.3, 97.6 (d, J_{C-F} = 192.4 Hz), 80.9 (d, J_{C-F} = 4.2 Hz), 43.4 (d, J_{C-F} = 16.0 Hz), 39.8, 29.9, 29.8 (d, J_{C-F} = 8.8 Hz), 24.7, (for minor isomer) δ 205.0 (d, J_{C-F} = 18.7 Hz), 137.8, 137.1, 135.0(4), 134.9(8), 129.8, 129.4(4), 129.4(0), 94.1 (d, J_{C-F} = 188.0 Hz), 81.3, 41.6 (d, J_{C-F} = 18.7 Hz), 38.8, 25.9 (d, J_{C-F} = 5.9 Hz), 25.3, 23.5; HRMS (ESI) Calcd for $C_{20}H_{20}O_5FNaS_2^+$ ([M+Na]$^+$) 447.0707. Found 447.0703.

TBSO ... SO$_2$Ph / SO$_2$Ph **3i** + allyl methyl carbonate (O ... O—OMe) → Pd$_2$dba$_3$·CHCl$_3$, PPh$_3$, Et$_3$N, CH$_2$Cl$_2$, r.t. → TBSO ... SO$_2$Ph / SO$_2$Ph **5b**
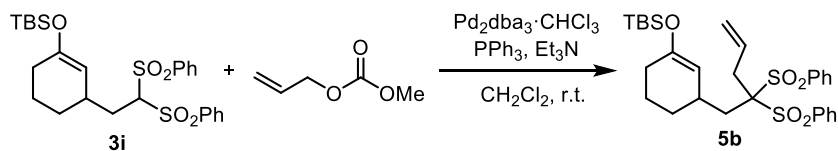
To a flame-dried Schlenk tube were added **3i** (72.9 mg, 0.14 mmol, 1 equiv), Pd$_2$dba$_3$·CHCl$_3$ (4.35 mg, 0.0042 mmol, [Pd] 6 mol%) and PPh$_3$ (5.51 mg, 0.021 mmol, 15 mol%) and the tube was degassed by alternating vacuum evacuation/Ar backfill. Then, CH$_2$Cl$_2$ (0.7 mL, 0.2 M) was introduced via syringe and the mixture was stirred for 10 min. After the addition of a solution of allyl methyl carbonate (19.1 μL, 0.17 mmol, 1.2 equiv) and Et$_3$N (21.5 μL, 0.15 mmol, 1.1 equiv) in CH$_2$Cl$_2$ (0.7 mL, 0.2 M), the whole reaction mixture was stirred at room temperature for 24 h and then diluted with

CH$_2$Cl$_2$ and brine. The extractive work-up was carried out with CH$_2$Cl$_2$ and the combined organic layers were dried over Na$_2$SO$_4$, filtered, and concentrated. The crude product was purified by column chromatography on silica gel (hexane/EtOAc = 5:1 as eluent) to afford **5b** in 86% yield (67.3 mg, 0.12 mmol, 86%): ^{1}H NMR (600 MHz, CDCl$_3$) δ 8.06-8.02 (4H, m), 7.70 (2H, t, J = 7.8 Hz), 7.57 (4H, t, J = 7.8 Hz), 6.05-5.97 (1H, m), 5.22 (1H, br), 5.20-5.18 (1H, brm), 4.78 (1H, br), 3.21-3.12 (2H, m), 2.91-2.85 (1H, m), 2.26 (1H, dd, J = 15.6, 5.1 Hz), 2.18 (1H, dd, J = 15.6, 5.1 Hz), 2.00-1.88 (2H, m), 1.82-1.75 (1H, m), 1.69-1.62 (1H, m), 1.60-1.51 (1H, m), 1.27-1.19 (1H, m), 0.90 (9H, s), 0.09 (6H, s); ^{13}C NMR (151 MHz, CDCl$_3$) δ 151.6, 137.6, 137.5, 134.6, 131.6, 131.1, 128.6(8), 128.6(5), 120.0, 109.7, 92.5, 37.3, 34.4, 31.0, 29.9, 29.6, 25.8, 21.2, 18.2, –4.2, –4.3; HRMS (ESI) Calcd for C$_{29}$H$_{40}$O$_5$NaS$_2$Si$^+$ ([M+Na]$^+$) 583.1979. Found 583.1974.
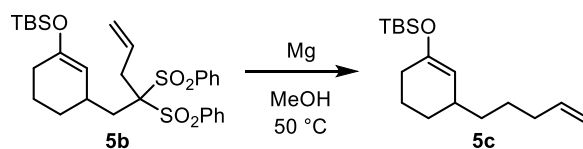
To a flame-dried test tube were added **5b** (26.4 mg, 0.047 mmol, 1 equiv) and anhydrous MeOH (1.2 mL, 0.04 M), and the reaction mixture was heated to 50 °C. To this solution was added Mg (22.9 mg, 0.94 mmol, 20 equiv) in three portions over 3 h at the same temperature. After stirring for additional 4 h, the reaction mixture was cooled to room temperature, filtered through a pad of Celite, and evaporated to remove the solvent. The crude residue was diluted with CH$_2$Cl$_2$ and brine, and then extractive work-up was carried out with CH$_2$Cl$_2$. The combined organic layers were dried over Na$_2$SO$_4$, filtered, and concentrated. The crude product was purified by silica gel column chromatography (hexane/EtOAc = 5:1 as eluent) to afford **5c** in 60% yield (7.9 mg, 0.028 mmol). ^{1}H NMR (400 MHz, CDCl$_3$) δ 5.88-5.76 (1H, m), 5.04-4.91 (2H, m), 4.79 (1H, brs), 2.16-1.89 (5H, m), 1.80-1.64 (2H, m), 1.61-1.48 (1H, m), 1.41 (2H, quin, J = 7.6 Hz), 1.34-1.20 (2H, m) 1.14-1.03 (1H, m), 0.92 (9H, s), 0.12 (6H, s); ^{13}C NMR (151 MHz, CDCl$_3$) δ 150.7, 139.3, 114.4, 109.8, 36.7, 34.7, 34.2, 30.2, 29.0, 26.5, 25.9, 21.9, 18.2, –4.2, –4.3.
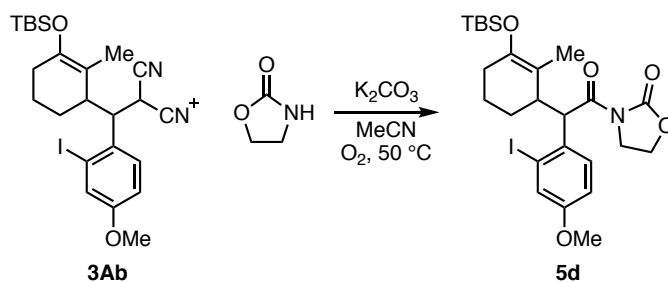
To a round-bottom flask were added **3Ab** (107.3 mg, 0.20 mmol, 1 equiv), K$_2$CO$_3$ (110.6 mg, 0.80 mmol, 4 equiv), and MeCN (2.0 mL, 0.1 M). The flask was then degassed and backfilled with O$_2$. To

this mixture was added 2-oxazolidone (69.7 mg, 0.80 mmol, 4 equiv). The reaction mixture was heated to 50 °C and stirred there for 24 h under O$_2$ atmosphere (balloon), and then diluted with CH$_2$Cl$_2$ and filtered through a pad of Celite. The filtrates were concentrated and the crude material was purified by column chromatography on silica gel (hexane/EtOAc = 5:1) to afford **5d** in 70% yield (82.5 mg, 0.14 mmol). ^{1}H NMR (600 MHz, CDCl$_3$) δ 7.41 (1H, d, J = 3.0 Hz), 7.21 (1H, d, J = 8.7 Hz), 6.81 (1H, dd, J = 8.7, 3.0 Hz), 5.53 (1H, d, J = 6.6 Hz), 4.38-4.33 (1H, m), 4.31-4.26 (1H, m), 4.05-3.99 (1H, m), 3.97-3.92 (1H, m), 3.76 (3H, s), 2.92-2.85 (1H, m), 2.16-2.09 (1H, m), 2.03-1.96 (1H, m), 1.92-1.85 (1H, m), 1.81-1.75 (1H, m), 1.54-1.47 (1H, m), 1.39-1.32 (1H, m), 1.30 (3H, s), 0.92 (9H, s), 0.12 (3H, s), 0.10 (3H, s); ^{13}C NMR (151 MHz, CDCl$_3$) δ 173.0, 158.8, 152.7, 146.8, 131.9, 129.5, 125.5, 114.1, 111.9, 102.5, 61.7, 55.6, 53.7, 43.3, 43.2, 30.6, 26.6, 26.0, 21.2, 18.3, 15.6, –3.3, –3.4;   HRMS (ESI) Calcd for C$_{25}$H$_{36}$O$_5$NINaSi$^+$ ([M+Na]$^+$) 608.1300. Found 608.1294.
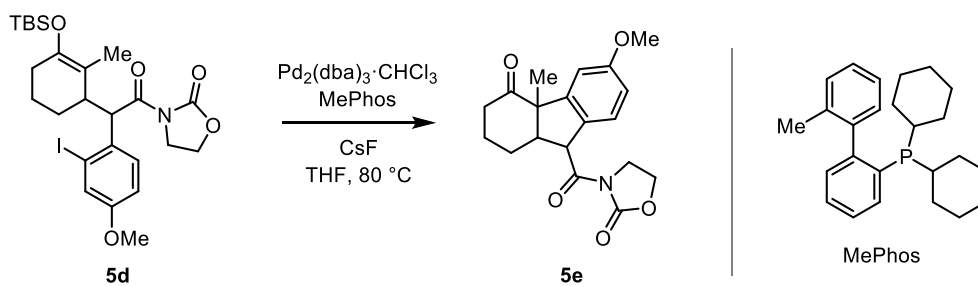
To a flame-dried Schlenk were added **5d** (82.0 mg, 0.14 mmol, 1 equiv), Pd$_2$dba$_3$·CHCl$_3$ (7.25 mg, 0.007 mmol, [Pd] 10 mol%), MePhos (6.12 mg, 0.017 mmol, 12 mol%), and CsF (33.0 mg, 0.21 mmol, 1.5 equiv). The Schlenk was then elaborately degassed and backfilled with Ar. Toluene (2.8 mL, 0.05 M) was added via syringe, and the reaction mixture was heated to 100 °C. After stirring overnight, the reaction mixture was cooled to room temperature and diluted with CH$_2$Cl$_2$. The mixture was filtered through a short pad of silica gel with the aid of EtOAc, and the filtrates were concentrated. The crude material was purified by column chromatography on silica gel (hexane/EtOAc = 3:1 to 1:3 as eluent) to afford **5e** in 56% yield (27.0 mg, 0.078 mmol, dr = 4.2:1). ^{1}H NMR (400 MHz, CDCl$_3$) (for major diastereomer) δ 7.02 (1H, d, J = 8.7 Hz), 6.79 (1H, dd, J = 8.7, 2.4 Hz), 6.75 (1H, d, J = 2.4 Hz), 5.14 (1H, d, J = 6.0 Hz), 4.48 (2H, t, J = 8.0 Hz), 4.10 (2H, t, J = 8.0 Hz), 3.79 (3H, s), 2.97 (1H, q, J = 6.0 Hz), 2.46 (1H, ddd, J = 16.0, 9.0, 6.0 Hz), 2.31 (1H, dt, J = 16.0, 6.0 Hz), 2.18-2.11 (1H, m), 1.99-1.91 (1H, m), 1.89-1.81 (1H, m), 1.75-1.68 (1H, m), 1.50 (3H, s), (for minor diastereomer) δ 7.21 (1H, d, J = 8.4 Hz), 6.82 (1H, dd, J = 8.4, 1.8 Hz), 6.53 (1H, d, J = 1.8 Hz), 5.36 (1H, d, J = 6.0 Hz), 4.54-4.45 (2H, m), 4.23-4.17 (1H, m), 4.10-4.05 (1H, m), 3.76 (3H, s), 3.15 (1H, dt, J = 11.4, 6.0 Hz), 2.45-2.40 (1H, m), 2.23 (1H, ddd, J = 15.6, 13.8, 5.4 Hz), 1.92-1.86 (1H, m), 1.68-1.59 (1H, m), 1.53-1.42 (2H, m), 1.39 (3H, s); ^{13}C NMR (151 MHz, CDCl$_3$) (for major diastereomer) δ 212.7, 174.4, 160.0, 153.7, 147.6, 131.7, 125.6, 114.5, 110.1, 62.2, 59.9, 55.6, 54.0, 52.2, 43.3, 38.7, 27.1, 25.2, 22.0, (for minor diastereomer) δ 211.2, 172.1, 160.0, 153.4, 147.8, 130.1, 127.9, 114.0, 108.0, 62.3, 59.6, 55.6,

52.6, 52.1, 42.9, 39.5, 25.4, 23.5, 23.2; HRMS (ESI) Calcd for Calcd for $C_{19}H_{21}O_5NNa^+$ ([M+Na]$^+$) 366.1312. Found 366.1317.

3u → **S9**

Selectfluor
MeCN
0 °C, r.t.
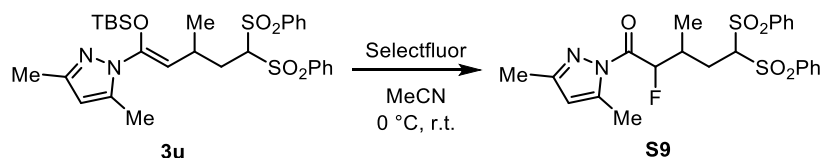
To a solution of **3u** (58.9 mg, 0.10 mmol, 1 equiv) in MeCN (1.0 mL, 0.1 M) was added Selectfluor (35.4 mg, 0.10 mmol, 1 equiv) at 0 °C, and the reaction mixture was allowed to warm to room temperature. After stirring for 24 h, the solvent was removed under reduced pressure. The crude product was purified by column chromatography on silica gel (hexane/EtOAc = 3:1 as eluent) to afford **S9** in 68% yield (33.3 mg, 0.068 mmol, dr = 2.5:1). ^{1}H NMR (400 MHz, CDCl$_3$) (for major diastereomer) δ 7.93 (2H, d, J = 7.6 Hz), 7.88 (2H, d, J = 7.2 Hz), 7.76-7.64 (2H, m), 7.64-7.51 (4H, m), 6.01 (1H, s), 5.92 (1H, dd, $J_{H–F}$ = 50.0 Hz, $J_{H–H}$ = 3.2 Hz), 4.57 (1H, dd, J = 7.6, 4.4 Hz), 2.86-2.65 (1H, m), 2.56 (3H, s), 2.37 (1H, ddd, J = 16.0, 7.2, 5.3 Hz), 2.23 (3H, s), 2.10 (1H, ddd, J = 16.0, 8.9, 4.5 Hz), 1.03 (3H, d, J = 7.2 Hz), (for minor diastereomer) δ 8.05 (2H, d, J = 7.6 Hz), 8.01 (2H, d, J = 7.2 Hz), 7.76-7.64 (2H, m), 7.64-7.51 (4H, m), 6.01 (1H, s), 5.75 (1H, brd, $J_{H–F}$ = 50.4 Hz), 4.97 (1H, dd, J = 6.0, 4.4 Hz), 2.67-2.58 (1H, m), 2.55 (3H, s), 2.42 (1H, ddd, J = 15.2, 8.4, 4.0 Hz), 2.28-2.16 (1H, m), 2.24 (3H, s), 0.94 (3H, d, J = 7.6 Hz); ^{13}C NMR (151 MHz, CDCl$_3$) (for major diastereomer) δ 168.7 (d, $J_{C–F}$ = 24.5 Hz), 153.5, 144.9, 137.8, 137.6, 134.8, 134.7, 129.8, 129.7, 129.3, 129.2, 111.9, 91.9 (d, $J_{C–F}$ = 182.3 Hz), 81.5, 34.7 (d, $J_{C–F}$ = 18.7 Hz), 27.2 (d, $J_{C–F}$ = 5.9 Hz), 16.7, 14.3, 14.0, (for minor diastereomer) δ 167.9 (d, $J_{C–F}$ = 23.1 Hz), 153.6, 145.0, 137.9, 137.3, 135.0, 134.9, 130.0, 129.9, 129.4, 129.3, 111.7, 89.1 (d, $J_{C–F}$ = 185.0 Hz), 81.4, 35.3 (d, $J_{C–F}$ = 20.2 Hz), 29.6, 14.2, 14.1, 12.9 (d, $J_{C–F}$ = 8.8 Hz); HRMS (ESI) Calcd for $C_{23}H_{25}O_5N_2FNaS_2^+$ ([M+Na]$^+$) 515.1081. Found 515.1087.

S9 → **5f**
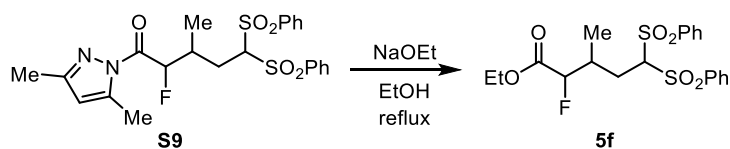
NaOEt
EtOH
reflux

To a flame-dried test tube were added **S9** (49.3 mg, 0.10 mmol, 1 equiv) and anhydrous EtOH (1.0 mL, 0.1 M), and the test tube was degassed and backfilled with Ar. NaOEt (15.2 mg, 0.22 mmol, 2.2 equiv) was added at 0 °C, and the reaction mixture was refluxed with stirring overnight. After cooling to room temperature, the reaction was quenched with aqueous solution of 1 N HCl. The extractive work-up was carried out with EtOAc and the combined organic layers were dried over Na$_2$SO$_4$, filtered,

and concentrated. The crude residue was purified by column chromatography on silica gel (hexane/EtOAc = 3:1) to afford **5g** in 90% yield (39.8 mg, 0.090 mmol). ^{1}H NMR (400 MHz, CDCl$_3$) (for major diastereomer) δ 7.99-7.91 (4H, m), 7.75-7.67 (2H, m), 7.63-7.56 (4H, m), 4.72 (1H, dd, J_{H-F} = 48.8 Hz, J_{H-H} = 4.4 Hz), 4.55 (1H, dd, J = 7.4, 4.6 Hz), 4.27 (2H, q, J = 7.2 Hz), 2.69-2.50 (1H, m), 2.38-2.27 (1H, m), 2.11 (1H, ddd, J = 15.8, 8.8, 4.8 Hz), 1.30 (3H, t, J = 7.2 Hz), 0.98 (3H, d, J = 6.8 Hz), (for minor diastereomer) δ 7.99-7.91 (4H, m), 7.75-7.67 (2H, m), 7.63-7.56 (4H, m), 4.80 (1H, dd, J_{H-F} = 49.2 Hz, J_{H-H} = 2.8 Hz), 4.49 (1H, t, J = 6.0 Hz), 4.26 (2H, q, J = 7.2 Hz), 2.69-2.50 (1H, m), 2.38-2.27 (1H, m), 2.24-2.16 (1H, m), 1.30 (3H, t, J = 7.2 Hz), 0.89 (3H, d, J = 6.8 Hz); ^{13}C NMR (151 MHz, CDCl$_3$) (for major diastereomer) δ 168.7 (d, J_{C-F} = 24.6 Hz), 137.7, 137.6, 134.9, 129.9, 129.8, 129.3(7), 129.3(5), 92.2 (d, J_{C-F} = 187.2 Hz), 81.4, 62.0, 34.5, 27.6 (d, J_{C-F} = 5.7 Hz), 15.58 (d, J_{C-F} = 2.9 Hz), 14.2, (for minor diastereomer) δ 168.5 (d, J_{C-F} = 24.6 Hz), 137.7, 137.5, 135.0, 134.9, 129.9, 129.8, 129.3, 90.7 (d, J_{C-F} = 188.0 Hz), 81.5, 61.9, 34.6, 28.8, 14.3, 13.2 (d, J_{C-F} = 4.4 Hz); HRMS (ESI) Calcd for C$_{20}$H$_{23}$O$_6$FNaS$_2^+$ ([M+Na]$^+$) 465.0812. Found 465.0820.

To a solution of **3u** (41.2 mg, 0.07 mmol, 1 equiv) in THF (0.7 mL, 0.1 M) was added a 1 M THF solution of TBAF (70 µL, 0.07 mmol, 1 equiv) dropwise at 0 °C. The reaction mixture was stirred at 0 °C for 1 h and then quenched with saturated aqueous solution of NaHCO$_3$. The extractive work-up was performed with EtOAc. The combined organic layers were dried over Na$_2$SO$_4$, filtered, and concentrated. The crude material was purified by column chromatography on silica gel (hexane/EtOAc = 3:1 as eluent) to afford **S10** in 96% yield (31.9 mg, 0.067 mmol). ^{1}H NMR (400 MHz, CDCl$_3$) δ 8.01 (2H, d, J = 7.2 Hz), 7.97 (2H, d, J = 7.2 Hz), 7.69 (1H, t, J = 7.6 Hz), 7.67 (1H, t, J = 7.2 Hz), 7.60-7.52 (4H, m), 5.96 (1H, s), 4.95 (1H, t, J = 5.4 Hz), 3.10 (1H, dd, J = 16.2, 4.8 Hz), 2.78 (1H, dd, J = 16.2, 7.4 Hz), 2.52 (3H, s), 2.40-2.31 (1H, m), 2.27-2.10 (2H, m), 2.21 (3H, s), 0.99 (3H, d, J = 6.8 Hz). ^{13}C NMR (151 MHz, CDCl$_3$) δ 172.4, 152.2, 144.3, 138.1, 137.7, 134.7, 130.0, 129.8, 129.2(0), 129.1(5), 111.4, 81.5, 41.8, 32.5, 29.2, 20.2, 14.7, 14.0; HRMS (ESI) Calcd for C$_{23}$H$_{26}$O$_5$N$_2$NaS$_2^+$ ([M+Na]$^+$) 497.1175. Found 497.1170.

The solution of **S10** (47.5 mg, 0.10 mmol, 1 equiv) and benzylamine (22 μL, 0.20 mmol, 2 equiv) in toluene (0.4 mL, 0.25 M) was stirred at 50 °C for 3 h. After cooling to room temperature, the reaction was quenched with 1 N aqueous solution of HCl and extractive work-up was carried out with CH_2Cl_2. The combined organic layers were washed with saturated aqueous solution of $NaHCO_3$ and dried over Na_2SO_4, filtered, and concentrated. The crude product was purified by column chromatography on silica gel (hexane/EtOAc = 1:1) to afford **5g** in 88% yield (42.8 mg, 0.088 mmol). ^{1}H NMR (400 MHz, CDCl$_3$) δ 7.95-7.92 (4H, m), 7.69-7.65 (2H, m), 7.57-7.52 (4H, m), 7.34-7.30 (2H, m), 7.29-7.25 (3H, m), 5.93 (1H, brs), 4.86 (1H, t, J = 3.4 Hz), 4.45 (1H, dd, J = 15.2, 6.3 Hz), 4.41 (1H, dd, J = 15.2, 6.3 Hz), 2.30-2.17 (3H, m), 2.15-2.07 (2H, m), 0.92 (3H, d, J = 7.2 Hz); ^{13}C NMR (151 MHz, CDCl$_3$) δ 171.3, 138.2, 138.0, 137.7, 134.7(0), 134.6(7), 129.9, 129.6, 129.3, 129.2, 128.9, 128.0, 127.7, 81.4, 43.8, 43.5, 32.3, 29.5, 20.4; HRMS (ESI) Calcd for $C_{25}H_{26}O_5NS_2^-$ ([M−H]$^-$) 484.1247. Found 484.1251.

Square Wave Voltammetry

   Square wave voltammetry (SWV) measurements of representative enol silyl ether **1a**, electron deficient olefin **2a**, and alkylated enol silyl ether **3a** were performed on ALS/CH Instruments Electrochemical Analyzer using a glassy carbon working electrode, a Pt wire counter electrode, and a ferrocene/ferrocenium reference electrode. Voltammograms were taken at room temperature in a 100 mM MeCN solution of tetrabutylammonium perchlorate ($Bu_4N \cdot ClO_4$) containing 1 mM of the designated substance. For conversion to the SCE couple, it is known that Fc/Fc^+ is 380 mV more positive than SCE in MeCN; this value was added from obtained potentials in Fc/Fc^+ to determine potentials against SCE.


TBSO

E_{ox} = 1.52 V (vs SCE in CH_3CN)

NC   CN

E_{red} = -0.70 V (vs SCE in CH_3CN)
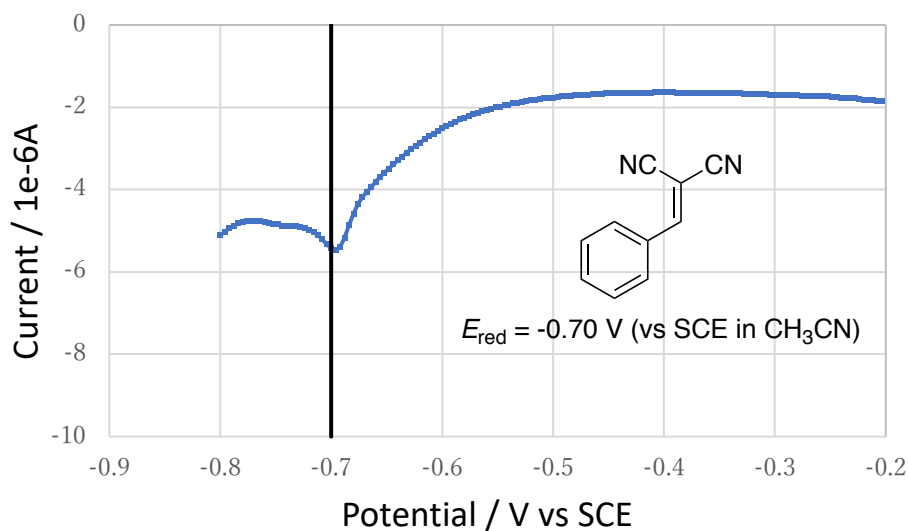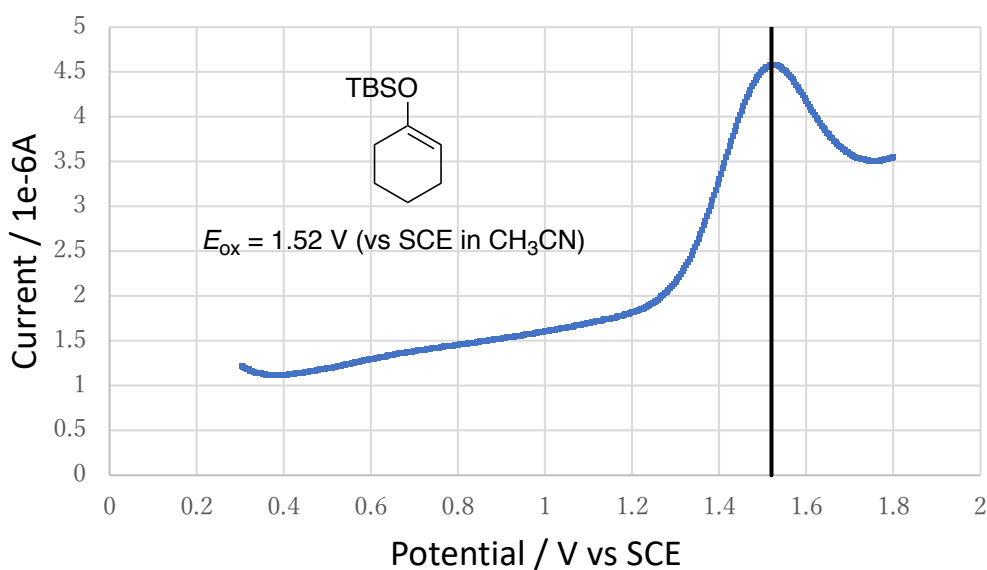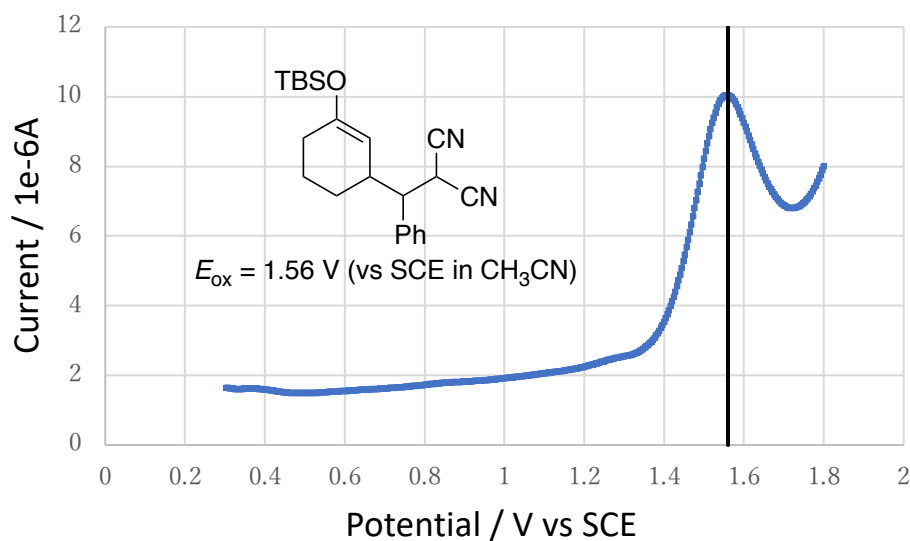
Fig. S2. SWV plots.

Stern-Volmer Experiments

Emission intensities were recorded on a HORIBA FluoroMax-4P spectrometer. The solutions were excited at 420 nm and the luminescence was measured at 564 nm. Stern-Volmer luminescence quenching experiments were run with freshly prepared a 0.1 mM solutions of $[Ir(dF(CF_3)ppy)_2(4,4'-dCF_3bpy)]PF_6$ in dry dichloroethane (DCE) at room temperature under N_2 atmosphere. In a typical experiment, the solution of Ir complex was added to an appropriate amount of quencher in 5 mL volumetric flask under N_2. The solution was transferred to 1 cm^2 quartz cell and the emission spectrum of the sample was collected. The data show that enol silyl ether **1a** and alkylated enol silyl ether **3a** are competent at quenching the excited state of the photocatalyst. On the other hand, benzalmalononitrile (**2a**) and 2,4,6-collidine are shown to be unable to quench this excited state.
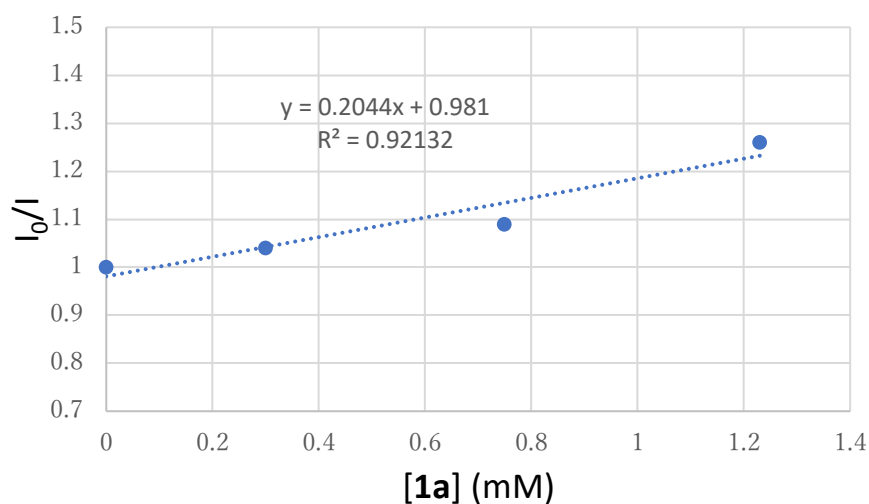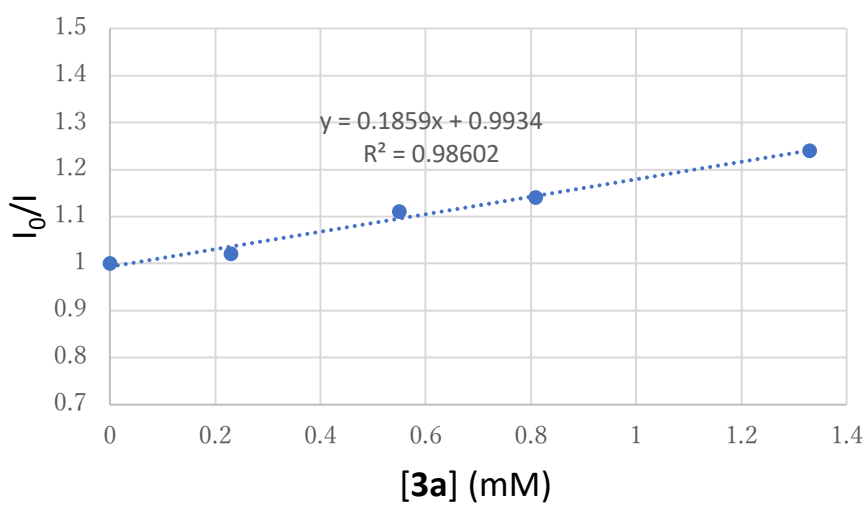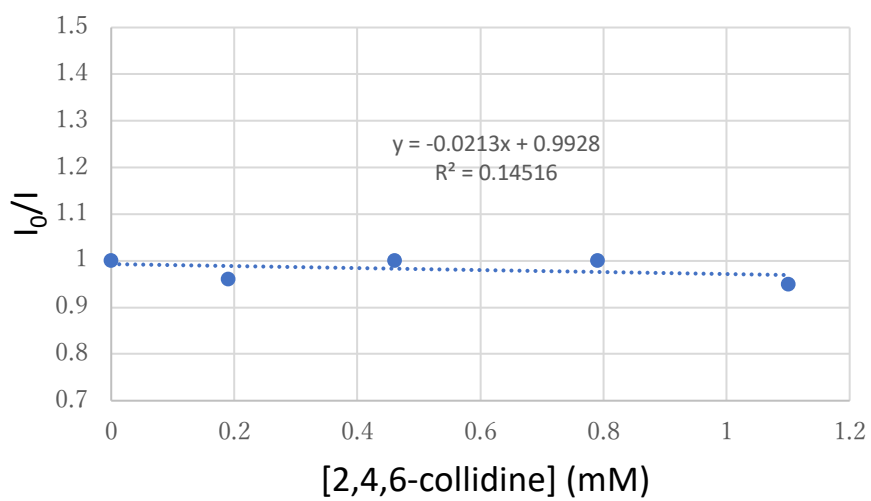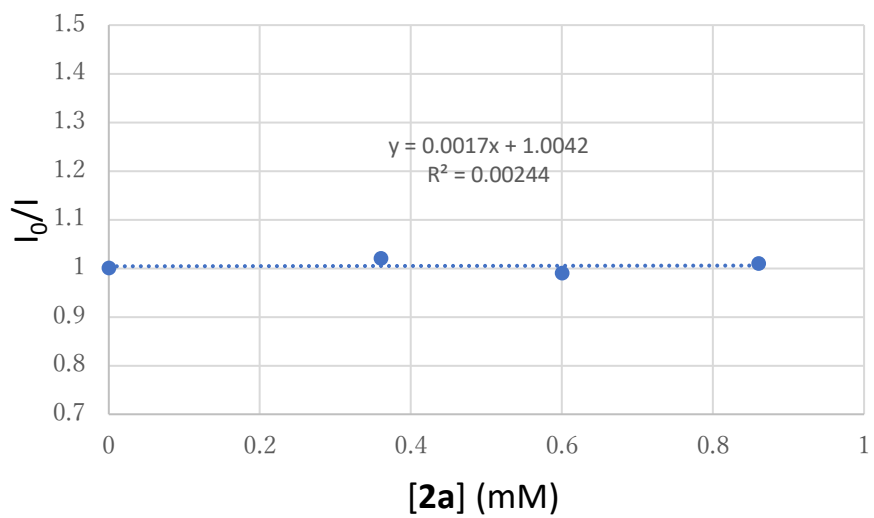
Fig. S3. Stern-Volmer Experiments.

Computational Details

The Gaussian 09 Revision D.01 program was used for all calculations.[41] The 3D molecular structures were depicted by using the CYLview v1.0.561 β.[42] Local minima and transition states (TS) were located by using the (U)CAM-B3LYP functional[43] with the 6-311+G(d,p) basis set in the dichloroethane (DCE) continuum solvent of the solvation model based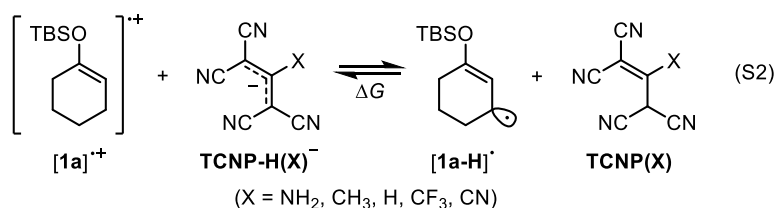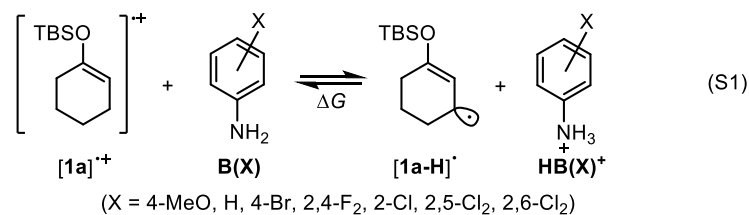 on density (SMD)[44] and "int=ultrafine" option to aid in better description of a DFT grid. As discussed in the main text, we need to estimate Kohn-Sham SOMO levels of TBS enol ether radicals for comparing the radical reactivity in the addition to olefins.

Since no global functional to treat radical cations properly was reported so far, in addition to CAM-B3LYP, B3LYP[45] (one of the most popular functional for calculating organic molecules) and LC-BLYP[46] (used in predicting several orbital properties of radical cationic systems[47]) were also examined for comparison. Harmonic frequency analyses were also performed to identify the stationary points (no/one imaginary frequency for local minima/TSs) and to estimate thermodynamic parameters at 298.15 K and 1 atm. Intrinsic reaction coordinate (IRC) analyses were conducted on the representative TS structures to confirm that the desired chemical transformations occurred through the TSs. The Cartesian coordinates and energies of optimized structures are summarized in the "**Cartesian coordinates**" section.

Estimation of pK_a of Enol Silyl Ether Radical Cations

It has been recognized that direct determination of pK_a of radical cations, based on thermochemical cycle, deviated by several unit, while relative tendency was reproduced. Therefore, statistical manipulation is required to obtain the pK_a values comparable with the experimentally determined values.[48,49]

Here, the pK_a values of radical cation [**1a**]$^{\bullet+}$ of cyclohexanone-derived enol silyl ether was simply estimated by considering acid-base equilibria with various substituted anilines **B(X)**, whose pK_a were experimentally determined (range of –6–16 in MeCN), and tetracyanopropenes **TCNP(X)** (range of –3-5 in MeCN). A linear free energy plot was shown in Figure S4 and S5, where the x-axis is the calculated reaction free energy (ΔG) of the equilibrium eq. S1 or eq. S2 with MeCN of the SMD solvent model and the y-axis is experimental pK_a values of substituted anilines or tetracyanopropenes. Both plots show excellent linear correlations: $R^2 = 0.988$ with a slope = –0.6 and intercept = 8.4 for eq. S1 and $R^2 = 0.997$ with a slope = –0.7 and intercept = 8.4 for eq. S2. According to the equilibrium eq. S1 and S2, the intercept of the plot corresponds to pK_a of [**1a**]$^{\bullet+}$: pK_a (MeCN) = 8.4.

(S1)

(X = 4-MeO, H, 4-Br, 2,4-F$_2$, 2-Cl, 2,5-Cl$_2$, 2,6-Cl$_2$)

[1a]$^{•+}$ **B(X)**   **[1a-H]**$^{•}$ **HB(X)**$^{+}$

(S2)

[1a]$^{•+}$ **TCNP-H(X)**$^{-}$ **[1a-H]**$^{•}$ **TCNP(X)**

(X = NH$_2$, CH$_3$, H, CF$_3$, CN)

These analyses were also applied to linear TBS enol ethers **1o** (R = tBu), **1r** (R = Mes), and **1s** (R = Ph), and their pK_a were determined to be 8.4 (**1o**), 6.5 (**1r**), and 4.8 (**1s**), respectively (eq. S3, Table S1-S6). B3LYP and LC-BLYP always give higher and lower pK_a values compared with CAM-B3LYP, and the difference becomes larger for aryl substituted systems (**[1r]**$^{•+}$ and **[1s]**$^{•+}$). While the absolute pK_a values depend on the functionals and the reference systems, the acidity order of the radical cations (**[1a]**$^{•+}$ ≈ **[1o]**$^{•+}$ < **[1r]**$^{•+}$ < **[1s]**$^{•+}$) is not changed. Therefore, the conclusion that **[1s]**$^{•+}$ is the most acidic of all calculated radical cations would be acceptable.

(S3)

[1o]$^{•+}$ (R^1 = t-Bu)   **B(X)**   **[1o-H]**$^{•}$ **HB(X)**$^{+}$
[1r]$^{•+}$ (R^1 = 2,4,6-Me$_3$C$_6$H$_2$)   **[1r-H]**$^{•}$
[1s]$^{•+}$ (R^1 = Ph)   **[1s-H]**$^{•}$

(X = 4-MeO, H, 4-Br, 2,4-F$_2$, 2-Cl, 2,5-Cl$_2$, 2,6-Cl$_2$)

(S4)

[1o]$^{•+}$ (R^1 = t-Bu)   **TCNP-H(X)**$^{-}$ **[1o-H]**$^{•}$ **TCNP(X)**
[1r]$^{•+}$ (R^1 = 2,4,6-Me$_3$C$_6$H$_2$)   **[1r-H]**$^{•}$
[1s]$^{•+}$ (R^1 = Ph)   **[1s-H]**$^{•}$

(X = NH$_2$, CH$_3$, H, CF$_3$, CN)
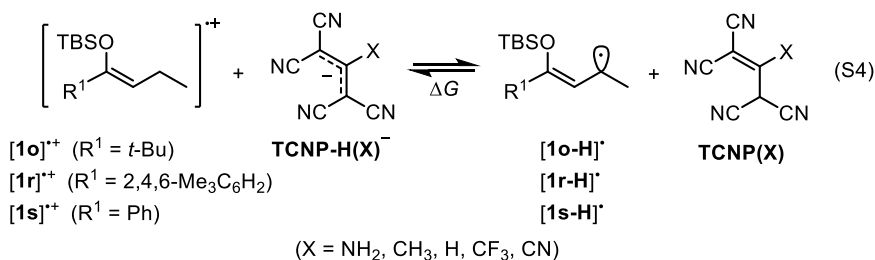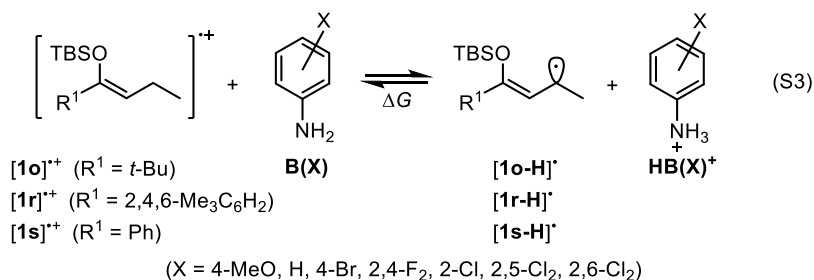
Fig. S4. Linear free energy plot of eq. S1.

Fig. S5. Linear free energy plot of eq. S2.
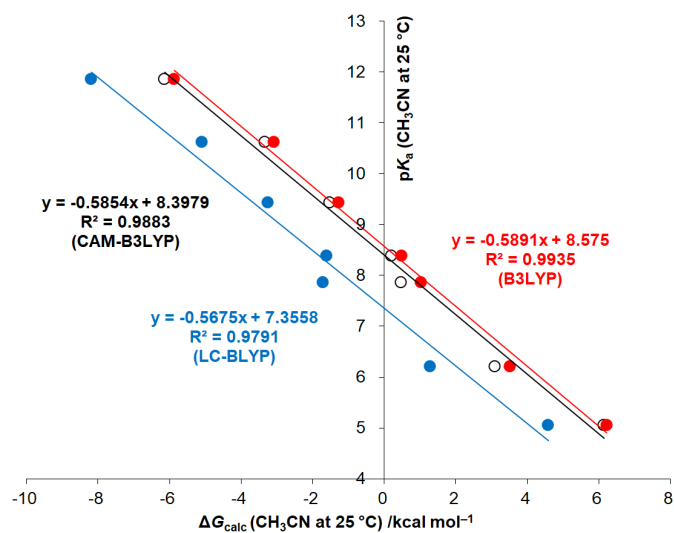
Fig. S6. Linear free energy plot of eq. S3 (R^1 = *t*-Bu).
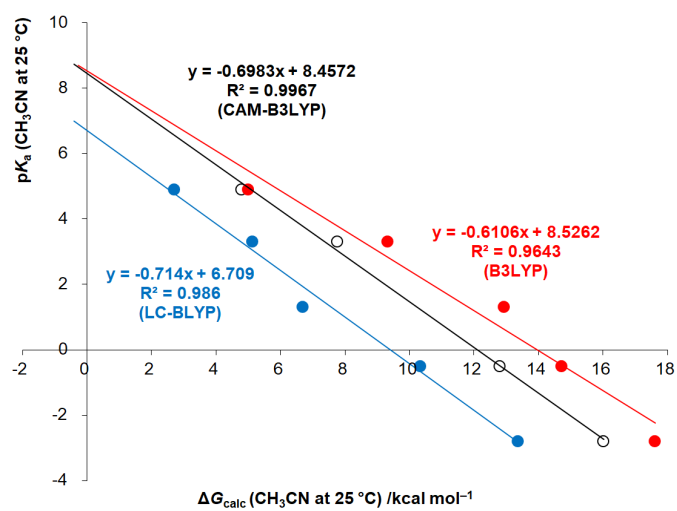
Fig. S7. Linear free energy plot of eq. S4 (R^1 = *t*-Bu).
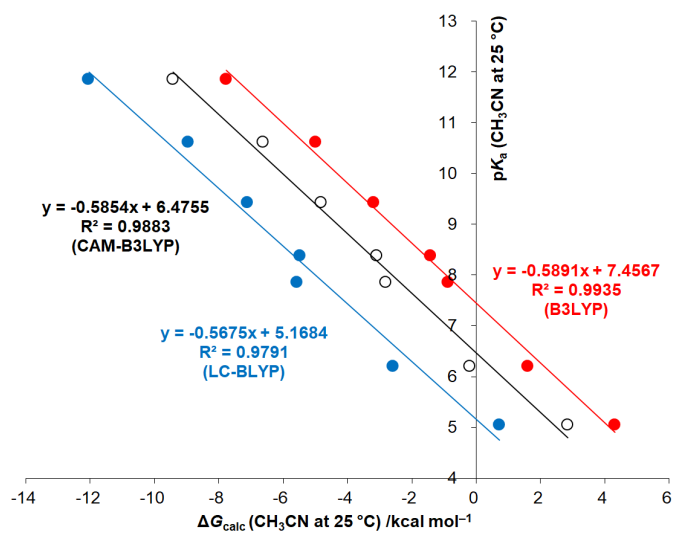
Fig. S8. Linear free energy plot of eq. S3 (R^1 = Mes).

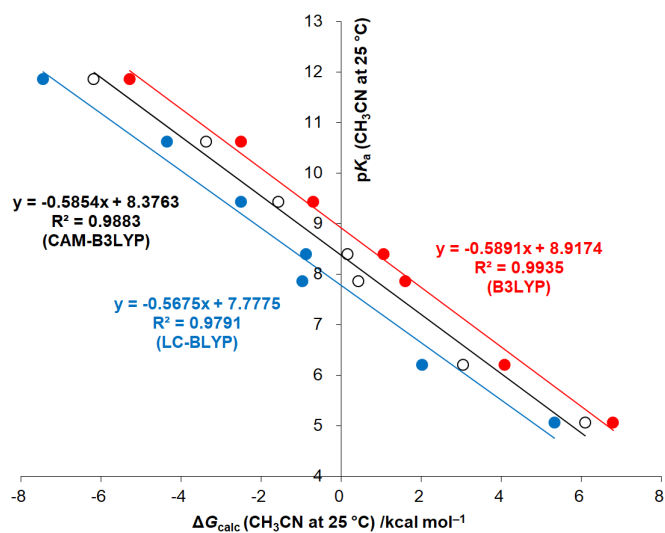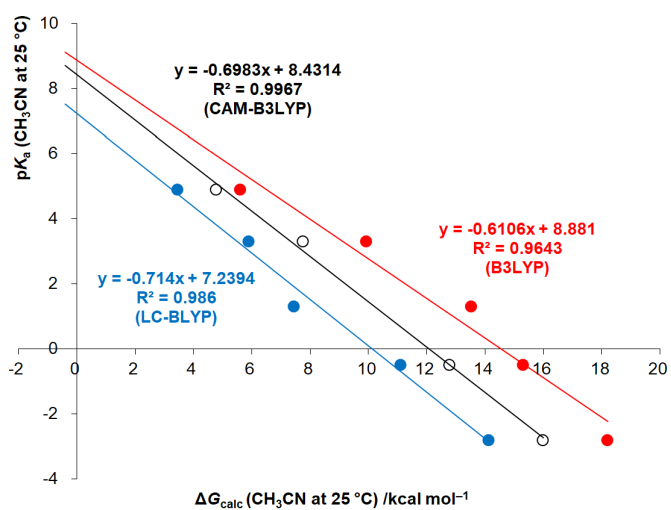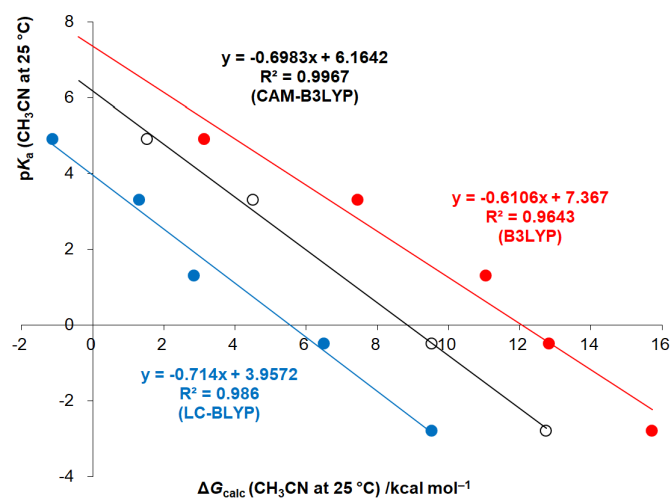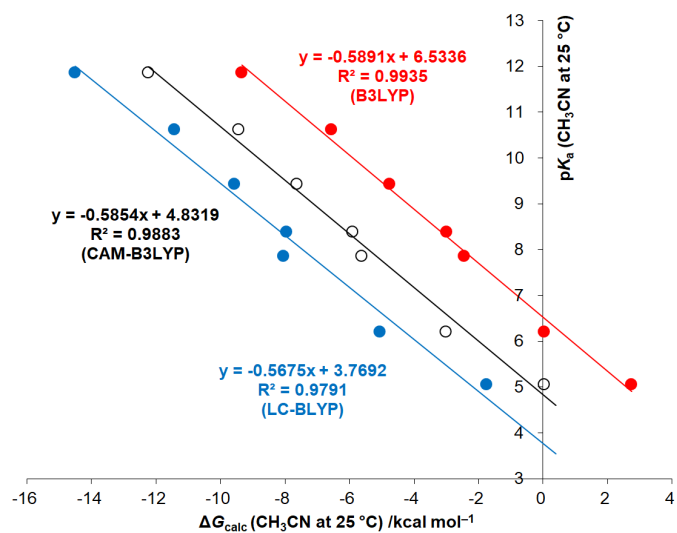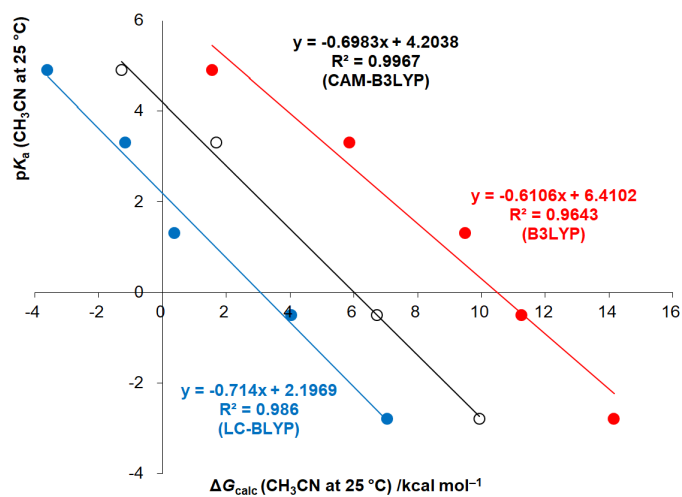**Fig. S9.** Linear free energy plot of eq. S4 (R^1 = Mes).

Fig. S10. Linear free energy plot of eq. S3 (R^1 = Ph).

Fig. S11. Linear free energy plot of eq. S4 (R^1 = Ph).

Table S1. Raw Gibbs free energy at SMD(MeCN)-CAM-B3LYP/6-311+G(d,p) and Gibbs free energy change in the equilibrium of eq. 1 and 3

	G /au		G /au	ΔG /kcal mol^{-1}				$pK_a(CH_3CN)^a$
				$[1a]^{\bullet+}$	$[1o]^{\bullet+}$	$[1r]^{\bullet+}$	$[1s]^{\bullet+}$	
TBS enol ether		*anilines*						
$[1a]^{\bullet+}$	-835.887634	B(4-MeO)	-401.928893	-6.18	-6.14	-9.43	-12.23	11.86
$[1a\text{-}H]^{\bullet}$	-835.461696	HB(4-MeO)$^+$	-402.364678					
$[1o]^{\bullet+}$	-915.608993	B(H)	-287.447382	-3.37	-3.33	-6.62	-9.42	10.62
$[1o\text{-}H]^{\bullet}$	-915.182996	HB(H)$^+$	-287.878690					
$[1r]^{\bullet+}$	-1107.248251	B(4-Br)	-2861.107170	-1.56	-1.52	-4.81	-7.62	9.43
$[1r\text{-}H]^{\bullet}$	-1106.827487	HB(4-Br)$^+$	-2861.535596					
$[1s]^{\bullet+}$	-989.422853	B(2,4-F$_2$)	-485.966607	0.16	0.20	-3.08	-5.89	8.39
$[1s\text{-}H]^{\bullet}$	-989.006563	HB(2,4-F$_2$)$^+$	-486.392287					
		B(2-Cl)	-747.085815	0.44	0.47	-2.81	-5.62	7.86
		HB(2-Cl)$^+$	-747.511057					
		B(2,5-Cl$_2$)	-1206.724615	3.05	3.09	-0.20	-3.00	6.21
		HB(2,5-Cl$_2$)$^+$	-1207.145693					
		B(2,6-Cl$_2$)	-1206.722090	6.10	6.14	2.86	0.05	5.06
		HB(2,6-Cl$_2$)$^+$	-1207.138304					

[a] See ref 48

Table S2. Raw Gibbs free energy at SMD(MeCN)-CAM-B3LYP/6-311+G(d,p) and Gibbs free energy change in the equilibrium of eq. 2 and 4

	G /au		G /au	ΔG /kcal mol^{-1}				$pK_a(CH_3CN)^a$
				$[1a]^{\bullet+}$	$[1o]^{\bullet+}$	$[1r]^{\bullet+}$	$[1s]^{\bullet+}$	
TBS enol ether		*tetracyanopropene*						
$[1a]^{\bullet+}$	-835.887634	TCNP(NH$_2$)	-542.072517	4.77	4.81	1.52	-1.28	4.90
$[1a\text{-}H]^{\bullet}$	-835.461696	TCNP-H(NH$_2$)$^-$	-541.654181					
$[1o]^{\bullet+}$	-915.608993	TCNP(Me)	-525.990880	7.75	7.78	4.50	1.69	3.30
$[1o\text{-}H]^{\bullet}$	-915.182996	TCNP-H(Me)$^-$	-525.577285					
$[1r]^{\bullet+}$	-1107.248251	TCNP(H)	*nd^b*					1.30
$[1r\text{-}H]^{\bullet}$	-1106.827487	TCNP-H(N)$^-$	-486.300151					
$[1s]^{\bullet+}$	-989.422853	TCNP(CF$_3$)	-823.758622	12.77	12.81	9.53	6.72	-0.50
$[1s\text{-}H]^{\bullet}$	-989.006563	TCNP-H(CF$_3$)$^-$	-823.353040					
		TCNP(CN)	-578.917068	15.99	16.03	12.74	9.94	-2.80
		TCNP-H(CN)$^-$	-578.516613					

[a] See ref 49

[b] Converged to 1st order saddle point and not used for the LFER plot

61

Table S3. Raw Gibbs free energy at SMD(MeCN)-(U)B3LYP/6-311+G(d,p) and Gibbs free energy change in the equilibrium of eq. 1 and 3

	G /au		G /au	ΔG /kcal mol^{-1}				pK_a(CH$_3$CN)[a]
				[1a]$^{•+}$	[1o]$^{•+}$	[1r]$^{•+}$	[1s]$^{•+}$	
TBS enol ether		*anilines*						
[1a]$^{•+}$	-836.226460	B(4-MeO)	-402.141285	-5.29	-5.87	-7.77	-9.33	11.86
[1a-H]$^{•}$	-835.797546	HB(4-MeO)$^{+}$	-402.578624					
[1o]$^{•+}$	-916.002889	B(H)	-287.614588	-2.51	-3.09	-4.98	-6.55	10.62
[1o-H]$^{•}$	-915.574901	HB(H)$^{+}$	-288.047495					
[1r]$^{•+}$	-1107.754289	B(4-Br)	-2861.173071	-0.70	-1.28	-3.18	-4.74	9.43
[1r-H]$^{•}$	-1107.329326	HB(4-Br)$^{+}$	-2861.603094					
[1s]$^{•+}$	-989.857161	B(2,4-F$_2$)	-486.166904	1.06	0.48	-1.42	-2.99	8.39
[1s-H]$^{•}$	-989.434695	HB(2,4-F$_2$)$^{+}$	-486.594127					
		B(2-Cl)	-747.249464	1.61	1.03	-0.87	-2.43	7.86
		HB(2-Cl)$^{+}$	-747.675809					
		B(2,5-Cl$_2$)	-1206.884794	4.09	3.51	1.61	0.05	6.21
		HB(2,5-Cl$_2$)$^{+}$	-1207.307185					
		B(2,6-Cl$_2$)	-1206.882174	6.80	6.22	4.32	2.75	5.06
		HB(2,6-Cl$_2$)$^{+}$	-1207.300252					

[a] See ref 48

Table S4. Raw Gibbs free energy at SMD(MeCN)-(U)B3LYP/6-311+G(d,p) and Gibbs free energy change in the equilibrium of eq. 2 and 4

	G /au		G /au	ΔG /kcal mol^{-1}				pK_a(CH$_3$CN)[a]
				[1a]$^{•+}$	[1o]$^{•+}$	[1r]$^{•+}$	[1s]$^{•+}$	
TBS enol ether		*tetracyanopropene*						
[1a]$^{•+}$	-836.226460	TCNP(NH$_2$)	-542.338339	5.61	5.03	3.13	1.56	11.86
[1a-H]$^{•}$	-835.797546	TCNP-H(NH$_2$)$^{-}$	-541.918360					
[1o]$^{•+}$	-916.002889	TCNP(Me)	-526.258520	9.92	9.34	7.44	5.87	10.62
[1o-H]$^{•}$	-915.574901	TCNP-H(Me)$^{-}$	-525.845410					
[1r]$^{•+}$	-1107.754289	TCNP(H)	-486.952191	13.53	12.95	11.05	9.48	9.43
[1r-H]$^{•}$	-1107.329326	TCNP-H(N)$^{-}$	-486.544838					
[1s]$^{•+}$	-989.857161	TCNP(CF$_3$)	-824.074635	15.31	14.73	12.83	11.26	8.39
[1s-H]$^{•}$	-989.434695	TCNP-H(CF$_3$)$^{-}$	-823.670116					
		TCNP(CN)	-579.201573	18.20	17.62	15.72	14.16	7.86
		TCNP-H(CN)$^{-}$	-578.801669					

[a] See ref 49

Table S5. Raw Gibbs free energy at SMD(MeCN)-(U)LC-BLYP/6-311+G(d,p) and Gibbs free energy change in the equilibrium of eq. 1 and 3

	G /au		G /au	ΔG /kcal mol^{-1}				pK$_a$(CH$_3$CN)[a]
				[1a]$^{•+}$	[1o]$^{•+}$	[1r]$^{•+}$	[1s]$^{•+}$	
TBS enol ether		*anilines*						
[1a]$^{•+}$	-834.331589	**B(4-MeO)**	-401.015234	-7.44	-8.19	-12.04	-14.51	11.86
[1a-H]$^{•}$	-833.910699	**HB(4-MeO)$^{+}$**	-401.447988					
[1o]$^{•+}$	-913.840835	**B(H)**	-286.745068	-4.36	-5.10	-8.95	-11.42	10.62
[1o-H]$^{•}$	-913.421129	**HB(H)$^{+}$**	-287.172899					
[1r]$^{•+}$	-1104.996066	**B(4-Br)**	-2859.902665	-2.50	-3.25	-7.10	-9.57	9.43
[1r-H]$^{•}$	-1104.582502	**HB(4-Br)$^{+}$**	-2860.327543					
[1s]$^{•+}$	-987.472908	**B(2,4-F$_2$)**	-485.028459	-0.87	-1.61	-5.47	-7.93	8.39
[1s-H]$^{•}$	-987.063273	**HB(2,4-F$_2$)$^{+}$**	-485.450734					
		B(2-Cl)	-746.120811	-0.97	-1.71	-5.57	-8.03	7.86
		HB(2-Cl)$^{+}$	-746.543245					
		B(2,5-Cl$_2$)	-1205.496649	2.02	1.28	-2.57	-5.04	6.21
		HB(2,5-Cl$_2$)$^{+}$	-1205.914312					
		B(2,6-Cl$_2$)	-1205.494467	5.33	4.58	0.73	-1.74	5.06
		HB(2,6-Cl$_2$)$^{+}$	-1205.906867					

[a] See ref 48

Table S6. Raw Gibbs free energy at SMD(MeCN)-(U)LC-BLYP/6-311+G(d,p) and Gibbs free energy change in the equilibrium of eq. 2 and 4

|	G /au		G /au	ΔG /kcal mol^{-1}				pK$_a$(CH$_3$CN)[a]
				[1a]$^{•+}$	[1o]$^{•+}$	[1r]$^{•+}$	[1s]$^{•+}$	
TBS enol ether		*tetracyanopropene*						
[1a]$^{•+}$	-834.331589	**TCNP(NH$_2$)**	-540.871671	3.46	2.72	-1.14	-3.60	11.86
[1a-H]$^{•}$	-833.910699	**TCNP-H(NH$_2$)$^{-}$**	-540.456294					
[1o]$^{•+}$	-913.840835	**TCNP(Me)**	-524.793872	5.90	5.15	1.30	-1.16	10.62
[1o-H]$^{•}$	-913.421129	**TCNP-H(Me)$^{-}$**	-524.382381					
[1r]$^{•+}$	-1104.996066	**TCNP(H)**	-485.613673	7.44	6.70	2.85	0.38	9.43
[1r-H]$^{•}$	-1104.582502	**TCNP-H(N)$^{-}$**	-485.204643					
[1s]$^{•+}$	-987.472908	**TCNP(CF$_3$)**	-822.207167	11.10	10.35	6.50	4.03	8.39
[1s-H]$^{•}$	-987.063273	**TCNP-H(CF$_3$)$^{-}$**	-821.803961					
		TCNP(CN)	-577.622417	14.12	13.37	9.52	7.06	7.86
		TCNP-H(CN)$^{-}$	-577.224025					

[a] See ref 49

Calculation for Radical addition

(TBS enol ether radical to 1,1-bis(phenylsulfonyl)ethylene)

The reactivity of enol silyl ether-derived allylic radicals was examined by calculating frontier orbital properties and TS of radical addition to 1,1-bis(phenylsulfonyl)ethylene (eq. S5).
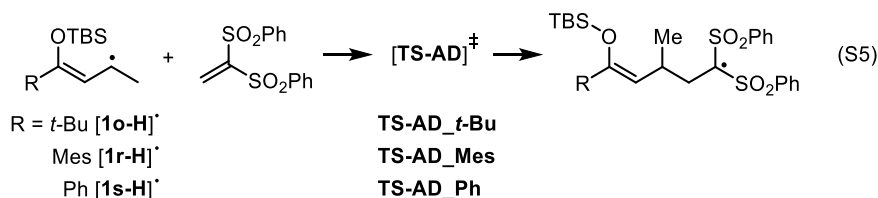

Optimized structures of these radicals at UCAM-B3LYP/6-311+G(d,p) level were summarized in Figure S7. As described in the main manuscript, spin density at the allylic carbon of each radical correlates with the experimental yield: 0.70 ([**1o-H**]$^\bullet$), 0.64 ([**1r-H**]$^\bullet$), and 0.51 ([**1s-H**]$^\bullet$).   For [**1s-H**]$^\bullet$, the spin is localized to the Ph group, which is reflected in the bond distance between the oxygen-bearing carbon and the carbon of the Ph group (*a* in Figure S7).   The C–C distance changes from 1.52 Å to 1.45 Å by substituting *t*-Bu to Ph, indicating the existence of radical delocalization toward an aromatic Ph ring. When Mes is introduced instead of Ph, *a* is elongated again from 1.45 Å to 1.48 Å, and the spin density at the γ-carbon increases from 0.51 to 0.64. The Mes group cannot adopt a coplanar orientation with the olefin moiety due to the steric repulsion caused by the two *o*-Me groups (the dihedral angle of $C_{ortho}C_{ipso}$-$C_\alpha C_\beta$ is 60.1°; highlighted in green in Figure S7). Since radical conjugation with the Mes group is partially inhibited in [**1r-H**]$^\bullet$, its spin density at the allylic position and reactivity are comparable with those of [**1o-H**]$^\bullet$.

In exploring the most stable TS for the radical addition, 8 kinds of conformers were examined: different orientations of 1) radical and olefin fragments about the forming C–C bond and 2) SO$_2$Ph groups in olefin about the approaching radical (Figure S8-S10, Table S3). The lowest values of $\Delta G^{\ddagger}$ for each substituent (21.2 kcal mol^{-1} (**TS-AD_*t*-Bu_1b**), 21.6 kcal mol^{-1} (**TS-AD_Mes_2b**), and 23.3 kcal mol^{-1} (**TS-AD_Ph_2b**)) are reported in Table 3 in the main text. These values correlate with the spin density of the C3-carbon and the experimental yield (90% (**1o**), 81% (**1r**), 53% (**1s**)). The proper balance of the radical cation acidity and the activation barrier of the radical addition may be a source of the superior reactivity of **1r** in the C–H alkylation.
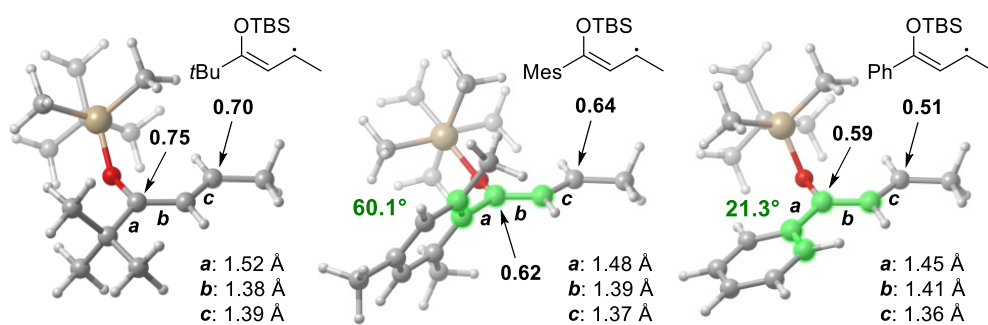
Fig. S12. Optimized structures of [**1o-H**]•, [**1r-H**]•, and [**1s-H**]• at UCAM-B3LYP/6-311+G(d,p). Representative bond distances, spin densities, and dihedral angles between an aromatic ring and an olefin moiety (green) are also shown for [**1r-H**]• and [**1s-H**]•.
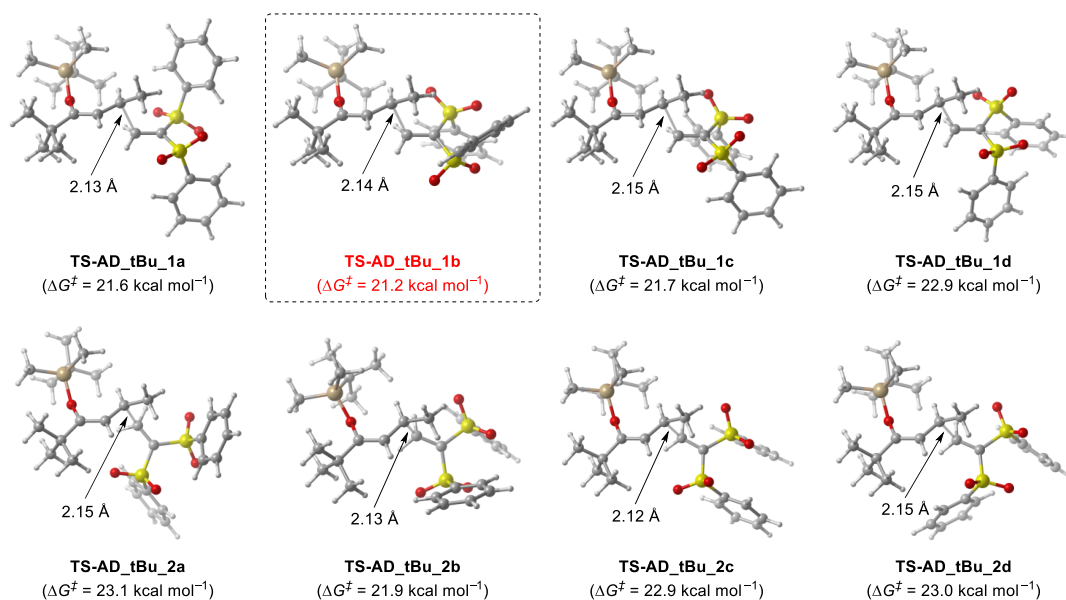
Fig. S13. Optimized TS structures of radical addition of [**1o-H**]• to 1,1-bis(phenylsulfonyl)ethylene.

TS-AD_Mes_1a
($\Delta G^{\ddagger}$ = 22.3 kcal mol^{-1})

TS-AD_Mes_1b
($\Delta G^{\ddagger}$ = 23.1 kcal mol^{-1})

TS-AD_Mes_1c
($\Delta G^{\ddagger}$ = 22.6 kcal mol^{-1})

TS-AD_Mes_1d
($\Delta G^{\ddagger}$ = 22.2 kcal mol^{-1})

2.14 Å   2.14 Å   2.16 Å   2.14 Å

TS-AD_Mes_2a
(*not determined*)

TS-AD_Mes_2b
($\Delta G^{\ddagger}$ = 21.6 kcal mol^{-1})

TS-AD_Mes_2c
($\Delta G^{\ddagger}$ = 23.0 kcal mol^{-1})

TS-AD_Mes_2d
($\Delta G^{\ddagger}$ = 24.0 kcal mol^{-1})

2.12 Å   2.13 Å   2.15 Å
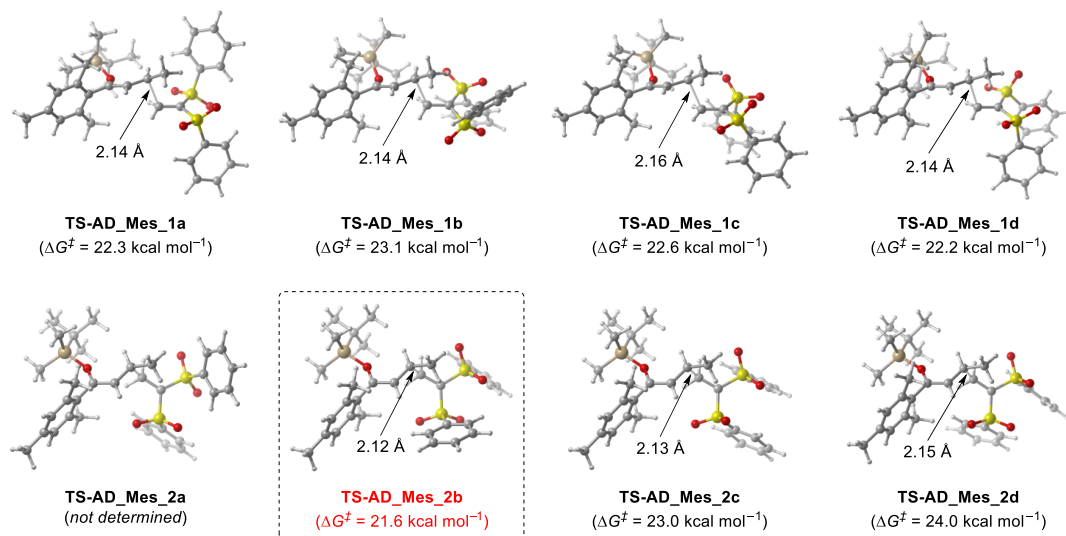
Fig. S14. Optimized TS structures of radical addition of [**1r-H**]$^{\bullet}$ to
1,1-bis(phenylsulfonyl)ethylene.

TS-AD_Ph_1a
($\Delta G^{\ddagger}$ = 24.4 kcal mol^{-1})

TS-AD_Ph_1b
($\Delta G^{\ddagger}$ = 24.4 kcal mol^{-1})

TS-AD_Ph_1c
($\Delta G^{\ddagger}$ = 25.9 kcal mol^{-1})

TS-AD_Ph_1d
($\Delta G^{\ddagger}$ = 25.2 kcal mol^{-1})

2.10 Å   2.10 Å   2.12 Å   2.10 Å

TS-AD_Ph_2a
($\Delta G^{\ddagger}$ = 25.7 kcal mol^{-1})

TS-AD_Ph_2b
($\Delta G^{\ddagger}$ = 23.3 kcal mol^{-1})

TS-AD_Ph_2c
($\Delta G^{\ddagger}$ = 25.4 kcal mol^{-1})

TS-AD_Ph_2d
($\Delta G^{\ddagger}$ = 24.8 kcal mol^{-1})

2.10 Å   2.10 Å   2.12 Å   2.10 Å
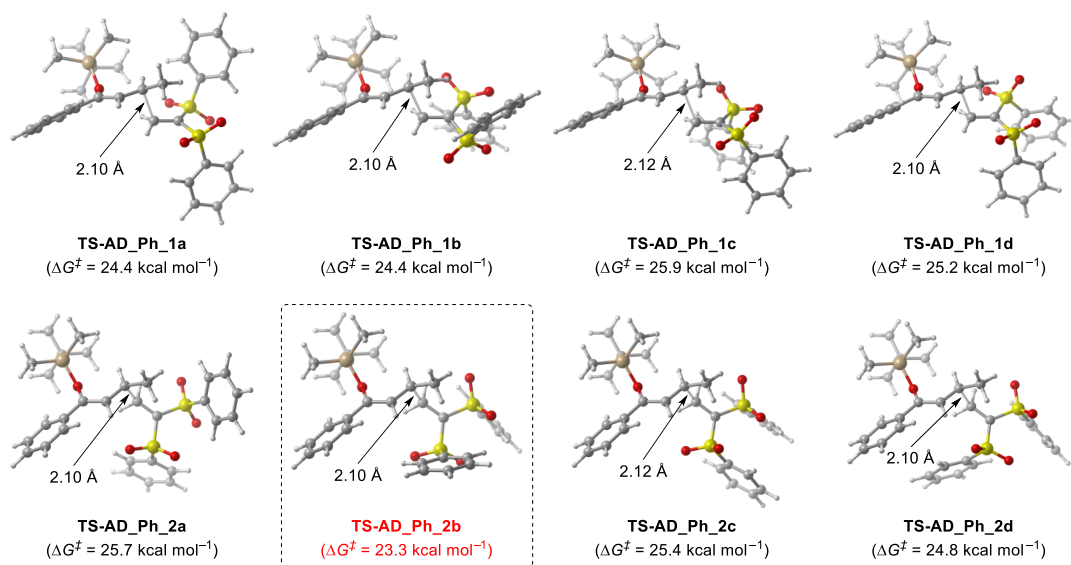
Fig. S15. Optimized TS structures of radical addition of [**1s-H**]$^{\bullet}$ to
1,1-bis(phenylsulfonyl)ethylene.

Table S7. Electron energy, enthalpy, entropy, Gibbs free energy, relative electron energy and relative Gibbs free energy of eq. S5 at SMD(CH₃CN)-(U)CAM-B3LYP/6-311+G(d,p)

| (R^1, R^2)	E /au	H /au	S /eu	G /au	ΔE /kcal mol^{-1}	ΔG /kcal mol^{-1}
1,1-bis(phenylsulfonyl)ethylene	-1637.714023	-1637.458874	139.527	-1637.525168		
[1o-H]$^{\cdot}$	-915.532276	-915.108818	156.782	-915.183310		
TS-AD_tBu_1a	-2553.236443	-2552.555665	249.277	-2552.674104	6.18	21.57
TS-AD_tBu_1b^a	-2553.235171	-2552.554233	253.409	-2552.674636	6.98	21.24
TS-AD_tBu_1c	-2553.233933	-2552.553140	254.256	-2552.673945	7.76	21.67
TS-AD_tBu_1d	-2553.233498	-2552.552567	251.254	-2552.671946	8.03	22.92
TS-AD_tBu_2a	-2553.233131	-2552.552260	251.276	-2552.671650	8.26	23.11
TS-AD_tBu_2b	-2553.234706	-2552.553594	252.479	-2552.673555	7.27	21.91
TS-AD_tBu_2c	-2553.233127	-2552.552212	252.024	-2552.671957	8.27	22.92
TS-AD_tBu_2d	-2553.233387	-2552.552397	251.324	-2552.671809	8.10	23.01
[1r-H]$^{\cdot}$	-1107.221441	-1106.742045	180.532	-1106.827822		
TS-AD_Mes_1a	-2744.925381	-2744.188832	270.677	-2744.317439	6.33	22.31
TS-AD_Mes_1b	-2744.923264	-2744.186774	272.275	-2744.316140	7.66	23.12
TS-AD_Mes_1c	-2744.921565	-2744.185228	277.444	-2744.317050	8.72	22.55
TS-AD_Mes_1d	-2744.921742	-2744.185555	277.911	-2744.317599	8.61	22.21
TS-AD_Mes_2a	=> converged to **TS-AD_Mes_1a**					
TS-AD_Mes_2b^a	-2744.923877	-2744.187270	276.201	-2744.318502	7.27	21.64
TS-AD_Mes_2c	-2744.920545	-2744.184310	278.007	-2744.316400	9.36	22.96
TS-AD_Mes_2d	-2744.919603	-2744.183163	277.032	-2744.314790	9.95	23.97
[1s-H]$^{\cdot}$	-989.323605	-988.932114	156.857	-989.006642		
TS-AD_Ph_1a	-2627.023676	-2626.374740	248.702	-2626.492907	8.76	24.41
TS-AD_Ph_1b	-2627.022089	-2626.373270	251.686	-2626.492854	9.75	24.45
TS-AD_Ph_1c	-2627.021267	-2626.372448	248.423	-2626.490482	10.27	25.93
TS-AD_Ph_1d	-2627.020483	-2626.371708	252.369	-2626.491617	10.76	25.22
TS-AD_Ph_2a	-2627.018974	-2626.370125	253.966	-2626.490792	11.71	25.74
TS-AD_Ph_2b^a	-2627.021894	-2626.373039	255.865	-2626.494609	9.87	23.34
TS-AD_Ph_2c	-2627.018844	-2626.370112	255.047	-2626.491293	11.79	25.42
TS-AD_Ph_2d	-2627.020143	-2626.371438	254.258	-2626.492244	10.97	24.83

^{a} Reported in the main text (Table 3).

References and Notes

(1) Stork, G.; Hudrlik, P. F. *J. Am. Chem. Soc.* **1968**, *90*, 4462.

(2) Kan, S. B. J.; Ng, K. K. H.; Paterson, I. *Angew. Chem. Int. Ed.* **2013**, *52*, 9097.

(3) Matsuo, J.; Murakami, M. *Angew. Chem. Int. Ed.* **2013**, *52*, 9109.

(4) Magnus, P.; Lacour, J.; Evans, P. A.; Roe, M. B.; Hulme, C. *J. Am. Chem, Soc.* **1996**, *118*, 3406.

(5) Tietze, L. F. *Domino Reactions: Concepts for Efficient Organic Synthesis* (Wiley, Weinheim, **2014**).

(6) Bhanja, C.; Jena, S.; Nayak, S.; Mohapatra, S. *J. Org. Chem.* **2012**, *8*, 1668.

(7) Serrano-Molina, D.; Martín-Castro, A. M. *Synthesis* **2016**, *48*, 3459.

(8) Davies, H. M. L.; Ren, P. *J. Am. Chem. Soc.* **2001**, *123*, 2070.

(9) Cuthbertson, J. D.; MacMillan, D. W. C. *Nature* **2015**, *519*, 74.

(10) Gassman, P. G.; Bottorff, K. J. *J. Org. Chem.* **1988**, *53*, 1097.

(11) Bhattacharya, A.; DiMichele, L. M.; Dolling, U.-H.; Grabowski, E. J. J.; Grenda, V. J. *J. Org. Chem.* **1989**, *54*, 6118.

(12) Bockman, T. M.; Shukla, D.; Kochi, J. K. *J. Chern, Soc. Perkin Trans.* **1996**, *2*, 1623.

(13) Bockman, T. M.; Kochi, J. K. *J. Chern, Soc. Perkin Trans.* **1996**, *2*, 1633.

(14) Rathore, R.; Kochi, J. K. *J. Org. Chem.* **1996**, *61*, 627.

(15) Ramsden, C. A.; Smith, R. G. *Org. Lett.* **1999**, *1*, 1591.

(16) Hudson, C. M.; Marzabadi, M. R.; Moeller, K. D.; New, D. G. *J. Am. Chem. Soc.* **1991**, *113*, 7372.

(17) Snider, B. B.; Kwon, T. *J. Org. Chem.* **1992**, *57*, 2399.

(18) Heidbreder, A.; Mattay, J. *Tetrahedron Lett.* **1992**, *33*, 1973.

(19) Hintz, S.; Mattay, J.; van Eldik, R.; Fu, W.-F. *Eur. J. Org. Chem.* **1998**, *1998*, 1583.

(20) Wright, D. L.; Whitehead, C. R.; Sessions, E. H.; Ghiviriga, I.; Frey. D. A. *Org. Lett.* **1999**, *1*, 1535.

(21) Ackermann, L.; Heidbreder, A.; Wurche, F.; Klärner, F.-G.; Mattay, J. *J. Chern. Soc. Perkin Trans.* **1999**, *2*, 863.

(22) Bunte, J. O.; Rinne, S.; Schäfer, C.; Neumann, B.; Stammler, H.-G.; Mattay, J. *Tetrahedron Lett.* **2003**, *44*, 45.

(23) Schmittel, M.; Burghart, A. *Angew. Chem. Int. Ed. Engl.* **1997**, *36*, 2550.

(24) Nakajima, K.; Miyake, Y.; Nishibayashi, Y. *Acc. Chem. Res.* **2016**, *49*, 1946.

(25) Lee, K. N.; Ngai, M.-Y. *Chem. Commun.* **2017**, *53*, 13093.

(26) Zhou, R.; Liu, H.; Tao, H.; Yu, X.; Wu, J. *Chem. Sci.* **2017**, *8*, 4654.

(27) McManus, J. B.; Onuska, N. P. R.; Nicewicz, D. A. *J. Am. Chem. Soc.* **2018**, *140*, 9056.

(28) Pirnot, M. T.; Rankic, D. A.; Martin, D. B. C.; MacMillan, D. W. C. *Science* **2013**, *339*, 1593.

(29) Petronijević, F. R.; Nappi, M.; MacMillan, D. W. C. *J. Am. Chem. Soc.* **2013**, *135*, 18323.

(30) Terrett, J. A.; Clift, M. D.; MacMillan, D. W. C. *J. Am. Chem. Soc.* **2014**, *136*, 6858.

(31) Jeffrey, J. L.; Petronijević, F. R.; MacMillan, D. W. C. *J. Am. Chem. Soc.* **2015**, *137*, 8404.

(32) Kaljurand, I.; Kütt, A.; Soovāli, L.; Rodima, T.; Mäemets, V.; Leito, I.; Koppel, I. A. *J. Org. Chem.* **2005**, *70*, 1019.

(33) Kütt, A.; Leito, I.; Kaljurand, I.; Soovāli, L.; Vlasov, V. M.; Yagupolskii, L. M.; Koppel, I. A. *J. Org. Chem.* **2006**, *71*, 2829.

(34) Choi, G. J.; Zhu, Q.; Miller, D. C.; Gu, C. J.; Knowles, R. R. *Nature* **2016**, *539*, 268.

(35) Li, J.; Lear, M. J.; Hayashi, Y. *Angew. Chem. Int. Ed.* **2016**, *55*, 9060.

(36) Thommen, C.; Jana, C. K.; Neuburger, M.; Gademann, K. *Org, Lett.*

(37) Lowry, M. S.; Hudson, W. R.; Pascal, R. A. Jr.; Bernhard, S. *J. Am. Chem. Soc.* **2004**, *126*, 14129.

(38) Sarabèr, F. C. E.; Dratch, S.; Bosselaar, G.; Jansen, B. J. M.; de Groot, A. *Tetrahedron* **2006**, *62*, 1717.

(39) Ito, H.; Ohmiya, H.; Sawamura, M. *Org. Lett.* **2010**, *12*, 4380.

(40) Sumida, Y., Yorimitsu, H. & Oshima, K. *J. Org. Chem.* **2009**, *74*, 7986.

(41) Gaussian 09, Revision D.01, Frisch, M. J.; Trucks, G. W.; Schlegel, H. B.; Scuseria, G. E.; Robb, M. A.; Cheeseman, J. R.; Scalmani, G.; Barone, V.; Mennucci, B.; Petersson, G. A.; Nakatsuji, H.; Caricato, M.; Li, X.; Hratchian, H. P.; Izmaylov, A. F.; Bloino, J.; Zheng, G.; Sonnenberg, J. L.; Hada, M.; Ehara, M.; Toyota, K.; Fukuda, R.; Hasegawa, J.; Ishida, M.; Nakajima, T.; Honda, Y.; Kitao, O.; Nakai, H.; Vreven, T.; Montgomery, Jr., J. A.; Peralta, J. E.; Ogliaro, F.; Bearpark, M.; Heyd, J. J.; Brothers, E.; Kudin, K. N.; Staroverov, V. N.; Keith, T.; Kobayashi, R.; Normand, J.; Raghavachari, K.; Rendell, A.; Burant, J. C.; Iyengar, S. S.; Tomasi, J.; Cossi, M.; Rega, N.; Millam, J. M.; Klene, M.; Knox, J. E.; Cross, J. B.; Bakken, V.; Adamo, C.; Jaramillo, J.; Gomperts, R.; Stratmann, R. E.; Yazyev, O.; Austin, A. J.; Cammi, R.; Pomelli, C.; Ochterski, J. W.; Martin, R. L.; Morokuma, K.; Zakrzewski, V. G.; Voth, G. A.; Salvador, P.; Dannenberg, J. J.; Dapprich, S.; Daniels, A. D.; Farkas, O.; Foresman, J. B.; Ortiz, J. V.; Cioslowski, J.; Fox, D. J. Gaussian, Inc., Wallingford CT, 2013.

(42) Legault, C. Y. CYLview, 1.0b, Université de Sherbrooke, 2009.

(43) Yanai, T.; Tew, D.; Handy, N. *Chem. Phys. Lett.* **2004**, *393*, 51.

(44) Marenich, A. V.; Cramer, C. J.; Truhlar, D. G. *J. Phys. Chem. B* **2009**, *113*, 6378.

(45) Becke, A. D. *J. Chem. Phys.* **1993**, *98*, 5648.

(46) Iikura, H.; Tsuneda, T.; Yanai, T.; Hirao, K. *J. Chem. Phys.* **2001**, *115*, 3540.

(47) Riffet, V.; Jacquemin, D.; Cauët, E.; Frison, G. *J. Chem. Theory Comput.* **2014**, *10*, 3308.

(48) Kütt, A.; Leito, I,; Kaljurand, I.; Soovāli, L.; Vlasov, V. M.; Yagupolskii, L. M.; Koppel, I. A. *J. Org. Chem.* **2006**, *71*, 2829.

(49) Kütt, A.; Rodima, T.; Saame, J.; Raamat, E.; Mäemets, V.; Kaljurand, I.; Koppel, I. A.; Garlyauskayte, R. Y.; Yagupolskii, Y. L.; Yagupolskii, L. M.; Bernhardt, E.; Willner, H.; Leito, I. *J. Org. Chem.* **2011**, *76*, 391.

Chapter 3

## Radical Cations as Catalytically Generated Brønsted Acids for Allylic C−H Heteroarylation of Enol Silyl Ethers

23 examples: 50-95%
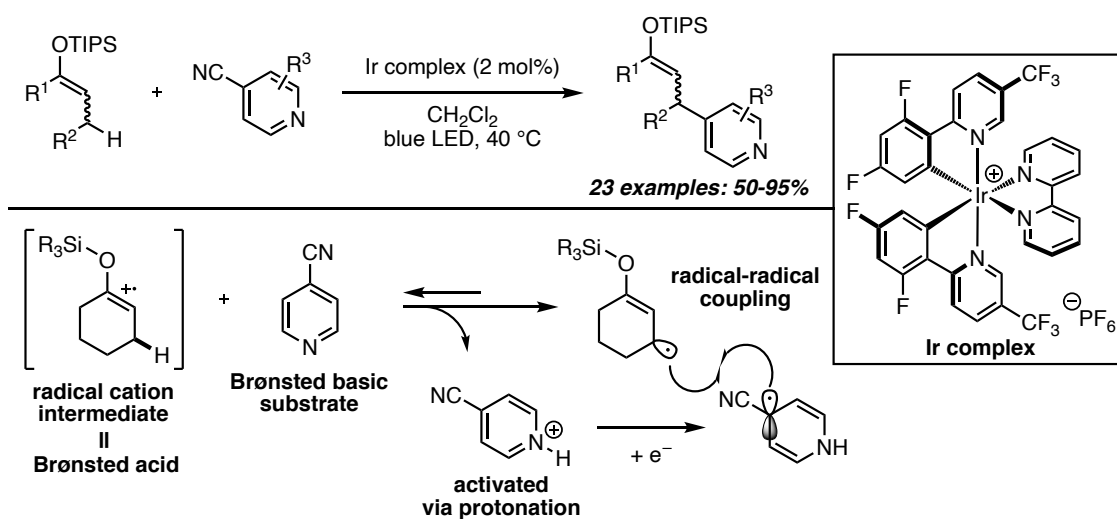
Abstract:

The intermediary radical cations, generated through single-electron oxidation of enol silyl ethers by the excited Ir-based photocatalyst, can be exploited as Brønsted acids for the activation of heteroarylcyanides. This strategy enables the direct allylic C−H heteroarylation of enol silyl ethers under visible light irradiation.

1. Introduction

Radical cations are open-shell reactive intermediates that typically generated from electron-rich compounds through chemical,[1] electrochemical,[2] or photochemical single-electron oxidation.[3] Owing to their electrophilic nature, radical cations can act as versatile intermediates for a range of reactions, such as cycloaddition with electron-rich diene[4] and intramolecular bond formation with nucleophilic functional groups.[5] Another distinctive character is represented in the mesolytic cleavage of the neighboring σ-bonds, such as C−H, C−C, C−S, and C−Si bonds, etc.[6] This type of bond cleavages is triggered by the weakening of α-C−X bond through the overlap of its σ orbital and the SOMO. Therefore, the mesolytic cleavage is a relatively facile process and radical cations can behave as strong carbon acids when X = H. For instance, α-benzylic C−H bond of the radical cation of toluene exhibits extremely high acidity, of which pK_a value was estimated to be −6.[7]

The radical cations of enol silyl ethers and their analogues have been known to readily undergo the elimination of silyl cation to afford the desilylated, electrophilic α-carbonyl radicals.[8] On the other hand, we recently reported a methodology to generate the nucleophilic allylic radicals from enol silyl ethers through single-electron oxidation and deprotonation sequence by using photoredox and appropriate Brønsted base catalysts (Figure 1a).[9] The predominant deprotonation of radical cations relied on the intrinsic high acidity of their allylic proton, of which pK_a was estimated to be close to *p*-toluenesulfonic acid (TsOH). Upon consideration of such high acidity of radical cations, these intermediates could be utilized as catalytically generated Brønsted acids for the activation of electrophiles having a basic functionality via protonation, which would concomitantly generate nucleophilic radicals to be engaged in the bond formation with the activated electrophiles. We envisioned that cyanopyridines were promising substrates for the demonstration of the ability of radical cations because (i) cyanopyridines would be protonated by acidic radical cations and (ii) the resulting pyridinium ion would smoothly undergo the single-electron transfer (SET) and subsequent radical−radical coupling (Figure 1b).[10,11] Here, we report the successful implementation of the use of radical cation as an activator of substrate through the development of an allylic heteroarylation of enol silyl ethers with heteroarylcyanides (Figure 1b).
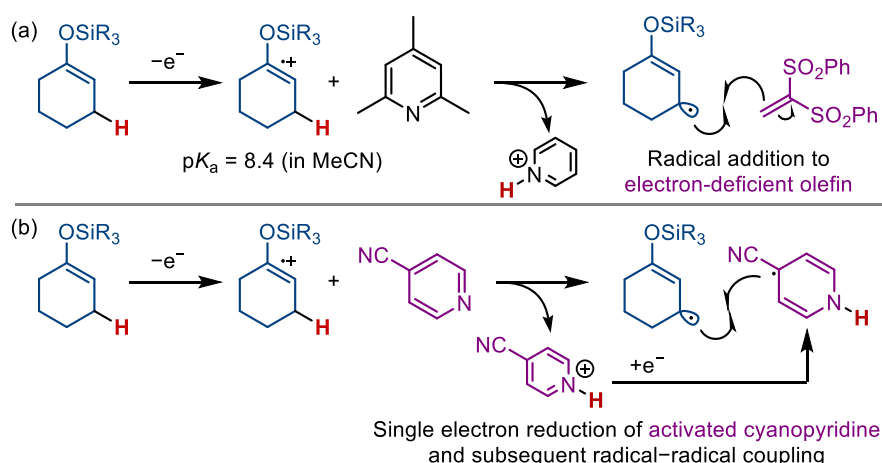
Scheme 1. Allylic C−H functionalization of enol silyl ethers based on single-electron oxidation-deprotonation sequence to generate nucleophilic allylic radical. (a) C−H alkylation through radidcal addition to electron-deficient olefins. (b) C−H heteroarylation triggered by the activation of caynopyridines.

2. Results and Discussion

At the outset of research, we selected cyclohexanone-derived enol silyl ether **1a** and 4-cyanopyridine (**2a**) as model substrates for allylic heteroarylation (Table 1). Since **1a** and **2a** have large electronic potential (E_{ox} of **1a** = 1.43 V vs SCE and E_{red} of **2a** = −1.81 V vs SCE, respectively), the single molecular photoredox catalysts in general are not capable of promoting SET for both of these substrates. However, upon irradiation of visible light at 40 °C[12] for 6 h, the reaction of **1a** and **2a** in the presence of [Ir(dFCF₃ppy)₂(4,4′-dCF₃bpy)]PF₆ (**4a**) proceeded to give allylic heteroarylation product **3a**, albeit in low yield (entry 1). While SET cannot occur from excited Ir(III) complex **4a** ($E_{1/2}*^{III/IV}$ = −0.51 V) as well as persistent Ir(II) complex ($E_{1/2}^{II/III}$ = −0.79 V) to **2a**, the intermediary radical cation of **1a** would facilitate this process via protonation of **2a**. In fact, the addition of Brønsted acid led to the notable shift of reduction potential of **2a** to −0.89 vs SCE.[11i,13] We then examined the reaction using photocatalysts **4b** or **4c**, of which Ir(II) complexes exhibit stronger reducing ability, and identified [Ir(dFCF₃ppy)₂(bpy)]PF₆ (**4c**) as an optimal catalyst candidate (entries 2 and 3). Subsequent optimization of reaction conditions uncovered that lowering the temperature led to the notable decrease of reaction efficiency. When the reaction was conducted with a fun to keep the reaction setup at ambient temperature, **3a** was obtained in reduced yield (entry 3 vs 4). Prolonged reaction time resulted in slightly improved yield of **3a** (entry 5). Following examination of solvent effects revealed that dichloromethane and acetonitrile were suitable for the present heteroarylation while acetone, ethyl acetate, and methanol seemed to retard the reaction (entries 6-9). No product formation was observed in the attempted reactions without

photocatalyst **4** or light irradiation, confirming that excited Ir complex was essential for promoting desired allylic heteroarylation (entries 10 and 11).

Table 1. Optimization of reaction conditions[a]
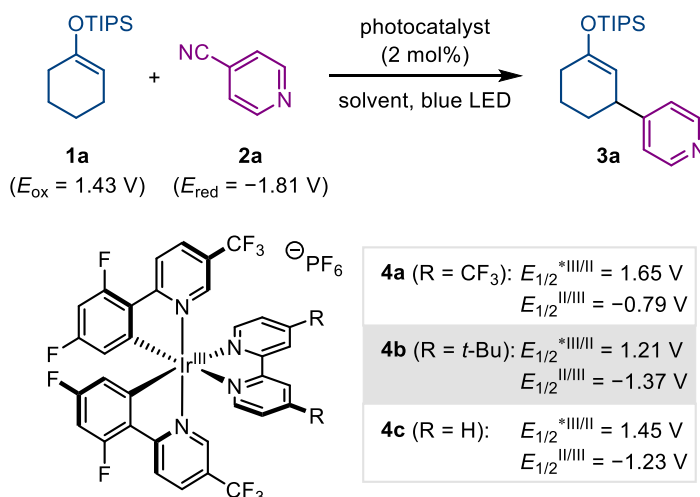
Entry	Photocatalyst	Solvent	Time (h)	Yield (%)[b]
1	**4a**	CH_2Cl_2	6	15
2	**4b**	CH_2Cl_2	6	42
3	**4c**	CH_2Cl_2	6	57
4[c]	**4c**	CH_2Cl_2	6	39
5	**4c**	CH_2Cl_2	12	65
6	**4c**	acetone	12	6
7	**4c**	EtOAc	12	4
8	**4c**	MeOH	12	34
9	**4c**	MeCN	12	63
10	None	CH_2Cl_2	12	0
11[d]	**4c**	CH_2Cl_2	12	0

[a] Unless otherwise indicated, the reactions were performed with 0.12 mmol of **1a** and 0.10 mmol of **2b** with photocatalyst **4** (2 mol%) in solvent (1.0 mL) under argon atmosphere at 40 °C with light irradiation (blue LED, 250 Wm^{-2}). [b] NMR yield with styrene as an internal standard. [c] With a fan to keep the reaction setup at room temperature. [d] Under dark.

3. Mechanistic Investigations

To gain an insight into the reaction mechanism, we then conducted Stern-Volmer luminescence quenching experiments with Ir complex **4c** in acetonitrile, confirming that the excited state of **4c** could be quenched by enol silyl ether **1a**. The quenching rate constant (K_{q1a})

was determined to be 4.36×10^7 [M^{-1}s^{-1}]. In addition, 4-cyanopyridine hydromesylate (**2a**·HOMs) could also act as a quencher, and its quenching rate constant was higher than that with **1a** ($K_{q2a\cdot HOMs} = 2.0 \times 10^8$ [M^{-1}s^{-1}]). This result indicated that the excited state of **4c** could undergo the reductive quenching with **1a** as well as oxidative quenching with **2a**·H when acidic radical cation generated in sufficient concentration.

A plausible reaction mechanism is outlined in Figure 1. The excited state of Ir^{III} complex **4c** initially undergoes the single-electron transfer (SET) with enol silyl ether **1a** to form the radical cation **A** and the reduced Ir^{II} complex. The subsequent deprotonation of acidic radical cation **A** by cyanopyridine **2a** generates the nucleophilic allylic radical **B** and pyridinium ion **C**. The single-electron reduction of **C** by Ir^{II} complex regenerates Ir^{III} complex to close the reductive quenching cycle with the concomitant formation of radical intermediate **D**, followed by radical−radical coupling with **A** and the elimination of cyanide to furnish hydrogen cyanide salt of **3a**. The excited state of Ir^{III} complex **4c** (Ir*$^{III/IV}$ = −0.87 V) can also promote the single-electron reduction of **C** to generate **D**. This SET process is relayed by single-electron oxidation of **1a** by the transient Ir^{IV} complex (Ir$^{IV/III}$ = 1.81 V) to close the oxidative quenching cycle.
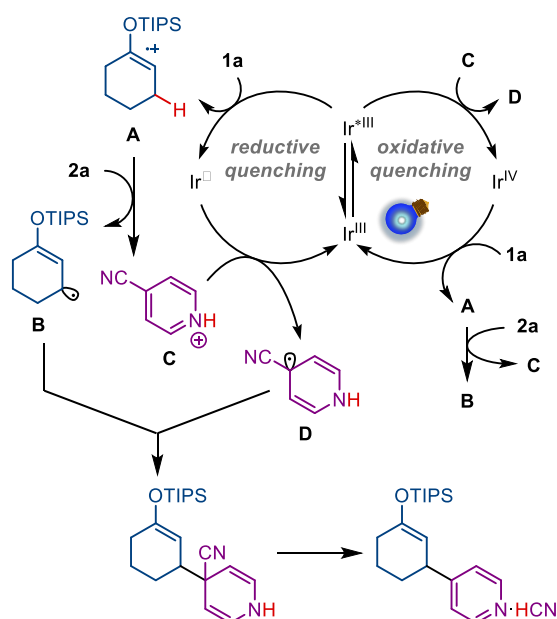
Figure 1. Proposed reaction mechanism.

4. Investigation of Substrate Scope

We subsequently explored the scope of this allylic heteroarylation reaction under photoredox catalysis of **4c** (Figure 2). A series of cyclic enol silyl ethers having five-, six-, seven-, and eight-membered ring systems underwent the radical heteroaromatic substitution to give the corresponding products **3b-3f** in uniformly good yields, while the reactions of seven-

and eight-membered cyclic enol silyl ethers gave slightly higher yield in acetonitrile than in dichloromethane. The present heteroarylation reaction was tolerant to various acyclic ketone-derived enol silyl ethers, and pyridyl-substituted enol silyl ethers **3g-3i** were obtained in good to excellent yields. The C−H functionalization at terminal methyl site also smoothly proceeded to furnish **3j** in good yield. The reactions with a range of substituted cyanopyridines were then examined. 4-Cyanopyidines possessing 2-alkyl- and 2-aryl substituents could be used as coupling partners, providing access to heteroarylation products **3k-3q**. 3-Substituted 4-cyanopyridines and 2,6-disubstituted one were also suitable substrates, giving rise to the corresponding products **3r-3u**. The enol silyl ether **3v** with 7-azaindole ring was obtained in moderate yield through the reaction of **1a** with *N*-Boc 4-cyano-1H-pyrrolo[2,3-b]pyridine.
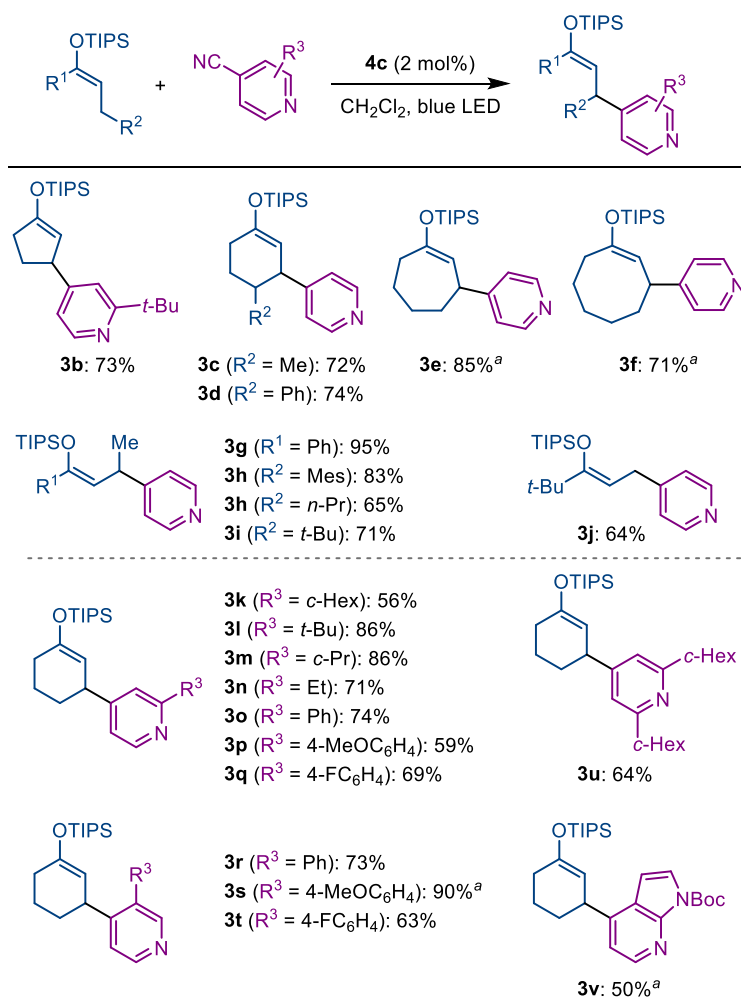
Figure 2. Substrate scope. Isolated yields are indicated. [a] Conducted in MeCN.

5. Conclusions

In conclusion, we have developed a simple synthetic protocol for direct allylic C−H heteroarylation of enol silyl ethers with heteroaryl cyanides. This protocol is based on the utilization of intermediary generated radical cations as Brønsted acid for the activation of heteroaryl cyanides, facilitating the single-electron reduction and subsequent radical−radical coupling. We believe that this study expands the versatility of radical cations and paves the way for the development of new transformations.

6. Experimental Section

Information: ^{1}H NMR spectra were recorded on a JEOL JNM-ECS400 (400 MHz) and JEOL JNMECA600II (600 MHz) spectrometer. Chemical shifts are reported in ppm from the tetramethylsilane (0.0 ppm) resonance as the internal standard ($CDCl_3$). Data are reported as follows: chemical shift, integration, multiplicity (s = singlet, d = doublet, t = triplet, q = quartet, sept =septet, m = multiplet, and br = broad) and coupling constants (Hz). ^{13}C NMR spectra were recorded on a JEOL JNM-ECA600II (151 MHz) spectrometer with complete proton decoupling. Chemical shifts are reported in ppm from the solvent resonance as the internal standard ($CDCl_3$; 77.16 ppm). The high-resolution mass spectra were conducted on Thermo Fisher Scientific Exactive Plus (ESI). Analytical thin layer chromatography (TLC) was performed on Merck precoated TLC plates (silica gel 60 GF254, 0.25 mm). Flash column chromatography was performed on Silica gel 60 N (spherical, neutral, 40~50μm; Kanto Chemical Co., Inc.). All air- and moisture-sensitive reactions were performed under an atmosphere of argon (Ar) in dried glassware. Dichloromethane (CH_2Cl_2) and 1,2-dichloroethane (1,2-DCE) were supplied from Kanto Chemical Co., Inc. as "Dehydrated" and further purified by both A2 alumina and Q5 reactant using a GlassContour solvent dispensing system. The photocatalysts (4a-4c) and enol silyl ethers were synthesized according to the previously reported procedures.[14-16] Other simple chemicals were purchased and used as such.

General Experimental Procedure for Allylic Heteroarylation of Enol Silyl Ethers

To a flame-dried test tube were added heteroarylcyanide (0.10 mmol, 1 equiv), [Ir(dFCF$_3$ppy)$_2$(bpy))]PF$_6$ (2.02 mg, 0.002 mmol, 2 mol%) and CH$_2$Cl$_2$ (1.0 mL, 0.1 M). The reaction tube was sealed with a rubber septum and then evacuated in *vacuo* and backfilled with Ar five times. Enol silyl ether (0.12 mmol, 1.2 equiv) was introduced via syringe. Then, a septum was removed and quickly sealed with a screw cap under a flow of Ar. The whole reaction mixture was stirred at 40 °C under the irradiation of blue LED (448 nm, 250 W/m^2). After indicated time, the reaction mixture was evaporated. Purification of the resulting crude residue by column chromatography on silica gel (hexane 100% to hexane/EtOAc = 5:1) afforded the corresponding heteroarylated enol silyl ether.

Note

In some cases, the desired heteroarylated products were obtained with a slight amount of isomerized products probably through the protonation and deprotonation sequence with hydrogen cyanide in the reaction system. The ratio of product and isomer was indicated respectively if observed.
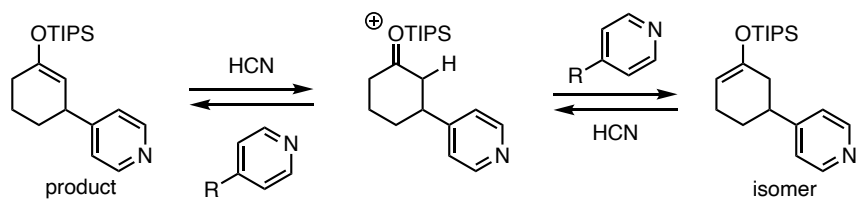
Characterization of Heteroarylated Enol Silyl Ethers
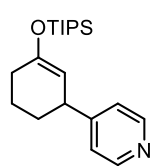
3a: ^{1}H NMR (400 MHz, CDCl$_3$) δ 8.50 (1H, d, J = 4.8 Hz), 7.15 (2H, d, J = 4.8 Hz), 4.86 (1H, brs), 3.50-3.42 (1H, m), 2.26-2.06 (2H, m), 1.98-1.88 (1H, m), 1.83-1.73 (1H, m), 1.73-1.58 (2H, m), 1.47-1.38 (1H, m), 1.23-1.39 (3H, m), 1.11 (12H, d, J = 3.2 Hz), 1.09 (6H, d, J = 3.2 Hz); ^{13}C NMR (151 MHz, CDCl$_3$) δ 156.7, 153.4, 149.5, 123.3, 104.9, 41.2, 31.9, 29.8, 21.6, 18.2, 12.8; HRMS (ESI) Calcd for C$_{20}$H$_{34}$ONSi$^+$ ([M+H]$^+$) 332.2404. Found 332.2399.
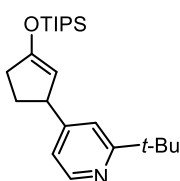
3b (product/isomer > 20:1): ^{1}H NMR (400 MHz, CDCl$_3$) δ 8.44 (2H, d, J = 4.8 Hz), 7.18 (1H, s,), 4.70 (1H, brs), 6.94 (1H, dd, J = 4.8, 1.2 Hz), 4.68 (1H, brs), 3.86-3.77 (1H, m), 2.47-2.33 (3H, m), 1.80-1.61 (1H, m), 1.35 (9H, s), 1.30-1.16 (3H, m), 1.13 (9H, d, J = 1.6 Hz), 1.11 (9H, d, J = 2.4 Hz); ^{13}C NMR (151 MHz, CDCl$_3$) δ 169.4, 157.9, 157.0, 148.7, 119.7, 117.8, 104.9, 47.7, 37.4, 33.8, 31.7, 30.4, 18.0(7), 18.0(6), 12.6; HRMS (ESI) Calcd for C$_{23}$H$_{40}$ONSi$^+$ ([M+H]$^+$) 374.2874. Found 374.2875.
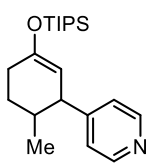
3c (dr = 5.4:1): The reaction was performed for 18 h.
^{1}H NMR (400 MHz, CDCl$_3$) δ 8.50 (2H, d, J = 4.6 Hz), 7.13 (2H, d, J = 4.6 Hz), 4.70 (1H, brs), 2.97 (1H, dd, J = 5.2, 2.4 Hz), 2.39-2.28 (1H, m), 2.18-2.09 (1H, m), 1.84-1.76 (1H, m), 1.64-1.42 (2H, m), 1.09 (12H, d, J = 2.8 Hz), 1.07 (6H, d, J = 2.8 Hz), 0.85 (3H, d, J = 6.4 Hz); ^{13}C NMR (151 MHz, CDCl$_3$) δ 155.9, 152.5, 149.6, 123.9, 105.7, 49.6, 36.3, 31.0, 29.8, 19.5, 18.1, 12.8; HRMS (ESI) Calcd for C$_{21}$H$_{36}$ONSi$^+$ ([M+H]$^+$) 346.2561. Found 346.2560.
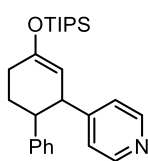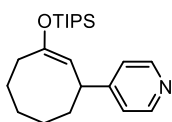
3d (dr > 20:1): The reaction was performed for 18 h.
^{1}H NMR (400 MHz, CDCl$_3$) δ 8.34 (2H, d, J = 6.4 Hz), 7.20-7.09 (3H, m), 6.95 (2H, d, J = 8.0 Hz), 6.83 (2H, d, J = 4.6 Hz), 4.86 (1H, brs), 3.57-3.50 (1H, m), 2.63-2.53 (1H, m), 2.53-2.37 (1H, m), 2.28-2.19 (1H, m), 2.19-2.03 (1H, m), 2.03-1.95 (1H, m), 1.30-1.16 (3H, m), 1.13 (12H, d, J = 4.0 Hz), 1.11 (6H, d, J = 4.0 Hz); ^{13}C NMR (151 MHz, CDCl$_3$) δ 154.7, 152.7, 149.5, 143.9, 128.3, 127.6, 126.6, 123.6, 105.7, 49.1(2), 49.0(6), 30.5, 30.4, 18.1(9), 18.1(7), 12.8; HRMS (ESI) Calcd for C$_{26}$H$_{38}$ONSi$^+$ ([M+H]$^+$) 408.2717. Found 408.2718.
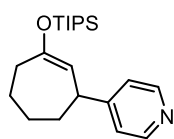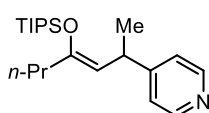
3e: The reaction was performed in MeCN for 36 h.
^{1}H NMR (400 MHz, CDCl$_3$) δ 8.50 (2H, d, J = 4.6 Hz), 7.15 (2H, d, J = 4.6 Hz), 4.91 (1H, d, J = 4.0 Hz), 3.47-3.40 (1H, m), 2.51-2.40 (1H, m), 2.34-2.25 (1H, m), 1.91-1.70 (4H, m), 1.70-1.54 (2H, m), 1.19-1.10 (3H, m), 1.10-1.04 (18H, m); [13]C

NMR (151 MHz, CDCl$_3$) δ 157.2, 156.7, 150.0, 122.8, 110.3, 42.9, 35.7, 35.3, 29.3, 25.0, 18.2, 12.7; HRMS (ESI) Calcd for C$_{21}$H$_{36}$ONSi$^+$ ([M+H]$^+$) 346.2561. Found 346.2562.

3f: The reaction was performed in MeCN for 36 h.
^{1}H NMR (400 MHz, CDCl$_3$) δ 8.50 (2H, d, J = 6.0 Hz), 7.16 (2H, d, J = 6.0 Hz), 4.62 (1H, d, J = 9.2 Hz), 3.52-3.41 (1H, m), 2.55 (1H, td, J = 13.2, 3.6 Hz), 2.08 (1H, dt, J = 14.0, 3.6 Hz), 1.94-1.77 (2H, m), 1.77-1.71 (1H, m), 1.71-1.68 (4H, m), 1.53-1.41 (1H, m), 1.20-1.09 (3H, m), 1.10-1.03 (18H, m); ^{13}C NMR (151 MHz, CDCl$_3$) δ 156.1, 153.7, 149.9, 122.7, 106.5, 42.1, 37.9, 32.7, 28.6, 26.9, 26.2, 18.2, 12.8; HRMS (ESI) Calcd for C$_{22}$H$_{38}$ONSi$^+$ ([M+H]$^+$) 360.2717. Found 360.2717.
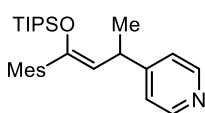
3g (*Z/E* = 1.1:1): The reaction was performed for 18 h.
^{1}H NMR (400 MHz, CDCl$_3$) (for *Z* isomer) δ 8.43 (2H, d, J = 5.2 Hz), 7.23 (2H, d, J = 6.0 Hz), 6.82 (1H, s), 6.79 (1H, s), 5.10 (d, 1H, J = 10.8 Hz), 2.95 (1H, dq, J = 10.4, 7.2 Hz), 2.34(9) (3H, s), 2.29 (3H, s), 1.94 (3H, s), 1,24 (3H, d, J = 7.2 Hz), 1.22-1.15 (3H, m), 1.07 (12H, d, J = 3.6 Hz), 1.06 (6H, d, J = 4.0 Hz), (for *E* isomer) δ 8.49 (2H, d, J = 5.6 Hz), 6.94 (2H, d, J = 5.6 Hz), 6.88 (1H, s), 6.79 (1H, s), 4.60 (d, 1H, J = 9.6 Hz), 4.19-4.07(1H, m), 2.34(5) (3H, s), 2.25 (3H, s), 2.20 (3H, s), 1,38 (3H, d, J = 7.2 Hz), 1.03-0.95 (3H, m), 0.92 (9H, d, J = 7.2 Hz), 0.90 (9H, d, J = 7.2 Hz); ^{13}C NMR (151 MHz, CDCl$_3$) (for *Z* isomer) 156.2, 149.8, 137.2, 136.4, 135.8, 134.2, 128.2(6), 128.1, 122.3, 111.2, 38.0, 23.0, 21.2, 20.1, 19.9, 18.3, 13.1, (for *E* isomer) δ 156.4, 149.8, 147.2, 137.5, 136.8, 136.3, 128.4, 128.3(1), 122.6, 115.4, 35.2, 21.7, 21.1, 20.3, 18.0, 13.2; HRMS (ESI) Calcd for C$_{27}$H$_{42}$ONSi$^+$ ([M+H]$^+$) 424.3030. Found 424.3029.

3h (*Z/E* = 1.2:1): The reaction was performed in MeCN for 48 h.
^{1}H NMR (400 MHz, CDCl$_3$) (for *Z* isomer) δ 8.48 (2H, d, J = 6.4 Hz), 7.14 (2H, d, J = 6.4 Hz), 4.66 (1H, d, J = 10.0 Hz), 3.51 (1H, dq, J = 9.6, J = 6.8), 2.12-2.06 (2H, m), 1.59-1.43 (2H, m), 1.31 (3H, d, J = 7.2 Hz), 1.21-1.10 (3H, m), 1.10-1.03 (18H, m), 0.88 (3H, t, J = 7.2 Hz), (for *E* isomer), δ 8.46 (2H, d, J = 6.4 Hz), 7.17 (2H, d, J = 5.6 Hz), 4.45 (1H, d, J = 9.2 Hz), 3.94 (1H, dq, J = 9.6, 7.6 Hz), 2.05 (2H, t, J = 8.0 Hz), 1.59-1.43 (2H, m), 1.28 (3H, d, J = 6.8 Hz), 1.21-1.10 (3H, m), 1.10-1.03 (18H, m), 0.92 (3H, t, J = 7.2 Hz); ^{13}C NMR (151 MHz, CDCl$_3$) (for *Z* isomer) δ 156.6, 152.6, 149.9, 122.4, 109.7, 37.2, 33.9, 22.8, 20.5, 18.2, 14.0, 12.8, (for *E* isomer) δ 156.7, 151.2, 149.7, 122.6, 109.9, 38.5, 34.7, 21.8, 20.7, 18.2, 13.9, 13.5; HRMS (ESI) Calcd for C$_{21}$H$_{38}$ONSi$^+$ ([M+H]$^+$) 348.2717. Found 348.2712.
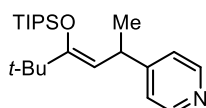
3i (*Z/E* = 11.1:1): ^{1}H NMR (400 MHz, CDCl$_3$) δ 8.48 (2H, d, J = 4.6 Hz), 7.17 (2H, d, J = 4.8 Hz), 4.58 (1H, d, J = 10.0 Hz), 3.75-3.63 (1H, m), 1.27 (3H, d, *J*

= 6.6 Hz), 1.24-1.15 (3H, m), 1.13 (9H, s), 1.10 (9H, d, J = 6.8 Hz), 1.05 (9H, d, J = 7.2 Hz); ^{13}C NMR (151 MHz, CDCl$_3$) δ 158.6, 156.2, 149.7, 122.5, 104.4, 37.4, 34.4, 29.1, 23.0, 18.5, 14.7; HRMS (ESI) Calcd for C$_{22}$H$_{40}$ONSi$^+$ ([M+H]$^+$) 362.2874. Found 362.2877.
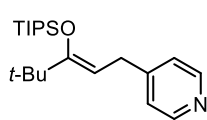
3j (*Z/E* = 7.7:1, determined after purification): ^{1}H NMR (400 MHz, CDCl$_3$) δ 8.48 (2H, d, J = 5.6 Hz), 7.12 (2H, d, J = 6.0 Hz), 4.53 (1H, t, J = 7.2 Hz), 3.33 (2H, d, J = 7.2), 1.31-1.16 (3H, m), 1.13(3) (9H, s), 1.12(5) (12H, brd), 1.11 (6H, brd); ^{13}C NMR (151 MHz, CDCl$_3$) δ 160.7, 151.6, 149.6, 123.9, 97.7, 37.5, 31.7, 29.1, 18.5, 14.7; HRMS (ESI) Calcd for C$_{21}$H$_{38}$ONSi$^+$ ([M+H]$^+$) 348.2717. Found 348.2718.
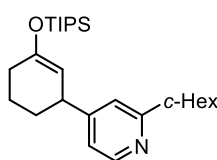
3k: ^{1}H NMR (400 MHz, CDCl$_3$) δ 8.40 (1H, d, J = 5.2 Hz), 7.01 (1H, s), 6.95 (1H, dd, J = 5.0, 1.6 Hz), 4.86(1H, brs), 3.47-3.39 (1H, m), 2.67 (1H, tt, J = 12.0, 3.6 Hz), 2.28-2.08 (2H, m), 1.98-1.89 (3H, m), 1.89-1.81 (2H, m), 1.81-1.70 (2H, m), 1.70-1.60 (1H, m), 1.58-1.45 (2H, m), 1.45-1.34 (2H, m), 1.34-1.24 (2H, m), 1.24-1.15 (3H, m), 1.12 (12H, d, J = 4.0 Hz), 1.10 (6H, d, J = 4.4 Hz); ^{13}C NMR (151 MHz, CDCl$_3$) δ 166.6, 156.7, 153.1, 149.0, 120.7, 120.3, 105.4, 46.8, 41.3, 33.2, 33.1, 32.1, 29.9, 26.8, 26.3, 21.8, 18.2(0), 18.1(8), 12.8; HRMS (ESI) Calcd for C$_{26}$H$_{44}$ONSi$^+$ ([M+H]$^+$) 414.3187. Found 414.3187.
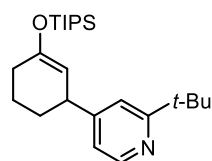
3l (product/isomer = 12.7:1): ^{1}H NMR (400 MHz, CDCl$_3$) δ 8.45 (1H, d, J = 4.8 Hz), 7.19 (1H, s), 6.95 (1H, dd, J = 5.2, 0.8 Hz), 4.87 (1H, brs), 3.48-3.40 (1H, m), 2.29-2.06 (2H, m), 1.98-1.87 (1H, m), 1.85-1.75 (1H, m), 1.75-1.60 (1H, m), 1.45-1.35(1H, m) 1.36 (9H, s), 1.27-1.13 (3H, m), 1.12 (12H, d, J = 3.2 Hz), 1.10 (6H, d, J = 3.2 Hz); ^{13}C NMR (151 MHz, CDCl$_3$) δ 169.4, 156.5, 153.1, 148.5, 120.4, 118.4, 105.4, 41.6, 37.5, 32.3, 30.4, 29.8, 21.9, 18.2, 12.8; HRMS (ESI) Calcd for C$_{24}$H$_{42}$ONSi$^+$ ([M+H]$^+$) 388.3030. Found 388.3028.
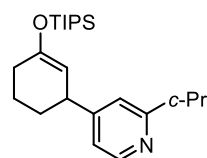
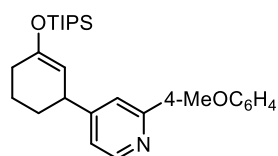**3m** (product/isomer = 10.1:1): ^{1}H NMR (400 MHz, CDCl$_3$) δ 8.32 (1H, d, J = 4.8 Hz), 6.98 (1H, s), 6.89 (1H, dd, J = 4.8, 1.6 Hz), 4.85 (1H, brs), 3.45-3.87 (1H, m), 2.27-2.06 (2H, m), 2.03-1.96 (1H, m), 1.96-1.87 (1H, m), 1.86-1.73 (1H, m), 1.71-1.59 (1H, m), 1.45-1.34 (1H, m), 1.24-1.13 (3H, m), 1.11 (12H, d, J = 3.6 Hz), 1.10 (6H, d, J = 3.6 Hz), 1.01-0.94 (4H, m); ^{13}C NMR (151 MHz, CDCl$_3$) δ 162.8, 156.2, 153.1, 149.2, 120.5, 120.2, 105.3., 41.1, 32.0, 29.9, 21.7, 18.2, 17.3, 12.8, 9.81, 9.74; HRMS (ESI) Calcd for C$_{23}$H$_{38}$ONSi$^+$ ([M+H]$^+$) 372.2717. Found 372.2716.
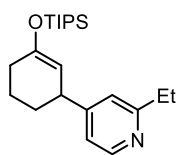
3n (product/isomer = >20:1): ^{1}H NMR (400 MHz, CDCl$_3$) δ 8.40 (1H, d, J = 4.4 Hz), 7.02 (1H, s), 6.96 (1H, dd, J = 4.8, 1.6 Hz), 4.86(1H, brs), 3.47-3.39 (1H, m), 2.79 (2H, q, J = 7.6 Hz), 2.28-2.07 (2H, m), 1.98-1.88 (1H, m), 1.83-1.73 (1H, m), 1.73-1.55 (1H, m), 1.46-1.34 (1H, m), 1.30 (3H, t, J = 7.6 Hz), 1.24-1.15 (3H, m), 1.11 (12H, d, J = 3.2 Hz), 1.10 (6H, d, J = 3.2 Hz); ^{13}C NMR (151 MHz, CDCl$_3$) δ 163.5, 156.8, 153.1, 149.2, 121.4, 120.6, 105.3, 41.2, 32.0, 31.5, 29.9, 21.7, 18.1(8), 18.1(6), 14.1, 13.0; HRMS (ESI) Calcd for C$_{22}$H$_{38}$ONSi$^+$ ([M+H]$^+$) 360.2717. Found 360.2714.
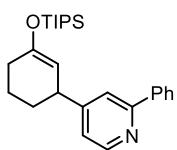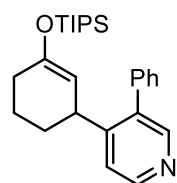
3o: The reaction was performed in MeCN.
^{1}H NMR (400 MHz, CDCl$_3$) δ 8.58 (1H, d, J = 4.0 Hz), 7.97 (2H, d, J = 8.4 Hz), 7.60 (1H, s), 7.47 (2H, td, J = 7.8, 1.6 Hz), 7.43-7.37 (1H, m), 7.10 (1H, d, J = 4.8 Hz), 4.93 (1H, brs), 3.54 (1H, brs), 2.28-2.10 (2H, m), 2.03-1.93 (1H, m), 1.87-1.76 (1H, m), 1.76-1.63 (1H, m), 1.52-1.41 (1H, m), 1.32-1.16 (3H, m), 1.13 (12H, d, J = 2.4 Hz), 1.12 (6H, d, J = 3.2 Hz); ^{13}C NMR (151 MHz, CDCl$_3$) δ 157.7, 157.2, 153.4, 149.7, 139.9, 128.9, 128.8, 127.1, 121.9, 120.1, 105.0, 41.4, 32.1, 29.9, 21.7, 17.9, 18.2, 12.8. 12.4; HRMS (ESI) Calcd for C$_{26}$H$_{38}$ONSi$^+$ ([M+H]$^+$) 408.2717. Found 408.2718.
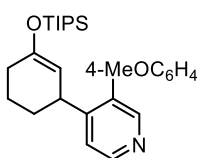
3p (product/isomer = >20:1): The reaction was performed in 1,2-DCE.
^{1}H NMR (400 MHz, CDCl$_3$) δ 8.53 (1H, d, J = 4.4 Hz), 7.93 (2H, d, J = 6.8 Hz), 7.53 (1H, s), 7.04 (1H, dd, J = 5.2, 1.6 Hz), 6.99 (2H, d, J = 6.8 Hz), 4.92 (1H, brs), 3.55-3.48 (1H, m), 3.87 (3H, s), 2.28-2.08 (2H, m), 2.02-1.92 (1H, m), 1.87-1.76 (1H, m), 1.75-1.63 (1H, m), 1.51-1.40 (1H, m), 1.30-1.16 (3H, m), 1.13 (12H, d, J = 3.2 Hz), 1.11 (6H, d, J =4.0 Hz); ^{13}C NMR (151 MHz, CDCl$_3$) δ 160.5, 157.3, 157.1, 153.3, 149.5, 132.5, 128.3, 121.2, 119.3, 114.2, 105.1, 55.5 41.4, 32.1, 29.9, 21.8, 18.2, 12.8; HRMS (ESI) Calcd for C$_{27}$H$_{40}$O$_2$NSi$^+$ ([M+H]$^+$) 438.2823. Found 426.2824.
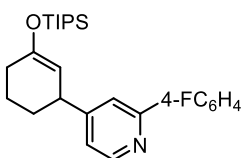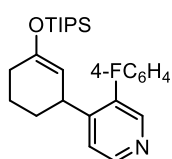
3q: The reaction was performed in MeCN.
^{1}H NMR (400 MHz, CDCl$_3$) δ 8.55 (1H, d, J = 4.8 Hz), 7.98-7.92 (2H, m), 7.54 (1H, s), 7.18-7.12 (2H, m), 7.10 (1H, dd, J = 5.0, 1.6 Hz), 4.91 (1H, brs), 3.57-3.48 (1H, m), 2.28-2.09 (2H, m), 2.02-1.93 (1H, m), 1.86-1.76 (1H, m), 1.76-1.63 (1H, m), 1.51-1.40 (1H, m), 1.30-1.15 (3H, m), 1.13 (12H, d, J = 2.8 Hz), 1.11 (6H, d, J = 3.2 Hz); ^{13}C NMR (151 MHz, CDCl$_3$) δ 163.6 (d, J_{C-F} = 247.2 Hz), 157.4, 156.7, 153.5, 149.7, 136.0, 128.9 (d, J_{C-F} = 8.6 Hz), 121.8, 119.8, 115.7 (d, J_{C-F} = 21.6 Hz), 105.0, 41.4, 32.1, 29.9, 21.7, 18.2, 17.9, 12.8, 12.4; HRMS (ESI) Calcd for C$_{26}$H$_{37}$ONFSi$^+$ ([M+H]$^+$) 426.2623. Found 426.2624.

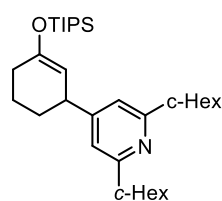**3r**: [structure: OTIPS-substituted cyclohexene with Ph group on pyridine] ^{1}H NMR (400 MHz, CDCl$_3$) δ 8.50 (1H, d, J = 5.6 Hz), 8.39 (1H, s), 7.48-7.37 (3H, m), 7.32-7.27(3H, m), 4.76 (1H, brs), 3.64 (1H, br), 2.26-2.14 (1H, m), 2.10-1.99 (1H, m), 1.81-1.70 (2H, m), 1.57-1.45 (1H, m), 1.39-1.22 (1H, m), 1.22-1.11 (3H, m), 1.11-1.05 (18H, m); ^{13}C NMR (151 MHz, CDCl$_3$) δ 153.7, 152.9, 150.4, 148.8, 138.0, 137.3, 129.6, 128.5, 127.7, 122.8, 105.9, 37.0, 31.3, 29.8, 21.9, 18.2, 12.8; HRMS (ESI) Calcd for C$_{26}$H$_{38}$ONSi$^+$ ([M+H]$^+$) 408.2717. Found 408.2724.

3s: The reaction was performed in MeCN for 18 h. [structure: OTIPS-substituted cyclohexene with 4-MeOC$_6$H$_4$ group on pyridine] ^{1}H NMR (400 MHz, CDCl$_3$) δ 8.48 (1H, d, J = 5.6 Hz), 8.38 (1H, s), 7.27 (1H, d, J = 4.4 Hz), 7.22 (2H, d, J = 6.6 Hz), 6.98 (2H, d, J = 7.6 Hz), 4.76 (1H,brs), 3.87 (3H, s), 3.69-3.61 (1H, m), 2.26-2.15 (1H, m), 2.10-2.00 (1H, m), 1.81-1.70 (2H, m), 1.58-1.45 (1H, m), 1.38-1.22 (1H, m), 1.21-1.11 (3H, m), 1.10 (12H, d, J = 4.8 Hz), 1.08 (6H, d, J = 4.4 Hz); ^{13}C NMR (151 MHz, CDCl$_3$) δ 159.2, 153.9, 152.8, 150.6, 148.5, 136.9, 130.7, 130.3, 122.8, 114.0, 106.0, 55.5, 37.0, 31.3, 29.8, 21.9, 18.2, 12.8; HRMS (ESI) Calcd for C$_{27}$H$_{40}$O$_2$NSi$^+$ ([M+H]$^+$) 438.2823. Found 438.2825.

3t: [structure: OTIPS-substituted cyclohexene with 4-FC$_6$H$_4$ group on pyridine] ^{1}H NMR (400 MHz, CDCl$_3$) δ 8.51 (1H, d, J = 4.8 Hz), 8.37(1H, s), 7.30-7.24 (3H, m), 7.17-7.10 (2H, m), 4.75 (1H, brs), 3.62-3.52 (1H, m), 2.26-2.15 (1H, m), 2.10-2.00 (1H, m), 1.82-1.68 (2H, m), 1.57-1.44 (1H, m), 1.37-1.23 (1H, m), 1.21-1.11 (3H, m), 1.10 (12H, d, J = 4.8 Hz), 1.08 (6H, d, J = 4.4 Hz); ^{13}C NMR (151 MHz, CDCl$_3$) δ 162.6 (d, J_{C-F} = 247.2 Hz), 153.9, 153.1, 150.4, 149.0, 136.3, 133.9, 131.3 (d, J_{C-F} = 7.2 Hz), 122.8, 115.5 (d, J_{C-F} = 21.7 Hz), 105.6, 105.0, 37.1, 31.3, 29.8, 21.9, 18.2, 12.8; HRMS (ESI) Calcd for C$_{26}$H$_{37}$ONFSi$^+$ ([M+H]$^+$) 426.2623. Found 426.2636.

3u (product/isomer = 8.7:1): The reaction was performed in MeCN. [structure: OTIPS-substituted cyclohexene with 2,6-di-c-Hex pyridine] ^{1}H NMR (400 MHz, CDCl$_3$) δ 6.81 (2H, s), 4.85 (1H, brs), 3.39 (1H, brd), 2.65 (2H, brd), 2.26-2.04 (2H, m), 2.02-1.86 (5H, m), 1.86-1.68 (7H, m), 1.68-1.54 (1H, m), 1.50-1.32 (9H, m), 1.32-1.15 (5H, m), 1.14-1.08 (18H, m) δ 6.81 (2H, s), 5.01 (1H, brs), 3.31 (1H, brd), 2.65 (2H, brd), 2.26-2.04 (2H, m), 2.02-1.86 (5H, m), 1.86-1.68 (7H, m), 1.68-1.54 (1H, m), 1.50-1.32 (9H, m), 1.32-1.15 (5H, m), 1.05-0.95 (3H, m), 0.91 (12H, d, J = 3.2 Hz), 0.89 (6H, d, J = 3.6 Hz); ^{13}C NMR (151 MHz, CDCl$_3$) δ 165.7, 156.8, 152.8, 117.1, 105.8, 46.8, 41.6, 33.4(1), 33.3(8), 32.4, 29.9, 26.8, 26.4, 22.0, 18.2(2), 18.1(9), 12.8; HRMS (ESI) Calcd for C$_{32}$H$_{54}$ONSi$^+$ ([M+H]$^+$) 496.3969. Found 496.3964.

3v: The reaction was performed in MeCN.

[structure: OTIPS-substituted cyclohexene attached to a 7-azaindole bearing NBoc]
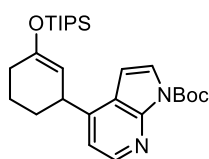
^{1}H NMR (400 MHz, CDCl$_3$) δ 8.41 (1H, dd, J = 5.2, 0.8 Hz), 7.59 (1H, dd, J = 4.4, 1.6 Hz), 7.06 (1H, dd, J = 4.4, J = 0.8 Hz), 6.59 (1H, dd, J = 4.0, 2.0 Hz), 4.93 (1H, brs), 3.87 (1H, brs), 2.30-2.10 (2H, m), 2.40-1.93 (1H, m), 1.85-1.74 (1H, m), 1.74-1.68 (1H, m), 1.28-1.23 (1H, m), 1.67 (9H, brs), 1.24-1.13 (3H, m), 1.11 (12H, brd), 1.09 (6H, brd); ^{13}C NMR (151 MHz, CDCl$_3$) δ 153.1, 149.2, 148.6, 148.1, 145.5, 125.7, 122.0, 117.3, 105.0, 103.0, 83.9, 38.6, 30.6, 29.9, 28.3, 21.8, 18.2, 12.8; HRMS (ESI) Calcd for C$_{27}$H$_{43}$O$_3$N$_2$Si$^+$ ([M+H]$^+$) 471.3037. Found 471.3040.

Square Wave Voltammetry

Square wave voltammetry (SWV) measurements of representative enol silyl ether **1a**, 4-cyanopyridine **2a**, 4-cyanopyridine hydromesylate (2a·HOMs), and heteroarylated enol silyl ether **3a** were performed on ALS/CH Instruments Electrochemical Analyzer using a glassy carbon working electrode, a Pt wire counter electrode, and a ferrocene/ferrocenium reference electrode. Voltammograms were taken at room temperature in a 100 mM MeCN solution of tetrabutylammonium perchlorate (Bu$_4$N·ClO$_4$) containing 1 mM of the designated substance. For conversion to the SCE couple, it is known that Fc/Fc+ is 380 mV more positive than SCE in MeCN; this value was added from obtained potentials in Fc/Fc+ to determine potentials against SCE.

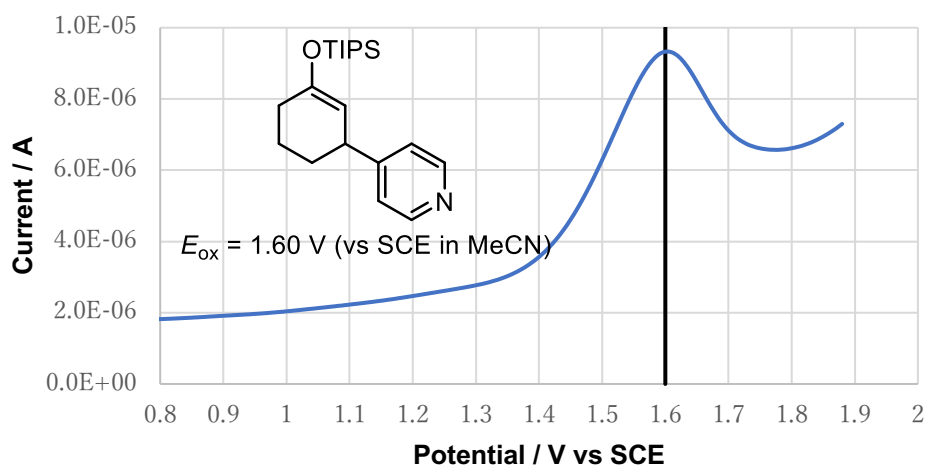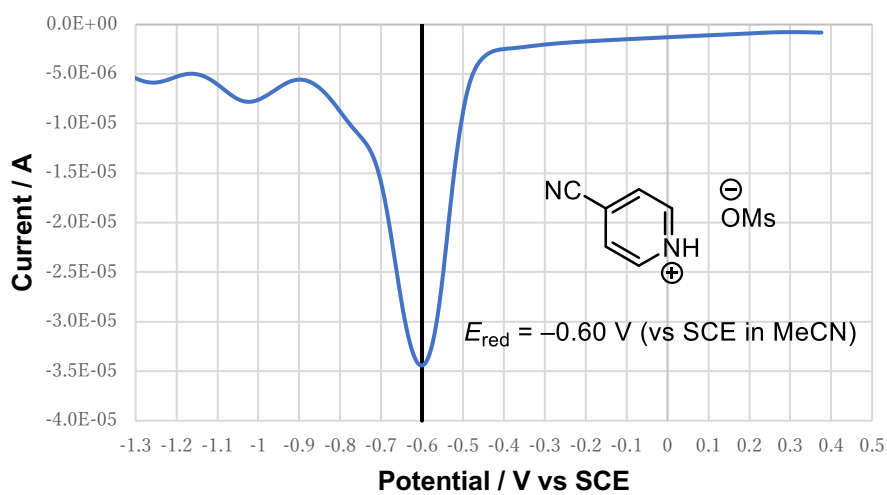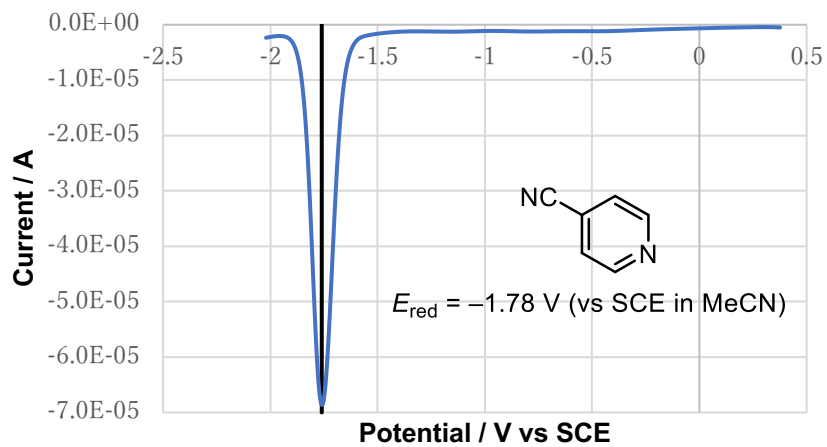E_{ox} = 1.46 V (vs SCE in MeCN)

$E_\text{red} = -1.78$ V (vs SCE in MeCN)

$E_\text{red} = -0.60$ V (vs SCE in MeCN)

$E_\text{ox} = 1.60$ V (vs SCE in MeCN)

Figure S1. SWV measurements.

Stern-Volmer Experiments

Emission intensities were recorded on a HORIBA FluoroMax-4P spectrometer. The solutions were excited at 420 nm and the luminescence was measured at 468 nm. Stern-Volmer luminescence quenching experiments were run with freshly prepared a 0.1 mM solutions of [Ir(dF(CF3)ppy)$_2$(bpy)]PF$_6$ in dry 1,2-dichloroethane (1,2-DCE) at room temperature under N$_2$ atmosphere. In a typical experiment, the solution of Ir complex was added to an appropriate amount of quencher in 5 mL volumetric flask under N$_2$. The solution was transferred to 1 cm^2 quartz cell and the emission spectrum of the sample was collected. The data show that enol silyl ether **1a**, 4-cyanopyridinium hydromesylate (**2a·HOMs**), and heteroarylated enol silyl ether **3a** are competent at quenching the excited state of the photocatalyst. On the other hand, 4-cyanopyridine (**2a**) are shown to be unable to quench this excited state.
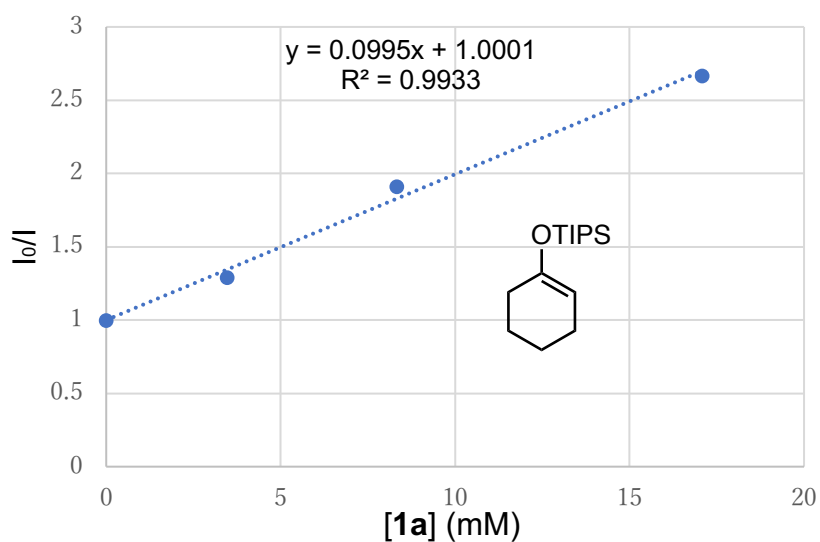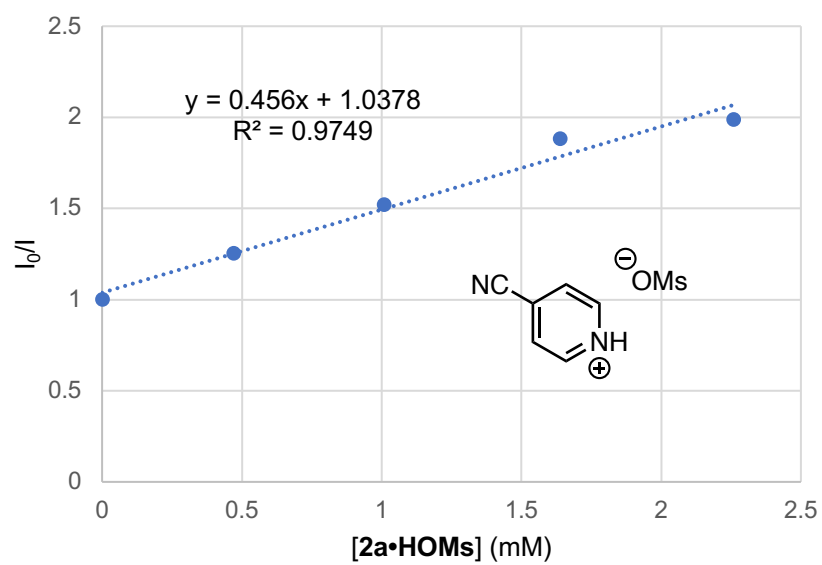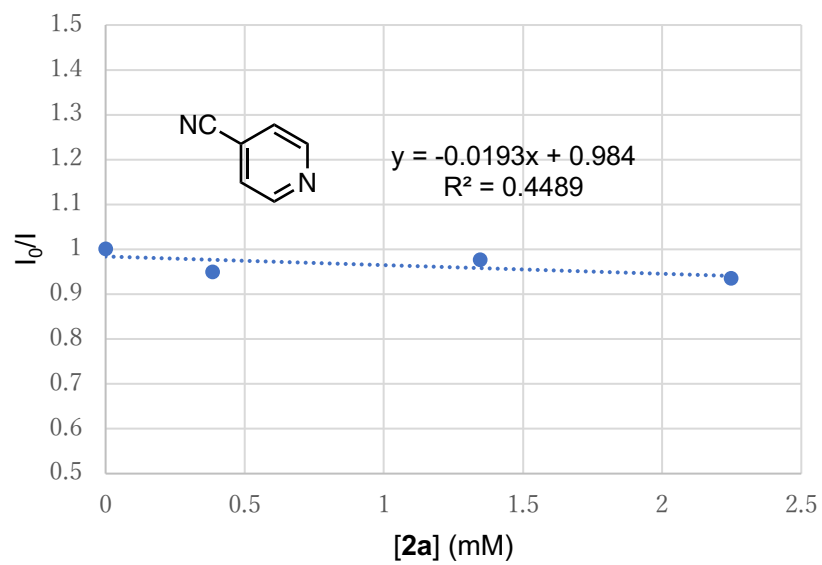
**Figure S2.** Stern-Volmer Experiments.

References and Notes

(1) Bauld, N. L. *Tetrahedron* **1989**, *45*, 5307.

(2) (a) Moeller, K. D. *Tetrahedron* **2000**, *56*, 9527; (b) Reddy, S. H. K.; Chiba, K.; Sun, Y. M.; Moeller, K. D. *Tetrahedron* **2001**, *57*, 5183.

(3) Mangion, D.; Arnold, D. R. *Acc. Chem. Res.* **2002**, *35*, 297

(4) (a) Gürtler, C. F.; Blechert, S.; Steckhan, E. *Angew. Chem. Int. Ed. Engl.* **1995**, *34*, 1900. (b) Schepp, N. P.; Johnston, L. J. *J. Am. Chem. Soc.* **1996**, *118*, 2872. (c) Nakamura, M.; Toganoh, M; Ohara, H; Nakamura, E. *Org. Lett.* **1999**, *1*, 7. (d) Ischay, M. A.; Lu, Z.; Yoon, T. P. *J. Am. Chem. Soc.* **2010**, *132*, 8572. (e) Lin, S.; Ischay, M. A.; Fry, C. G.; Yoon, T. P. *J. Am. Chem. Soc.* **2011**, *133*, 19350. (f) Horibe, T.; Ohmura, S.; Ishihara, K. *J. Am. Chem. Soc.* **2019**, *141*, 1877.

(5) (a) Schmittel, M; Burghart, A. *Angew. Chem. Int. Ed. Engl.* **1997**, *36*, 2550. (b) Sutterer, A.; Moeller, K. D. *J. Am. Chem. Soc.* **2000**, *122*, 5636. (c) Hamilton, D. S.; Nicewicz, D. A. *J. Am. Chem. Soc.* **2012**, *134*, 18577. (d) Musacchio, A. J.; Nguyen, L. Q.; Beard, G. H.; Knowles, R. R. *J. Am. Chem. Soc.* **2014**, *136*, 12217.

(6) Baciocchi, E.; Bietti, M.; Lanzalunga, O. *Acc. Chem. Res.* **2000**, *33*, 243.

(7) Nicholas, A. M. de P.; Arnold, D. R. *Can. J. Chem.* **1982**, *60*, 2165.

(8) Gassman, P. G.; Bottorff, K. J. *J. Org. Chem.* **1988**, *53*, 1097.

(9) Ohmatsu, K.; Nakashima, T.; Sato, M.; Ooi, T. *Nat. Commun.* **2019**, *10*, 2706.

(10) Vittimberga, B. M.; Minisci, F.; Morrocchi, S. *J. Am. Chem. Soc.* **1975**, *97*, 4397.

(11) For examples of photoredox-catalyzed substitutions of heteroarylcyanides: (a) Zuo, Z.; MacMillan, D. W. C. *J. Am. Chem. Soc.* **2014**, *136*, 5257. (b) Cuthbertson, J. D.; MacMillan, D. W. C. *Nature* **2015**, *519*, 74. (c) Nakajima, K.; Nojima, S.; Sakata, K.; Nishibayashi, Y. *ChemCatChem* **2016**, *8*, 1028. (d) Chen, M.; Zhao, X.; Yang, C.; Xia, W. *Org. Lett.* **2017**, *19*, 3807. (e) Zhu, S.; Qin, J.; Wang, F.; Li, H.; Chu, L. *Nat. Commun.* **2019**, *10*, 749. (f) Lipp, B.; Kammer, L. M.; Kücükdisli, M.; Luque, A.; Kühlborn, J.; Pusch, S.; Matulevičiūtė, G.; Schollmeyer, D.; Šačkus, A.; Opatz, T. *Chem. Eur. J.* **2019**, *25*, 8965. (g) Lehnherr, D.; Lam, Y.; Nicastri, M. C.; Liu, J.; Newman, J. A.; Regalado, E. L.; DiRocco, D. A.; Rovis, T. *J. Am. Chem. Soc.* **2020**, *142*, 468. (h) Nicastri, M. C.; Lehnherr, D.; Lam, Y.; DiRocco, D. A.; Rovis, T. *J. Am. Chem. Soc.* **2020**, *142*, 987. (i) Zhou, C.; Lei, T.; Wei, X.-Z.; Ye, C.; Liu, Z.; Chen, B.; Tung, C.-H.; Wu, L.-Z. *J. Am. Chem. Soc.* **2020**, *142*, 16805. (j) Shen, J.; Zhang, Y.; Yu, Y.; Wang, M. *Org. Chem. Front.* **2021**, doi: 10.1039/d0qo01218a.

(12) Light irradiation without a fan to cool reaction vessel led to the increase of reaction temperature to 40 °C. For details, see the ESI.

(13) For details, see the Supplementary Information.

(14) Choi, G. J.; Zhu, Q.; Miller, D. C.; Gu, C. J.; Knowles, R. R. *Nature* **2016**, *539*, 268.

(15) Lowry, M. S.; Hudson, W. R.; Pascal, R. A. Jr.; Bernhard, S. *J. Am. Chem. Soc.* **2004**, *126*, 14129.

(16) Ito, H.; Ohmiya, H.; Sawamura, M. *Org. Lett.* **2010**, *12*, 4380.

Chapter 3

Mannich-type Allylic C−H Functionalization of Enol Silyl Ethers under Photoredox-Thiol Hybrid Catalysis
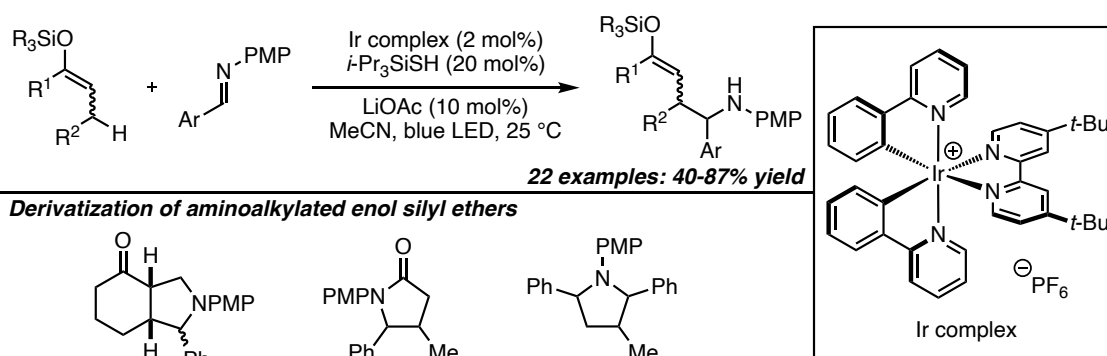
**Abstract:**

The synergy of an Ir-based photosensitizer with mild oxidizing ability and a thiol catalyst enables efficient allylic C−H functionalization of enol silyl ethers with imines under visible light irradiation. Subsequent transformations of the aminoalkylated enol silyl ethers allow for the facile construction of unique molecular frameworks such as functionalized octahydroisoindol-4-one.

1. Introduction

Aminocarbonyls serve as valuable building blocks for the assembly of biologically active and medicinally relevant organic molecules, especially those containing this structural motif as the core component.[1] Hence, there is strong demand for the development of reliable yet practical methods for rapid access to a diverse array of nitrogen-containing carbonyl compounds in the field of synthetic chemistry and pharmaceutical science.[2] One of the most versatile reaction manifolds in this regard is the Mannich-type bond connection, including vinylogous Mannich addition, wherein a wide variety of carbonyl nucleophiles and imine electrophiles can be employed for the construction of β- or δ-aminocarbonyl architectures.[3]

To access γ-aminocarbonyl compounds *via* the nucleophilic addition of carbonyl compounds to imines, activation of the inherently electrophilic or inert carbonyl β-carbons as nucleophiles is necessary. Although this mode of bond formation is attractive given the potential diversity in the structures of accessible γ-aminocarbonyl compounds, research on the development of strategies for enabling the requisite nucleophilic activation of carbonyl β-carbons have met with limited success.[4,5] A representative means for implementing the nucleophilic activation of carbonyl β-carbons relies on the polarity inversion of α,β-unsaturated aldehydes using *N*-heterocyclic carbenes as catalysts.[4] Activation of the β-sp³ carbons in saturated carbonyl substrates was also achieved, although the scope was limited to β-arylpropionic acid esters (Scheme 1a).[5]

Recently, the synergy of photoredox and other molecular catalysts has created a basis for devising methodologies that allow for the formal activation of carbonyl β-carbons. In the seminal contribution by MacMillan and coworkers, the single-electron oxidation of an enamine and subsequent deprotonation of the resulting radical cation generated an intermediate with a nucleophilic carbon radical at the allylic position.[6] This strategy has been successfully applied to establish β-Mannich-type reactions of saturated cyclic ketones with imines (Scheme 1b).[7] On the other hand, the author has introduced a photoredox−Brønsted base co-catalyzed allylic C−H alkylation of enol silyl ethers with electron-deficient olefins.[8] One of the salient features of this protocol is the broad substrate scope, as a series of cyclic and acyclic ketone-derived enol silyl ethers undergo allylic C−H alkylation to afford β-functionalized ketone derivatives. Herein, the author extend the allylic C−H functionalization strategy to the reaction of enol silyl ethers with imines (Scheme 1c). The present transformation and subsequent derivatization of the resulting functionalized enol silyl ethers provide facile access to a range of γ-aminocarbonyl compounds.
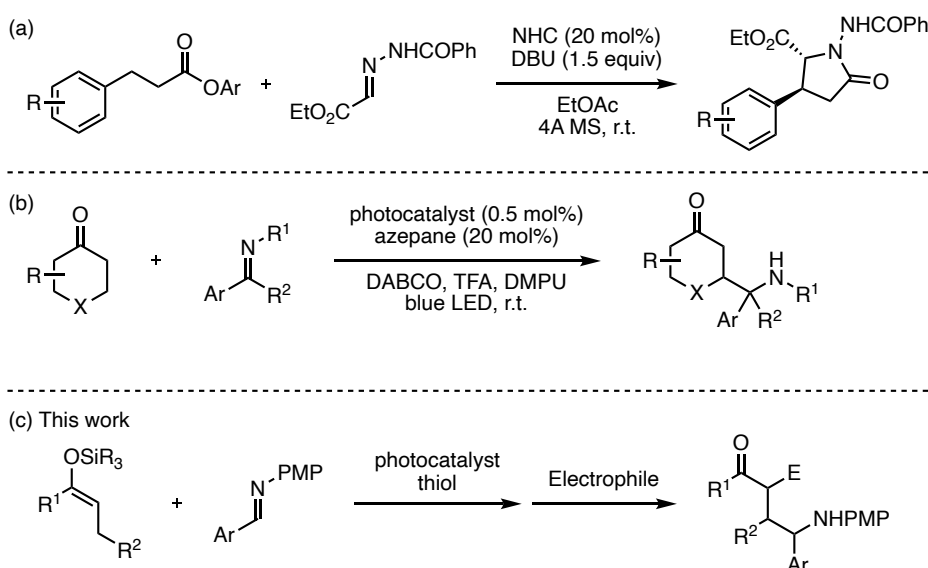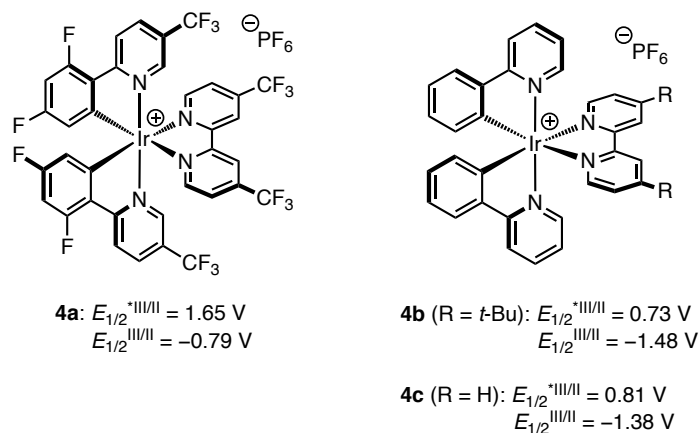
Scheme 1. (a) NHC-catalyzed β-Mannich-type addition-cyclization reaction; (b) β-Mannich-type reaction by photoredox-enamine catalysis; (c) allylic Mannich-type addition of enol silyl ethers.

2. Results and Discussion

For the preliminary experiment, we selected cyclohexanone-derived enol silyl ether **1a** and *N*-methanesulfonyl imine **2a** as model substrates and subjected them to the reaction conditions previously optimized for the allylic C−H alkylation (Scheme 2).[8] Thus, [Ir(dFCF$_3$ppy)$_2$(4,4′-dCF$_3$bpy)]PF$_6$ (**4a** in Figure 1, 2 mol%) and 2,4,6-collidine (10 mol%) were employed as the photoredox and Brønsted base catalysts, respectively, to generate an allylic radical from **1a** (E_{ox} = 1.52 V vs. SCE) via a single-electron oxidation-deprotonation sequence in the presence of **2a** as a radical acceptor in 1,2-dichlororethane under visible-light irradiation. In this trial, however, the desired Mannich-type allylic C−H functionalization did not occur at all. The author inferred that the addition of the **1a**-derived allylic radical to **2a** would be unfavorable because of the relative instability of the nitrogen-centered radical generated after carbon-carbon bond formation.[9] Because aromatic substituents with electron-donating groups effectively stabilize nitrogen radicals,[9a] *N*-aryl imines, such as *N*-PMP imines, would be more suitable electrophilic partners for promoting the nucleophilic radical addition. Nevertheless, the corresponding products bearing an *N*-arylamino functionality would have lower oxidation potential than that of enol silyl ethers (the oxidation potential of anilines is typically below 1.0 V vs. SCE),[10] thus being incompatible with the catalysis of **4a** ($E_{1/2}^{*III/II}$ = 1.65 V). These assumptions led us to reconsider the catalytic system for realizing the Mannich-type allylic C−H alkylation of enol silyl ethers.
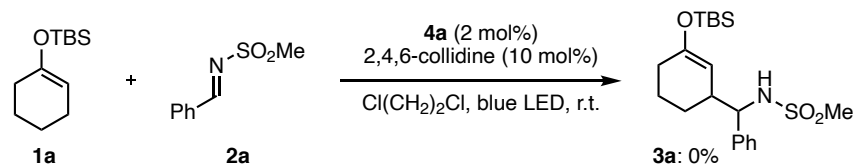
Scheme 2. Preliminary investigation of Mannich-type C−H alkylation of enol silyl ethers


4a: $E_{1/2}^{*\text{III/II}} = 1.65$ V
$E_{1/2}^{\text{III/II}} = -0.79$ V

4b (R = *t*-Bu): $E_{1/2}^{*\text{III/II}} = 0.73$ V
$E_{1/2}^{\text{III/II}} = -1.48$ V

4c (R = H): $E_{1/2}^{*\text{III/II}} = 0.81$ V
$E_{1/2}^{\text{III/II}} = -1.38$ V

Figure 1. Photoredox catalysts used in this study.

Considering the weak bond dissociation energy of allylic C−H bonds (about 80 kcal mol^{-1})[11] and the leading examples of photoredox-catalyzed hydrogen-atom transfer (HAT) C−H functionalization with imines,[12,13] the author envisioned that hybrid catalysis of photosensitizer with mild oxidizing ability and thiol catalyst would be effective for the generation of an allylic radical from enol silyl ethers via HAT, while accommodating electron-rich imines as acceptors. Toward this end, we attempted the reaction of **1a** with *N*-PMP imine **2b** under the influence of [Ir(ppy)$_2$(dtbbpy)]PF$_6$ (**4b**) (2 mol%), triisopropylsilylthiol (20 mol%), and 2,4,6-collidine (10 mol%) in acetonitrile under irradiation by a blue LED, which involved the catalytic generation of a thiyl radical as an HAT-active species via proton-coupled electron transfer (Table 1, entry 1).[14] As expected, this attempt afforded the desired aminoalkylation product **3b** in moderate yield (46%). The parallel reaction of **1a** with *N*-sulfonyl imine **2a** under otherwise identical conditions did not furnish the product (entry 2), confirming the appropriate reactivity of *N*-aryl imines. Subsequent evaluation of the effect of the Brønsted base revealed that lithium acetate significantly improved the reaction efficiency (entries 3-6). On the other hand, switching the photocatalyst to **4c**, which is a slightly stronger oxidant in its excited state and a weaker reductant in its reduced form, led to a notable decrease in the reaction conversion (entry 7). A decrease in the yield of **3b** was also observed when the reaction was conducted with methyl thioglycolate as a thiol catalyst (entry 8). Screening of solvents revealed that acetonitrile was the optimal choice (entries 9-11). Eventually, we found that slightly increasing the amount of

1a (1.5 equiv.) had a beneficial impact on the reactivity profile, furnishing **3b** in satisfactory yield (entry 12).

Table 1. Optimization of reaction conditions.[a]
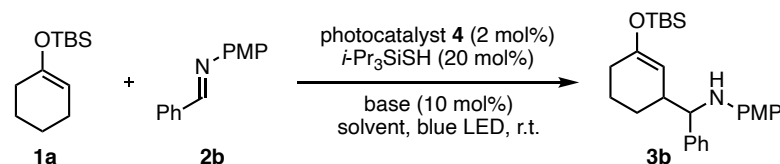
| Entry	4	Base	Solvent	Yield[b] (%)
1	**4b**	2,4,6-Collidine	MeCN	46
2[c]	**4b**	2,4,6-Collidine	MeCN	0
3	**4b**	KOAc	MeCN	21
4	**4b**	NaOAc	MeCN	43
5	**4b**	LiOAc	MeCN	66
6	**4b**	Li_2CO_3	MeCN	16
7	**4c**	LiOAc	MeCN	41
8[d]	**4b**	LiOAc	MeCN	20
9	**4b**	LiOAc	Acetone	49
10	**4b**	LiOAc	$PhCF_3$	11
11	**4b**	LiOAc	EtCN	53
12[e]	**4b**	LiOAc	MeCN	87 (79)

[a] Unless otherwise indicated, the reactions were performed with 0.12 mmol of **1a** and 0.10 mmol of **2b** with photocatalyst **4** (2 mol%), i-Pr$_3$SiSH (20 mol%), and base (10 mol%) in solvent (1.0 mL) at ambient temperature under an argon atmosphere with light irradiation (blue LED, 750 W m^{-2}).
[b] NMR yield with styrene as an internal standard. The value in parentheses is the isolated yield. Diastereomeric ratio (d.r.) of **3b** ranged from 1.0:1 to 1.2:1. [c] With **2a** instead of **2b**. [d] With MeO$_2$CCH$_2$SH instead of i-Pr$_3$SiSH. [e] With 0.15 mmol of **1a**.

3. Investigation of Substrate Scope

With the optimized reaction conditions in hand, the author next explored the substrate scope of this Mannich-type C−H alkylation of enol silyl ethers. As shown in Figure 2, *N*-PMP imines bearing *ortho*-, *meta*-, or *para*-methylphenyl substituents underwent radical addition to give the corresponding products **3c-3e** in moderate to high yields. Sterically demanding mesityl-substituted imine and fused-aromatic imines, typically 2-naphthylimine, were also amenable to the present hybrid catalytic system, affording **3f** and **3g**, respectively. Imines with additional functional groups such as ether, thioether,

and pyridine proved to be good substrates for furnishing the Mannich-type adducts **3h-3k** in moderate to good yields. Moreover, the reaction with the imine bearing *N-ortho*-methoxyphenyl group as a radical acceptor proceeded smoothly to yield **3l**. With respect to enol silyl ethers, cyclohexanone-derived triethylsilyl and triisopropylsilyl ethers were tolerated, leading to the formation of **3m** and **3n**. Other cyclic enol silyl ethers with five- and seven-membered rings, as well as those with oxygen-containing six-membered rings, were also suitable candidates for the nucleophile components and the corresponding adducts **3o-3q** were obtained in good yields. Notably, various acyclic ketone-derived enol silyl ethers and butyryl pyrazole-derived ketene silyl hemiaminal could be converted into aminoalkylated products **3r-3w** with moderate to high efficiency.
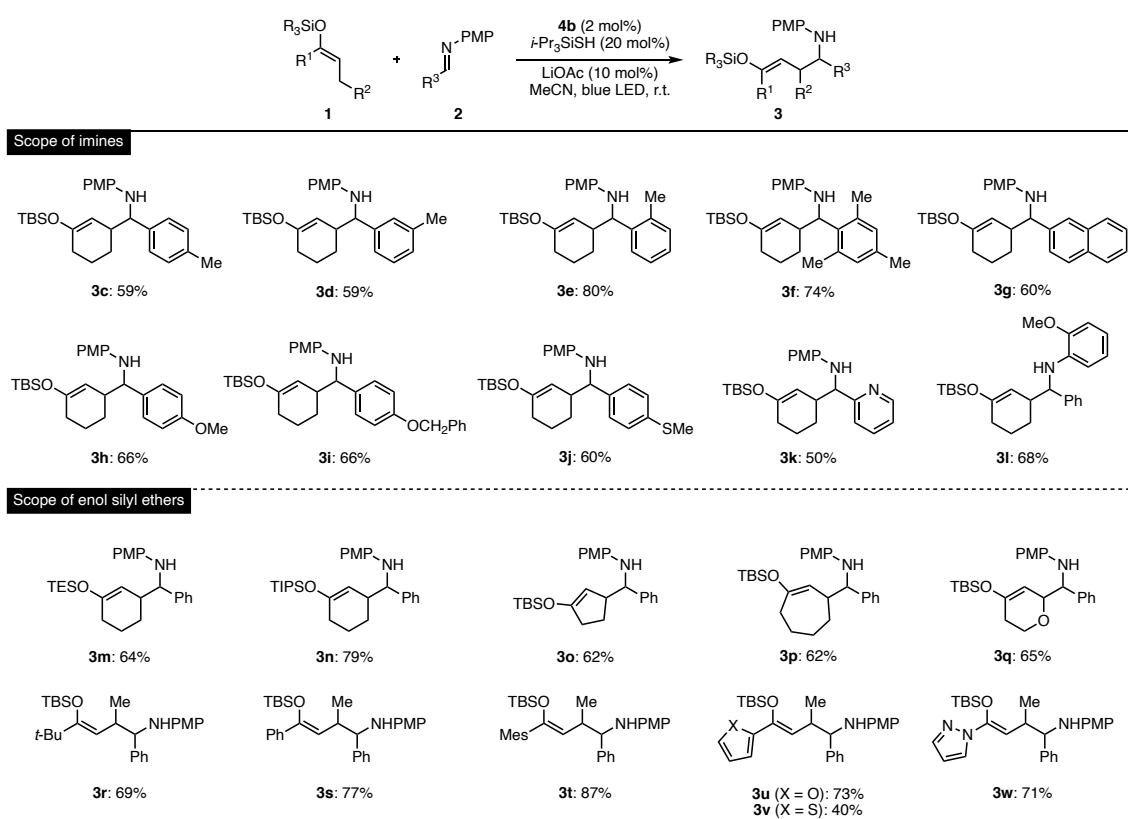

Figure 2. Scope of substrates. Isolated yields are indicated. Diastereomeric ratios (d.r.) of the products were 1.0:1-1.3:1. See the ESI for details.

4. Derivatization

Finally, the synthetic utility of this Mannich-type C−H functionalization of enol silyl ethers was demonstrated through the derivatization of aminoalkylated products (Scheme 3). For instance, the Mukaiyama−Mannich cyclization of **3b** with formaldehyde proceeded smoothly under the action of a catalytic amount of diarylborinate[15] to form fused bicyclic product **5**. The octahydroisoindol-4-one structure of **5** is often encountered in natural products and biologically active compounds.[16] In addition,

the treatment of **3w** with trifluoroacetic acid facilitated the protonation of the enol silyl ether and sequential cyclization to furnish β,γ-disubstituted γ-lactam **6** in high yield.
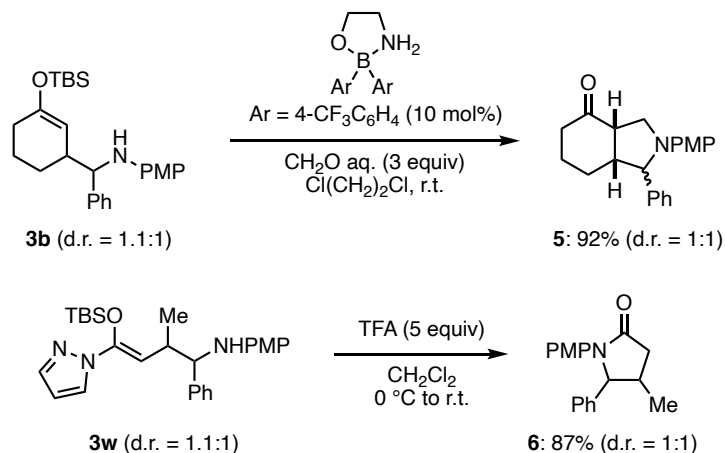
Scheme 3. Derivatization of aminoalkylated enol silyl ethers.

5. Conclusoins

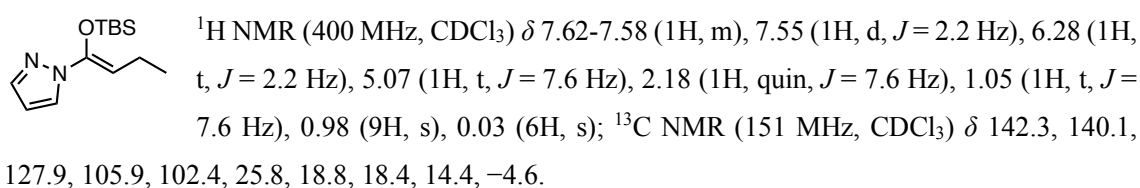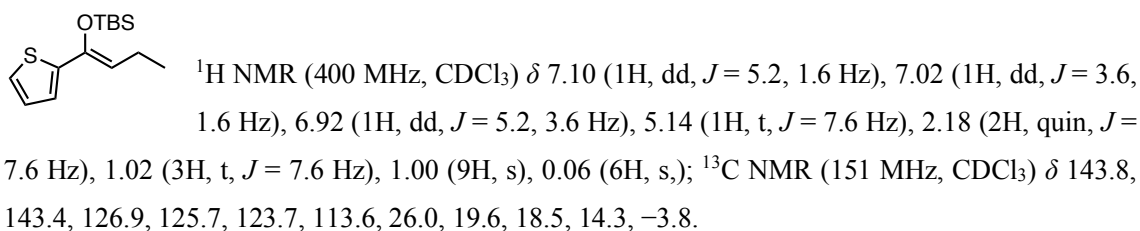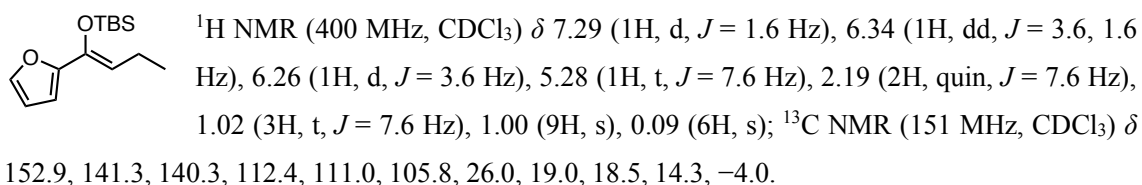The author have developed a Mannich-type allylic C−H functionalization of enol silyl ethers with *N*-aryl imines by exploiting photoredox−thiol hybrid catalysis. This catalytic system is applicable to a series of cyclic and acyclic ketone-derived enol silyl ethers, thus providing facile access to diverse γ-aminocarbonyl derivatives. We believe that this study expands the utility of enol silyl ethers for the efficient and diverse synthesis of functionalized carbonyl compounds on demand.

Experimental Section

General Information: ^{1}H NMR spectra were recorded on a JEOL JNM-ECS400 (400 MHz) and JEOL spectrometer. Chemical shifts are reported in ppm from the tetramethylsilane (0.0 ppm) resonance as the internal standard (CDCl$_3$). Data are reported as follows: chemical shift, integration, multiplicity (s = singlet, d = doublet, t = triplet, q = quartet, quin = quintet, m = multiplet, and br = broad) and coupling constants (Hz). ^{13}C NMR spectra were recorded on a JEOL JNM-ECA600II (151 MHz) spectrometer with complete proton decoupling. Chemical shifts are reported in ppm from the solvent resonance as the internal standard (CDCl$_3$; 77.16 ppm). The high-resolution mass spectra were measured on Thermo Fisher Scientific Exactive Plus (ESI). Analytical thin layer chromatography (TLC) was performed on Merck precoated TLC plates (silica gel 60 GF254, 0.25 mm). Flash column chromatography was conducted on Silica gel 60 N (spherical, neutral, 40~50 μm; Kanto Chemical Co., Inc.). Preparative thin layer chromatography (PTLC) was performed on TLC plates (silica gel 70 F254; FUJIFILM Wako Pure Chemical Corporation).

All air- and moisture-sensitive reactions were performed under an atmosphere of argon (Ar) in dried glassware. Acetonitrile (MeCN), 1,2-dichloroethane, and dichloromethane were supplied from Kanto Chemical Co., Inc. as "Dehydrated" and further purified by both A2 alumina and Q5 reactant using a GlassContour solvent dispensing system. The photocatalysts (**4a-4c**),[18,19] imines,[12e] and enol silyl ethers[8] were synthesized according to the previously reported procedures. Other simple chemicals were purchased and used as such.

Characterization of Enol Silyl Ethers

OTIPS (cyclohexenyl) ^{1}H NMR (400 MHz, CDCl$_3$) δ 4.90-4.86 (1H, m), 2.08-1.97 (4H, m), 1.70-1.62 (2H, m), 1.54 -1.47 (2H, m), 1.20-1.05 (3H, m), 1.08 (18H, d, J = 6.0 Hz); ^{13}C NMR (151 MHz, CDCl$_3$) δ 150.8, 103.8, 30.1, 24.0, 23.4, 22.5, 18.2, 12.8.

OTBS (cyclopentenyl) ^{1}H NMR (400 MHz, CDCl$_3$) δ 4.64-4.60 (1H, m), 2.29-2.21 (4H, m), 1.90-1.80 (2H, m), 0.92 (9H, s), 0.15 (6H, s); ^{13}C NMR (151 MHz, CDCl$_3$) δ 155.5, 102.6, 33.6, 28.8, 25.8, 21.5, 18.3, −4.4.

OTBS (dihydropyranyl) ^{1}H NMR (400 MHz, CDCl$_3$) δ 4.84-4.81 (1H, m), 4.14 (2H, dd, J = 5.2, 2.8 Hz), 3.81 (2H, t, J = 5.8 Hz), 2.16-2.10 (2H, m), 0.93 (9H, s), 0.15 (6H, s); ^{13}C NMR (151 MHz, CDCl$_3$) δ 148.1, 102.4, 64.9, 30.6, 25.8, −4.2.

OTBS (furanyl) ^{1}H NMR (400 MHz, CDCl$_3$) δ 7.29 (1H, d, J = 1.6 Hz), 6.34 (1H, dd, J = 3.6, 1.6 Hz), 6.26 (1H, d, J = 3.6 Hz), 5.28 (1H, t, J = 7.6 Hz), 2.19 (2H, quin, J = 7.6 Hz), 1.02 (3H, t, J = 7.6 Hz), 1.00 (9H, s), 0.09 (6H, s); ^{13}C NMR (151 MHz, CDCl$_3$) δ 152.9, 141.3, 140.3, 112.4, 111.0, 105.8, 26.0, 19.0, 18.5, 14.3, −4.0.

OTBS (thienyl) ^{1}H NMR (400 MHz, CDCl$_3$) δ 7.10 (1H, dd, J = 5.2, 1.6 Hz), 7.02 (1H, dd, J = 3.6, 1.6 Hz), 6.92 (1H, dd, J = 5.2, 3.6 Hz), 5.14 (1H, t, J = 7.6 Hz), 2.18 (2H, quin, J = 7.6 Hz), 1.02 (3H, t, J = 7.6 Hz), 1.00 (9H, s), 0.06 (6H, s,); ^{13}C NMR (151 MHz, CDCl$_3$) δ 143.8, 143.4, 126.9, 125.7, 123.7, 113.6, 26.0, 19.6, 18.5, 14.3, −3.8.

OTBS (pyrazolyl) ^{1}H NMR (400 MHz, CDCl$_3$) δ 7.62-7.58 (1H, m), 7.55 (1H, d, J = 2.2 Hz), 6.28 (1H, t, J = 2.2 Hz), 5.07 (1H, t, J = 7.6 Hz), 2.18 (1H, quin, J = 7.6 Hz), 1.05 (1H, t, J = 7.6 Hz), 0.98 (9H, s), 0.03 (6H, s); ^{13}C NMR (151 MHz, CDCl$_3$) δ 142.3, 140.1, 127.9, 105.9, 102.4, 25.8, 18.8, 18.4, 14.4, −4.6.

General Experimental Procedures for Mannich-type C−H Alkylation of Enol Silyl Ethers
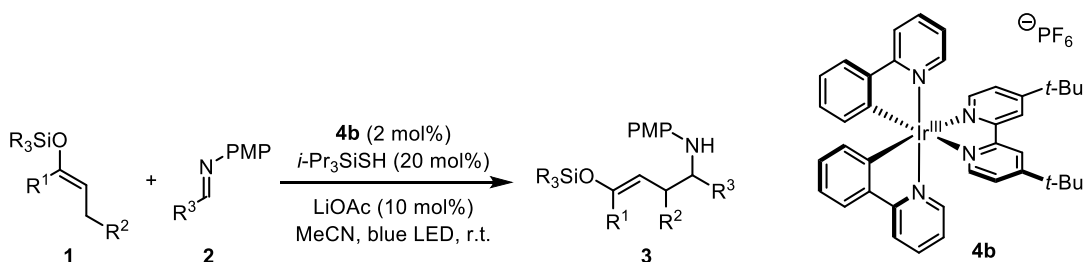
To a flame-dried test tube were added *N*-(4-methoxyphenyl) imine **2** (0.10 mmol, 1 equiv), [Ir(ppy)$_2$(dtbbpy)]PF$_6$ (**4b**) (1.83 mg, 0.002 mmol, 2 mol%), LiOAc (0.66 mg, 0.01 mmol, 10 mol%), and MeCN (1 mL, 0.1 M). The reaction tube was sealed with a rubber septum and then evacuated in *vacuo* and backfilled with Ar five times. Enol silyl ether **1** (0.15 mmol, 1.5 equiv) and *i*-Pr$_3$SiSH (4.3 μL, 0.02 mmol, 20 mol%) were successively introduced via syringe. The whole reaction mixture was stirred at 25 °C under the irradiation of blue LED (448 nm, 750 W/m^2) with a fan to keep the temperature. After appropriate reaction time (indicated with the characterization data for the reaction products), the mixture was directly evaporated. Purification of the resulting crude residue by column chromatography on silica gel (hexane 100% to hexane/Et$_2$O = 30:1 to 15:1) or preparative TLC (hexane/Et$_2$O = 10:1) afforded the corresponding aminoalkylated enol silyl ether **3**.

Measurement of Quantum Yield of Catalytic Reaction

Photon flux was measured by Shimadzu-QYM-01. Irradiation was carried out with Asahi Spectra-MAX 303 equipped with band pass filter. A 1 cm^2 quartz cuvette was charged with a solution of enol silyl ether **1a** (91.6 μL, 0.38 mmol), imine **2b** (52.8 mg, 0.25 mmol), photocatalyst **4b** (4.6 mg, 0.005 mmol), and LiOAc (1.6 mg, 0.025 mmol) in CH$_3$CN (2.5 mL). The solution was carefully evacuated in *vacuo* and backfilled with Ar five times (great care was taken to ensure that the solution was kept in the dark before light irradiation), and then *i*-Pr$_3$SiSH (10.7 μL, 0.05 mmol) was introduced via syringe. The reaction mixture was irradiated for 9 h or 12 h. After evaporation to remove solvent, the yield of the corresponding product **3b** was determined by ^{1}H NMR with styrene as an internal standard. Quantum yield (Φ) was calculated by the following formula.

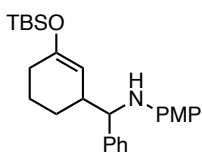$$\Phi = \frac{n_{\mathbf{3b}} \cdot N_A}{n_{ph}}$$

$$\left(
\begin{array}{ll}
\Phi: & \text{quantum yield} \\
n_{\mathbf{3b}}: & \text{amount of product } \mathbf{3b} \text{ [mol]} \\
N_A: & \text{Avogadro constant } (6.02 \cdot 10^{23} \text{ mol}^{-1}) \\
n_{ph}: & \text{number of absorbed photons}
\end{array}
\right)$$

9 h: $n_{\mathbf{3b}} = 4.25 \cdot 10^{-5}$, $n_{ph} = 2.95 \cdot 10^{20}$: $\Phi = 0.087$

12 h: $n_{\mathbf{3b}} = 6.25 \cdot 10^{-5}$, $n_{ph} = 3.89 \cdot 10^{20}$: $\Phi = 0.097$

Average of quantum yield: $\Phi = 0.092$
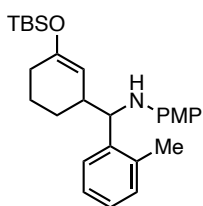
Characterization of Aminoalkylated Enol Silyl Ether
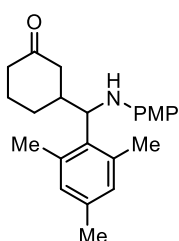
3b (mixture of diastereomers in the ratio of 1.1:1): The reaction was performed for 18 h. ^{1}H NMR (400 MHz, CDCl$_3$) δ 7.35-7.27 (8H, m), 7.24-7.18 (2H, m), 6.69-6.63 (4H, m), 6.44-6.37 (4H, m), 4.74 (1H, brs), 4.69 (1H, brs), 4.23 (1H, d, J = 4.0 Hz), 4.12 (1H, d, J = 5.6 Hz), 3.89 (2H, brs), 3.68 (6H, s), 2.70-2.60 (2H, m), 2.12-2.03 (2H, m), 2.01-1.92 (2H, m), 1.87-1.70 (3H, m), 1.52-1.30 (5H, m), 0.92 (9H, s), 0.91 (9H, s), 0.15 (3H, s), 0.11(4) (3H, s), 0.11(2) (3H, s), 0.10 (3H, s); ^{13}C NMR (151 MHz, CDCl$_3$) δ 154.2, 153.8, 152.0, 151.6, 143.2, 142.7, 142.5, 142.1, 128.4, 127.2, 126.8(9), 126.8(5), 126.8, 115.0, 114.8(3), 114.7(7), 114.1, 106.7, 103.1, 63.3, 62.3, 56.0, 55.9, 43.2, 43.1, 30.2, 30.1, 27.6, 25.9, 25.8, 23.7, 22.3, 22.2, 18.2(4), 18.1(7), −4.0, −4.1, −4.2, −4.3, one peak was not found probably due to overlapping; HRMS (ESI): Calcd for C$_{26}$H$_{38}$O$_2$NSi$^+$ ([M+H]$^+$) 424.2666. Found 424.2673.
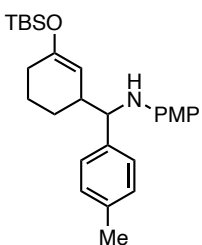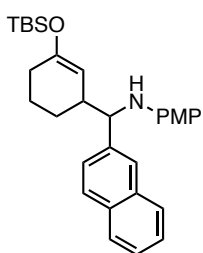
3c (mixture of diastereomers in the ratio of 1.2:1): The reaction was performed for 18 h. ^{1}H NMR (400 MHz, CDCl$_3$) δ 7.21 (2H, d, J = 8.4 Hz), 7.17 (2H, d, J = 8.4 Hz), 7.10(4) (2H, d, J = 8.4 Hz), 7.09(7) (2H, d, J = 8.4 Hz), 6.69-6.63 (4H, m), 6.44-6.37 (4H, m), 4.76 (1H, brs), 4.70 (1H, brs), 4.19 (1H, d, J = 4.4 Hz), 4.09 (1H, d, J = 5.2 Hz), 3.85 (2H, brs), 3.68 (6H, s), 2.66-2.58 (2H, m), 2.32 (3H, s), 2.31 (3H, s), 2.13-2.02 (2H, m), 2.00-1.91 (2H, m), 1.86-1.68 (3H, m), 1.65-1.25 (5H, m), 0.92 (9H, s), 0.91 (9H, s), 0.15 (3H, s), 0.12 (3H, s), 0.11 (3H, s), 0.10 (3H, s); ^{13}C NMR (151 MHz, CDCl$_3$) δ 154.1, 153.8, 151.9, 151.5, 142.6, 142.2, 140.2, 139.6, 136.3, 136.2, 129.1(3), 129.0(9), 127.0, 126.8, 115.0, 114.8(0), 114.7(6), 114.1, 106.8, 103.3, 63.0, 62.1, 56.0, 55.9, 43.2, 43.1, 30.2, 30.1, 27.6, 25.9, 25.8, 23.7, 22.3(3), 22.2(8), 21.2(2), 21.2(0), 18.2(3), 18.1(7), −4.0, −4.1, −4.2, −4.3; HRMS (ESI): Calcd for C$_{27}$H$_{40}$O$_2$NSi$^+$ ([M+H]$^+$) 438.2823. Found 438.2820.
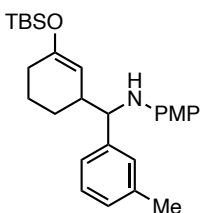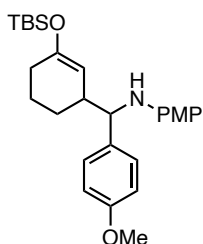
3d (mixture of diastereomers in the ratio of 1.1:1): The reaction was performed for 18 h. ^{1}H NMR (400 MHz, CDCl$_3$) δ 7.22-7.06 (6H, m), 7.05-6.99 (2H, m), 6.70-6.64 (4H, m), 6.45-6.39 (4H, m), 4.76 (1H, brs), 4.68 (1H, brs), 4.19 (1H, d, J = 3.6 Hz), 4.07 (1H, d, J = 5.6 Hz), 3.87 (2H, brs), 3.69 (6H, s), 2.67-2.59 (2H, m), 2.33(2) (3H, s), 2.32(5) (3H, s), 2.15-2.03 (2H, m), 2.02-1.92 (2H, m), 1.88-1.70 (3H, m), 1.53-1.25 (5H, m), 0.92 (9H, s), 0.91 (9H, s), 0.16 (3H, s), 0.13 (3H, s), 0.12 (3H, s), 0.10 (3H, s); ^{13}C NMR (151 MHz, CDCl$_3$) δ 154.2, 153.7, 151.9, 151.6, 143.3, 142.7, 142.6, 142.3, 137.8(9), 137.8(5), 128.3, 127.9, 127.6(3), 127.5(9), 124.2, 124.0, 115.0, 114.8(0), 114.7(7), 114.0, 106.7, 103.1, 63.4, 62.4, 56.0, 55.9, 43.2, 43.1, 30.2, 30.1, 27.7, 25.9, 25.8, 23.9, 22.4, 22.3, 21.7, 18.3, 18.2, −4.0, −4.1, −4.2, −4.4, three peaks were not found probably due to overlapping; HRMS (ESI): Calcd for C$_{27}$H$_{40}$O$_2$NSi$^+$ ([M+H]$^+$) 438.2823. Found 438.2820.

3e (mixture of diastereomers in the ratio of 1.1:1): The reaction was performed for 18 h. ^{1}H NMR (400 MHz, CDCl$_3$) δ 7.43-7.37 (1H, m), 7.30-7.25 (1H, m), 7.19-7.06 (6H, m), 6.68-6.62 (4H, m), 6.36-6.29 (4H, m), 4.76 (1H, brs), 4.65 (1H, brs), 4.43 (1H, d, J = 2.8 Hz), 4.35 (1H, d, J = 5.6 Hz), 3.90 (2H, brs), 3.67 (6H, s), 2.68-2.54 (2H, m), 2.43 (3H, s), 2.42 (3H, s), 2.19-2.05 (2H, m), 2.02-1.92 (2H, m), 1.91-1.74 (3H, m), 1.62-1.38 (5H, m), 0.94 (9H, s), 0.91 (9H, s), 0.20 (3H, s), 0.14 (3H, s), 0.12 (3H, s), 0.10 (3H, s); ^{13}C NMR (151 MHz, CDCl$_3$) δ 154.6, 154.0, 152.0, 151.5, 142.6, 142.1, 140.8, 140.3, 134.9, 134.7, 130.8, 130.7, 127.1, 126.6, 126.1(2), 126.0(6), 126.0, 115.0, 114.8, 114.6, 113.8, 106.6, 102.4, 59.4, 58.3, 56.0, 55.9, 40.7, 40.5, 30.2, 30.1, 28.1, 25.9, 25.8, 23.9, 22.5, 22.3, 19.5, 19.3, 18.3, 18.2, −4.0, −4.0(5), −4.1(3), −4.3, one carbon atom was not found probably due to overlapping; HRMS (ESI): Calcd for C$_{27}$H$_{40}$O$_2$NSi$^+$ ([M+H]$^+$) 438.2823. Found 438.2818.

3f (purified and characterized after the conversion of enol silyl ether to the corresponding ketone. Mixture of diastereomers in the ratio of 1.2:1): The reaction was performed for 18 h. ^{1}H NMR (400 MHz, CDCl$_3$) δ 6.77 (2H, brs), 6.75 (2H, brs), 6.68 (2H, d, J = 8.4 Hz), 6.66 (2H, d, J = 8.4 Hz), 6.45 (2H, d, J = 8.4 Hz), 6.40 (2H, d, J = 8.4 Hz), 4.59 (1H, brs), 4.57 (1H, brs), 4.54 (2H, brs), 3.69 (3H, s), 3.68 (3H, s), 3.00-2.92 (1H, m), 2.41 (6H, s), 2.38 (6H, s), 2.35-2.23 (6H, m), 2.21 (3H, s), 2.20 (3H, s), 2.18-2.11 (2H, m), 2.10-1.96 (4H, m), 1.80-1.36 (5H, m); ^{13}C NMR (151 MHz, CDCl$_3$) δ 211.3, 152.1, 152.0, 142.1, 142.0, 136.4, 136.3, 135.8, 134.7, 134.0, 132.0, 129.9, 115.0, 114.3, 114.2, 60.5, 60.2, 55.9, 47.1, 45.6, 44.6, 44.3, 41.6, 41.5, 30.1, 28.9, 25.6, 25.3, 21.7, 20.8(1), 20.7(7), five peaks were not found probably due to overlapping; HRMS (ESI): Calcd for C$_{23}$H$_{29}$O$_2$NNa$^+$ ([M+Na]$^+$) 374.2091. Found 374.2088.
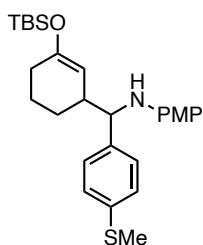
3g (mixture of diastereomers in the ratio of 1.1:1): The reaction was performed for 18 h. ^{1}H NMR (400 MHz, CDCl$_3$) δ 7.83-7.73 (8H, m), 7.50-7.39 (6H, m), 6.68-6.61 (4H, m), 6.47-6.41 (4H, m), 4.80 (1H, brs), 4.74 (1H, brs), 4.38 (1H, d, J = 4.0 Hz), 4.29 (1H, d, J = 5.6 Hz), 3.99 (2H, brs), 3.66 (6H, s), 2.80-2.70 (2H, m), 2.15-2.03 (2H, m), 2.01-1.92 (2H, m), 1.88-1.72 (3H, m), 1.62-1.35 (5H, m), 0.92 (9H, s), 0.91 (9H, s), 0.15 (3H, s), 0.11(0) (3H, s), 0.10(6) (3H, s), 0.09 (3H, s); ^{13}C NMR (151 MHz, CDCl$_3$) δ 154.3, 154.0, 152.0, 151.7, 142.5, 142.1, 140.8, 140.4, 133.5(9), 133.5(6), 132.9, 132.8, 128.2, 128.1, 128.0, 127.7(8), 127.7(6), 126.0(3), 125.9(8), 125.9, 125.6, 125.5, 125.4, 115.0(0), 114.9(4), 114.8, 114.2, 106.7, 103.1, 63.5, 62.7, 56.0, 55.9, 43.1, 30.2, 30.1, 27.7, 25.9, 25.8, 23.7, 22.3(4), 22.2(5), 18.2(4), 18.1(7), −4.0, −4.1, −4.2, −4.3, two peaks were not found probably due to overlapping; HRMS (ESI): Calcd for C$_{30}$H$_{40}$O$_2$NSi$^+$ ([M+H]$^+$) 474.2823. Found 474.2821.
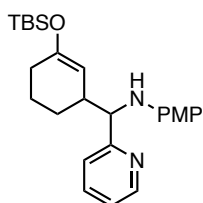
3h (mixture of diastereomers in the ratio of 1.1:1): The reaction was performed for 18 h. ^{1}H NMR (400 MHz, CDCl$_3$) δ 7.24 (2H, d, $J = 8.8$ Hz), 7.20 (2H, d, $J = 9.2$ Hz), 6.84(2) (2H, d, $J = 9.2$ Hz), 6.83(5) (2H, d, $J = 8.8$ Hz), 6.66 (2H, d, $J = 9.2$ Hz), 6.65 (2H, d, $J = 9.2$ Hz), 6.41 (2H, d, $J = 8.8$ Hz), 6.40 (2H, d, $J = 8.8$ Hz), 4.76 (1H, brs), 4.69 (1H, brs), 4.18 (1H, d, $J = 4.4$ Hz), 4.07 (1H, d, $J = 5.2$ Hz), 3.85 (2H, brs), 3.79 (3H, s), 3.78 (3H, s), 3.68 (6H, s), 2.65-2.56 (2H, m), 2.13-2.02 (2H, m), 2.01-1.91 (2H, m), 1.86-1.67 (3H, m), 1.62-1.25 (5H, m), 0.92 (9H, s), 0.91 (9H, s), 0.15 (3H, s), 0.12 (3H, s), 0.11 (3H, s), 0.10 (3H, s); ^{13}C NMR (151 MHz, CDCl$_3$) δ 158.5(2), 158.4(6), 154.1, 153.7, 151.9, 151.6, 142.5, 142.2, 135.2, 134.7, 128.1, 127.8, 115.0, 114.9, 114.8, 114.1, 113.8(3), 113.8(1), 106.7, 103.3, 62.7, 61.8, 56.0, 55.9, 55.4, 43.3, 43.2, 30.2, 30.1, 27.6, 25.9, 25.8, 23.8, 22.3(3), 22.2(7), 18.2(4), 18.1(7), −3.9(8), −4.0(4), −4.2, −4.3, one peak was not found probably due to overlapping; HRMS (ESI): Calcd for C$_{27}$H$_{39}$O$_3$NNaSi$^+$ ([M+Na]$^+$) 476.2591. Found 476.2589.
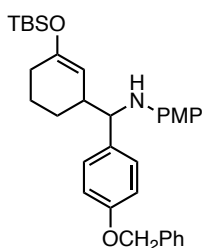
3i (mixture of diastereomers in the ratio of 1.1:1): The reaction was performed for 18 h. ^{1}H NMR (400 MHz, CDCl$_3$) δ 7.45-7.28 (10H, m), 7.24 (2H, d, $J = 9.0$ Hz), 7.20 (2H, d, $J = 9.0$ Hz), 6.92 (2H, d, $J = 8.8$ Hz), 6.91 (2H, d, $J = 8.8$ Hz), 6.67 (2H, d, $J = 8.8$ Hz), 6.66 (2H, d, $J = 8.8$ Hz), 6.42 (2H, d, $J = 9.0$ Hz), 6.40 (2H, d, $J = 9.0$ Hz), 5.03 (2H, s), 5.02 (2H, s), 4.75 (1H, brs), 4.72 (1H, brs), 4.18 (1H, d, $J = 4.0$ Hz), 4.07 (1H, d, $J = 5.6$ Hz), 3.89-3.81 (2H, brm), 3.68 (6H, s), 2.65-2.56 (2H, m), 2.13-2.02 (2H, m), 2.01-1.91 (2H, m), 1.87-1.68 (3H, m), 1.61-1.21 (5H, m), 0.92 (9H, s), 0.91 (9H, s), 0.15 (3H, s), 0.12 (3H, s), 0.11 (3H, s), 0.10 (3H, s); ^{13}C NMR (151 MHz, CDCl$_3$) δ 157.8(3), 157.7(7), 154.1, 153.7, 151.9, 151.6, 142.5, 142.2, 137.3(3), 137.2(9), 135.5, 135.0, 128.7, 128.1(3), 128.0(5), 127.9, 127.7, 115.0, 114.9, 114.8, 114.7, 114.1, 106.7, 103.2, 70.2, 62.7, 61.7, 56.0, 55.9, 43.3, 43.1, 30.2, 30.1, 27.5, 25.9, 25.8, 23.8, 22.3(3), 22.2(5), 18.2(4), 18.1(7), −3.9(8), −4.0(4), −4.2, −4.3, five peaks were not found probably due to overlapping; HRMS (ESI): Calcd for C$_{33}$H$_{43}$O$_3$NNaSi$^+$ ([M+Na]$^+$) 552.2904. Found 552.2911.
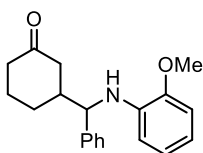
3j (mixture of diastereomers in the ratio of 1.1:1): The reaction was performed for 18 h. ^{1}H NMR (400 MHz, CDCl$_3$) δ 7.29-7.17 (8H, m), 6.67 (2H, d, $J = 8.8$ Hz), 6.66 (2H, d, $J = 8.8$ Hz), 6.40 (2H, d, $J = 8.8$ Hz), 6.39 (2H, d, $J = 8.8$ Hz), 4.73 (1H, brs), 4.69 (1H, brs), 4.19 (1H, d, $J = 4.0$ Hz), 4.09 (1H, d, $J = 5.2$ Hz), 3.86 (2H, brs), 3.68 (6H, s), 2.66-2.58 (2H, m), 2.47 (3H, s), 2.46 (3H, s), 2.14-2.02 (2H, m), 2.01-1.92 (2H, m), 1.87-1.69 (3H, m), 1.52-1.24 (5H, m), 0.92 (9H, s), 0.91 (9H, s), 0.15 (3H, s), 0.12 (3H, s), 0.11(4) (3H, s), 0.10(6) (3H, s); ^{13}C NMR (151 MHz, CDCl$_3$) δ 154.3, 154.0, 152.0, 151.7, 142.3, 142.0, 140.4, 139.9, 136.3(9), 136.3(6), 127.7, 127.4,

126.9, 115.0, 114.9, 114.8, 114.1, 106.5, 103.0, 62.8, 61.9, 55.9(4), 55.8(5), 43.2, 43.0, 30.2, 30.1, 27.6, 25.9, 25.8, 23.6, 22.3, 22.2, 18.2(3), 18.1(7), 16.1(9), 16.1(6), −4.0, −4.1, −4.2, −4.3, one carbon atom was not found probably due to overlapping; HRMS (ESI): Calcd for $C_{27}H_{40}O_2NSSi^+$ ([M+H]$^+$) 470.2544. Found 470.2544.

3k (mixture of diastereomers in the ratio of 1.2:1): The reaction was performed for 18 h. ^{1}H NMR (400 MHz, CDCl$_3$) δ 8.60 (2H, d, J = 4.4 Hz), 7.57 (2H, t, J = 7.6 Hz), 7.31 (1H, d, J = 7.6 Hz), 7.27 (1H, d, J = 7.6 Hz), 7.15-7.08 (2H, m), 6.69 (2H, d, J = 8.2 Hz), 6.67 (2H, d, J = 8.2 Hz), 6.44 (4H, d, J = 8.2 Hz), 4.69 (1H, brs), 4.64 (1H, brs), 4.34 (1H, d, J = 3.6 Hz), 4.24 (1H, d, J = 5.2 Hz), 4.13 (2H, brs), 3.69 (6H, s), 2.96-2.87 (2H, m), 2.14-2.02 (2H, m), 2.01-1.91 (2H, m), 1.86-1.70 (3H, m), 1.64-1.35 (5H, m), 0.92 (9H, s), 0.90 (9H, s), 0.14 (3H, s), 0.11 (3H, s), 0.08(4) (3H, s), 0.08(0) (3H, s); ^{13}C NMR (151 MHz, CDCl$_3$) 162.6, 162.2, 154.2, 153.6, 152.2, 151.8, 149.7, 149.6, 142.2, 142.0, 136.3(0), 136.2(6), 122.2, 121.9, 121.4, 115.0(1), 114.9(7), 114.8, 114.3, 106.4, 103.3, 64.5, 63.9, 55.9(4), 55.8(5), 41.4, 30.1(1), 30.0(9), 27.4, 25.9, 25.8, 23.9, 22.3, 22.1, 18.2(4), 18.1(7), −4.0, −4.1, −4.2, −4.3, two peaks were not found probably due to overlapping; HRMS (ESI): Calcd for $C_{25}H_{37}O_2N_2Si^+$ ([M+H]$^+$) 425.2619. Found 425.2623.

3l (purified and characterized after the conversion of enol silyl ether to the corresponding ketone. Mixture of diastereomers in the ratio of 1.2:1): The reaction was performed for 18 h. ^{1}H NMR (400 MHz, CDCl$_3$) δ 7.34-7.19 (10H, m), 6.76 (1H, dd, J = 4.2, 1.4 Hz), 6.74 (1H, dd, J = 3.8, 1.4 Hz), 6.70-6.64 (2H, m), 6.63-6.56 (2H, m), 6.35 (1H, dd, J = 3.0, 1.8 Hz), 6.33 (1H, dd, J = 3.0, 1.4 Hz), 4.76 (2H, brs), 4.29 (1H, d, J = 4.0 Hz), 4.23 (1H, d, J = 4.0 Hz), 3.89 (3H, s), 3.88 (3H, s), 2.72-2.60 (1H, m), 2.40-2.31 (3H, m), 2.31-2.16 (6H, m), 2.13-2.01 (3H, m), 1.81-1.73 (1H, m), 1.68-1.38 (4H, m); ^{13}C NMR (151 MHz, CDCl$_3$) δ 211.4, 211.3, 146.9, 141.5, 141.2, 137.1(2), 137.1(0), 128.6(4), 128.6(2), 127.4(3), 127.4(1), 127.3, 127.2, 121.3, 121.2, 116.7(4), 116.7(0), 111.0, 110.9, 109.5, 109.4, 62.6, 62.1, 55.6, 45.6, 45.4, 45.2, 41.4(8), 41.4(5), 28.5, 27.7, 25.2, 25.1, three carbon atoms were not found probably due to overlapping; HRMS (ESI): Calcd for $C_{20}H_{24}O_2N^+$ ([M+H]$^+$) 310.1802. Found 310.1802.
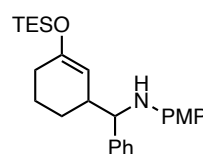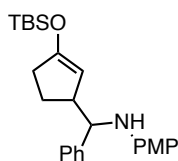
3m (mixture of diastereomers in the ratio of 1.1:1): The reaction was performed for 18 h. ^{1}H NMR (400 MHz, CDCl$_3$) δ 7.35-7.27 (8H, m), 7.24-7.17 (2H, m), 6.70-6.63 (4H, m), 6.43-6.36 (4H, m), 4.73 (1H, brs), 4.67 (1H, brs), 4.24 (1H, d, J = 3.6 Hz), 4.11 (1H, d, J = 5.6 Hz), 3.90 (2H, brs), 3.68 (6H, s), 2.70-2.60 (2H, m), 2.17-2.04 (2H, m), 2.03-1.93 (2H, m), 1.88-1.71 (3H, m), 1.62-1.24 (5H, m), 0.95(3) (9H, t, J =

8.0 Hz), 0.95(0) (9H, t, J = 8.0 Hz), 0.65 (6H, q, J = 8.0 Hz), 0.63 (6H, q, J = 8.0 Hz); ^{13}C NMR (151 MHz, CDCl₃) δ 154.2, 153.8, 152.0, 151.6, 143.2, 142.8, 142.5, 142.1, 128.4, 127.2, 126.9, 126.8, 115.0, 114.7(8), 114.7(5), 114.0, 106.1, 102.4, 63.3, 62.2, 56.0, 55.9, 43.2, 43.1, 30.1, 30.0, 27.7, 23.8, 22.4, 22.3, 6.9, 5.2(2), 5.1(7), three peaks were not found probably due to overlapping; HRMS (ESI): Calcd for C₂₆H₃₈O₂NSi⁺ ([M+H]⁺) 424.2666. Found 424.2664.
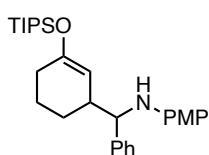
3n (mixture of diastereomers in the ratio of 1.1:1): The reaction was performed for 18 h. ^{1}H NMR (400 MHz, CDCl₃) δ 7.34-7.26 (8H, m), 7.23-7.16 (2H, m), 6.69-6.62 (4H, m), 6.42-6.35 (4H, m), 4.72 (1H, brs), 4.65 (1H, brs), 4.24 (1H, d, J = 4.0 Hz), 4.10 (1H, d, J = 6.0 Hz), 3.88 (2H, brs), 3.67 (6H, s), 2.70-2.58 (2H, m), 2.21-2.09 (2H, m), 2.06-1.97 (2H, m), 1.89-1.71 (3H, m), 1.63-1.30 (5H, m), 1.18-1.02 (42H, m); ^{13}C NMR (151 MHz, CDCl₃) δ 154.3, 153.9, 151.9, 151.6, 143.3, 142.8, 142.5, 142.2, 128.4, 127.2, 126.9, 126.8(2), 126.7(6), 115.0, 114.8, 114.7, 114.0, 105.6, 101.9, 63.4, 62.3, 56.0, 55.9, 43.3, 43.2, 30.1, 30.0, 27.7, 23.9, 22.4, 22.3, 18.2, 18.1, 12.7(0), 12.6(7), one peak was not found probably due to overlapping; HRMS (ESI): Calcd for C₂₉H₄₄O₂NSi⁺ ([M+H]⁺) 466.3136. Found 466.3131.
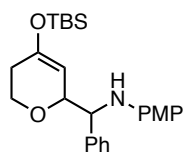
3o (mixture of diastereomers in the ratio of 1.1:1): The reaction was performed for 18 h. ^{1}H NMR (400 MHz, CDCl₃) δ 7.36-7.24 (8H, m), 7.24-7.16 (2H, m), 6.70-6.63 (4H, m), 6.46-6.39 (4H, m), 4.48 (1H, brs), 4.40 (1H, brs), 4.21 (1H, d, J = 3.6 Hz), 4.10 (1H, d, J = 6.4 Hz), 3.98 (2H, brs), 3.67 (6H, s), 3.17-3.02 (2H, m), 2.40-2.22 (4H, m), 2.12-1.99 (1H, m), 1.89-1.75 (3H, m), 0.94 (9H, s), 0.92 (9H, s), 0.19 (3H, s), 0.16 (6H, s), 0.14 (3H, s); ^{13}C NMR (151 MHz, CDCl₃) δ 158.2, 157.6, 152.0, 151.6, 143.8, 143.3, 142.4, 142.1, 128.5, 128.4, 127.0, 126.8, 126.7, 115.0, 114.8, 114.2, 104.1, 101.6, 63.1, 62.3, 55.9(4), 55.8(9), 50.1, 33.8, 33.3, 25.8, 23.7, 18.3(2), 18.3(0), −4.3(6), −4.4(2), −4.5, six peaks were not found probably due to overlapping; HRMS (ESI): Calcd for C₂₅H₃₆O₂NSi⁺ ([M+H]⁺) 410.2510. Found 410.2519.
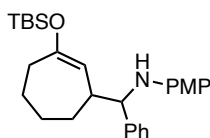
3p (mixture of diastereomers in the ratio of 1.1:1): The reaction was performed for 18 h. ^{1}H NMR (400 MHz, CDCl₃) δ 7.36-7.24 (8H, m), 7.23-7.17 (2H, m), 6.67 (4H, d, J = 8.4 Hz), 6.41 (4H, d, J = 8.4 Hz), 4.90 (1H, d, J = 4.8 Hz), 4.89 (1H, d, J = 4.8 Hz), 4.20 (1H, d, J = 4.4 Hz), 4.16 (1H, d, J = 5.6 Hz), 3.89 (2H, brs), 3.68(4) (3H, s), 3.68(0) (3H, s), 2.65-2.55 (2H, m), 2.40-2.24 (2H, m), 2.18-2.07 (2H, m), 2.00-1.62 (6H, m), 1.60-1.24 (6H, m), 0.88 (9H, s), 0.87 (9H, s), 0.05 (3H, s), 0.03 (6H, s), 0.00 (3H, s); ^{13}C NMR (151 MHz, CDCl₃) δ 157.0, 156.4, 151.9, 151.8, 143.2, 142.4, 142.3, 142.2, 128.5, 128.4, 127.5, 127.2, 126.9, 114.9, 114.8, 114.5, 114.2, 111.0, 108.7, 64.3, 63.9, 55.9(3), 55.8(7), 44.3, 43.8, 35.2(2), 35.1(8), 32.6, 30.0, 29.8, 29.2, 25.9, 25.0, −4.2, −4.3(1), −4.3(4), −4.4, three peaks were not

found probably due to overlapping; HRMS (ESI): Calcd for $C_{27}H_{40}O_2NSi^+$ ([M+H]$^+$) 438.2823. Found 438.2820.

3q (mixture of diastereomers in the ratio of 1.2:1): The reaction was performed for 18 h. ^{1}H NMR (400 MHz, CDCl$_3$) δ 7.44-7.20 (10H, m), 6.68-6.62 (4H, m), 6.48-6.39 (4H, m), 4.65 (1H, brs), 4.61 (1H, brs), 4.49 (2H, brs), 4.30-4.24 (1H, m), 4.12 (1H, d, J = 6.0 Hz), 4.12-3.99 (2H, m), 3.72-3.61 (2H, m), 3.67 (6H, s), 2.46-2.24 (2H, m), 2.05-1.95 (1H, m), 1.91-1.82 (1H, m), 0.91 (9H, s), 0.90 (9H, s), 0.12 (3H, s), 0.11 (3H, s), 0.10 (3H, s), 0.09 (3H, s); ^{13}C NMR (151 MHz, CDCl$_3$) δ 152.1, 152.0, 151.2, 150.5, 142.3, 142.0, 141.3, 140.0, 128.6, 128.5, 127.8, 127.6, 127.5, 127.3, 115.0, 114.8(4), 114.8(1), 114.7(6), 103.4, 101.3, 78.2, 77.9, 64.6, 63.8, 63.6, 62.5, 55.8(9), 55.8(7), 30.5, 30.4, 25.7(9), 25.7(7), 18.1(8), 18.1(7), −4.0, −4.1, −4.4, −4.5; HRMS (ESI): Calcd for $C_{25}H_{36}O_3NSi^+$ ([M+H]$^+$) 426.2459. Found 426.2454.
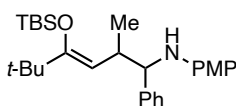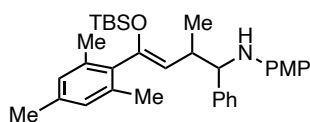
3r (Z/E > 20:1, dr of Z-isomer is 1.2:1): The reaction was performed with **1q** (0.2 mmol, 2 equiv), i-Pr$_3$SiSH (0.04 mmol, 40 mol%) and LiOAc (0.02 mmol, 20 mol%) for 48 hours. ^{1}H NMR (400 MHz, CDCl$_3$) δ 7.40 (2H, d, J = 7.2 Hz), 7.31 (2H, t, J = 7.2 Hz), 7.28-7.17 (6H, m), 6.62 (4H, d, J = 9.2 Hz), 6.35 (2H, d, J = 9.2 Hz), 6.32 (2H, d, J = 9.2 Hz), 4.45 (1H, d, J = 10.8 Hz), 4.30 (2H, brs), 4.21 (1H, d, J = 2.4 Hz), 4.19 (1H, d, J = 3.2 Hz), 3.66 (3H, s), 3.65 (3H, s), 3.61 (1H, d, J = 9.6 Hz), 3.18-3.07 (1H, m), 2.80-2.68 (1H, m), 1.11 (9H, s), 1.08 (9H, s), 1.05 (9H, s), 1.02 (9H, s), 0.90 (3H, d, J = 6.8 Hz), 0.75 (3H, d, J = 6.8 Hz), 0.23 (3H, s), 0.22(4) (3H, s), 0.22(1) (3H, s), 0.20 (3H, s); ^{13}C NMR (151 MHz, CDCl$_3$) δ 160.1, 159.3, 151.8, 151.2, 143.8, 143.2, 141.8, 140.8, 128.4, 128.3, 127.8(3), 127.8(0), 127.0, 126.9, 114.9, 114.8, 114.5, 113.8, 108.1, 105.5, 66.6, 63.5, 55.9, 37.5, 37.0, 36.9, 34.9, 29.2, 29.1, 26.7(2), 26.6(7), 19.4(2), 19.3(7), 18.5, 18.3, −2.5(9), −2.6(1), −2.7, −2.9, one peak was not found probably due to overlapping; HRMS (ESI): Calcd for $C_{28}H_{44}O_2NSi^+$ ([M+H]$^+$) 454.3136. Found 454.3140.
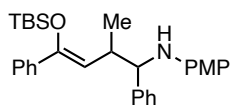
3s (Z/E = 8.7:1, dr of Z isomer is 1.3:1): The reaction was performed with **1r** (0.2 mmol, 2 equiv) for 18 h. ^{1}H NMR (400 MHz, CDCl$_3$) (for Z isomer) δ 7.46-7.38 (8H, m), 7.37-7.16 (12H, m), 6.66-6.59 (4H, m), 6.42-6.35 (4H, m), 5.00 (1H, d, J = 10.0 Hz), 4.78 (1H, d, J = 10.0 Hz), 4.67 (2H, br), 4.31 (1H, d, J = 4.4 Hz), 3.78 (1H, d, J = 9.2 Hz), 3.66 (3H, s), 3.64 (3H, s), 3.38-3.26 (1H, m), 3.02-2.90 (1H, m), 1.07 (9H, s), 1.02(0) (9H, s), 1.01(6) (3H, d, J = 7.6 Hz), 0.86 (3H, d, J = 6.8 Hz), 0.03 (3H, s), 0.02 (3H, s), −0.08 (3H, s), −0.12 (3H, s); ^{13}C NMR (151 MHz, CDCl$_3$) (for Z isomer) δ 151.7, 151.4, 151.2, 150.6, 144.0, 143.0, 142.1, 141.1, 139.4, 139.3, 128.5, 128.1(4), 128.1(0), 128.0(9), 128.0(7), 128.0(0), 127.9(7), 127.7, 127.1, 126.9, 126.6, 126.5, 115.6, 114.9(0), 114.8(9), 114.3, 113.9, 113.1, 66.3, 64.1, 56.0, 55.9, 38.3,

36.3, 26.1, 18.4, 18.2, 17.8, −3.4(7), −3.5(4), −4.1, −4.2, two peaks were not found probably due to overlapping; HRMS (ESI): Calcd for $C_{31}H_{40}O_2NSi^+$ ([M+H]$^+$) 474.2823. Found 474.2826.
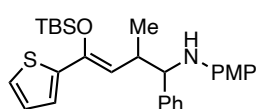
3t (isolated as a mixture of geometrical isomers (Z/E = 3.0:1), both of which consist of two diastereomers (dr = 1:1)): The reaction was performed with **1s** (0.2 mmol, 2 equiv), i-Pr$_3$SiSH (0.04 mmol, 40 mol%) and LiOAc (0.02 mmol, 20 mol%) for 48 h. ^{1}H NMR (400 MHz, CDCl$_3$) (for Z isomer) δ 7.42 (2H, d, J = 7.2 Hz), 7.34-7.13 (8H, m), 6.84 (2H, brs), 6.81 (2H, brs), 6.67-6.58 (4H, m), 6.42-6.36 (4H, m), 4.50 (1H, d, J = 9.6 Hz), 4.27 (1H, d, J = 4.8 Hz), 4.23 (1H, d, J = 10.0 Hz), 3.80 (1H, d, J = 9.2 Hz), 3.67 (3H, s), 3.66 (3H, s), 3.50-3.37 (1H, m), 3.14-3.02 (1H, m), 2.33(3) (3H, s), 2.32(5) (3H, s), 2.30 (3H, s), 2.26 (6H, s), 2.23 (3H, s), 1.04 (3H, d, J = 9.6 Hz), 1.00 (9H, s), 0.97 (9H, s), 0.90 (3H, d, J = 6.8 Hz), −0.11 (3H, s), −0.12 (3H, s), −0.25 (3H, s), −0.27 (3H, s) , (for E isomer) δ 7.34-7.13 (10H, m), 6.94 (2H, brs), 6.90 (2H, brs), 6.67-6.58 (4H, m), 6.33 (2H, d, J = 9.2 Hz), 6.25 (2H, d, J = 8.8 Hz), 4.80 (1H, d, J = 10.0 Hz), 4.64 (1H, d, J = 10.8 Hz), 4.02 (1H, d, J = 3.6 Hz), 3.84 (1H, d, J = 8.0 Hz), 3.67 (3H, s), 3.65 (3H, s), 3.50-3.37 (1H, m), 3.14-3.02 (1H, m), 2.40 (12 H, s), 2.25 (3H, s), 2.24 (3H, s), 0.93 (3H, d, J = 7.2 Hz), 0.87 (9H, s), 0.85 (9H, s), 0.81 (3H, d, J = 6.8 Hz), 0.09 (3H, s), 0.07 (3H, s), 0.05 (3H, s), 0.02 (3H, s); ^{13}C NMR (151 MHz, CDCl$_3$) (for Z isomer) δ 151.5, 151.3, 148.1, 147.4, 144.1, 142.6, 142.2, 141.1, 137.5(4), 137.4(7), 137.0, 136.7, 136.0, 135.9, 135.7, 135.5, 128.5, 128.4, 128.3, 128.1, 128.0, 127.7, 127.0, 126.8, 114.9, 114.8, 114.1, 113.8, 65.3, 64.1, 56.0, 55.9, 38.0, 35.9, 25.9, 21.2, 20.8, 20.5, 20.4, 18.5, 18.4, −4.2, −4.2(7), −4.3(4), −4.4, three carbon atoms were not found probably due to overlapping, (for E isomer) δ 151.8, 149.8, 149.2, 142.8, 142.1, 141.3, 137.4, 137.3, 136.5, 135.9, 135.8, 134.1, 133.9, 128.5, 128.4, 128.3, 128.0, 127.9, 127.0, 126.9, 116.4, 114.8, 114.5, 114.4, 112.5, 110.6, 64.8, 64.1, 55.9(0), 55.8(7), 39.3, 38.6, 25.8, 21.3, 20.2, 20.1, 20.0, 18.3, 17.9, −4.4, eight carbon atoms were not found probably due to overlapping; HRMS (ESI): Calcd for $C_{33}H_{46}O_2NSi^+$ ([M+H]$^+$) 516.3292. Found 516.3304.
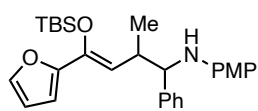
3u (isolated as a mixture of geometrical isomers (Z/E = 1.2:1), both of which consist of two diastereomers (dr = 1.2:1)): The reaction was performed for 18 h. ^{1}H NMR (400 MHz, CDCl$_3$) (for Z isomers) δ 7.42-7.38 (2H, m), 7.36-7.18 (10H, m), 6.66-6.59 (4H, m), 6.51-6.47 (2H, m), 6.44-6.30 (6H, m), 5.22 (1H, d, J = 10.4 Hz), 5.00 (1H, d, J = 10.8 Hz), 3.85 (1H, d, J = 9.2 Hz), 3.80 (1H, d, J = 9.6 Hz), 3.66 (6H, s), 3.32-3.22 (1H, m), 3.00-2.87 (1H, m), 1.08 (9H, s), 0.96 (9H, s), 0.91 (3H, d, J = 6.8 Hz), 0.85 (3H, d, J = 6.8 Hz), 0.15 (3H, s), 0.12 (9H, s), (for E isomer) δ 7.44 (2H, d, J = 1.2 Hz), 7.42-7.38 (2H, m), 7.36-7.18 (8H, m), 6.66-6.59 (4H, m), 6.44-6.30 (8H, m), 4.86 (1H, d, J = 10.4 Hz), 4.71 (1H, d, J = 10.8 Hz), 4.31 (2H, d, J = 4.4 Hz), 3.70-3.56 (1H, m), 3.66 (3H, s), 3.64 (3H, s), 3.32-3.22 (1H, m), 1.04 (9H, s), 1.02 (3H, d, J = 7.2 Hz), 1.00 (3H, d, J = 7.2 Hz), 0.94 (9H, s), 0.12 (3H, s), 0.11 (3H, s), 0.08 (3H,

s), 0.07 (3H, s); ^{13}C NMR (151 MHz, CDCl$_3$) (for all isomers) δ 152.1(3), 152,0(8), 151.9, 151.8(2), 151.7(8), 151.7, 151.4, 143.7, 143.4, 142.7, 142.3, 142.1(9), 142.1(5), 142.1(2), 142.0, 141.9, 141.7(9), 141.7(6), 141.7, 141.6, 141.2, 141.0, 140.9, 128.5, 128.4, 128.1(1), 128.0(9), 128.0, 127.8, 127.7, 127.2, 127.1, 127.0(2), 126.9(5), 115.2, 115.0, 114.9, 114.8, 114.7, 114.6, 114.5, 114.3, 114.0, 113.8, 112.7, 111.6, 111.1(3), 111.0(8), 111.0(2), 110.9(9), 109.8, 109.7, 107.0, 106.9, 66.0, 65.4, 63.8, 63.6, 55.9(4), 55.9(1), 55.8(6), 38.7, 37.7, 36.6, 35.6, 26.1, 25.9, 19.2, 19.0, 18.7, 18.5, 18.3, 18.1, 17.7, −3.6, −3.7, −4.1(2), −4.1(3), −4.3(5), −4.4(2), −4.6, nine peaks were not found probably due to overlapping; HRMS (ESI): Calcd for C$_{28}$H$_{38}$O$_3$NSi$^+$ ([M+H]$^+$) 464.2615. Found 464.2614.

3v (isolated as a mixture of geometrical isomers (*Z*/*E* = 1.5:1), both of which consist of two diastereomers (dr = 1.1:1)): The reaction was performed for 18 h. ^1H NMR (400 MHz, CDCl$_3$) (for *Z* isomer) δ 7.39 (2H, t, *J* = 8.0 Hz), 7.35-7.20 (10H, m), 7.17-7.13 (1H, m), 7.07 (1H, dd, *J* = 3.6, 0.8 Hz), 7.03-6.98 (1H, m), 6.94 (1H, t, *J* = 4.4 Hz), 6.66-6.59 (4H, m), 6.44-6.35 (4H, m), 5.08 (1H, d, *J* = 9.6 Hz), 4.90 (1H, d, *J* = 10.8 Hz), 3.88 (1H, d, *J* = 8.8 Hz), 3.79 (1H, d, *J* = 9.2 Hz), 3.66 (6H, s), 3.03-2.85 (2H, m), 1.08 (9H, s), 0.97 (9H, s), 0.95 (3H, d, *J* = 6.8 Hz), 0.85 (3H, d, *J* = 6.8 Hz), 0.13(2) (3H, s), 0.12(6) (3H, s), 0.07 (3H, s), 0.04 (3H, s), (for *E* isomer) δ 7.39 (2H, t, *J* = 8.0 Hz), 7.35-7.20 (10H, m), 7.18 (1H, d, *J* = 3.6 Hz), 7.04 (1H, dd, *J* = 3.6, 0.8 Hz), 7.03-6.98 (1H, m), 6.94 (1H, t, *J* = 4.4 Hz), 6.66-6.59 (4H, m), 6.44-6.35 (4H, m), 4.86 (1H, d, *J* = 10.8 Hz), 4.81 (1H, d, *J* = 10.8 Hz), 4.31 (1H, d, *J* = 8.4 Hz), 4.30 (1H, d, *J* = 7.2 Hz), 3.65 (6H, s), 3.35-3.20 (2H, m), 1.04(3) (3H, d, *J* = 7.2 Hz), 1.03(8) (9H, s), 1.00 (3H, d, *J* = 7.2 Hz), 0.94 (9H, s), 0.11 (6H, s), 0.09 (6H, s); ^{13}C NMR (151 MHz, CDCl$_3$) (for *Z* isomer) δ 152.0, 151.8, 145.4, 145.3, 143.1, 142.9, 142.1, 141.6, 140.6, 128.5, 128.2, 128.1, 127.8, 127.7, 127.3, 127.1, 127.0(1), 126.9(8), 126.9, 126.3, 125.7, 124.6, 124.5, 115.3, 114.9, 114.7, 114.4, 114.0, 112.1, 66.2, 65.4, 56.0, 55.9, 40.1, 38.2, 25.9, 18.8, 18.6, 18.0, −3.4, −4.0, −4.2, −4.4, two peaks were not found probably due to overlapping, (for *E* isomer) δ 152.6, 151.4, 144.9, 144.7, 143.7, 142.6, 141.9, 141.3, 140.8(4), 140.8(0), 128.0(4), 127.9(9), 127.0, 126.8, 126.4, 125.6, 124.5(4), 124.4(7), 114.9(1), 114.8(5), 114.5, 114.4, 112.9, 64.0, 63.2, 55.9(3), 55.8(9), 38.1, 36.2, 26.1, 18.5, 18.4, 17.7, −3.5, −3.9, −4.3, −4.4, seven peaks were not found probably due to overlapping; HRMS (ESI): Calcd for C$_{28}$H$_{38}$O$_2$NSSi$^+$ ([M+H]$^+$) 480.2387. Found 480.2382.
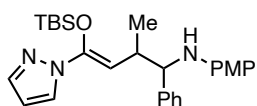
3w (*Z*/*E* > 20:1, dr of *Z*-isomer is 1.1:1): The reaction was performed for 18 h. ^1H NMR (400 MHz, CDCl$_3$) δ 7.59 (1H, d, *J* = 2.0 Hz), 7.58 (1H, d, *J* = 2.0 Hz), 7.56 (1H, d, *J* = 2.0 Hz), 7.53 (1H, d, *J* = 2.0 Hz), 7.39 (2H, d, *J* = 7.2 Hz), 7.35-7.17 (8H, m), 6.68-6.60 (4H, m), 6.45-6.38 (4H, m), 6.30 (1H, t, *J* = 2.0 Hz), 6.29 (1H, t, *J* = 2.0 Hz), 4.99 (1H, d, *J* = 10.4 Hz), 4.80 (1H, d, *J* = 10.4 Hz), 4.33 (1H, d, *J* = 4.4 Hz), 3.89 (1H, d, *J* = 9.2 Hz), 3.67 (3H, s), 3.66 (3H, s), 3.21-3.10 (1H, m), 2.92-2.80 (1H, m), 1.07 (3H, d, *J* = 7.6

Hz), 1.04 (9H ,s), 1.01 (9H, s), 0.94 (3H, d, $J = 6.8$ Hz), 0.09 (3H, s), 0.07 (3H, s), 0.02 (3H, s), −0.02 (3H, s); ^{13}C NMR (151 MHz, CDCl$_3$) δ 151.9, 151.7, 144.1, 143.4(1), 143.3(5), 142.4, 141.8, 141.0, 140.5, 140.4, 128.6, 128.5, 128.4, 128.2, 127.9, 127.6, 127.2, 127.0, 114.9, 114.8, 114.6, 114.3, 106.4, 106.2, 104.0, 102.4, 65.5, 63.6, 55.9(2), 55.9(0), 37.9, 36.4, 25.9, 18.4, 18.3, 17.7, −4.4, −4.6, −4.7(0), −4.7(2), two peaks were not found probably due to overlapping; HRMS (ESI): the peak pattern corresponding to **3w** was not observed probably due to the loss of pyrazole group under the measurement condition.

Derivatization of Alkylated Enol Silyl Ethers
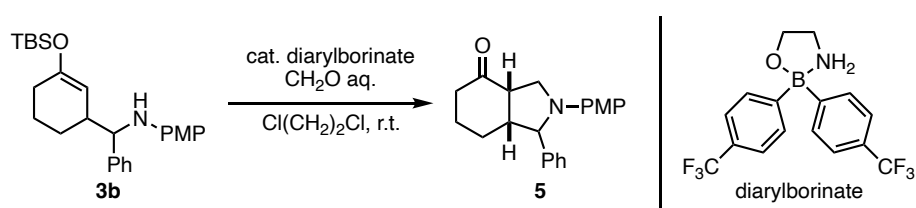
To a flame-dried test tube were added **3b** (21.2 mg, 0.05 mmol), diarylborinate (1.8 mg, 0.005 mmol, 10 mol%) and 1,2-dichloroethane (1 mL, 0.05 M). The reaction tube was sealed with rubber septum and then evacuated in *vacuo* and backfilled with Ar five times. A 37% aqueous solution of formaldehyde (14.9 μL, 0.15 mmol, 3 equiv) was introduced via syringe. After stirring overnight, the reaction mixture was concentrated. The resulting crude material was purified by column chromatography on silica gel (hexane/EtOAc = 15: to 5:1 as eluent) to afford **5** in 92% yield (14.8 mg, 0.046 mmol, dr = 1:1). ^{1}H NMR (400 MHz, CDCl$_3$) δ 7.33-7.15 (10H, m), 6.74 (2H, d, $J = 9.0$ Hz), 6.72 (2H, d, $J = 9.0$ Hz), 6.42 (2H, d, $J = 9.0$ Hz), 6.41 (2H, d, $J = 9.0$ Hz), 4.70 (1H, d, $J = 7.2$ Hz), 4.43 (1H, d, $J = 3.2$ Hz), 4.24 (1H, dd, $J = 9.0, 6.4$ Hz), 3.80 (2H, d, $J = 8.0$ Hz), 3.70 (3H, s), 3.69 (3H, s), 3.51 (1H, t, $J = 9.0$ Hz), 3.17 (1H, q, $J = 8.0$ Hz), 3.12-2.99 (2H, m), 2.63-2.46 (1H, m), 2.44-2.35 (1H, m), 2.30 (2H, t, $J = 6.6$ Hz), 2.13-1.98 (2H, m), 1.86-1.67 (2H, m), 1.65-1.44 (3H, m), 1.44-1.34 (1H, m); ^{13}C NMR (151 MHz, CDCl$_3$) δ 211.0, 210.5, 151.5, 151.4, 143.2, 142.0, 141.5, 140.2, 128.9, 128.6, 127.2, 125.9, 114.9, 114.6(9), 114.6(7), 113.4, 68.9, 67.3, 56.0, 55.9, 52.1, 51.3, 51.0, 50.1, 49.9, 46.9, 39.3(4), 39.2(8), 26.5, 24.2, 23.7, 23.6, two peaks were not found probably due to overlapping; HRMS (ESI): Calcd for C$_{21}$H$_{23}$O$_2$NNa$^+$ ([M+Na]$^+$) 344.1621. Found 344.1611.
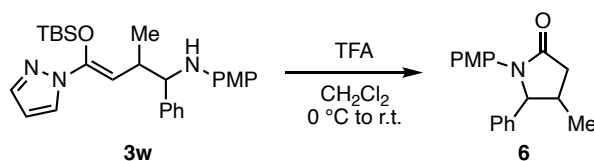
To a solution of **3w** (32.7 mg, 0.071 mmol, 1 equiv) in CH$_2$Cl$_2$ (1.4 mL, 0.05 M) was added trifluoroacetic acid (TFA) (27.2 μL, 0.36 mmol, 5 equiv) dropwise at 0 °C, and the resulting mixture

was allowed to warm to room temperature. After stirring for 2 h, the reaction mixture was diluted with water and the extractive work-up was conducted with CH_2Cl_2. The combined organic layers were washed with saturated aqueous solution of $NaHCO_3$, dried over Na_2SO_4, filtered and concentrated. The resulting crude material was purified by column chromatography on silica gel (hexane/EtOAc = 3:1 to 1:1 as eluent) to give **6** in 87% yield (17.5 mg, 0.062 mmol, dr = 1:1). ^{1}H NMR (400 MHz, $CDCl_3$) δ 7.38-7.13 (10H, m), 6.80-6.73 (4H, m), 5.09 (1H, d, J = 8.0 Hz), 4.65 (1H, d, J = 5.6 Hz), 3.72 (3H, s), 3.71 (3H, s), 2.98-2.83 (1H, m), 2.88 (1H, dd, J = 19.2, 9.2 Hz), 2.69 (1H, dd, J = 17.0, 9.8 Hz), 2.42 (1H, dd, J = 17.0, 9.8 Hz), 2.37-2.27 (1H, m), 2.30 (1H, dd, J = 19.2, 9.2 Hz), 1.25 (3H, d, J = 6.4 Hz), 0.71 (3H, d, J = 6.8 Hz); ^{13}C NMR (151 MHz, $CDCl_3$) δ 174.5, 174.4, 157.0, 156.8, 140.3, 137.5, 131.9, 131.3, 128.9, 128.8, 128.1, 128.0, 127.2, 126.7, 124.6, 123.7, 114.0(9), 114.0(5), 72.1, 68.8, 55.4(8), 55.4(5), 39.5, 38.8, 37.7, 32.7, 18.9, 16.1; HRMS (ESI): Calcd for $C_{18}H_{19}O_2NNa^+$ ([M+Na][+]) 304.1308. Found 304.1308.

References and Notes

(1) Ricci, A. *Amino Group Chemistry: From Synthesis to the Life Sciences*, Willey-VCH, **2008**.

(2) Hili, R.; Yudin, A. K. *Nat. Chem. Biol.* **2006**, *2*, 284.

(3) For selected recent reviews, see: (a) Shi, Y.; Wang, Q.; Gao, S. *Org. Chem. Front.* **2018**, *5*, 1049. (b) Saranya, S.; Harry, N. A.; Krishnan, K. K.; Anilkumar, G. *Asian. J. Org. Chem.* **2018**, *7*, 613. (c) Frías, M.; Cieślik, W.; Fraile, A.; Rosado-Abón, A.; Garrido-Castro, A. F.; Yuste, F.; Alemán, J. *Chem. Eur. J.* **2018**, *24*, 10906. (d) Cheng, D.-J.; Shao, Y.-D. *ChemCatChem* **2019**, *11*, 2575. (e) Meyer, C. C.; Ortiz, E.; Krische, M. J. *Chem. Rev.* **2020**, *120*, 3721. (f) Morisaki, K.; Morimoto, H.; Ohshima, T. *ACS Catal.* **2020**, *10*, 6924.

(4) For examples of β-functionalization of α,β-unsaturated aldehydes with imines using N-heterocyclic carbene (NHC) as a catalyst, see: (a) He, M; Bode, J. W. *Org. Lett.* **2005**, *7*, 3131. (b) Phillips, E. M.; Reynolds, T. E.; Scheidt, K. A. *J. Am. Chem. Soc.* **2008**, *130*, 2416. (c) Rommel, M.; Fukuzumi, T.; Bode, J. W. *J. Am. Chem. Soc.* **2008**, *130*, 17266. (d) Raup, D. E. A.; Cardinal-David, B.; Holte, D.; Scheidt, K. A. *Nat. Chem.* **2010**, *2*, 766. (e) Zhao, X.; DiRocco, D. A.; Rovis, T. *J. Am. Chem. Soc.* **2011**, *133*, 12466. (f) Lv, H.; Tiwari, B.; Mo, J.; Xing, C.; Chi, R. *Org. Lett.* **2012**, *14*, 5412. (g) Zhang, B.; Feng, P.; Sun, L.-H.; Cui, Y.; Ye, S.; Jiao, N. *Chem. Eur. J.* **2012**, *18*, 9198. (h) Xu, W.-Y.; Iwaki, R.; Jia, Y.-M.; Zhang, W.; Kato, A.; Yu, C.-Y. *Org. Biomol. Chem.* **2013**, *11*, 4622. (i) Guo, C.; Fleige, M.; Janssen-Müller, D.; Daniliuc, C. G.; Glorius, F. *Nat. Chem.* **2015**, *7*, 842. (j) Xu, J.; Hu, S.; Lu, Y.; Dong, Y.; Tang, W.; Lu, T.; Dua, D. *Adv. Synth. Catal.* **2015**, *357*, 923. (k) Dong, S.; Frings, M.; Zhang, D.; Guo, Q.; Daniliuc, C. G.; Cheng, H.;

Bolm, C. *Chem. Eur. J.* **2017**, *23*, 13888. (l) Chen, X.-Y.; Xiong, J.-W.; Liu, Q.; Li, S.; Sheng, H.; von Essen, C.; Rissanen, K.; Enders, D. *Angew. Chem. Int. Ed.* **2018**, *57*, 300.

(5) Fu, Z.; Xu, J.; Zhu, T.; Leong, W. W. Y.; Chi, Y. R. *Nat. Chem.* **2013**, *5*, 835.

(6) Pirnot, M. T.; Rankic, D. A.; Martin, D. B. C.; MacMillan, D. W. C. *Science* **2013**, *339*, 1593.

(7) Jeffrey, J. L.; Petronijević, F. R.; MacMillan, D. W. C. *J. Am. Chem. Soc.* **2015**, *137*, 8404.

(8) Ohmatsu, K.; Nakashima, T.; Sato, M.; Ooi, T. *Nat. Commun.* **2019**, *10*, 2706.

(9) (a) Hioe, J.; Šakić, D.; Vrček, V.; Zipse, H. *Org. Biomol. Chem.* **2015**, *13*, 157. (b) Šakić, D.; Zipse, H. *Adv. Synth. Catal.* **2016**, *358*, 3983.

(10) Roth, H. G.; Romero, N. A.; Nicewicz, D. A. *Synlett* **2016**, *27*, 714.

(11) (a) Khursan, S. L.; Mikhailov, D. A.; Yanborisov, V. M.; Borisov, D. I. *React. Kinet. Catal. Lett.* **1997**, *61*, 91. (b) Luo, Y.-R. *Handbook of Bond Dissociation Energies in Organic Compounds* CRC Press, Boca Raton, FL, **2003**.

(12) (a) Hager, D.; MacMillan, D. W. C. *J. Am. Chem. Soc.* **2014**, *136*, 16986. (b) Uraguchi, D. Kinoshita, N.; Kizu, T.; Ooi, T. *J. Am. Chem. Soc.* **2015**, *137*, 13768. (c) Fava, E.; Millet, A.; Nakajima, M.; Loescher, S.; Rueping, M. *Angew, Chem. Int. Ed.* **2016**, *55*, 6776. (d) Patel, N. R.; Kelly, C. B.; Siegenfeld, A. P.; Molander, G. A. *ACS Catal.* **2017**, *7*, 1766. (e) Jia, J.; Kancherla, R.; Rueping, M.; Huang, L. *Chem. Sci.* **2020**, *11*, 4954.

(13) Leitch, J. A.; Rossolini, T.; Rogova, T.; Maitland, J. A. P.; Dixon, D. J. *ACS Catal.* **2020**, *10*, 2009.

(14) (a) Knowles, R.; Yayla, H. *Synlett* **2014**, *25*, 2819. (b) Gentry, E. C.; Knowles, R. R. *Acc. Chem. Res.* **2016**, *49*, 1546. (c) Miller, D. C.; Tarantino, K. T.; Knowles, R. R. *Top. Curr. Chem.* **2016**, *374*, 30. (d) Hoffmann, N. *Eur. J. Org. Chem.* **2017**, 1982.

(15) The present Mannich-type reaction was not tolerant to aliphatic imines. For instance, the reactions of **1a** with pivalaldehyde- or cyclohexanecarboxaldehyde-derived imines resulted in no reaction or the formation of a complex mixture, including the parent 4-methoxyaniline and aldehyde generated through imine hydrolysis.

(16) Tanaka, Y.; Hasui, T.; Suginome, M. *Synlett* **2008**, 1239.

(17) (a) Li, Y.-J.; Huang, H.-M.; Dong, H.-Q.; Jia, J.-H.; Han, L.; Ye, Q.; Gao, J.-R. *J. Org. Chem.* **2013**, *78*, 9424. (b) Spanò, V.; Pennati, M.; Parrino, B.; Carbone, A.; Montalbano, A.; Cilibrasi, V.; Zuco, V.; Lopergolo, A.; Cominetti, D.; Diana, P.; Cirrincione, G.; Barraja, P.; Zaffaroni, N. *J. Med. Chem.* **2016**, *59*, 7223. (c) Annamalai, M.; Hristeva, S.; Bielska, M.; Ortega, R.; Kumar, K. *Molecules* **2017**, *22*, 827. (d) Liu, L.; Bao, L.; Wang, L.; Ma, K.; Han, J.; Yang, Y.; Liu, R.; Ren, J.; Yin, W.; Wang, W.; Liu, H. *J. Org. Chem.* **2018**, *83*, 812.

(18) Choi, G. J.; Zhu, Q.; Miller, D. C.; Gu, C. J.; Knowles, R. R. *Nature* **2016**, *539*. 268.

(19) Lowry, M. S.; Hudson, W. R.; Pascal, R. A. Jr.; Bernhard, S. *J. Am. Chem. Soc.* **2004**, *126*, 14129.

List of Publications

Chapter 2

(1) Direct Allylic C−H Alkylation of Enol Silyl Ethers Enabled by Photoredox-Brønsted Base Hybrid Catalysis

Ohmatsu, K.; Nakashima, T.; Sato, M.; Ooi, T. *Nat. Commun.* **2019**, *10*, 2706.

Chapter 4

(2) Mannich-Type Allylic C−H Functionalization of Enol Silyl Ethers under Photoredox-Thiol Hybrid Catalysis

Nakashima, T.; Ohmatsu, K.; Ooi, T. *Org. Biomol. Chem.* **2021**, *19*, 141.

Acknowledgement